Identification of genetic modifiers of *ACCELERATED CELL DEATH 6* (*ACD6*) in natural *Arabidopsis thaliana* accessions

Dissertation

der Mathematisch-Naturwissenschaftlichen Fakultät

der Eberhard Karls Universität Tübingen

zur Erlangung des Grades eines

Doktors der Naturwissenschaften

(Dr. rer. nat.)

vorgelegt von

Maricris Lanuzo Zaidem

aus Quezon City, Philippinen

Tübingen

2016

Gedruckt mit Genehmigung der Mathematisch-Naturwissenschaftlichen Fakultät der Eberhard Karls Universität Tübingen.

Tag der mündlichen Qualifikation: 29.07.2016
Dekan: Prof. Dr. Wolfgang Rosenstiel
1. Berichterstatter: Prof. Dr. Detlef Weigel
2. Berichterstatter: Prof. Dr. Thorsten Nürnberger

Acknowledgements

For the opportunity of a lifetime, and for extraordinary patience and generosity,

Prof. Dr. Detlef Weigel

For agreeing to be part of my PhD and Thesis Advisory committee,

Prof. Dr. Thorsten Nürnberger, Prof. Dr. Klaus Harter, Prof. Dr. Ulrike Zentgraf, and Dr. Karsten Borgwardt

For introducing me to the idea of pursuing a PhD in Europe,

Norman Warthmann

For the invaluable help by answering my questions and fruitful discussions,

Marco Todesco, Dan Koenig, Gautam Shirsekar, Sang-tae Kim, Eunyoung Chae, Norman Warthmann, Ignacio Rubio, Hernán Burbano, Rafał Gutaker, Patrice Salome, Rebecca Schwab, Lisa Smith, Chang Liu, Christa Lanz, Josip Percovic, Frank Kuettner, Moises Exposito Alonso, Danelle Seymour, George Wang, Joerg Hagmann, Francois Vasseur, Anette Habring-Mueller, Sonja Kersten and Hülya Wicher

For translating my Zusammenfassung, better than Google Translate can,

Patricia Lang, Rebecca Schwab and Detlef Weigel

For all kinds of awesomeness at work and otherwise,

Rafał Gutaker, Eshita Sharma, Subhashini Muralidharan, Johannes Kaut, Diep Tran, Patricia Lang, Efythimia Symeonidi, Giovanna Capovilla, Silvio Collani, Gautam Shirsekar, Marco Todesco, and Juan Diego Santillana Ortiz and Moises Exposito Alonso

For taking care of me when I had “the operation”; for being there at my lowest,

Subhashini Muralidharan, Sridhar Venkatakrishnan and Rafał Gutaker

For the long-distance sisterly talks and encouragements,

Erin Tanchico and Charisma Love Gado

For love, joy, inspiration and unconditional support,

Mama, Tomo, Moshe, Zaine, Sofia and Ollie

For my current scattered brain,

My little “Peanut butter”

For reminding me to watch the sun rise and set, the birds fly, and for everything else,

Rafał

Table of Contents

Abbreviations

Genes

ACD6	*ACCELERATED CELL DEATH 6*
ADR2	*ACTIVATED DISEASE RESISTANCE 2*
BAK1	*BRASSINOSTEROID INSENSITIVE 1-ASSOCIATED KINASE 1*
CERK1	*CHITIN ELICITOR RECEPTOR KINASE*
DM3	*DANGEROUS MIX 3*
DM5	*DANGEROUS MIX 5*
EDS1	*ENHANCED DISEASE SUSCEPTIBILITY 1*
EF-TU	*ELONGATION FACTOR THERMO UNSTABLE*
FLS2	*FLAGELLIN SENSING 2*
FRK1	*FLG22-INDUCED RECEPTOR KINASE*
HSP90	*HEAT SHOCK PROTEIN 90*
NDR1	*NON-RACE SPECIFIC DISEASE RESISTANCE PROTEIN 1*
NPR1	*NONEXPRESSER OF PR GENES 1*
PAD4	*PHYTOALEXIN DEFICIENT 4*
PR1	*PATHOGENESIS RELATED GENE 1*
RAR1	*REQUIRED FOR MLA1 RESISTANCE 1*
RPM1	*RESISTANCE TO P. SYRINGAE PV MACULICOLA 1*
RPP1	*RECOGNITION OF PERONOSPORA PARASITICA 1*
RPP2	*RECOGNITION OF PERONOSPORA PARASITICA 2*
RPP4	*RECOGNITION OF PERONOSPORA PARASITICA 4*
RPP5	*RECOGNITION OF PERONOSPORA PARASITICA 5*
RPP7	*RECOGNITION OF PERONOSPORA PARASITICA 7*
RPP8	*RECOGNITION OF PERONOSPORA PARASITICA 8*
RPS6	*RESISTANT TO P. SYRINGAE 6*
RPW8	*RESISTANCE TO POWDERY MILDEW8*
RRS1	*RESISTANT TO RALSTONIA SOLANACEARUM 1*
SAG12	*SENESCENCE-ASSOCIATED GENE 12*
SGT1b	*SGT1 HOMOLOG b*
SNC1	*SUPPRESSOR OF NPR1-1, CONSTITUTIVE 1*
SSI4	*SUPPRESSOR OF SALICYLIC ACID INSENSITIVITY OF NPR1-5*
WRKY29	*WRKY TRANSCRIPTION FACTOR 29*
WRKY46	*WRKY TRANSCRIPTION FACTOR 46*

Other

ABA	Abscisic acid
amiR	Artificial microRNA
Avr	Avirulence
BAM	Binary alignment/mapping
bp	Base pair
BR	Brassinosteroids
BTH	Benzo (1,2,3) thiadiazole-7-carbothioic acid S-methyl ester
BWA	Burrows-Wheeler Aligner

CaMV	Cauliflower mosaic virus
cDNA	Complementary DNA
CK	Cytokinin
cM	Centimorgan
CNBH	Carbon:Nutrient Balance Hypothesis
CTAB	Cetyl trimethylammonium bromide
DAMP	Damage-associated molecular pattern
DAS	Days after sowing
DNA	Deoxyribonucleic acid
DNAse	Deoxyribonuclease
dNTP	Deoxyribose nucleoside triphosphate
EDTA	Ethylenediaminetetraacetic acid
EFR	EF-Tu receptor
ET	Ethylene
ETI	Effector-triggered immunity
F_1	Filial 1 hybrid
F_2	Second filial generation
flg22	22 amino acid flagellin peptide
GA	Gibberellic acid or gibberellins
GATK	Genome Analysis Toolkit
GDBH	Growth-Differentiation Balance Hypothesis
GOF	Gain-of-function
GRH	Growth Rate Hypothesis
GWAS	Genome-wide association study
HR	Hypersensitive response
INA	2,6,-dichloroisonicotinic acid
JA	Jasmonic acid
k-mer	String of length *k*
LB	Luria-Bertani broth
LOD	Logarithm of odds
LOF	Loss-of-function
LRR-RLK	Leucine-rich repeat receptor-like kinase
LYK	Lysin motif receptor kinase
LysM RLK	Lysin motif receptor-like kinase
LysM RLP	Lysin motif receptor-like proteins
MAMP	Microbe-associated molecular pattern
MAP kinase	Mitogen-activated protein kinase
Mb	Megabase
MS	Murashige and Skoog
NB-LRR	Nucleotide-binding domain and leucine-rich repeat protein
NLR	Nucleotide-binding domain and leucine-rich repeat protein
ODT	Optimal Defense Theory
oligo(dT)	Oligo-deoxythymine
PAMP	Pathogen associated molecular pattern
PCR	Polymerase chain reaction
PRR	Pattern recognition receptor
Psm	*Pseudomonas syringae* pv. *maculicola*
Pst HrcC-	*Pseudomonas syringae* pv. *tomato HrcC-*
PTI	PAMP-triggered immunity
pv.	Pathovar

qRT-PCR	Quantitative reverse-transcriptase polymerase chain reaction
QTL	Quantitative trait locus
RAD-Seq	Restriction-site Associated DNA Sequencing
RNA	Ribonucleic acid
ROS	Reactive oxygen species
RQH	Red Queen hypothesis
SA	Salicylic acid
SAM	Sequence alignment/mapping
SAR	Systemic-acquired resistance
SNP	Single nucleotide polymorphism
T_1	First transgenic generation
TAE	Tris base, acetic acid and EDTA buffer
Taq	*Thermus aquaticus*
TLR	Toll-like receptor
UTR	Untranslated region
WAK	Wall-associated kinase
WAS	Weeks after sowing
WMD	Web MicroRNA Designer

Abstract

Plants defend themselves against pathogens by activating responses that can also cause unintended collateral damage to the plant itself. Improved understanding of the evolutionary constraints and molecular mechanisms affecting these responses can provide means to minimize the tradeoff between disease-related losses and hyperimmunity-related yield drag in crops. As a model to investigate this problem, I have exploited natural variation at the *ACCELERATED CELL DEATH 6* (*ACD6*) gene, which controls a major trade-off between growth and disease resistance among natural accessions of *Arabidopsis thaliana*. The hyperactive allele *ACD6*-Est-1 is known to confer broad-spectrum immunity, but at the same time to also negatively affect growth in many *A. thaliana* accessions.

Here, I first surveyed a large collection of *A. thaliana* genomes for the presence of Est-like *ACD6* alleles. I confirmed that not all accessions with this allele express overt hyperimmunity. I then demonstrated that Est-like *ACD6* alleles from accessions that do not show the typical autoimmune phenotype normally associated with this allele could confer hyperimmunity when transformed into a different genetic background, indicating that the attenuation of the Est-like *ACD6* phenotype was likely due to extragenic modifiers. I then investigated pathogen responses of several of these accessions more closely. My experiments revealed that reduced growth and immune responses were partially uncoupled in some of these accessions. These findings dovetailed with genetic results suggesting that different accessions contain genetically distinct modifiers of the typical Est-like *ACD6* phenotype. Finally, I demonstrated by quantitative trait loci (QTL) mapping that these modifiers are located in different regions of the genome, with one of the modifiers potentially being a gene in cluster of genes encoding nucleotide-binding domain and leucine-rich repeat (NLR) immune receptors. This is an important finding, as *ACD6* had previously been linked only to PAMP-triggered immunity (PTI), but not to effector-triggered immunity (ETI), which predominantly relies on NLR immune receptors. My study thus provides new insights into the complex genetic interactions that affect disease resistance and growth.

Zusammenfassung

Pflanzen verteidigen sich gegen Krankheitserreger, indem sie Verteidigungsmechanismen abrufen, mit denen sie sich auch selbst unbeabsichtigt Schaden zufügen können. Ein verbessertes Verständnis evolutionärer Beschränkungen und molekularer Mechanismen, die die Ausprägung der Verteidigungsmechanismen beeinflussen, kann dazu beitragen, das Gleichgewicht zwischen krankheitsbedingten Verlusten und durch Hyperimmunität verursachten Ertragsminderungen zu steuern. Zur näheren Untersuchung dieses Problems habe ich die natürliche Variation des *ACCELERATED CELL DEATH 6* (*ACD6*) Genes genutzt, welches in natürlichen Akzessionen von *Arabidopsis thaliana* die Balance zwischen Wachstum und Krankheitsresistenz kontrolliert. Das hyperaktive Allel *ACD6*-Est-1 ist bekannt dafür, breitgefächert Immunität zu verleihen und gleichzeitig das Wachstum in vielen *A. thaliana* Akzessionen zu beeinträchtigen.

Hier untersuchte ich zunächst eine große Sammlung von *A. thaliana* Genomen auf das Vorhandensein von Est-ähnlichen *ACD6*-Allelen. Ich bestätigte, dass nicht alle Akzessionen mit diesem Allel offensichtliche Anzeichen von Hyperimmunität besitzen. Dann zeigte ich, dass Est-ähnliche *ACD6*-Allele aus solchen Akzessionen trotzdem Hyperimmunität vermitteln können, wenn sie in einen anderen genetischen Hintergrund transformiert werden. Das weist darauf hin, dass die Abschwächung des Est-ähnlichen *ACD6*-Phänotyps wahrscheinlich extragenischen Modifikatoren zuzuschreiben ist. Anschließend untersuchte ich die molekularen Antworten auf Pathogenbefall in einigen dieser Akzessionen genauer. Meine Experimente zeigten, dass verringertes Wachstum und Immunantwort in manchen dieser Akzessionen teilweise entkoppelt sind. Diese Erkenntnisse ergänzen meine genetische Experimente, die andeuteten, dass verschiedene Akzessionen unterschiedliche Modifikatoren des typischen Est-ähnlichen *ACD6*-Phänotyps enthalten. Schließlich zeigte ich mit Hilfe von QTL (= *quantitative trait loci*) Kartierung, dass diese Modifikatoren in verschiedenen Regionen des Genoms angesiedelt sind, und dass einer der Modifikatoren eventuell ein Gen in einem Cluster von *nucleotide-binding leucine-rich repeat*

(NLR) Genen ist. Dies ist eine wichtige Erkenntnis, da *ACD6* bisher nur mit PAMP-ausgelöster Immunität (PAMP-triggered immunity, PTI) in Verbindung gebracht wurde, nicht aber mit Effektor ausgelöster Immunität (effector-triggered immunity, ETI), welche hauptsächlich auf NLR Immunrezeptoren basiert. Meine Studie gibt daher neue Einblicke in die komplexen genetischen Interaktionen, die Krankheitsresistenz und Wachstum beeinflussen.

1 Introduction

Organisms are continuously besieged by pathogens of various phyla (e.g. bacteria, fungi, oomycetes, and viruses) and have to defend themselves to survive infection by these pathogens. Plants, being immobile, cannot actively escape from these often more mobile and more numerous pathogens. However, disease in natural populations is the exception, such that most of the individuals are usually healthy (Allen, Bittner-Eddy et al. 2004, Partida-Martinez and Heil 2011). For protection, plant cells have developed a diverse system of defense mechanisms. Unlike vertebrates, plants lack the circulatory system with specialized defense cells or an adaptive immune machinery to fight pathogen invasion (Dangl and Jones 2001). Instead, plant cells rely on an array of predetermined or induced structural, chemical and protein-based defenses that culminate in a highly effective immune response against most potential pathogens.

1.1 Plant pathogens

In pursuance of understanding how plants protect themselves we must first know the pathogens that assail them. There are three broad groups of plant pathogens based on their different substrate requirements, biotrophs, necrotrophs and hemibiotrophs (Laluk and Mengiste 2010). **Biotrophs** are pathogens that penetrate or establish close contacts with the host for growth and reproduction in their life cycle. These types of pathogens are obligate parasites that obtain nutrients from living cells (Glazebrook 2005). Their continued development on the host relies on deception, such that the host's defense response is evaded. This fragile relationship between the biotroph and the plant host is biochemically and structurally complex to a degree that biotrophs have established specialized structures to obtain the sugars, amino acid and other nutrients that they need. There are several biotrophs that depend upon highly specialized feeding structures that penetrate the host cell wall, colonizing the intercellular space without disrupting the plasma membrane, called haustoria (Schulze-Lefert and Panstruga 2003, Garnica,

Nemri et al. 2014). An example of a biotrophic pathogen that employs haustoria is the barley powdery mildew fungus *Blumeria graminis*. Alternatively, there are biotrophic pathogens that do not form haustoria but remain in the apoplast such as the tomato pathogen *Cladosporium fulvum* (Vleeshouwers and Oliver 2014). Furthermore, there are biotrophic vesicular-arbuscular mycorrhizal fungi that form mutualistic relationships with the roots of their plant hosts, in which the fungus obtains sugars from the plant and provides phosphates and other minerals in return (Szabo and Bushnell 2001). **Necrotrophs**, as the name implies, employ a mode of infection by which death of the host plant cells precedes or follows colonization by the pathogen. Phytotoxic compounds, cell wall-degrading enzymes and other extracellular enzymes are released into the host tissue prior and during colonization to destroy plant cell walls and release nutrients (Alfano and Collmer 1996, Mengiste 2012). Examples of necrotrophic pathogens include the bacterial soft-rot *Erwinia carotovora* and the mold fungus *Botrytis cinerea*. A third group of pathogens, **hemibiotrophs**, first establishes a biotrophic interaction with the host and then switches to a necrotrophic lifestyle (Vargas, Martin et al. 2012). The duration of the biotrophic versus the necrotrophic phase varies significantly among hemibiotrophs (Mengiste 2012). During the early stages of infection, hemibiotrophs actively suppress the host's immune responses. In the later stages of infection, hemibiotrophs undergo a physiological transition from an asymptomatic growth to a destructive necrotrophic stage (Lee and Rose 2010). The oomycete that caused the potato famine in the 19th century, *Phytophthora infestans*, is one well-known example of a hemibiotroph. Another representative hemibiotroph is the bacterium *Pseudomonas syringae.* The divergent strategies of these pathogens further underpin the necessity for multiplicity and adaptability of plant immune responses.

1.2 Plant defense mechanisms

Depending on its lifestyle, an invading pathogen must grapple with a variety of detection mechanisms and physical or metabolic defenses deployed by the plant host (Spoel, Johnson et al. 2007, Bari and Jones 2009). Defense responses involve inducible networks of complex, tightly regulated molecular

pathways. These pathways often overlap and influence each other. At the same time, these pathways are integrated into the plant's developmental and life cycle strategy (Katagiri, Thilmony et al. 2002, de Wit 2007, Rodriguez, Petersen et al. 2010). After pathogen assault, defense ultimately culminates in characteristic downstream response such as reinforcement of the cell wall, reactive oxygen species (ROS) production, activation of defense genes and synthesis of secondary metabolites and defense hormones, and a form of programmed cell death called hypersensitive response (HR) (Pontier, Balague et al. 1998, Lam, Kato et al. 2001, Greenberg and Yao 2004, War, Paulraj et al. 2012, Ponce de Leon and Montesano 2013).

Precedent to these triggered immune responses are physical adaptations at common entry points that limit the access of pathogens and deter herbivore or insect feeding (Thaler 2002). Plants are equipped with (constitutively) produced plant defense chemicals. The multitude of these chemicals produced by plants during defense has often been called "secondary plant metabolites" owing to the fact that they are products of specialized biosynthetic pathways (Ryan and Jagendorf 1995). The plant inducible defense system has been rationalized to be predominantly via two main pathways that build upon recognition of compounds not typically produced by the plant's own tissues. The first, which relies on receptors at the cell membrane, is known as pathogen/microbe associated molecular pattern (P/MAMP) triggered immunity (PTI/MTI). The second and more specialized induced response is based on recognition of specific, often race-specific pathogenic ligands usually delivered into the plant; it is termed effector-triggered immunity (ETI) (Dangl and Jones 2001). Plant hormones as part of PTI and ETI play a substantial role in defense responses and have been shown to be involved in fine-tuning of defense and growth (Spoel and Dong 2008, Verhage, van Wees et al. 2010, Lozano-Duran, Macho et al. 2013)

The major mechanisms will be summarized in the subsequent sections separately.

1.2.1 Physical and preformed defenses

Plant organs are equipped with structural barriers that can be considered constitutive (continuous) defenses, which aid in limiting pathogen attachment, invasion and infection. Predominantly comprised of mechanical barriers embedded in plant morphology, these physical structures at the plant surface include thickened cell walls, waxy epidermal cuticles, spines, thorns (spinescence), trichomes (pubescence), toughened or hardened leaves (sclerophylly) and barks (Taiz and Zeiger 2010). Specifically these defensive preformed barriers are based on a lignin and cellulose-rich cell wall, thick waxy acyl lipid cuticle on the epidermal cells, and stomatal morphology and physiology that lessen pathogen connection with viable host cells. Highlighting these physical defenses, we focus on the cell wall as an important line of defense against bacterial and fungal invaders. Not just a structural impediment, the cell wall is equipped with chemical compounds that can be rapidly activated when a cell detects the presence of pathogens (Malinovsky, Fangel et al. 2014). Proteins and enzymes such as pectin methylesterases can reshape the cell wall during growth and strengthen the cell wall as a defense response. Recognition of invading pathogens, discussed further below, leads to activation of enzymes that result in bursts of superoxide (O_2^-) or hydrogen peroxide (H_2O_2), collectively known as reactive oxygen species (ROS) (Hammond-Kosack and Jones 1996). This ROS burst can damage the cells of invading organisms, but they also protect the plant from invasion by giving the plant strength and rigidity, strengthening the cell wall by catalyzing cross-linkages between cell wall polymers (Asselbergh, Curvers et al. 2007). Furthermore, ROS serves as a signal to neighboring cells that an attack is underway. Specific to a microbial attack, callose between the cell wall and cell membrane adjacent to the invading pathogen is rapidly synthesized and deposited (Luna, Pastor et al. 2011). Plant induced defense responses have been shown to include cell polarization, focal redistribution of the actin cytoskeleton, guided migration of organelles, targeted secretion, and callose deposition at the site of pathogen contact (Kwon, Neu et al. 2008). These callose deposits, called papillae, are polysaccharide polymers consisting of

(1-3)-β-D-glucan subunits that impede penetration at the site of infection. (Bestwick, Bennett et al. 1995, Maor and Shirasu 2005)

Proteinase inhibitors, proteolytic enzymes, phytoanticipins and plant defensins are natural chemical barriers generated by plants as part of their constitutive defenses (Morrissey and Osbourn 1999). These compounds are produced as part of normal growth and development. They are frequently kept in specialized organs or tissues such as trichomes, oil glands, or epidermal cell layers (Bednarek and Osbourn 2009). There is evidence seen in crucifers, that glucosinolates and thioglucosides, which are normally synthesized in healthy cells, may be mobilized to the pathogen challenged site (Bednarek and Osbourn 2009, Clay, Adio et al. 2009). Unsurprisingly, polar vesicle trafficking of natural products, proteins and other cargo is an important component of disease resistance (Robatzek 2007, Leborgne-Castel and Bouhidel 2014).

1.2.2 PAMP-triggered immunity

PTI begins with detection of pathogens at the plant cell surface. At the cell membrane are pattern recognition receptors (PRRs). These receptors contain extracellular domains that detect PAMPs, also called elicitors, which are conserved motifs/ligands found in pathogens that trigger defense signaling downstream (Boller and Felix 2009, Hamdoun, Liu et al. 2013). Another indicator of pathogen presence similar to PAMPs may also arise from the plant itself because of subsequent damage from pathogens. These endogenous elicitors are described as damage-associated molecular patterns (DAMPs) (Boller and Felix 2009). Most known PRRs in plants are leucine-rich repeat receptor like kinases (LRR-RLKs) with extracellular leucine rich repeats (LRR) and an intracellular kinase domain. Upon recognition of their corresponding ligand, the intracellular kinase domain initiates activation of proximal interactors and trigger a signaling cascade. FLAGELLIN SENSING 2 (FLS2), the first identified receptor for a general elicitor in *A. thaliana* (Chinchilla, Bauer et al. 2006), is an analog of human TOLL LIKE RECEPTOR (TLR)5, which also recognizes flagellin, a principal component of bacterial flagella (Hayashi, Smith et al. 2001). FLS2 homologues have been

found in all higher plants for which genome information is available (Boller and Felix 2009), and at least the rice homologue has been shown to also function as a flagellin receptor (Takai, Isogai et al. 2008). Perception by FLS2 is through recognition of a highly conserved N-terminal epitope of flagellin, flg22. Upon flg22 binding, FLS2 heterodimerizes with another PRR, BRASSINOSTEROID INSENSITIVE 1-ASSOCIATED KINASE 1 (BAK1), activating downstream factors and plant immunity. Since the identification of FLS2, other PAMPs and their receptors have been found. ELONGATION FACTOR THERMO UNSTABLE (EF-TU), a protein responsible for delivering aminoacyl-tRNA to the ribosome during bacterial translation is another bacterial PAMP, which is recognized by the EF-TU RECEPTOR (EFR) LRK in *A. thaliana* (Zipfel, Kunze et al. 2006). Another protein, LYSIN MOTIF RECEPTOR KINASE (LYK) or CHITIN ELICITOR RECEPTOR KINASE (CERK1), is the major receptor for the fungal PAMP chitin in *O. sativa* and *A. thaliana* (Kaku, Nishizawa et al. 2006, Miya, Albert et al. 2007, Cao, Liang et al. 2014). Unlike FLS2 and EFR, instead of an LRR domain, CERK1 contain two extracellular LysM motifs (Miya, Albert et al. 2007). Chitin is a fungal β-1,4 linked N-acetyl-glucosamine oligomer (GlcNAc) found as a building block in fungal cell walls. A list of currently known Arabidopsis, rice and tomato PRRs and their corresponding ligands are shown in Table 1.1.

Challenge with flg22 and EF-Tu leads to up-regulation of similar sets of genes, suggesting that recognition of different PAMPs triggers a similar set of defense responses within the host cell (Zipfel, Kunze et al. 2006) Common processes initiated during PTI response are activation of MAP kinase cascades and oxidative burst (Nitta, Ding et al. 2014), followed by callose deposition (Luna, Pastor et al. 2011) and the release of ROS and flux of Ca^{2+} molecules (Bolwell 1995, Stael, Kmiecik et al. 2015).

Table 1.1 *A. thaliana*, tomato and rice PRRs

PRR	Subfamily*	Ligand†	Species	References
FLS2	LRR RLK	flg22	*A. thaliana*	(Gomez-Gomez and Boller 2000) (Chinchilla, Bauer et al. 2006)
EFR	LRR RLK	elf18	*A. thaliana*	(Kunze, Zipfel et al. 2004) (Zipfel, Kunze et al. 2006)
PEPR1/2	LRR RLK	PEPs	*A. thaliana*	(Yamaguchi, Pearce et al. 2006)
bCERK1 (OsCERK1)	LysM RLK	chitin	*A. thaliana* Rice	(Miya, Albert et al. 2007) (Petutschnig, Jones et al. 2010) (Shimizu, Nakano et al. 2010)
CEBiP	LysM RLP	chitin	Rice	(Kaku, Nishizawa et al. 2006)
LYM1/LYM3	LysM RLP	PGNs	*A. thaliana*	(Willmann, Lajunen et al. 2011)
LYP4/6	LysM RLP	PGNs/chitin	Rice	(Liu, Li et al. 2012)
LeEix2	LRR RLP	Eix	Tomato	(Ron and Avni 2004)
ReMax	LRR RLP	eMax	*A. thaliana*	(Jehle, Lipschis et al. 2013)
Ve1	LRR RLP	Ave1	Tomato	(de Jonge, van Esse et al. 2012)
WAK1	WAK[4]	OGs	*A. thaliana*	(Brutus, Sicilia et al. 2010)

*LRR RLK – Leucine-rice repeat receptor-like protein kinase; LysM RLK – Lysin motif receptor-like kinase; LysM RLP – Lysin motif receptor-like protein; WAK – cell wall-associated kinase
† flg22 – 22 amino acid flagellin peptide; elf18 - 18 amino acid elongation factor Tu peptide; PEP – 23 amino acid peptide that enhances resistance to root pathogen, *Phythium irregulare*; PGN – peptidoglycan; Eix – ethylene-inducing xylanase; eMax - Enigmatic MAMP of Xanthomonas; Ave1 – avirulence on Ve1; OGs - Oligogalacturonides

1.2.3 Effector-triggered immunity

The effectiveness of PAMP signaling in controlling pathogens is reflected by the many ways that pathogens try to overcome PTI by injecting a repertoire of effectors into the host cell to inhibit PTI (Dangl and Jones 2001). Effectors are defined as pathogen-produced molecules that have a specific effect on one or more genotypes of a host (Vleeshouwers and Oliver 2014). These effectors (virulence factors) are typically injected by bacteria, fungi, oomycetes or even nematodes into the host through specialized secretion systems (Cambronne and Roy 2006) and Roy, 2006; Ellis et al., 2009). About several hundred oomycete effectors (Tyler, Tripathy et al. 2006) and more than 30 bacterial effectors have been identified (Lindeberg, Cartinhour et al. 2006). Many more are yet to be discovered given the fluidity of pathogen genomes, i.e. rust (McDowell 2011) and complexity of pathogen genomes, i.e. *Phytophthora infestans* (Haas, Kamoun et al. 2009).

There are at least three major strategies for effectors to subvert host defenses: 1) alter turnover of proteins, 2) alter RNA metabolism or 3) inhibit signaling during immune response, employed by these effectors to shift host responses (Block, Li et al. 2008). Plant counter measures against these effectors rely on the products of resistance (R) genes that recognize the effectors either directly, or indirectly through host targets modified by effectors. Upon recognition, activate R proteins trigger ETI (Van der Biezen and Jones 1998, Dangl and Jones 2001). Successful pathogen colonization of plant tissue is described as a compatible interaction with a virulent pathogen. Alternately, a condition when the plant is able to perceive and stimulate a defense reaction indicates that the pathogen is avirulent, and this is referred to as an incompatible interaction (Katagiri, Thilmony et al. 2002). A compatible plant-pathogen interaction conforms to the Mendelian “gene-for-gene” model, a precept of which is that resistance only occurs when an R gene is able to recognize the corresponding effector encoded by a pathogen avirulence gene (Flor 1955, Ma, Dong et al. 2006). A number of diverse Avr/R gene pairs have been identified (Table 1.2). Most R genes encode proteins with a nucleotide-binding domain and leucine-rich repeat domain known as NB-LRRs/NLRs. The *A. thaliana* reference genome encodes about 150 (Meyers, Kozik et al. 2003, Guo, Fitz et al. 2011) NB-LRR proteins. Most R proteins act via indirect recognition of effectors, as guards of important host proteins that are recurrently targeted by diverse effectors (Van der Biezen and Jones 1998).

Several downstream events are shared between ETI and PTI, including protein phosphorylation, calcium fluxes, ROS, phytohormones, induction of defense related genes and synthesis of antimicrobial compounds (Grennan 2006, Thomma, Nurnberger et al. 2011). ETI-PTI crosstalk is further evidenced by how pathogens deliver effectors target and induce a complex interplay of transcriptional networks to modify and suppress PTI (basal) responses during pathogenesis (Hauck, Thilmony et al. 2003, Li, Lin et al. 2005, de Torres, Mansfield et al. 2006, Truman, de Zabala et al. 2006). Compared to PTI, ETI has been posited to evoke a more prolonged and robust immune response (Hamdoun, Liu et al. 2013). ETI is also more often associated with localized cell death called hypersensitive response (HR) that inhibits pathogen growth (Katagiri and

Table 1.2. Avr/R gene pairs

Effector	Pathogen species	Resistance (R) gene	Plant host	Reference
Avr1	*Phytophthora infestans*	R1	Potato	(Houterman, Cornelissen et al. 2008, Vleeshouwers, Raffaele et al. 2011)
Avr2	*Phytophthora infestans*	R2	Potato	(Vleeshouwers, Raffaele et al. 2011, Saunders, Breen et al. 2012)
Avr3a	*Phytophthora infestans*	R3a	Potato	(Bos, Armstrong et al. 2010)
Avr3b	*Phytophthora infestans*	R3b	Potato	(Rietman, Bijsterbosch et al. 2012)
Avr4	*Phytophthora infestans*	R4	Potato	(Rietman, Bijsterbosch et al. 2012)
Avrblb1	*Phytophthora infestans*	Rpi-blb1	Potato	(Vleeshouwers, Raffaele et al. 2011)
Avrblb2	*Phytophthora infestans*	Rpi-blb2	Potato	(Vleeshouwers, Raffaele et al. 2011)
Avrvnt1	*Phytophthora infestans*	Rpi-vnt1	Potato	(Vleeshouwers, Raffaele et al. 2011)
AvrSmira1	*Phytophthora infestans*	Rpi-Smira1	Potato	(Rietman, Bijsterbosch et al. 2012)
AvrSmira2	*Phytophthora infestans*	Rpi-Smira1	Potato	(Rietman, Bijsterbosch et al. 2012)
AvrB	*P. syringae pv. glycinea race 0*	RPM1 (RIN4/RIPK/RAR1//MPK4)	Tomato	(Russell, Ashfield et al. 2015)
AvrBs3	*X. campestris pv. vesicatoria race 1*	Bs3	Tomato and peppers	(Romer, Hahn et al. 2007, Boch and Bonas 2010)
AvrPphB	*P. syringae pv. phaseolicola race 3*	RPS5 (PBS1/BIK1/PBL1)	Bean	(Qi, Dubiella et al. 2014)
AvrPto	*P. syringae pv. tomato JL1065*	Pto and Prf (FLS2/EFR/BAK1/RIN4)	Tomato	(Xing, Zou et al. 2007, Zong, Xiang et al. 2008)
AvrPtoB	*P. syringae pv. tomato DC3000*	Pto and Prf (Fen/FLS2/BAK1/CERK1/RIN4)	Tomato	(Xiang, Zong et al. 2008)
AvrRpm1	*P. syringae pv. glycinea race 0*	RPM1 and RPS2 (RIN4)	Tomato	(Kim, Geng et al. 2009)
AvrRps4	*P. syringae pv. pisi 151*	RPS4 (EDS1)	Tomato	(Sohn, Zhang et al. 2009)
AvrRpt2	*P. syringae pv. tomato T1*	RPS2 (RIN4)	Tomato	(Day, Dahlbeck et al. 2005)
HopA1	*P. syringae pv. syringae 61*	RPS6 (EDS1)	Tomato	(Kim, Kwon et al. 2009)
HopI1	*P. syringae pv. maculicula ES4326*	Hsp70	Tomato	(Jelenska, van Hal et al. 2010)
HopF2	*P. syringae pv. tomato DC3000*	RIN4/MKK5, BAK1	Tomato	(Zhou, Wu et al. 2014)
HopM1	*P. syringae pv. tomato DC3000*	AtMIN7	Tomato	(Lozano-Duran, Macho et al. 2013)
HopN1	*P. syringae pv. tomato DC3000*	PsbQ	Tomato	(Rodriguez-Herva, Gonzalez-Melendi et al. 2012)
HopU1	*P. syringae pv. tomato DC3000*	GRP7/GRP8	Tomato	(Fu, Guo et al. 2007)
PopP2	*R. solanacearum GMI1000*	RRS1 (RD19)	Solanum	(Deslandes, Olivier et al. 2003)
XopD	*X. campestris*	AtMYB30	Brassica	(Canonne, Marino et al. 2011)

(Katagiri and Tsuda 2010). The two responses could mainly be distinguished by their timing and location in the host, with the early extracellular response due to PTI and the later intracellular responses chiefly coming from ETI (Abramovitch, Anderson et al. 2006).

1.2.4 Hormonal signaling and pathogen defense

Plant defense response is additionally modulated by phytohormones that work in a composite network that also regulates growth, development, reproduction and general response to environmental cues (Pieterse, Leon-Reyes et al. 2009). Specifically phytohormones such as SA, jasmonic acid (JA), ethylene (ET), gibberellins (GA), brassinosteroids (BR), auxins, abscisic acid (ABA), and even cytokinins (CK) act as signaling molecules during an induced immune response (Robert-Seilaniantz, Navarro et al. 2007, Bari and Jones 2009). Subsequent to a pathogen attack, the quantity, composition and the timing of the phytohormonal blend produced by the plant varies among species and depends greatly on the lifestyle and infection strategy of the invading attacker (Pieterse, Leon-Reyes et al. 2009). For example, SA-dependent defenses are effective primarily against biotrophic pathogens, while ET/JA dependent defenses confer resistance primarily to necrotrophic fungi (Bari and Jones 2009). Medleys of particular defense-related genes are triggered by 'signal signatures', which are induced by particular pathogens (De Vos, Van Oosten et al. 2005). Crosstalk between hormonal signaling pathways provides the plant with a powerful regulatory potential and allows the plant to tailor its defense response to the invaders encountered (Verhage, van Wees et al. 2010, Robert-Seilaniantz, Grant et al. 2011). Not to be left behind, some pathogens also manipulate hormone-regulated signaling pathways to evade host immune responses (Pieterse, Leon-Reyes et al. 2009). A well-studied example is the bacterium *Pseudomonas syringae* (Nomura, Melotto et al. 2005).

As a regulator of plant resistance to biotrophic and hemibiotrophic pathogens, such as *Hyaloperonospora arabidopsidis* and *P. syringae* (Robert-Seilaniantz, Navarro et al. 2007), SA is one of the most studied phytohormones (Vlot, Dempsey et al. 2009). Although affecting many plant

processes including growth and development, SA is primarily recognized for its role in local defense response and in the establishment of systemic acquired resistance (SAR) (Loake and Grant 2007, Rivas-San Vicente and Plasencia 2011). SA accumulation occurs upon either PTI or ETI activation (Dempsey, Vlot et al. 2011). Increased endogenous amounts of SA and its conjugates during pathogen infection concur with activation of disease resistance inclusive of elevated expression of defense genes (Shah 2003). This phenomenon is further reinforced by the fact that exogenous application of SA or synthetic functional analogs, such as 2,6,-dichloroisonicotinic (INA) or benzo(1,2,3) thiadiazole-7-carbothioic acid S-methyl ester (BTH), produces the same result (Gorlach, Volrath et al. 1996, Dong 2001). Along with this, blocking SA synthesis or preventing SA accumulation hinders activation of several defense responses (Gaffney, Friedrich et al. 1993, Delaney 1994, Wildermuth, Dewdney et al. 2001).

1.3 Fine-tuning and evolution of plant defense responses

Summarizing the aforementioned plant defense mechanisms, there are several key certitudes that hold during plant-microbe interactions. First, pathogens are detected through PAMPs, DAMPs and effectors by host cell receptors. During plant-microbe interaction, a number of these receptor-ligand interactions may be taking place simultaneously. The plant-microbe detection-evasion interrelation has pushed plants and pathogens into an evolutionary arms race (Ingle, Carstens et al. 2006, Jones and Dangl 2006, Burdon and Thrall 2009). The outcome is that plants have evolved multiple defense mechanisms with diverse arrays of receptors and disease resistance genes (Michelmore and Meyers 1998, Nagy and Bennetzen 2008, Horger, Ilyas et al. 2012, Huard-Chauveau, Perchepied et al. 2013, Yang, Li et al. 2013, Karasov, Kniskern et al. 2014). At the same time pathogens are evolving to a) avoid detection by loss, sequence diversification, or post-translational modification of the pathogen molecules detected by the host, or b) through direct corruption of host immunity with new effectors (Ma, Dong et al. 2006, Baltrus, Nishimura et al. 2011, Lovell, Jackson et al. 2011, Cook, Mesarich et al. 2015). And most importantly, the aforementioned immune responses must

require fine-tuning and coordination such that proper allocation and use of metabolites in plant resistance should not be at the expense of other physiological processes like growth and reproduction (Rasmann, Chassin et al. 2015). This section will be on the arguments for the forces governing plant-pathogen co-evolution with more focus on how plants cope with the dilemma of effectively sustaining simultaneous growth and defense.

Co-evolution is an evolutionary process that brings about reciprocal genetic change in interacting species owing to natural selection imposed by each one on the other (Turcotte, Corrin et al. 2012). It can occur between any interacting populations, but it is specifically appropriate for host-pathogen systems because of the close nature of the interaction and the selective pressure that each can exert on each other (Woolhouse, Webster et al. 2002). Two models have been put forward to describe the co-evolutionary process affecting plant-microbe interactions, “Red Queen hypothesis (RQH)” and “arms race”. The RQH describes cyclic dynamics of allele frequencies while the arms race portrays fixation of advantageous mutations (selective sweeps) (Raberg, Alacid et al. 2014). Arms race accounts for rapid evolution of the genes involved in plant-pathogen interactions albeit at generally low levels of standing genetic variation. The arms race hypothesis further postulates that at the center of the plant-pathogen interaction are the R-avr gene interactions. This is the interface that has been pinpointed to drive the plant-pathogen co-evolutionary system, comprising the characters that determine the outcome of confrontation between the host and the pathogen. Once an adaptation by one player (i.e. R-gene) has been attained, this adaptation leads to selection on and an evolutionary response in the second player (i.e. effector) (Bittner-Eddy and Beynon 2001, Allen, Bittner-Eddy et al. 2004, Lewis, Wu et al. 2010). In an arms race, the antagonist is propelled in a certain direction. On the contrary, Red Queen dynamics result in balanced polymorphisms with deep coalescence times. The name comes from what the Red Queen in Lewis Carroll’s “Through the Looking Glass” says to Alice, “Now, here, you see, it takes all the running you can do, to keep in the same place”. To explain this, let us look at a population of host plants and obligate host-specific pathogens. In this situation, obligate pathogens are pressured to constantly infect hosts of the same species. The hypothesis assumes that the pathogen after some

time becomes specialized on the most common host genotypes in the population. Rare genotypes then gain a fitness advantage that declines as they become more common. An oscillation between susceptible common genotypes and differentially virulent pathogens ensues governed by frequency-dependent selection (Clay and Kover 1996).

Having to face the dilemma of partitioning limited resources among growth, reproduction and defense also motivates the mechanism and evolution of plant defenses. There are several conjectures formulated that attempt to explain the dynamics of plant defense in relation to the partitioning dilemma, including: 1) Optimal Defense Theory (ODT), 2) Growth Rate Hypothesis (GRH), 3) Carbon:Nutrient Balance Hypothesis (CNBH) and 4) Growth-Differentiation Balance Hypothesis (GDBH). The ODT puts forward a framework for investigation of genotypic expression of plant defense, with emphasis on allocation cost of defense based on fitness value of different tissues and probability of attack (Barto and Cipollini 2005, Alba, Bowers et al. 2012, Meldau, Erb et al. 2012). The GRH relates the evolution of plant defense to resource availability and predicts that plants that have evolved in abiotically stressful environments grow more slowly although more constitutively resistant than plants in more productive habitats (Van Zandt 2007, Endara and Coley 2011). The CNB hypothesis, also called the Environmental Constraint Hypothesis, is a model structured to explain phenotypic expression of defense by plants based on the supply of carbon and nutrients in the environment (Hamilton, Zangerl et al. 2001, Massad, Dyer et al. 2012). The GDB hypothesis states that there is a physiological trade-off between growth and secondary metabolism; balance must be maintained between resources used for growth and differentiation which includes chemical defense production (Barto and Cipollini 2005, Glynn, 2007 #1509). Despite using different frameworks, these hypothesis are built on similar central assumptions: 1) defenses can incur cost to physiology and metabolism; 2) efficiency of defense response depends on certain selective pressures (i.e. competition, environmental condition, resource availability, genetic potential) (Coley, Bryant et al. 1985, Strauss, Rudgers et al. 2002, Siemens, Lischke et al. 2003, Fine, Miller et al. 2006, Boots 2011, Kempel, Schadler et al. 2011). Which of these theories describes the actual situation in

nature is still unclear. Studies such as the one from Barto and Cipollini (Barto and Cipollini 2005), testing ODT and the GDBH in *Arabidopsis thaliana*, show that expected patterns of responses followed neither ODT not GBDH consistently, while others, such as meta-analyses carried out by Endara and Coley (Endara and Coley 2011), claim that GRH has substantial explanatory power. These hypotheses have contributed to our current understanding of plant defense responses but each has its limitations.

1.4 Plant autoimmunity, natural variation and *ACD6*

Genetics has been used in two ways to further our understanding of immunity: first by identifying mutants in which responses to pathogens are compromised, such as knockouts of PPR and R genes as well as positive downstream signaling factors. An alternative approach is to look for mutants that mount an immune response in the absence of pathogens. A number of gain-of-function (GOF)/loss-of-function (LOF) mutants, collectively known as lesion-mimic mutants, have been linked to immunity and repeatedly described as positive/negative regulators of cell death (Bruggeman, Raynaud et al. 2015). Those mutants point to de-repression or activation of genes involved in immunity, especially some R-genes (generally *NLRs*) (Table 1.3).

Some of the genes identified through lesion-mimic mutants are themselves suppressed by LOF of important components for defense response (e.g. *ENHANCED DISEASE SUSCEPTIBILITY 1* (*EDS1*) and *PHYTOAELXIN DEFICIENT 4* (*PAD4*)) or by suppression or removal of SA accumulation (Bruggeman, Raynaud et al. 2015). An example of such lesion-mimic mutant is the dominant GOF mutant in Col-0 -- *ACCELERATED CELL DEATH 6* (*ACD6*) *acd6-1*. *acd6-1* shows spontaneous cell death, small stature and constitutively elevated defenses (Rate, Cuenca et al. 1999). *ACD6* is described as a positive regulator of cell death and defenses in *Arabidopsis thaliana* acting in part via the major SA transducer *NONEXPRESSER OF PR GENES* 1 (*NPR1*) (Rate, Cuenca et al. 1999). Operating in a positive feedback loop with SA, ACD6 localizes at the plasma membrane and the endoplasmic reticulum (Zhang, Shrestha et al. 2014).

Table 1.3 *A. thaliana* lesion mimic mutants

Mutant	Lesion phenotype	Resistance	Hypersensitive response*	Putative function	References
acd5	Disease-like lesions	Decreased	Normal	Lipid kinase	(Greenberg 2000)
acd6	HR-like lesions	Increased	Reduced	ND	(Rate, Cuenca et al. 1999)
agd2	Few necrotic lesions	Increased	Reduced	ND	(Rate and Greenberg 2001)
cpn1	Necrotic lesions	Increased r	Accelerated	Copine protein	(Jambunathan, Siani et al. 2001)
cpr5	Chlorotic lesions	Increased	Normal	Type IIIa transmembrane protein	(Bowling, Guo et al. 1994, Stokes, Kunkel et al. 2002, Boch and Bonas 2010)
dnd1	Rare necrotic lesions	Increased r	Reduced	AtCNGC2, cyclic nucleotide gated channel	(Yu, Parker et al. 1998, Clough, Fengler et al. 2000)
Y23	Disease-like lesions	Similar / Increased	Reduced	ND	(Yu, Parker et al. 1998)
hlm1	Necrotic lesions and chlorosis on leaves	Increased	Reduced	AtCNGC4, cyclic nucleotide gated channel	(Balague, Lin et al. 2003)
hrl1	HR-like lesions	Increased	Reduced	ND	(Devadas, Enyedi et al. 2002, Devadas and Raina 2002)
lsd2-lsd5	*lsd2*, *lsd4*: chlorotic lesions *lsd3*, *lsd5*: necrotic lesions	Increased	ND	ND	(Dietrich, Delaney et al. 1994)
lsd6-lsd7	Necrotic lesions	Increased	ND	ND	(Weymann, Hunt et al. 1995)
ssi1	HR-like lesions	Increased	ND	ND	(Greenberg 2000, Shah, Kachroo et al. 2001, Shah 2003)
ssi2	HR-like lesions	Increased	ND	Stearoyl-ACP desaturase	(Kachroo, Schopfer et al. 2001, Shah 2003)
ssi4	Chlorotic lesions	Increased	ND	TIR-NB-LRR protein	(Shirano, Kachroo et al. 2002)

*ND, not determined

Together with SA, ACD6 is part of a positive feedback loop that regulates the levels of several PAMP receptors including FLS2, EFR and CERK1 (Tateda, Zhang et al. 2015). Notably, a study capitalizing on natural variation identified a hyperactive allele of *ACD6*, *ACD6*-Est-1, which changes the balance between growth and defense in *A. thaliana* accessions (Todesco, Balasubramanian et al. 2010). While *NLR*s confer race-specific resistance, the hyperactive *ACD6* allele protects against a wide range of unrelated pathogens, including insects. This unusually large benefit of hyperactive *ACD6* allele equivalent to a constitutively active defense response, accordingly incurs a substantial handicap to the growth of the plant.

Natural *ACD6* variants offer an opportunity to study different plant survival and adaptation strategies, ranging from being small but well protected to being larger but less prepared to combat pathogens. Natural variation, broadly defined as the phenotypic variation caused by genetic variation brought about by mutations maintained in nature by any evolutionary process like genetic drift, artificial and natural selection (Alonso-Blanco, Aarts et al. 2009), is one of the most important basic resources for biology. This resource has been relevant to discover which specific allelic variants are present in nature, where they might either be neutral or have a selective advantage under specific conditions (Shindo, Bernasconi et al. 2007). Natural variation has been utilized for finding new genes involved in specific aspects of plant physiology or development (Koornneef, Alonso-Blanco et al. 2004, Weigel and Nordborg 2005). Natural variation in disease resistance is among the earliest examples of a Mendelian trait to be genetically described in plants (Holub 2001). As early as 1905, Biffen described a single locus responsible for the resistance of some wheat cultivars to yellow rust caused by *Puccinia striiformis*. Since then many more genes have been identified to confer resistance to an assortment of pathogens known to infect various plant species, as previously enumerated in Table 1.2.

1.5 Aims and objectives of this thesis

Much research has been focused on *NLR* conferred disease resistance (Martin, Bogdanove et al. 2003 2007). On the other hand, little is known about

variation in the more generalist PAMP perception system, whose components are often shared across distant genera (Boller and Felix 2009, Vetter, Kronholm et al. 2012). While many studies focus on merely pairwise plant-pathogen interactions, it is becoming progressively clear that a more comprehensive method to understand plant defense response is needed. One way is through inspecting specific plant defense mechanisms in their natural environment. At the same time, additional effort for understanding trade-offs during plant defense responses may uncover links for better understanding and production of pathogen resistant and durable crops with minimal physiological costs. *ACD6* offers an ecologically relevant genetically traceable system in which these can be addressed. Unlike the use of lesion mimic mutants, which are generated artificially, the natural allelic variation present in *ACD6* provides the system where differential responses are a product of natural selection due to the environment and pathogens present in the location where the accessions are originally from. Therefore, in the context of natural variation of the growth and defense trade-off phenotype imparted by having a hyperactive *ACD6* allele, I attempted to:

1) Determine the extent of *ACD6* natural variation in *A. thaliana* accessions and geographical distribution of the hyperactive *ACD6* allele type to deduce the evolutionary context of this variation;
2) Phenotypic and molecular characterization of *A. thaliana* accessions to dissect pathogen resistance pathways given the *ACD6* imparted autoimmune phenotypes;
3) Identify novel components of the *ACD6* defense response pathway through genetic analysis of *A. thaliana* accessions having variable *ACD6* activity.

2 Materials and Methods

General laboratory buffers, media and protocols were made and performed as instructed in (Sambrook and Russell 2001). Chemicals were mainly obtained from Sigma-Aldrich (Taufkirchen, Germany), Roth (Karlsruhe, Germany), and VWR/Merck (Darmstadt, Germany) unless otherwise stated. Buffers were prepared using double distilled water (ddH_2O), except when other solvents were required.

2.1 Plant material, growth conditions and phenotyping

Seeds for *A. thaliana* accessions were obtained from the European Arabidopsis Stock Centre (The European Arabidopsis Stock Center) and the Arabidopsis Biological Resource Center . Information for accessions used are given in Appendix Table 1. Prior to stratification, seeds were sterilized by washing with 70% ethanol for 5 minutes followed by washing with 100% ethanol for 10 minutes. After decanting the last ethanol wash, seeds were air-dried in a sterile hood until all the residual ethanol has evaporated. Seeds were stratified by immersion in 0.1% w/v Agar-agar for 4–7 days in the dark at 4°C prior to planting. Plants were grown in either short-day (8 h light) or long-day (16 h light) conditions under about 50 µmol m^{-2} s^{-1} light fluence rate in controlled 23°C temperature growth chambers, with 65% relative humidity. Plants meant for experiments testing temperature effects were concurrently grown in growth chambers with the same conditions but with 16°C temperature. For some experiments such as transgenic marker selection, seeds were stratified and sown in half-strength Murashige and Skoog (MS) medium prior to sowing in soil; 1 L of half-strength MS medium is made with:

- 2.15g, 1X MS salts (Duchefa, Haarlem, Netherlands),
- 0.5g MES (Duchefa, Haarlem, Netherlands),
- 0.8% w/v Agar-agar (Merck, Darmstadt, Germany)
- pH 5.8 with 1N KCl (Roth, Karlsruhe, Germany)

For most experiments, plants were sown in a completely randomized design with at least 4 replicates per genotype. An exception was the experimental design for the populations used for QTL mapping that did not allow for this since individual F_2 plants cannot be replicated. In order to minimize variation, plants were watered with the same amount of water and the flats were rotated every two days.

2.2 Quantification of salicylate and SA-conjugates

Salicylate and SA-conjugates was extracted from 4-week old rosettes, 8 biological replicates per genotype, grown in a randomized complete block design at 23°C short day conditions. The freeze-dried, ground plant material (Target: 10 mg ± 1 mg) was extracted twice with 400 µl methanol 20% (LCMS-grade) / 0.1% HFA (5 min ultrasonic extraction; 20 min on ice; centrifuge 10 min 13500 g). From the supernatant 320 µl were removed after each extraction step and combined in a new vial. A third extraction step with 400 µl methanol 100% (conditions as above) was performed yielding an additional volume of 420 µl. The end volume of 1060 µl was split in half before drying overnight in the speed vacuum. For the analysis of the conjugated and free SA, the pellets were resolved in 30 µl methanol 50% / 0,1% HFA (mixed 10 min; 1400 rpm; centrifuge 10 min 13500 g). Ultra Performance Liquid Chromatography Mass Spectrometry analysis was performed on a Waters Acquity UPLC system coupled to a SYNAPT G2 QTOF mass spectrometer equipped with a Zspray TM ESI-Source (Waters Corporation, Milford, MA, USA). Chromatographic conditions: Waters Acquity UPLC column (HSS T3; 1,8µM; 21x100mm). A binary solvent was utilized at 30°C, flow rate 0.2 ml/min, consisting of eluent A (water; 0.1% formic acid; Milli-Q-grade) and eluent B (Methanol; Roth – LCMS grade; 0,1% formic acid). The gradient starts – after a 2 min constant phase - from 99% A to 1% A in 10 min (total run time 15 min; injection volume 5 µL). The SYNAPT G2 was operated in negative mode (V-optics) to detect the compounds of interest (scan range 50-2000 Da; scan time 0,4 sec; capillary voltage 2 kV; sampling cone voltage 20 V; extraction cone at 3 V; source temperature 120°C; cone gas 10 l/h; desolvation gas 800 l/h, 450°C; nebulizer gas Nitrogen; collision gas Argon).

A lock mass calibration (leucine enkephalin (50 pg/mL) was automatically performed. The software used to control the LCMS system and to perform data integration was MassLynx V4.1 / TargetLynx (Waters Corporation, Manchester, UK). The quantifier ion used for the free salicylic acid and the salicylic acid conjugates were m/z 137.057 and 299.102, respectively.

2.3 Trypan blue staining

Cell death resulting from the hypersensitive response associated with increased *ACD6* activity was visualized through staining by Trypan blue.

First, lacto-phenol/Trypan blue solution (10 mL lactic acid, 10 mL glycerol, 10 mL phenol, 10 mg Trypan blue and 10 mL water) and 2.5g/mL chloral hydrate solution (25 g chloral hydrate in 10 mL water) were prepared. Freshly harvested leaf tissue was stained by completely immersing it in the lacto-phenol/Trypan blue stain and boiling the tube in a heat block set at 100°C for 30-60 seconds. After boiling, the tubes were then kept at room temperature for 10 to 25 minutes. Next, the staining solution was aspirated out and replaced by the chloral hydrate solution to destain/clear the leaf tissues. Tissues were then soaked over-night (~12-16 hours) in fresh chloral hydrate solution for better clearing. The samples are kept in 60% glycerol for long-term storage or prior to documentation.

2.4 Molecular characterization

2.4.1 Oligonucleotide primer design

PCR primers were usually initially designed from the Col-0 reference sequence using Primer3 (Untergasser, Nijveen et al. 2007). For cloning purposes, certain primers were also designed by hand with the aid of Gene Construction Kit® Version 4.0.0. A list of primers made in the conduct of experiments relevant to this thesis, together with other useful information about them, can be found in Appendix Table 2. All primers were ordered from MWG (Ebersberg, Germany). Dried primers were resuspended in sterile ddH_2O to produce a stock concentration of 100 µM. Working solutions for

PCR reactions were diluted 10 fold in sterile ddH_2O to give a working concentration of 10 µM. Working stocks were temporarily stored at 4°C, while concentrated stocks are kept at -20°C.

2.4.2 Plasmid DNA extraction

Small-scale routine plasmid DNA extractions for cloning experiments were conducted based on (Sambrook and Russell 2001). Alternatively, when high quality, large-scale amounts of plasmid DNA was needed the plasmid extraction kit from Promega® Pureyield™ Plasmid Miniprep System (Madison, WI, USA) was used as instructed by the manufacturer.

2.4.3 Genomic DNA extraction

The DNA extraction protocol was modified after Doyle and Doyle (Doyle and Dickson 1987). The same protocol was adapted for both 96-well plate format as well as individual tube format. Leaf samples were collected on ice and kept at -80°C overnight. With the aid of two steel beads per tube, maceration was done using a grinding mill (Retsch MM300, Haan, Germany) set at 20 beats per second for 1 minute or until the tissues were finely ground. In instances when larger amount of cleaner DNA was needed, plant tissue was collected in either 1.5 ml or 15 ml tubes that were immediately placed in liquid nitrogen. Frozen plant tissue was then ground using a mortar and pestle that had been pre-cooled with liquid nitrogen. Ensuring that no residual powdered tissue was stuck at the tube caps, 500 µL of pre-heated (65°C) extraction buffer (2% w/v CTAB, 1.42 M NaCl, 100 mM Tris pH 8.0, 20 mM EDTA, 0.2% v/v β-mercaptoethanol) supplemented with 5 µL 20 mg/mL RNAse A (Invitrogen, Carlsbad, California) was added to each sample (~200 mg of pulverized tissue). The mixture was then vigorously shaken and incubated at 65°C for 1 hour. Dissociation of proteins from nucleic acids was facilitated by the addition of 300 µL chloroform:isoamyl (24:1) and light inversion of the tubes. Subsequently, to separate the cellular components the samples were centrifuged at 16,000 x g for 20 minutes at room temperature. The resulting supernatant was transferred into a new tube. DNA precipitation

was then facilitated by mixing 0.7 volumes (~400 µL) of isopropanol with the collected supernatant. The tubes were temporarily kept at 4°C for a minimum of 20 minutes and then centrifuged at 16,000 x g for 30 minutes at room temperature. After decanting the supernatant, the resulting pellet was washed with 700 µL 70% v/v ethanol and centrifuged at 16,000 x g for 10 minutes. The resulting DNA pellet was air-dried and resuspended in double distilled sterile water. DNA quality and quantity was measured using a UV-Vis NanoDrop 2000 spectrophotometer (Thermo Scientific, Waltham, Massachusetts, USA). Samples that had ratios of 1.8 to 2.0, for absorbance at 260 nm and 280 nm (A_{260}/A_{280}), were considered as the acceptable. OD260 = 1 is equivalent to 50 µg/ml of double-stranded DNA.

2.4.4 Polymerase Chain Reaction (PCR)

PCR cycling conditions were optimized for each primer pair used. Reactions were performed in a PTC-200 Peltier thermal cycler from MJ Research (Waltham, Massachusetts, USA). The generic 20 µL PCR cocktail for amplifying fragments (especially for cloning) was composed of:

- Template (~ 5-10ng of plasmid DNA or 10-100 ng of genomic DNA),
- 4 µL of 5X Phusion® HF Buffer (New England Biolabs Inc., Ipswich, MA),
- 2 µL of 2mM dNTPs (10 mM each dNTP base, Invitrogen™),
- 2 µL of 10 µM Forward primer,
- 2 µL of 10 µM Reverse primer,
- 0.2 µL of Phusion® High-Fidelity DNA polymerase (5 U/µL, New England Biolabs Inc., Ipswich, MA),
- Sterile ddH_2O to make up the volume to 20 µL

For amplification and cloning of artificial microRNA (amiRNA) fragments, Pfu polymerase and the corresponding buffer was used, as instructed by the manufacturer. The highly efficient but less expensive, Thermo-Start *Taq* DNA polymerase (Thermo Scientific Waltham, Massachusetts, USA) was used for routine genotyping PCR. The following

reaction components per reaction was scaled-up depending on the number of samples to be genotyped:

- Template (~ 5-10ng of plasmid DNA or 10-100 ng of genomic DNA),
- 2 µL of 10X PCR Buffer
- 2 µL of 2 mM dNTPs (10 mM each dNTP base, Invitrogen^{TM}),
- 2 µL of Forward primer 10 µM,
- 2 µL of Reverse primer 10 µM,
- 0.5 µL of DNA polymerase
- Sterile ddH_2O to make up the volume to 20 µL

Thermal cycling programs were set up as follows:

1x Cycle	Initial denaturation	30 sec (Phusion)	98°C
		45 sec (Pfu)	94°C
		2 min (*Taq*)	94°C
34x Cycle	1) Denaturation	5 sec (Phusion)	98°C
		45 sec (Pfu)	94°C
		20 sec (*Taq*)	94°C
	2) Annealing	30 sec (Phusion)	50– 72°C*
		45 sec (Pfu)	50– 65°C*
		30 sec (*Taq*)	50– 65°C*
	3) Extension	30 sec/Kb (Phusion)	72°C
		1 min/Kb (Pfu)	72°C
		1 min/Kb (*Taq*)	72°C
1x Cycle	Final extension	5 min (Phusion)	72°C
		10 min (*Taq*)	72°C
1x Cycle	Incubation	as needed	14°C

* Annealing temperature was based on the calculated melting temperature (T_m) of the specific primer used in the PCR reaction.

PCR conditions and some reaction components had to be individually optimized for some primer pairs.

2.4.5 Agarose gel electrophoresis

PCR products and restriction enzyme fragments were separated in a submerged agarose gel prepared with 1x TAE [2.0 M Tris Acetate, 0.05 M EDTA buffered by glacial acetic acid (~57.1 mL per liter) to pH 8.2 – 8.4]. The concentration of the gel, in % w/v, varied with the expected fragment size of products loaded – a higher concentration was used when smaller fragments were to be separated. Loading buffer (10 mM Tris-HCl, 1 mM EDTA pH 8.0, 50% v/v glycerol, 0.05 g/mL bromophenol blue) was mixed with PCR products and restriction fragments, for visualization and tracking of the electrophoresis progression. A molecular marker was loaded on to wells adjacent to the samples being resolved. The gels were usually run at 10-20 V/cm for as long as needed to obtain the desired separation. The resulting separated fragments were visualized with UV light (302 nm) and documented using AlphaImager (Alpha Innotech, Genetic Technologies, Inc., Florida, USA).

2.4.6 RNA extraction

RNA was extracted using a modified TRIzol (Invitrogen^{TM}) method. Plant tissues, collected in 1.5 ml tubes containing two steel beads, were ground to powder using pre-frozen (cooled at -80°C) tube adaptors for the grinding mill (Retsch MM300). Carefully making sure that the plant tissue did not thaw, 1 mL of TRIzol was added per sample (~100 – 200 mg). The mixture was homogenized and incubated at room temperature for 5 minutes. Next, 500 µL chloroform was added and the tube was subsequently inverted around 24 times and centrifuged at 14,000 x g for 10 minutes at 4°C. The supernatant was transferred to a new 1.5 ml tube, after which 500 µL isopropanol was added and mixed by gentle inversion. This mixture was incubated on ice for 10 minutes and then centrifuged at 14,000 x g for 20 minutes at 4°C. After centrifugation, the resulting pellet was washed with 70% ethanol and re-precipitated again by centrifugation at 14,000 x g for 10 minutes at 4°C. Precipitated RNA was air-dried and dissolved in 30 – 50 µL of DEPC-treated ddH_2O. Quantity was measured using a UV-Vis NanoDrop 2000 spectrophotometer (Thermo Scientific) set to measure absorbance at 260 nm

and 280 nm. The presence of intact ribosomal RNA and comparative absorbance ratios A_{260}/A_{280} of ~2.0 was used to assess the quality of the RNA extracted. RNA samples were stored at -80°C.

2.4.7 DNAse I treatment

RNA samples were routinely treated with DNAse I to ensure that there was no contaminating DNA in the samples. Treatment was done using the RQ1 RNase-Free DNAse from Promega® kit, employed as per the manufacturer's instructions. RNA quality and quantity were re-checked after DNAse treatment and normalized by dilution to ~ 50 - 100 ng/µL.

2.4.8 First-strand complementary DNA (cDNA) synthesis

As soon as the RNA was cleaned-up and diluted to the desired concentration, first-strand complementary DNA (cDNA) was synthesized. The SuperScript® First-Strand Synthesis System for RT-PCR kit (Invitrogen™), was utilized for this purpose. Random hexamers and oligo(dT) primers were the oligonucleotides of choice for cDNA amplification. The protocol as suggested by the manufacturer was adapted. To unfold the RNA the 24 µL reaction, incubated at 65°C for 5 minutes, consisted of the following:

- 20 µL Template (~ 10 µg of normalized DNAse-treated RNA),
- 2 µL oligo(dT)18 primer,
- 2 µL random hexamer primer

The reactions were immediately flash-cooled at on ice to preserve the unfolded RNA structure, and the following reaction components are added:

- 8 µL Reaction buffer,
- 2 µL Ribolock RNAse Inhibitor,
- 4 µL 10 mM dNTP mix,
- 2 µL RevertAid M-MuLV Reverse Transcriptase

The total 40 µL reaction was incubated at 42°C for 60 minutes. The reaction was halted by incubation at 70°C for 5 minutes. The final single-stranded cDNA was then diluted 1:10 and used for succeeding PCR reactions.

2.4.9 Quantitative RT-PCR (qRT-PCR)

Gene expression changes were determined using reverse transcription followed by quantitative real-time RT-PCR (qRT-PCR) using gene specific primers (Appendix Table 2). The reaction was performed with Fast SYBR® Green Master Mix (Invitrogen™). The progression of the reaction cycles for real-time quantification of template amplification was monitored with CFX384 Touch™ Real-Time PCR Detection System (Biorad, Hercules, CA, USA). A minimum of three biological replicates was tested for most experiments except for routine checks of unstable transgenic lines (primary transformants) when replication is not possible. Two technical replicates of each genotype as well as the corresponding housekeeping gene for normalization were measured.

The relative expression ratio to the control, usually the accession Col-0, was quantified based on a formula from Pfaffl (Pfaffl 2001):

$$2^{-[(Ct_{\text{test sample}} - Ct_{\text{housekeeping gene}}) - (Ct_{\text{normalization sample}} - Ct_{\text{housekeeping gene}})]}$$

A typical 20 µL qPCR reaction consisted of the following:

- 5 µL Fast SYBR® Green Master Mix,
- 2 µL of 10 µM Forward primer,
- 2 µL of 10 µM Reverse primer,
- 4 µL single-stranded cDNA, diluted 1:10
- 7 µL water

2.4.10 Artificial microRNA (amiRNA), domain swaps, rescue and genomic complementation constructs

Constructs expressing amiRNAs under the control of the constitutive Cauliflower Mosaic Virus (CaMV) 35S promoter were designed and prepared as described (Schwab, Ossowski et al. 2006). First, the target cDNA sequence was submitted to the WMD online tool (Weigelworld , Ossowski, Schwab et al. 2008) to design the amiRNA primers. Sequence verified amiRNA constructs were then inserted into the *MIR319a* backbone and transferred behind the CaMV 35S promoter in a modified transformation

vector (pFK210) derived from pGREEN (Hellens, Edwards et al. 2000). A list of the amiRNA constructs used in this work can be found in Appendix Table 3.

Genomic constructs were prepared with restriction enzymes or Gateway cloning. *ACD6* alleles from Pro-0 and Rmx-A180 were isolated using specific primers (Appendix Table 2). In addition, domain swap constructs were made between Est-1 and Pro-0 *ACD6* allele types (Appendix Table 3). As with the amiRNA constructs, all binary vectors were based on the pGREEN system. Constructs were introduced into Col-0 and other genotypes (Appendix Table 3) using *Agrobacterium tumefaciens* mediated transformation (Weigel and Glazebrook 2006).

2.5 Pathogen-Associated-Molecular-Pattern (PAMP) assays and Pathogen response assays

2.5.1 PAMP-induced Reactive-oxygen species (ROS) assays

A two-day experimental set-up, excluding the growth of the plants used for the assay, was needed to perform PAMP-induced ROS assays. The scheme and the details are provided in Figure 2.1. Each assay for a particular genotype was repeated at least three times to ensure that the pattern shown by the assay was consistent. The Elicitation Solution (for composition refer to Figure 1) was always kept protected from direct light and was only added to the recovered leaf discs a few seconds prior to reading of ROS burst by the luminometer (TECAN Infinite ® 200 Pro). A multichannel pipette was used to aliquot the solution to each well to guarantee that sets of samples are treated with the solution at the same time.

The flg22 peptide was ordered from and synthesized by EZBiolab Inc. (Westfield IN, USA) at >85% purity with the following sequence: QRL STG SRI NSA KDD AAG LQI A.

2.5.2 Pseudomonas syringae storage and growth

Pseudomonas syringae pv. *maculicola* ES4326 (*Psm*) and *Pseudomonas syringae HrcC-* (*Pst HrcC-*) strains were provided by A.G.

Staphnill (JIC, UK). Long-term pathogen stocks were kept in 50% glycerol at -80°C before transfer to agar stock plates on LB medium supplemented with 50 µg/ml each of rifampicin and kanamycin kept at 28°C overnight (~12 to 16 hours). Those plates were stored for up to 2 weeks at 4°C. Single colony bacteria grown for actual assays were also taken from and re-inoculated to LB medium with the appropriate antibiotics. Approximately 250 µL of the growth culture was then lawn plated unto a fresh LB plate, again with the appropriate antibiotics, and grown at 28°C overnight (~12 to 16 hours).

2.5.3 Bacterial (Pseudomonas syringae) inoculation and counting

A typical experimental set-up and flow of the inoculation is shown in Figure 2.2. For each genotype tested, at least three individual plants (biological replicates) for infection and a corresponding set for mock inoculation were grown in a 23°C short-day growth chamber for four weeks. Three days before leaf disc collection, bacterial inoculum used for infiltration was prepared by re-suspending scrapings from fresh lawn-plated bacteria in 10mM $MgCl_2$. Bacterial density was measured using an Eppendorf Bio-photometer (Hamburg, Germany) and adjusted to OD_{600} 0.002 (equivalent to ~10^6 cfu/mL). Pressure infiltrations were made using 1 mL needleless syringe on the abaxial side of each leaf, until the whole leaf appeared to be water-soaked. At least 4 leaves were infiltrated per plant. Leaf discs (5 mm diameter) taken from two leaves of three plants amounted to a minimum of 6 data points per genotype per treatment. To assess bacterial content in comparative trials, dilution plating and colony counting were performed after macerating the collected leaf disc in 200 µL 10 mM $MgCl_2$ with two steel beads per tube using a grinding mill (Retsch MM300).

Serial dilutions of between 10^0 to 10^{-7} were dot-plated (~10 µL per spot) on LB plates (Figure 2.3) with the necessary antibiotics and incubated for two days at 28°C. At the same time, each dilution series was dot-plated twice as

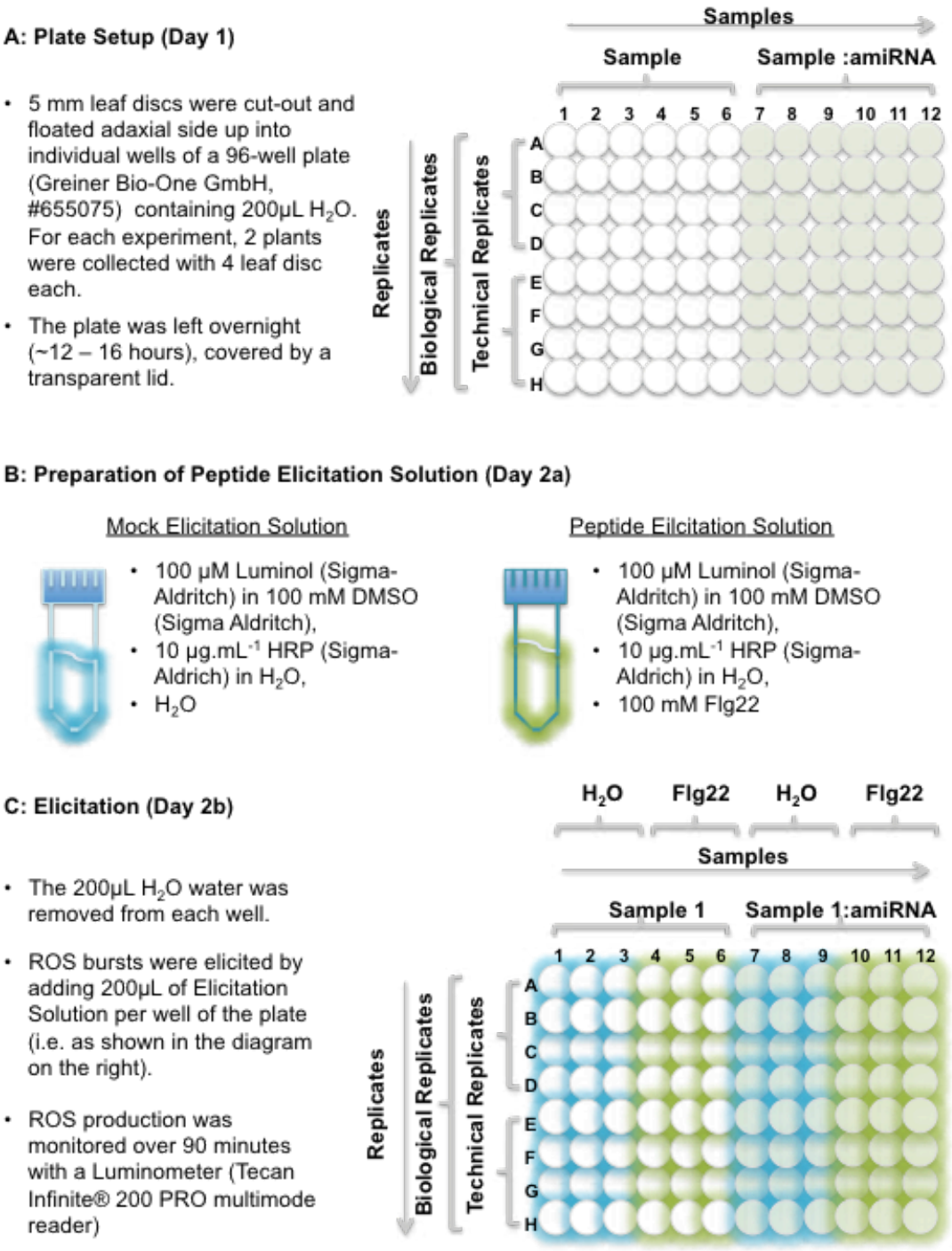

Figure 2.1 PAMP-induced Reactive-oxygen species (ROS) assay experimental set-up and scheme

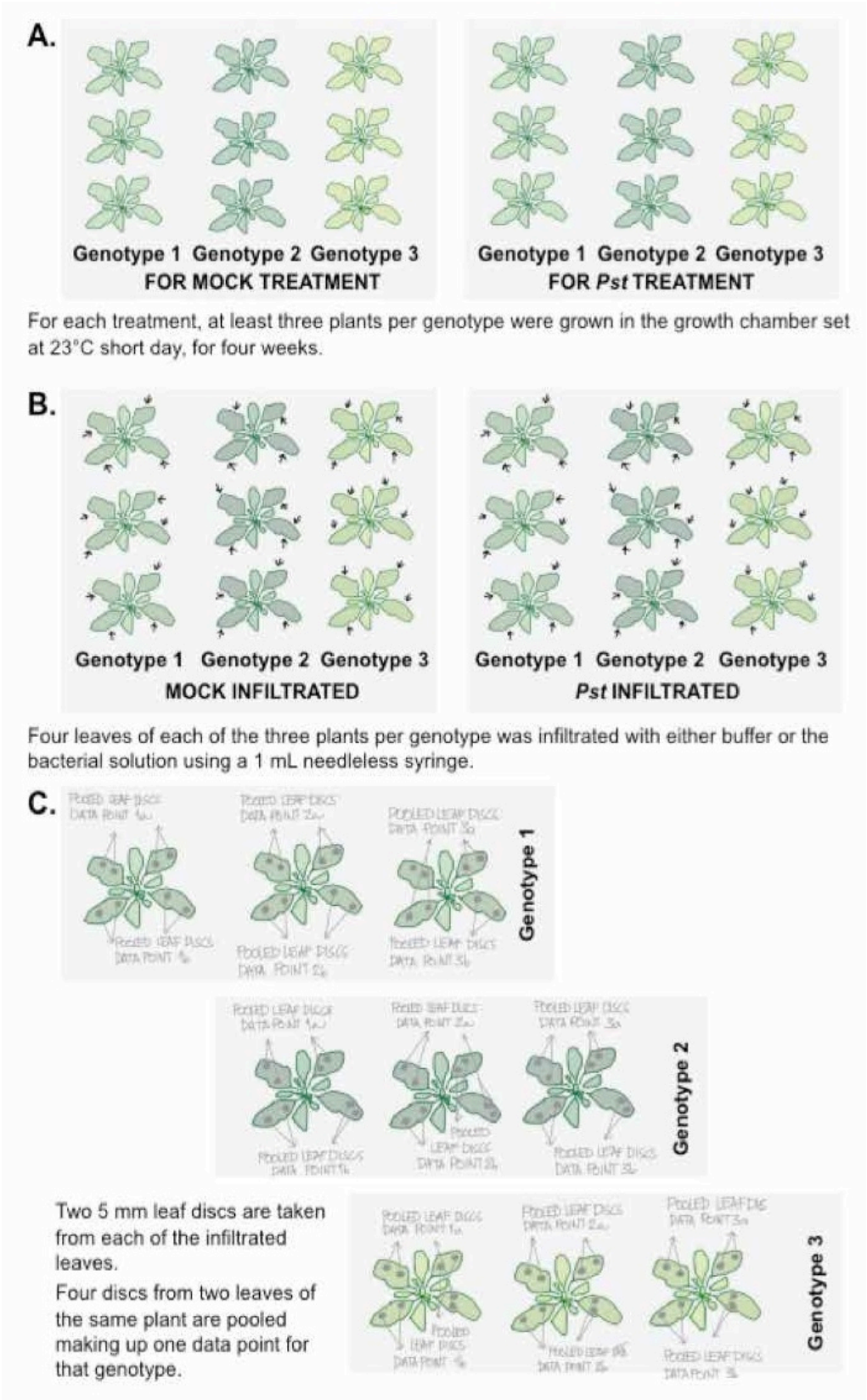

Figure 2.2 Plant experimental set-up for bacterial inoculation and sample collection for colony counting assay

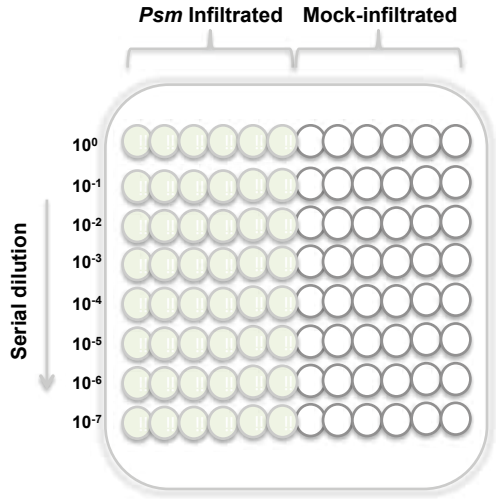

Figure 2.3 Agar plate set-up for bacterial dilution and colony counting from macerated leaf extracts of infected and non-infected leaves.

Equation for colony counting:

$$\text{Log cfu.cm}^2 = \frac{\left[\frac{\text{Number of colonies}}{\mu\text{L plated}}\right] \times \text{Highest dilution where colonies grew (Dilution at which colonies were counted)} \times \text{Number of leaf punches}}{\text{Area of leaf punch in cm}^2}$$

technical replicate. The number of colonies that formed was counted at the highest possible dilution and the average between the two technical replicates was recorded for each specific dilution. Finally, the number of colony forming units per leaf area taken was calculated with the final unit of measure in (log) cfu.cm^2.

2.6 Screening of accessions and generation of mapping populations

The collection of *Arabidopsis thaliana* accessions (Appendix Table 1) available in the laboratory was screened for the presence of *ACD6*-Est-1 allele. A fragment of the more variable 3'- end region of *ACD6* (At1g14400) was amplified by PCR using oligonucleotides G-12247

(AGCCGTAGACGCTGGAAATA) and G-18613 (AGAAGAAACATATCCTTGAA). Next, PCR fragments were Sanger sequenced and the presence of the causal amino acid change typical of *ACD6*-Est-1 allele was assessed. All accessions containing the causal SNPs for said amino acid changes were grown in 23°C SD and phenotyped for the presence of late-onset leaf necrosis. From that subset, six accessions showing none to mild late-onset leaf necrosis/ cell death patches were kept and tested further. Testcrosses and mapping populations were created simultaneously, as illustrated in Figure 2.4. Those plants were genotyped with markers (Appendix Table 2) distinguishing the *ACD6*-Est-1 allele from *ACD6*-Col-0 allele to determine if the late-onset phenotype co-segregated with the *ACD6* allele type.

2.6.1 Identification of Est-like ACD6 alleles using Illumina short reads of accessions from the 1001 Genomes Project

2.6.1.1 Mapping and SNPs calling

To map and find accession-specific SNPs, a home-made pipeline written in Nextflow language (group) was used to do the following:

- Mapping with BWA mem (Li and Durbin 2009)
- Sorting SAM file using Picard (Institute) SortSam
- Removing PCR duplicates using Picard MarkDuplicates
- Indexing BAM files using Picard BuildBamIndex
- Local realignment around indels using Genome Analysis Toolkit (GATK) (McKenna, Hanna et al. 2010) RealignerTargetCreator and IndelRealigner
- Calling variants (SNPs and indels) using GATK Haplotype Caller

After mapping and SNP calling, all individual vcf files were merged through GATK GenotypeGVCFs. A subset of the genome containing *ADC6* was extracted using vcftools (coordinates of *ACD6* -- chr Chr4 --from 8298043bp to 8298249bp). This fragment covers the two crucial triplets,

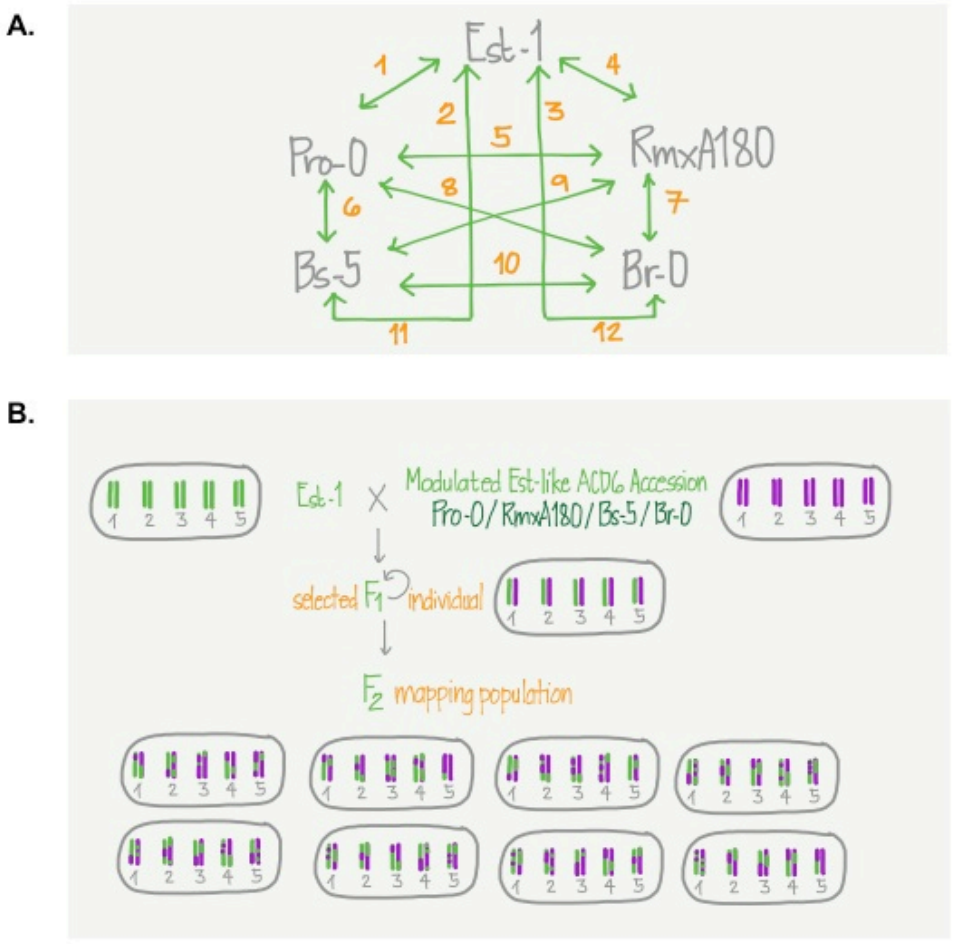

Figure 2.4 Schematics of A) crossing of testcross between candidate accessions with *ACD6* modifiers and B) generation of populations used for genetic/QTL mapping.

causal for Est-1 *ACD6* hyperactivity, and 243 bp between them. The critical CTT/TTT substitution occurs in position Chr4 8298247. Indels were removed using GATK SelectVariants. Finally, fasta sequences were produced for each accession, using GATK FastaAlternateReferenceMaker. If there was no coverage for a particular position, Col-0 reference SNP was taken instead.

Confirmation for a subset of accessions, having at least one of the crucial triplets as being Est-like, was done by Sanger sequencing of the transmembrane fragment amplified using oligonucleotides G-12247 and G-18613.

2.6.1.2 Plotting geographic distribution of accessions

Accessions were plotted on the world map based on the triplet sequence for the two causal amino acid changes using ggplot (Wickham 2009) package in R . For better resolution, a separate plot was made for the subset of accessions with confirmed Sanger sequencing SNPs and lesion phenotypes.

2.6.2 Restriction-site Associated DNA Sequencing (RAD-Seq)

Library preparation: Restriction-site Associated DNA Sequencing, a genotyping-by-sequencing method, was employed to genotype F_2 populations for QTL mapping. The method uses restriction enzyme digestion to create fragments of genomic DNA with a specific overhang. These overhangs are then exploited for adapter ligation. For our purpose, RAD-Seq library preparation and adapter sequences were adapted from the methods developed by (Poland, Brown et al. 2012). A set of 192 adapters based on *Pst-1* and *Mse1*, designed according to Poland et al. (Appendix Table 4), was used for pooled sequencing of a maximum of 192 individual samples per library.

Restriction Digest: Normalized genomic DNA (200 ng) for each individual sample was digested in 20 µl reaction volume of NEB Buffer 4 with 8 U of *PstI* HF (High- Fidelity, New England BioLabs Inc.) and 8 U of *MseI* (New England BioLabs Inc.). Samples were incubated at 37°C for 2 hours and then at 80°C for 20 minutes to inactivate the enzymes.

Ligation: Immediately after digestion, the adapters were ligated to the DNA fragments. In the same reaction tube, extra NEB Buffer 4 (#B7004S) and 1mM ATP (Thermo Scientific, #R0441) were added together with 200 U T4 DNA Ligase (ThermoFisher Scientific, Waltham, Massachusetts, USA), 0.1 pmol Adapter 1 and 15 pmol of the common Y-adapter (Appendix Table 2). Samples were incubated at 22°C for 2 hours and then at 65°C for 20 minutes to inactivate the ligase.

Multiplexing and Amplification: For each designated library, ligated samples were multiplexed in a single tube by pooling equal amounts from each sample. Prior to PCR amplification the multiplexed mixture was purified using a QIAquick PCR Purification Kit (Qiagen, Venlo, Limburg, Netherlands). A 200 µl total of pooled ligated DNA was combined with 1000 µl buffer PB in a fresh 2.0 mL tube. One spin column was used for each 600 µl of the mixture. Each column was spun at 16, 000 x g, and sequentially washed and air-dried. The ligated DNA fragments were eluted using 60 µl of buffer EB. PCR amplification of the cleaned up fragments was done in a single tube. Each library was amplified for 12 cycles of 95°C (10 seconds), 62°C (30 seconds), 72°C (30 seconds) and a final 5-minute extension at 72°C. After PCR amplification, the reactions were purified again purified using a QIAquick PCR Purification Kit. For different mapping populations, a single library consisted of either 96 or 192 samples, which was sequenced on a single lane of Illumina HiSeq2000.

Processing of Illumina Raw Data: Raw Illumina 100 bp reads was processed using custom Perl scripts supplemented with the mapping and analysis pipeline SHORE (2013). The (unfiltered QSeq) Illumina data were assigned to individual samples using the designated barcode sequence. Only sequences that had maximum of 2 mismatch in the barcode followed by the expected *PstI* cut-site were kept. A 10% leeway as the maximum amount of ambiguous base calls per read was set with the minimum trimmed read length as 30 bp. Low complexity filters as well as SHORE custom filters were also used. Trimmed and quality-filtered reads (from all the F_2 individuals as well as the parental genotypes) were then mapped to the preprocessed Col-0 reference sequence genome. Consensus analysis based on the SHORE homology scoring matrix resulted in a list of quality variant and quality reference SNPs with the corresponding quality scores and read support counts. The last 10 bases of each alignment were offset as more “suspicious” than the rest of the read. High quality co-dominant SNP markers were compiled from the quality reference and quality variant SNPs of each F_2 parental genotype. A matrix containing the genotypes at specific marker positions for all the F_2 individuals

genotyped for the mapping population was then created using a customized script.

2.6.3 QTL mapping and analysis

F_2 individuals from crosses between Pro-0 x Est-1, RmxA180 x Est-1, Br-0 x Est-1 and Bs-5 x Est-1 were phenotyped for the severity of late-onset necrosis. Phenotypic scores were supplied from the qualitative scoring of the phenotypes based on the severity of lesions formed on the plants. Phenotypes were entered as “0” when the individual did not develop lesions at the phenotyping time point and “1” otherwise. QTL mapping and testing for QTL effects and interactions were performed using the R/qtl package. The R/qtl software package is implemented as an add-on package for the command-line-based, open-source statistical software R. Lod scores were initially calculated with single-QTL model using the function ‘‘scanone’’. Subsequent results indicating more than one loci prompted re-computation of lod scores and testing interactions (epistatic, additive and dominant) using the functions “scantwo” and “fitqtl”. The lod score significance threshold was established using 1,000 permutations. In all the functions utilized the standard expectation-maximization algorithm was used for ‘‘method.’’

3 *ACD6* natural variation in *Arabidopsis thaliana* populations

“Biology is a science of three dimensions. The first is the study of each species across all levels of biological organization, molecule to cell to organism to population to ecosystem. The second dimension is the diversity of all the species in the biosphere. The third is the history of each species in turn, comprising both its genetic evolution and the environmental change that drove the evolution. Biology, by growing in all three dimensions, is progressing toward unification and will continue to do so.”

- Edward O. Wilson, 2005

The total number of characteristics in the genetic makeup of a species (genetic diversity) and the tendency of these genetic characteristics to vary (variation) remains core to the study of all living organisms (Koornneef, Alonso-Blanco et al. 2004, Arber 2011, Weigel and Nordborg 2015). An attestation to this, natural variation (genetic diversity in the wild) in different plant species has been increasingly utilized to identify the molecular basis of important agronomic traits (Alonso-Blanco, Aarts et al. 2009). Finding the molecular nature of important phenotypes starts by identifying genetic variation controlling the trait. Conjointly, the origin and the phenotypic effects of these genetic variations are central to obtaining knowledge on how species adapt to the environment. Molecular characterization of the allelic differences is a fundamental building block of plant molecular breeding.

As much as biodiversity is vast, genetic programs for several complex traits have been shown to be shared across groups of organisms (Weigel 2012). Accordingly, a few species have arisen as models for the study of traits typically found in a larger group of species. Some model plants have been selected based on their own value in biotechnology or agronomy. Examples of such are corn, rice and wheat. There are also newly emerging models such

as *Panicum virgatum* (switchgrass) and *Brachypodium distachyon* (purple false brome) that have become increasingly popular, either because of favorable properties for genetic research or their direct usefulness for biomass production.

The traditional genetic models were selected due to ease of investigating particular biological phenomena or just plain ease of handling of the species itself. *Arabidopsis thaliana* ("Arabidopsis"), selected initially as such, has now been adopted as a major model or reference plant especially suitable for genetic and molecular research. Although native to Europe and central Asia it is now naturalized in many places across the world, in a wide range of habitats (Koornneef, Alonso-Blanco et al. 2004). Natural accessions of Arabidopsis have often been called "ecotypes", a term that implies that individuals are type specimens for a particular ecological environment. The neutral term "accession" is more preferable (Alonso-Blanco and Koornneef 2000, Weigel 2012).

There are many studies of the effects of specific natural alleles found in Arabidopsis populations. Traits that have been investigated include resistances to biotic (Schiff, Wilson et al. 2001, Wilson, Schiff et al. 2001) and abiotic factors (Zhang and Lechowicz 1995), control of developmental processes and physiological traits (van Der Schaar, Alonso-Blanco et al. 1997, Perez-Perez, Serrano-Cartagena et al. 2002) and even production of biochemical compounds (Kliebenstein, Kroymann et al. 2001). Most of these studies focus on clear defined phenotypes responsible for specific traits. Recently, additional attention has been given to study trade-offs in Arabidopsis and in other plants that exemplify the adaptation consequences of acquiring advantage over one phenotype/trait at the expense of another (Kiani, Trontin et al. 2012, Oakley, Agren et al. 2014, Zhang, Shrestha et al. 2014, Rasmann, Chassin et al. 2015, Shyu and Brutnell 2015).

One example is alleles in the Arabidopsis gene *ACD6* that underlie a trade-off effect between growth and defense (Todesco, Balasubramanian et al. 2010). It has been shown that reduced size and autoimmune symptoms are correlated across Arabidopsis accessions. A conventional QTL mapping strategy identified the Est-1 allele type as causal for both late-onset necrosis (in the absence of pathogens), and slower leaf production and reduced

biomass. It has also been found that this hyperactive *ACD6* allele, compared to the reference allele, strongly enhances resistance to a broad range of pathogens from different phyla (e.g. *Golovinomyces orontii*, *Hyaloperonospora arabidopsidis*, and *Pseudomonas syringae*). Furthermore, the authors reported that approximately 20% of the 96 accessions they sequenced for *ACD6* had an allele similar to that of Est-1 (Figure 3.1).

The late-onset necrosis phenotype is reminiscent of the hypersensitive response induced by pathogen resistance. By this reason, and not just in the aforementioned study, the lesion response has been used as a proxy for autoimmunity or hyperactivation of plant defense response (Moeder and Yoshioka 2008). *ACD6* Est-1 like alleles have been assumed to generally associate with the proxy phenotype for *ACD6* hyperactivity late-onset necrosis (interchanged often with the simpler description appearance of “lesions” in the succeeding sections and Chapters). Notably, not all accessions (e.g., Pro-0 and Rmx-A180) that had the Est-like allele of *ACD6* showed strong lesions (Todesco, Balasubramanian et al. 2010). The genetic or evolutionary reasons for this variation were, however, not investigated further.

In this chapter, I focus on efforts to identify the extent of variation, distribution and maintenance of Est-like ACD6 alleles in natural *Arabidopsis* accessions. Specifically, I began with identification of a quick but robust method to assay *ACD6* allele type. Next, I used that information to substantiate the claim that the late-onset necrosis/lesion phenotype is a consequence of having an Est-like *ACD6* allele. Finally, after I had obtained *ACD6* genotype and phenotype information, I surveyed geographic patterns of variation, distribution and maintenance of Est-like *ACD6* alleles in Arabidopsis accessions.

3.1 Causal amino acids for *ACD6* hyperactivity

My first step into dissecting the possibility of natural modulation of the trade-off effect of *ACD6* on growth and defense potential was finding more cases of Est-1 like allele without lesion phenotype (like Pro-0 and Rmx-A180) (Todesco, Balasubramanian et al. 2010). This would not only give us

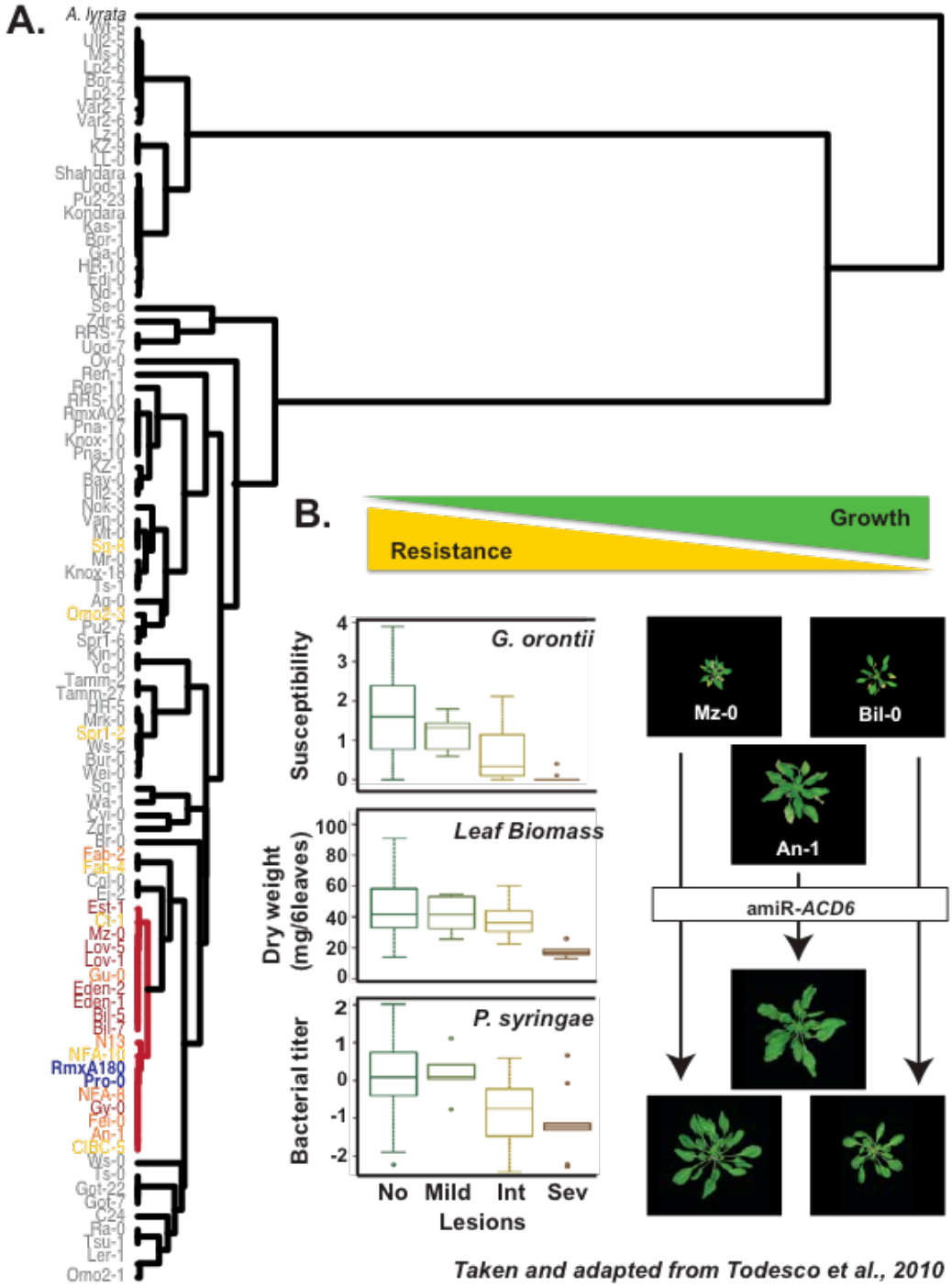

Figure 3.1 Known *ACD6* genetic variation and associated phenotypes before I began my thesis work. A) Hierarchical clustering of *ACD6* alleles in 96 accessions of *Arabidopsis thaliana* shows that accessions having Est-like *ACD6* alleles group together. Est-like *ACD6* alleles generally associate with late-onset necrosis, the severity of which varies among the accessions tested. As illustrated in the tree: yellow indicates mild, orange intermediate and red severe necrosis. B) The trade-off effect of *ACD6* on growth and defense. Severity of lesioning is inversely proportional to susceptibility to pathogens and biomass. Among accessions with Est-like *ACD6* alleles, amiR-*ACD6* knockdowns abolish the lesions and increase biomass.

information on how common they are but also provide more cases with which *ACD6* variability can be studied. Concurrent to that goal, I attempted to confirm the previously defined *ACD6*-Est-1 SNPs responsible for hyperactivity of the Est-1 *ACD6* allele. Transgenic tests have identified two causal amino acid changes that are together necessary and sufficient to change a Col-0 *ACD6* allele into an allele with the Est-1 activity (Figure 3.2): A566N and L634F (Todesco, Balasubramanian et al. 2010).

Using the Est-type nucleotide triplets AAC (encoding N566) and TTT (encoding F634), I used short reads from the 1001 Genomes Project (http://1001genomes.org/) to find accessions with these SNPs. Short-read data from 858 accessions passed the quality filter I used. Table 3.1 shows the distribution of nucleotide triplet types for these 858 accessions. Some of the nucleotides called from the short read sequences were ambiguous. For amino acid 566, the following triplets were observed in addition to GCA (Col-0-like, encoding Ala): GAA (Glu), GMA (Ala/Glu), GTA (Val), GWA (Ala/Val) and GYA (Ala/Val). AAC, the nucleotide triplet coding for Est-1, was not recovered from any of the mapped reads. For amino acid 634, I found in addition to CTT (Col-0-like, encoding Leu) and TTT (Est-1-like, encoding Phe): GTT (Val), KTT (Val/Phe), STT (Val/Leu) and YTT (Leu/Phe). Heterozygous calls question accuracy of SNP calling from short-read data, as *A. thaliana* mostly reproduces by self-fertilization (Platt, Horton et al. 2010). The species exists in metapopulations, with genetically identical plants in the native range being generally restricted to individual stands (Cao, Schneeberger et al. 2011). With self-fertilization and bi-parental breeding only 95% of *A. thaliana* have five or fewer heterozygous loci (Platt, Horton et al. 2010). Given these facts, heterozygosity is not characteristic of *A. thaliana* accessions. The ambiguous SNPs are likely pseudo-heterozygous and are due to sequencing errors or paramorphism (polymorphism between paralogs) (Fu, Emrich et al. 2005). In Col-0 there is an *ACD6* paralog (AT4G14390), located immediately upstream of the *ACD6* locus. This or any other paralog that is not included in the reference genome may be causal for this paramorphism. Illumina short reads are 100-250 bp short DNA fragments are when they are aligned to the reference. Short fragments from non-reference paralogs could still be aligned

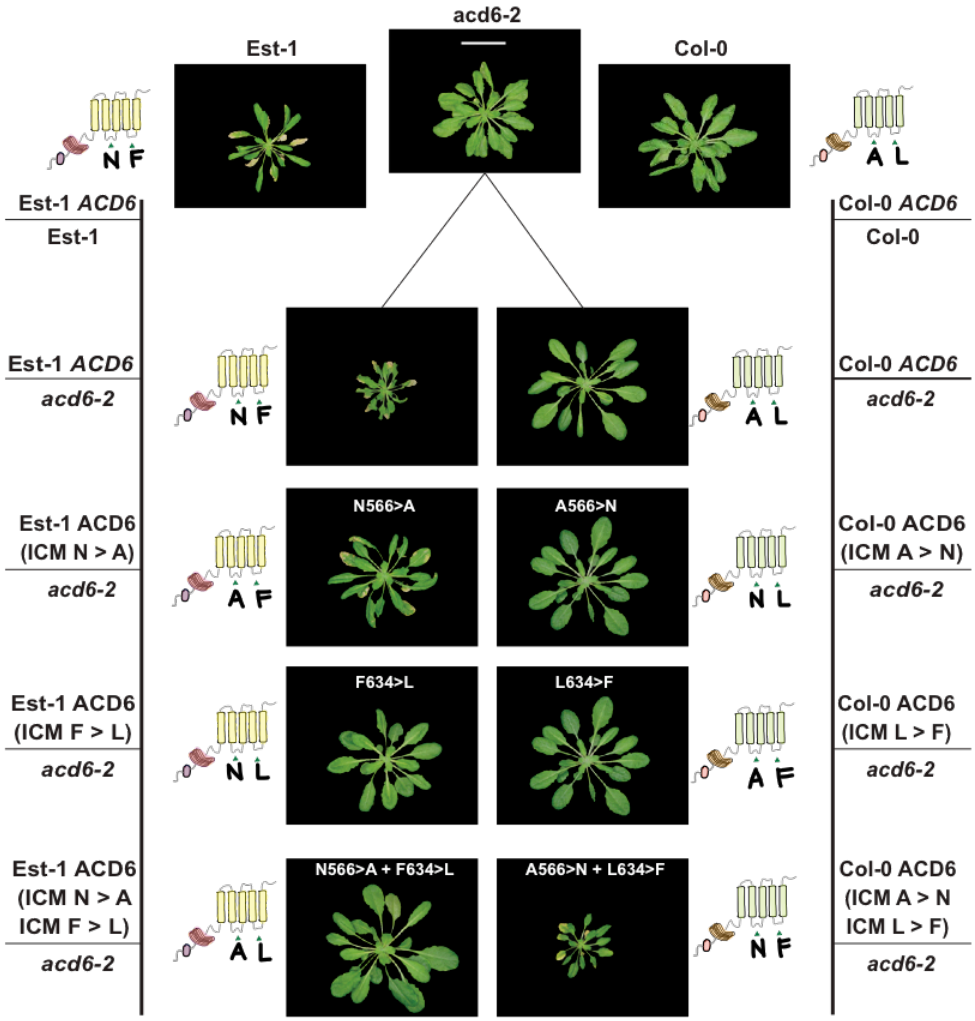

Figure 3.2 Representative *acd6-2* transgenics with induced point mutations showing the two causal amino acid changes that are sufficient to confer Est-like *ACD6* hyperactivity in Col-0-like *ACD6* alleles. Induced point mutations (ICMs) revert A) Col-0 type Alanine (Ala) at position 566 to Est-1 type Asparagine (Asn) and/or B) Col-0 type Leucine (Leu) at position 634 to Est-1 type Phenylalanine (Phe).

Note: Transgenics made by Dr. Marco Todesco, I did the phenotypic screening.

to the reference but with some mismatches that could result in ambiguous SNPs calls.

Given the nucleotide triplet type ambiguities seen, I wanted to test the robustness of this short read-based allele-type-designation, by deducing the likely genotype from Est-1-like necrosis and by parallel Sanger sequencing. I grew seedlings for a subset of 94 accessions with the respective nucleotide triplet combinations, shown in Table 3.2. Accessions with ambiguous nucleotide triplet combinations were prioritized. The selected accessions have nucleotide triplet combinations for which there was the highest probability that one of the pseudo heterozygous SNP results in a position 566 and 634 Est-like *ACD6* amino acid. Since there were assayed Est-1 F634 triplets, more focus was put into determining what position 566 triplets those were found in conjunction with. Serving as control, I also grew Est-1 and Col-0 together with these selected accessions. Genomic DNA samples were used to amplify an 800 bp fragment in the *ACD6* transmembrane domain where the causal SNPs for amino acid position 566 and 634 are located. This 800 bp was used for Sanger sequencing. In parallel, a set of 6 seedlings each was grown to maturity and phenotyped for appearance of spontaneous lesions.

Sanger results identified a new nucleotide triplet, AAA (encoding Lys), for amino acid 566 (Figure 3.3). Also at amino acid position 566, accessions with GMA ambiguous nucleotide triplet could be categorized either as having Col-0 like, GCA (Ala) or the new nucleotide triplet, AAA (Lys). Still at amino acid position 566, accessions with GWA ambiguous nucleotide triplet could be categorized either as having Est-1 like AAC (Asn) or the newly discovered AAA (Lys) nucleotide triplet. It seemed that the new nucleotide triplet for *ACD6* amino position 566 caused mistyping for some accessions. Comparison between Illumina and Sanger sequences showed that most selected accessions had Est-like nucleotide triplets for F634 (Figure 3.3), including those initially called as having KTT(Val/Phe) and YTT (Leu/Phe). Most of the accessions originally typed as having TTT (Phe) for *ACD6* amino acid 634 were indeed TTT. Contingent on Sanger sequencing results, prior designation of accessions as having Est-like *ACD6* based on F634 alone was 87% accurate.

Accessions with more severe HR-like lesions have Est-1 triplet nucleotides AAC and TTT at ACD6 amino acid 566 and 634 respectively (Figure 3.4A). Analysis of the two ACD6 amino acid positions showed that this observation holds although there is a lesion severity gradient for accessions having both AAC and TTT triplet nucleotides (Figure 3.4B). This gradient may be due to other SNPs in ACD6 that result in non-synonymous amino acid changes which could temper the effect of the identified Est-like amino acid causal for hyperactivity. Other than this, extragenic factors can reduce ACD6 hyperactivity in some of these accessions that have both Est-like causal amino acids. Accessions that contained the new triplet nucleotide AAA encoding for ACD6 amino acid position 566, can have mild HR-like lesions, when combined with either Col-like CTT or Est-like TTT at ACD6 amino acid position 634 (Figure 3.4B). There were two accessions that had Col-like triplet nucleotide combination, GCA/CTT and GCA/TTT respectively, which had severe lesions. The lesion phenotype observed in these accessions can be due to a gene different from *ACD6*, for which the allele present in the said accession could also result in an HR-like lesion. Otherwise, there might be other SNPs that are present in *ACD6* alleles different from Est-1 that could be causal for an *ACD6*-dependent lesion phenotype. Cloning and transforming the *ACD6* alleles from these accessions could be a way to check for the lesion phenotype causality.

Summarily, with the results from this section I have shown:

- With ~20% error, raw Illumina resequencing data analyzed using the pipeline I adapted can be used to designate accessions as having Est-like *ACD6* alleles. The errors might have been due to Illumina sequencing errors or the uncertainty of assigning Illumina short reads between paralogs. Follow up with experiments
- Most of the *A. thaliana* accessions having both Est-like ACD6 amino acids N566 and F634 showed strong HR-like lesions. Some had none or mild lesions which resembling Pro-0 and Rmx-A180 phenotypes.

Table 3.1 Frequency distribution of triplet types at positions coding for *ACD6*-Est-1 causal amino acids among *A. thaliana* accessions of the 1001 Genomes Project based on reconstituting SNPs from the raw Illumina short read sequences for *ACD6*

Combination	Position 566[1]	Similarity	Accessions	Position 634[1]	Similarity	Number of accessions with amino acid combination
1	GAA	New	229	CTT	Col-0	721
2	GCA	Col-0	523	GTT	New	17
3	GMA	New/Col-0	92	TTT	Est-1	102
4	GTA	New	3	KTT	New/Est-1	3
5	GWA	New/Col-0	7	STT	New/Col-0	12
6	GYA	New/Col-0	4	YTT	Col-0/Est-1	3
	total		858	total		858

[1]IUPAC nucleotide code: M- A or C, W- A or T, Y- C or T, K- G or T, and S- G or C.

Table 3.2 Frequency distribution of accessions selected for Sanger sequencing. Triplet types at positions coding for *ACD6*-Est-1 causal amino acids among Arabidopsis thaliana accessions of the 1001 Genomes Project based on reconstituting SNPs from short read sequences for *ACD6*

Combination	Position 566 [1]	Amino acid identity	Similarity	Position 634 [1]	Amino acid identity	Similarity	Number of accessions with amino acid combination
1	GCA	Ala	Col-0	YTT(CTT/TTT)	Leu or Phe	Col-0/Est-1	2
2	GCA	Ala	Col-0	KTT(GTT/TTT)	Val or Phe	New/Est-1	2
3	GCA	Ala	Col-0	TTT	Phe	Est-1	51
4	GMA(GCA/GAA)	Ala or Glu	New/Col-0	KTT(GTT/TTT)	Val or Phe	New/Est-1	1
5	GMA(GCA/GAA)	Ala or Glu	New/Col-0	TTT	Phe	Est-1	32
6	GWA(GAA/GTA)	Ala or Val	New/Col-0	CTT	Leu	New	6

[1]IUPAC nucleotide code: M- A or C, W- A or T, Y- C or T, K- G or T, and S- G or C.

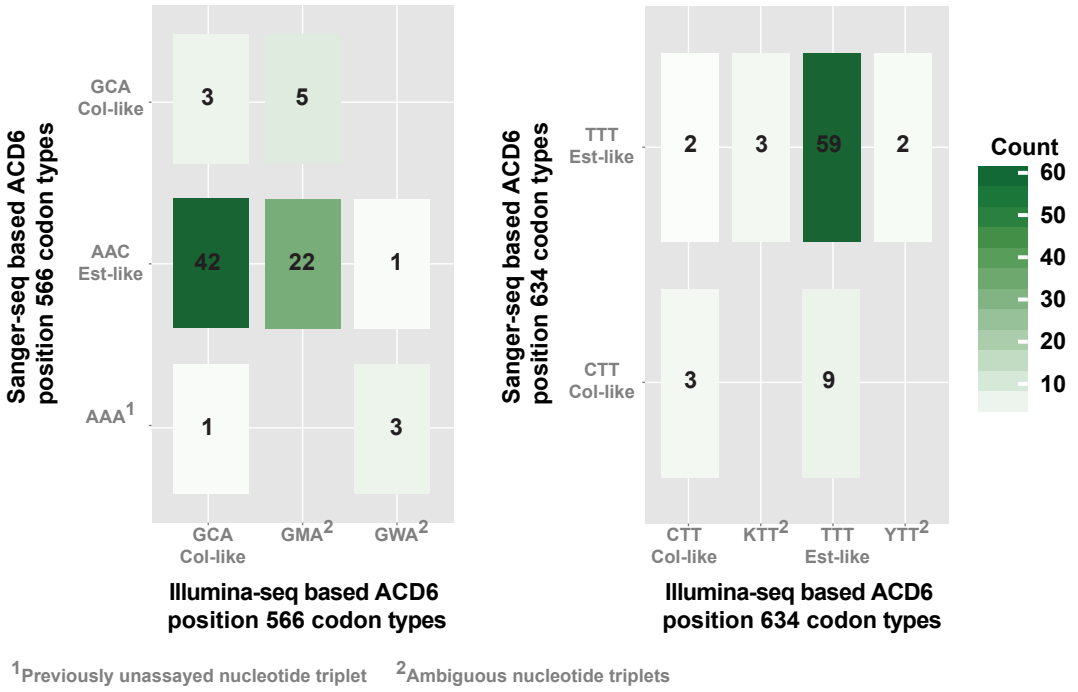

Figure 3.3 Illumina short-read sequencing and Sanger sequencing codon call concordance for *ACD6* nucleotides encoding amino acids 566 and 634.

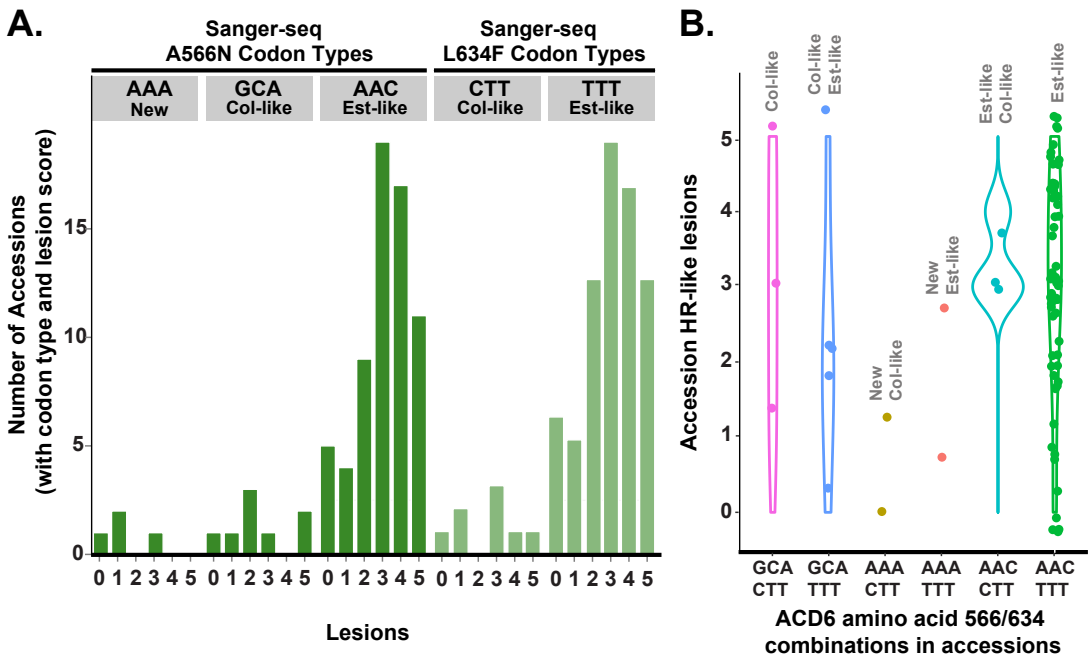

Figure 3.4 Correlation of lesions with codon types for ACD6 residues 566 and 634. A) Taking each codon type at position 566 and 634 separately, accessions with Est-like codons have more severe lesions. B) Codon type combination AAC(Asn)/TTT(Leu) was present in most of the accessions with severe lesions.

3.2 Diversity and maintenance of *ACD6* allele types

Based on nucleotide-triplets for *ACD6* amino acid 634 from the 858 *A. thaliana* accessions for classifying *ACD6* allele type, I could detect predominantly accessions with Col-0 *ACD6* alleles (Figure 3.5). Accessions with Est-like *ACD6* alleles consisted of 12% of the population tested, another 4% of the population had neither Col-0 nor Est-1 but other types of *ACD6* alleles. Shown in Figure 3.5 are the geographic origins of the accessions tested, from which it is clearly seen that these different *ACD6* allele types co-occurred with each other. As suggested by Todesco and colleagues (Todesco, Balasubramanian et al. 2010), co-occurrence of these functionally distinct *ACD6* alleles in both local and global populations of *A. thaliana* is congruous with this locus being under balancing selection.

To make further use of the short-read data from the 1001 Genomes project, I adapted an alternative method, Mash. Originally described by Ondov and colleagues (Ondov 2015) as rapid estimation of pairwise distances between genomes or metagenomes based on raw reads, I adapted Mash for estimating similarity of gene short-read sequences to reference allele types. Mash, which is based on an algorithm called MinHash, divides sequence information into k-mers, which in turn are reduced to a representative sketch before comparison. Reduction occurs through transforming all k-mers using hash function[1] and selection of a k-mer represented by minimum value. The reduction process is repeated thousands of times with different, arbitrary hash functions, in consequence of that thousands of independent minimal k-mers are saved into sketch. Similarity between sequences of different Arabidopsis accessions can be calculated by counting number of minimal k-mers that co-occur. Consequently, the more min-hashes (reduced k-mers) two sequences share, the more similar they are (Ondov 2015). K-mer similarity reflects not only shared substitutions but also shared structural variants such as indels and inversions. I calculated similarity of short-read sequences from 858 accessions of Arabidopsis to reference alleles of genes *ACD6*, *FLS2* and *PR1*. I used Est-1 *ACD6* and Col-0 *ACD6* as reference sequence. For comparing and for contrasting, I also estimated the diversity of two other

[1] function which allows transformation of character string into numeric

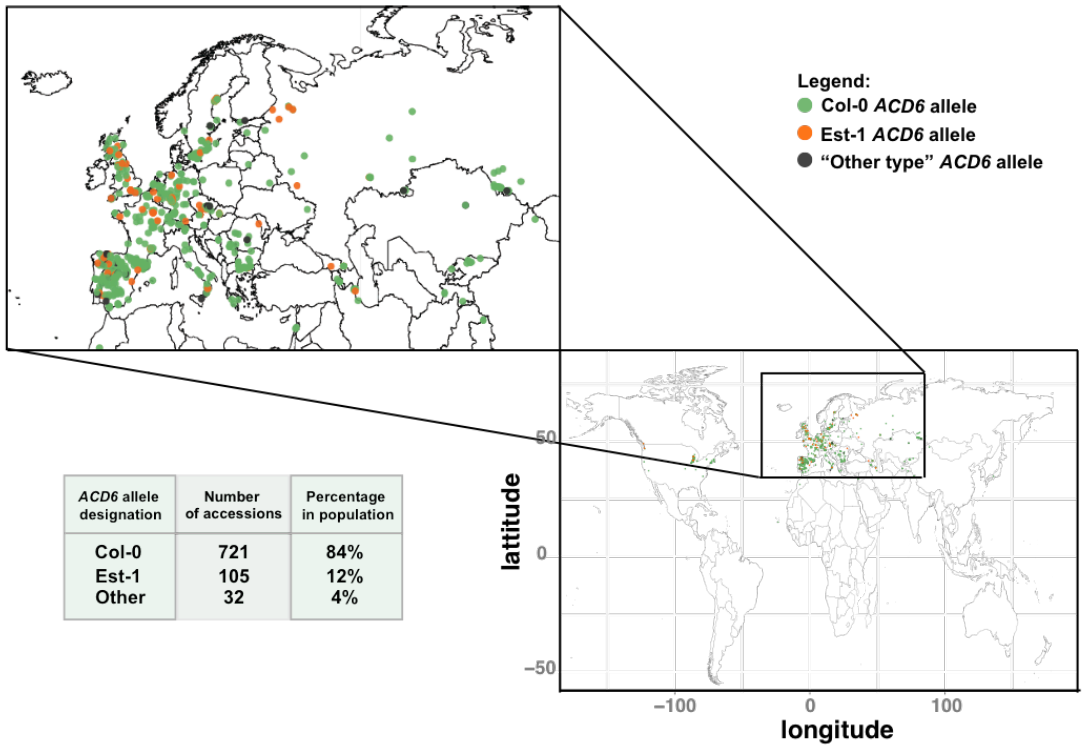

ACD6 allele designation	Number of accessions	Percentage in population
Col-0	721	84%
Est-1	105	12%
Other	32	4%

Figure 3.3 Worldwide distribution of tested *Arabidopsis thaliana* accessions; color-coded based on short-read sequencing reconstituted *ACD6* allele types. Accessions that are Est-like at amino acid position 634 are color-coded orange while accessions that are Col-like for the same amino acid position are color-coded as green.

ACD6-related immune genes, using Col-0 *FLS2* and Col-0 *PR1* sequences as reference. I found more sequence diversity in *ACD6* than *FLS2* and *PR1* (Figure 3.6A and 3.6B). This finding reflected data from Todesco and colleagues (Todesco, Kim et al. 2014) in which they found several other diverse *ACD6* allele types from accessions such as Se-0, Mir-0, Bla-1.

These alleles had duplications and deletions at different parts, which are very distinct from the *ACD6*-Est-1 and the *ACD6*-Col-0 alleles. Clearly, there are more *ACD6* allele types than what was previously known. By contrast, diversity of *FLS2* locus is characterized by fewer non-reference alleles than in *ACD6* alleles, as shown by the bulk of accessions sharing high number of k-mers with Col-0 *FLS2* reference sequence (Figure 3.6B and 3.6C). Similar pattern could be observed for *PR1* alleles except that there were 16 outlier accessions sharing less than 1000 k-mers with Col-0 *PR1* reference (Figure 3.6D). Those accessions all originate from Sweden.

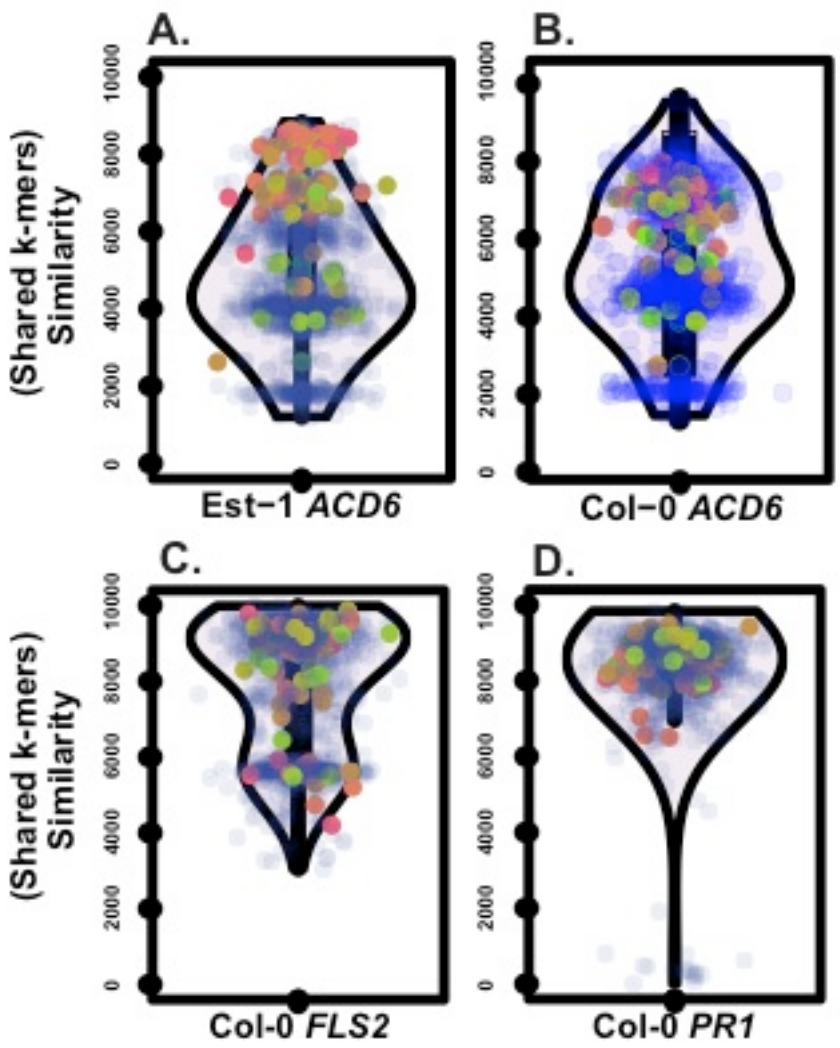

Figure 3.4 Diversity estimation of *Arabidopsis thaliana* accessions based on selected genes in the *ACD6* pathway. Mash (shared k-mers) similarity estimates were based on the following reference sequences: A) Est-1 *ACD6*, B) Col-0 *ACD6* C) Col-0 *FLS2*, and D) Col-0 *PR1*.

Accessions that were phenotyped for lesions are color-coded from light green to salmon based on the increasing severity of the lesion phenotype. Other accessions that have not been phenotyped for lesions are color-coded blue.

The bulk of *A. thaliana* accessions had ~5000 out of 10000 k-mers shared with either the Est-1 *ACD6* or Col-0 *ACD6* allele as reference. While the distribution trend for the tested accessions was similar when using either Est-1 *ACD6* or Col-0 *ACD6* allele as reference, severity of lesions in a subset of phenotyped *A. thaliana* accessions seemed to correlate with how similar their *ACD6* alleles were to Est-1 and not Col-0 (Figure 3.6A and 3.6B). The accessions phenotyped as having Est-like HR lesions are bulked as sharing >8000 out of 10000 k-mers with Est-1. These same accessions shift lower in the distribution when Col-0 *ACD6* allele is used as a reference, having >6000 out of 10000 but <8000 out of 10000 k-mers shared with Col-0 *ACD6*. Huge variability in shared k-mers in *ACD6* locus is likely caused by structural variants such as inversions and insertions described in Se-0, Bla-1 and Mir-0 accessions (Todesco, Kim et al. 2014). Substitutions and more specifically causative SNPs have little impact on the number of shared k-mers, which explains the close similarity of Est-1 like and Col-0 like alleles. In summary, Est-1 like and Col-0 like alleles are distinct by numerous SNPs, however, are similar by structural variation. It has been posited that there is a latitudinal gradient in species richness within the geographic range of growth (Hillebrand 2004). One longstanding hypothesis for the origin of the latitudinal richness gradient is the ‘‘biotic interactions hypothesis,’’ which posits that species interactions are stronger and more specialized at lower latitudes, promoting greater diversification rates and species richness (Schemske, Mittelbach et al. 2009). Indeed such a latitudinal gradient seemed to be apparent when one hones into accessions marked as having Est-like *ACD6* alleles. I plotted the geographical occurrence of each of these accessions with the corresponding lesion phenotype observed when they were grown in the lab (Figure 3.7). Based on this plot there were seemingly more diversified levels of *ACD6* hyperactivity in the accessions coming from the lower latitudes of *A. thaliana* geographic range. At the same time, a mild latitudinal gradient coinciding with increasing severity of lesions spanning from Portugal to Sweden could be observed.

I constructed a simple 3D scatterplot for an initial overview of *A. thaliana* lesion phenotype dependent on latitude and k-mer based *ACD6* allele

type. The plot also includes a plane overlay depicting the simple fitted relationship:

$$Y_i \sim A_i + B_i$$

where:

Y_i = Lesion phenotype severity

A_i = Individual *A. thaliana* accession latitudinal coordinate

B_i = k-mer based allele type of tested gene

This regression analysis showed that both *ACD6* allele type (p=2.37E-06) and latitudinal coordinate (p=0.05) had significant correlation with the lesion phenotype severity (Figure 3.8). Taken together, an *A. thaliana* accession's k-mer based *ACD6* allele type designation and latitudinal coordinate accounted for 33% (F-statistic 18.71, p-value: 2.76E-07) of the variation observed in the coordinate. Unlike in the *ACD6* case, neither *FLS2* nor *PR1* allele type to exhibit appositeness with lesion development (Figure 3.8). Although more formal testing should be done, these results suggest that *ACD6* alleles are distributed along a latitudinal gradient.

Substantiating these initial regression analyses, I fit all factorial information available, namely: *ACD6* allele type, latitudinal coordinate from place of accession origin, longitudinal coordinate, and genetic (kinship) group designation (Genomes Consortium. Electronic address and Genomes 2016). The factorial information was modeled following this equation:

$$A_i \sim B_i + C_i + D_i + E_i$$

where:

A_i = Lesion phenotype severity

B_i = k-mer based allele type of tested gene

C_i = Individual *A. thaliana* accession latitude coordinate

D_i = Individual *A. thaliana* accession longitude coordinate

E_i = Individual *A. thaliana* accession genetic group designation

The sample included 72 accessions with confirmed lesion phenotypes (Table 3.2). The model that explained the most variance (44%) in the lesion phenotype observed was a linear model of lesion phenotype as a function of all the factorial information available (F-statistic, p-value 8.3E-07, variable p-value 8.84E06, significance level 0.001). The model where the lesion phenotype was the direct consequence of *ACD6* allele type accounted for

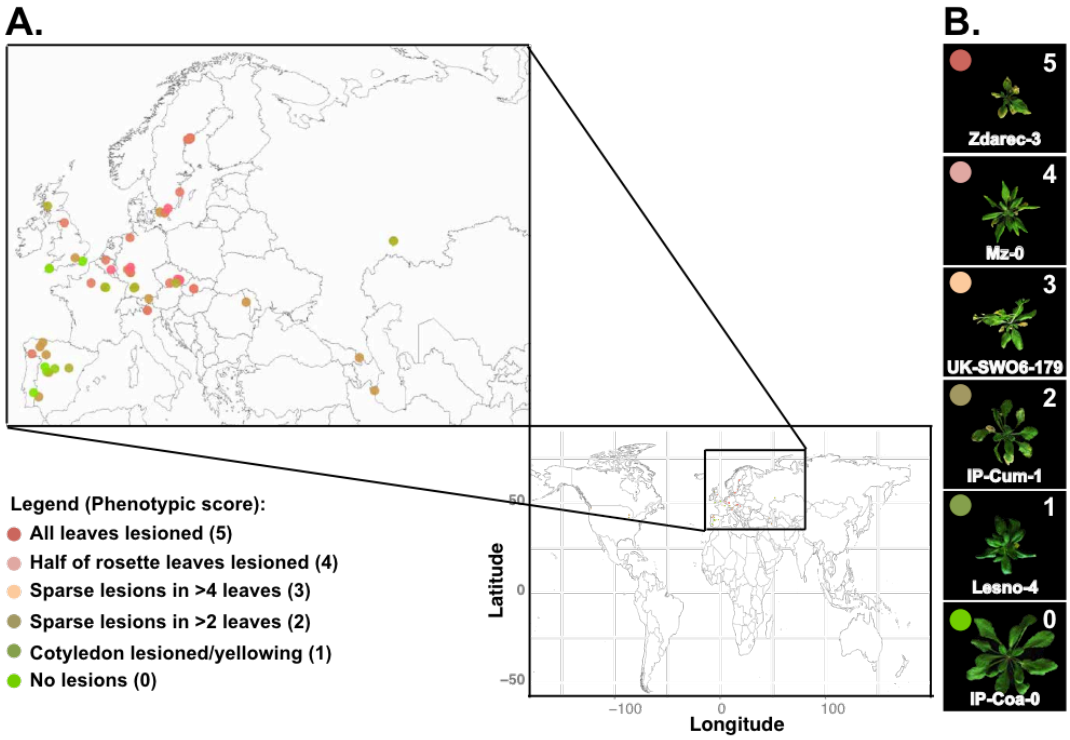

Figure 3.6 Distribution of Est-1 like *ACD6* alleles and lesioning among *A. thaliana* accessions. A) Est-like *ACD6* alleles color-coded based on the severity of the appearance of lesions (as shown in inset legend). B) Representative accessions for different lesion severity.

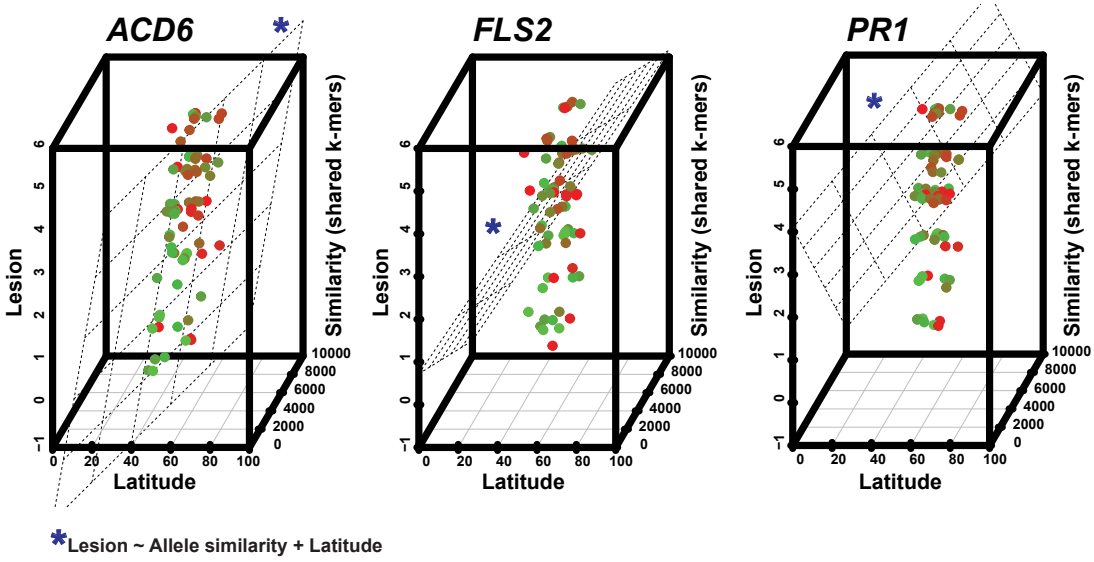

Figure 3.5 Interaction plot between the lesion phenotype, latitudinal coordinate and k-mer based gene similarity. A regression plane is plotted based on a fitted linear model where the lesion phenotype is the result of the linear combination between the accession's latitudinal coordinate and the k-mer based gene similarity.

30.74% of the variation observed (Table 3.3). Furthermore, sequentially dropping out a factor for each linear model constructed, yielded *ACD6* allele type as the most significant function that contributed to the lesion phenotype (Table 3.3). With this result, it seemed that an accessions lesion phenotype was significantly dependent on the *ACD6* allele type. As with the regression analyses, I also tested the same models for lesion phenotype development in which *ACD6* allele type was substituted for *PR1* or *FLS2* allele type. Comparable with the assumptions made from the 3D scatterplots, variance (10%) in lesion development given either an *FLS2* or *PR1* allele type could mostly be attributed to the latitudinal coordinate of the accessions tested (Table 3.4 and 3.5). The *FLS2* full factorial model explained 16.2% of the variance observed (F-statistic, p-value 3.6E-02, variable p-value 8.4E03, significance level 0.01). As with *FLS2*, the *PR1* full factorial model explained the most variance (17.36%) observed (F-statistic, p-value 2.6E-02, variable p-value 0.0716, significance level 0.1). Unlike for *ACD6*, the lesion phenotype is not strongly correlated with an accession's *FLS2* or *PR1* allele type.

Taking all these results together, it seems that lesion phenotype had a discernible dependence on latitudinal coordinates. However, it is clear that *ACD6* allele type predominantly contributed to development of the lesion phenotype and not the other genes tested.

3.1 Accessions with Est-like *ACD6* alleles differ in lesion phenotypes

The results from the previous sections confirmed Todesco and colleagues (2010) initial finding that there is variation in the expressivity of Est-like *ACD6* alleles (Figure 3.7). Simultaneously grown and phenotyped at 23°C LD, 10 of 102 accessions with an Est-like *ACD6* allele did not show clear lesion (Figure 3.9). *ACD6* activity in those accessions was modulated. Modulation could be an effect of either of intragenic, i.e. in *ACD6* itself, or extragenic nature. Intragenic modifiers might render the protein inactive or perturb the normal protein function of Est-*ACD6*. Extragenic suppressors could either directly or indirectly interfere with *ACD6*-mediated response. The nature of these modulators of *ACD6*-dependent phenotypes present in the identified accessions were investigated and discussed in Chapter 4.

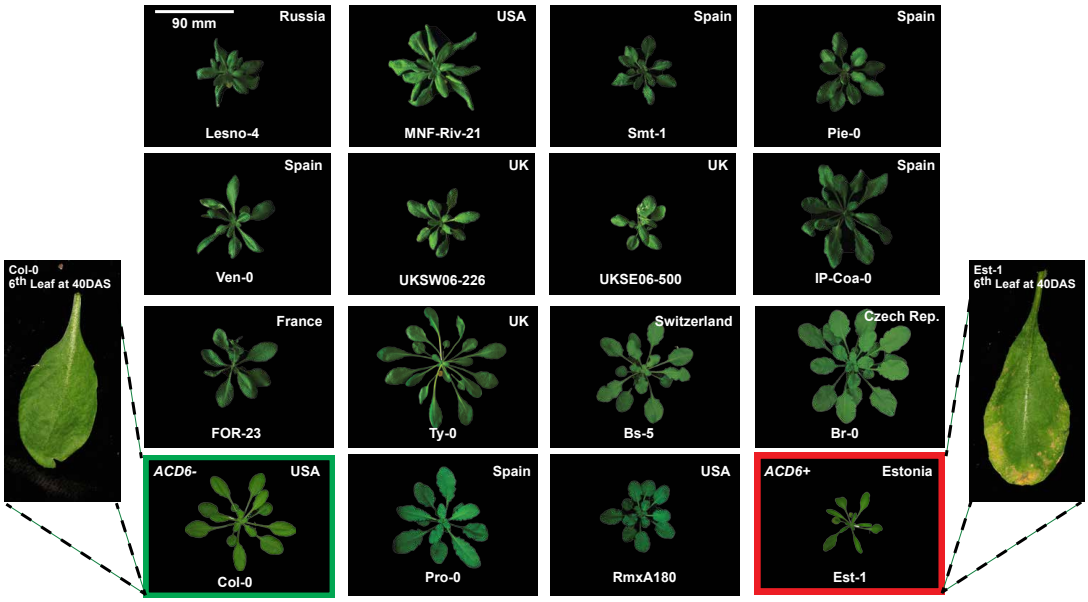

Figure 3.7 Accessions with an Est-like *ACD6* allele but without obvious lesions. Insets are the control accessions: bordered green is Col-0 with non-hyperactive *ACD6* allele; red bordered is Est-1 with a hyperactive *ACD6* allele.

Table 3.3 Comparison of linear model fits for explaining lesion phenotype variation in 72 accessions using factorial information -- *ACD6* allele type, geographical coordinates and genetic group

Linear Model	Variable having the significant effect	% Variation Explained	R-squared	F-statistic, p-value	Coefficients/variable	Variable p-value	Significance level
$A_i = B_i + C_i + D_i + E_i$	Allele type	44.1800	0.4418	8.3E-07	Intercept	0.034	*
					B	8.84E-06	***
					C	0.089	.
					D	0.783	
					E	0.537	
$A_i = B_i + C_i + D_i$	Allele type & an undefined factor	34.1000	0.3410	1.2E-06	Intercept	3.77E-02	*
					B	2.57E-06	***
					C	1.01E-01	
					D	6.28E-01	
$A_i = B_i + C_i$	Allele type, latitudinal vector and an undefined factor	33.8800	0.3388	2.8E-07	Intercept	2.18E-02	*
					B	2.37E-06	***
					C	5.04E-02	.
$A_i = B_i$	Allele type	30.7400	0.3074	1.7E-07	Intercept	2.04E-01	
					B	1.68E-07	***
$A_i = C_i$	Latitudinal vector	10.1100	0.1011	5.1E-03	Intercept	5.81E-01	
					C	5.12E-03	**
$A_i = D_i$	An undefined factor	0.5698	0.0057	5.2E-01	Intercept	<2e-16	***
					D	5.17E-01	
$A_i = E_i$	An undefined factor	0.2555	0.0026	7.0E-01	Intercept	<2e-16	***
					E	0.214	

Where: A – lesion phenotype, B – *ACD6* allele type, C – latitudinal vector, D – longitudinal vector, and E – genetic/kinship group; Significance codes: 0 '***' 0.001 '**' 0.01 '*' 0.05 '.' 0.1 ' ' 1

Table 3.4 Comparison of linear model fits for explaining lesion phenotype variation in 72 accessions using factorial information – *FLS2* allele type, geographical coordinates and genetic group

Linear Model	Variable having the significant effect	% Variation Explained	R-squared	F-statistic, p-value	Coefficients/variable	Variable p-value	Significance level
$A_i = B_i + C_i + D_i + E_i$	Latitudinal vector	16.2000	0.1620	3.6E-02	Intercept	0.8959	
					B	0.2684	
					C	0.0084	**
					D	0.8336	
					E	0.2672	
$A_i = B_i + C_i + D_i$	Latitudinal vector	12.0500	0.1205	2.5E-02	Intercept	0.703	
					B	0.225	
					C	0.0185	*
					D	0.9778	
$A_i = B_i + C_i$	Latitudinal vector	11.1800	0.1118	1.3E-02	Intercept	0.76869	
					B	0.3511	
					C	0.00633	**
$A_i = B_i$	An undefined factor	3.4420	0.0344	1.1E-01	Intercept	7.82E-06	***
					B	0.106	
$A_i = C_i$	Latitudinal vector	10.1100	0.1011	5.1E-03	Intercept	0.58141	
					C	0.00512	**
$A_i = D_i$	An undefined factor	0.5698	0.0057	5.2E-01	Intercept	<2e-16	***
					D	0.517	
$A_i = E_i$	An undefined factor	0.2555	0.0026	7.0E-01	Intercept	5.31E-13	***
					E	0.696	

Where: A – lesion phenotype, B – *FLS2* allele type, C – latitudinal vector, D – longitudinal vector, and E – genetic/kinship group; Significance codes: 0 '***' 0.001 '**' 0.01 '*' 0.05 '.' 0.1 ' ' 1

Table 3.5 Comparison of linear model fits for explaining lesion phenotype variation in 72 accessions using factorial information – *PR1* allele type, geographical coordinates and genetic group

Linear Model	Variable having the significant effect	% Variation Explained	R-squared	F-statistic, p-value	Coefficients/variable	Variable p-value	Significance level
$A_i = B_i + C_i + D_i + E_i$	Latitudinal vector	17.3600	0.1736	2.6E-02	Intercept	0.2904	
					B	0.1537	
					C	0.0716	.
					D	0.6918	
					E	0.2672	
$A_i = B_i + C_i + D_i$	Latitudinal vector	12.4200	0.1242	2.2E-02	Intercept	0.3034	
					B	0.1836	
					C	0.0708	.
					D	0.8189	
$A_i = B_i + C_i$	Latitudinal vector	12.3500	0.1235	8.1E-03	Intercept	0.2757	
					B	0.1759	
					C	0.0653	.
$A_i = B_i$	None	0.8745	0.0087	4.2E-01	Intercept	0.176	
					B	0.419	
$A_i = C_i$	Latitudinal vector	10.1100	0.1011	5.1E-03	Intercept	0.58141	
					C	0.00512	**
$A_i = D_i$	An undefined factor	0.5698	0.0057	5.2E-01	Intercept	<2e-16	***
					D	0.517	
$A_i = E_i$	An undefined factor	0.2555	0.0026	7.0E-01	Intercept	5.31E-13	***
					E	0.696	

Where: A – lesion phenotype, B – *PR1* allele type, C – latitudinal vector, D – longitudinal vector, and E – genetic/kinship group; Significance codes: 0 '***', 0.001 '**', 0.01 '*', 0.05 '.', 0.1 '.'

4 Responses associated with the modulation *of ACD6* activity

"Plant pathology has become a utilitarian science of vast possibilities."

- Joseph Charles Arthur.

1904

The fact that most plants appear healthy in an environment teeming with pathogens attests to plants' capability and development of effective defense repertoires.

Plant responses to pathogens generally progress from: 1) initial recognition of the pathogen, 2) a signaling cascade, often including hormones, to 3) broad transcriptional reprogramming for production of proteins to induce or repress key segments of the response pathway (Figure 4.1). Parts of plant defense pathways can be appraised using specific assays.

- To inspect pathogen recognition capability, a pathogen associated molecular pattern (PAMP) induced reactive oxygen species (ROS) production assay or direct pathogen-infection assays can be utilized.
- Some surveys to gauge reactivity of the defense-signaling cascade include hormone level quantification, and MAPK (mitogen-activated protein kinase) activity assays.
- Tests for downstream responses include: quantification of antimicrobial compounds, hypersensitive response severity, callose deposition and comprehensive growth changes (i.e. infection induced growth inhibition). Most importantly, differences in marker gene expression can be utilized to monitor each step of the reaction cascade.

Mechanisms for fine-tuning the trade-off between defense and growth are yet to be exhaustively described. To this end, the case of the hyperactive Est-1 *ACD6* allele that strongly enhances resistance to a broad range of pathogens

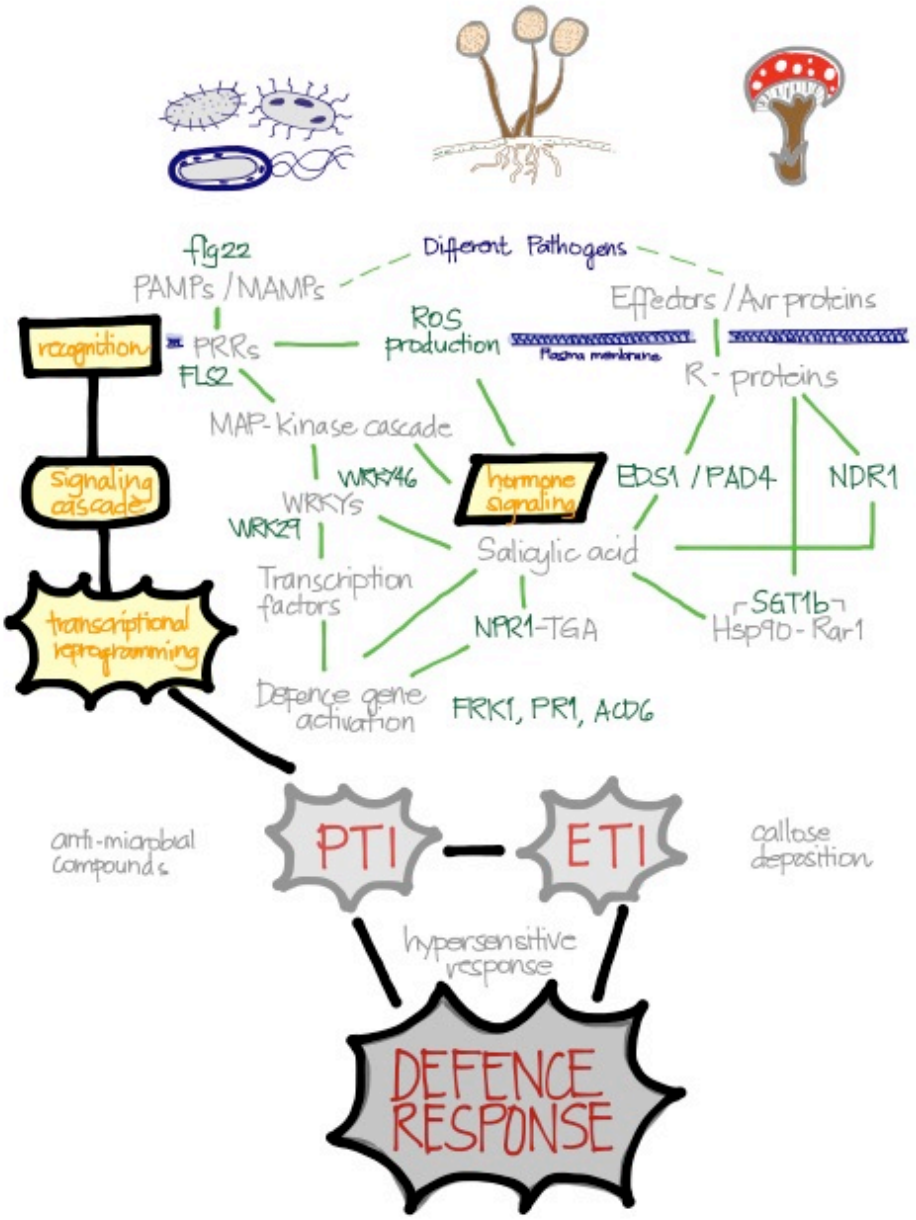

Figure 4.1 A generalized illustration of plant defense.

Abbreviations: flg22 – flagellin 22; P/MAMPs – pathogen/microbe associated molecular patterns; PRR – pattern recognition receptor; ROS – reactive oxygen species; Avr – avirulence; MAP-kinase – mitogen associated protein kinase; *EDS1 – ENHANCED DISEASE SUSCEPTIBILITY 1*; *PAD4 – PHYTOALEXIN DEFICIENT* 1; *NDR1 – NON-RACE SPECIFIC DISEASE RESISTANCE PROTEIN* 1; *SGT1b – SGT1 HOMOLOG b*; *HSP90 – HEAT SHOCK PROTEIN 90*; *RAR1 – REQUIRED FOR MLA1 RESISTANCE 1*; *NPR1 – NONEXPRESSER OF PR GENES* 1; *FRK1 – FLG22-INDUCED RECEPTOR KINASE*; *PR1 – PATHOGENESIS RELATED GENE* 1; *ACD6 – ACCELERATED CELL DEATH 6*; PTI – PAMP-triggered immunity; ETI – effector-triggered immunity.

while having a concomitant reduction in growth potential (Todesco, Balasubramanian et al. 2010) presents a useful case to supplement current knowledge. In this Chapter, I delve into the details of the *ACD6*-dependent trade-off between growth and defense with the aid of accessions that differ in expressivity of Est-like *ACD6* alleles. The objectives for this chapter were:

- To determine whether intragenic or extragenic modifiers are responsible for modulating hyperactive *ACD6*-dependent phenotypes,
- To characterize the variation in the *ACD6*-dependent phenotypes such as rosette size differences, appearance of late-onset necrosis/lesions, and defense response activation (SA accumulation, PAMP-induced ROS production and marker gene expression).
- To identify key pathways and candidate genes relevant for modulation of *ACD6*-dependent responses

To accomplish these objectives I mainly tested the accessions Pro-0 and Rmx-A180. For some assays I also included Bs-5 and Br-0, accessions that I identified later, which had Est-like *ACD6* alleles but with modulated *ACD6*-dependent phenotypes.

4.1 Pro-0 and Rmx-A180 have extragenic modifiers of *ACD6*-dependent phenotypes

ACD6 hyperactivity in Est-1 is not due to gene expression differences (Todesco, Balasubramanian et al. 2010). Nonetheless, it is possible that some Est-like *ACD6* alleles contain polymorphisms that will result in modifications of the gene expression profile of *ACD6* or in a truncated protein that can ultimately perturb the downstream pathways. As shown in Figure 4.2, *ACD6* gene expression increased in all the genotypes (Est-1, Col-0 and Pro-0) tested as the plants aged. At the last stage of Est-1 development the increase in *ACD6* level was more pronounced compared to Col-0 or Pro-0. High *ACD6* expression has been shown to activated expression of downstream gene *PR1* (Todesco, Balasubramanian et al. 2010). However, *PR1* gene expression was concurrently induced only in Est-1(Todesco, Balasubramanian et al. 2010). Consistent with this, appearance of lesions was only apparent in Est-1.

Together, these findings show that the *ACD6* allele of Pro-0 did not induce the defense response as in Est-1 despite encoding the causal amino acid changes for the hyperactivity of the *ACD6*-Est-1 allele.

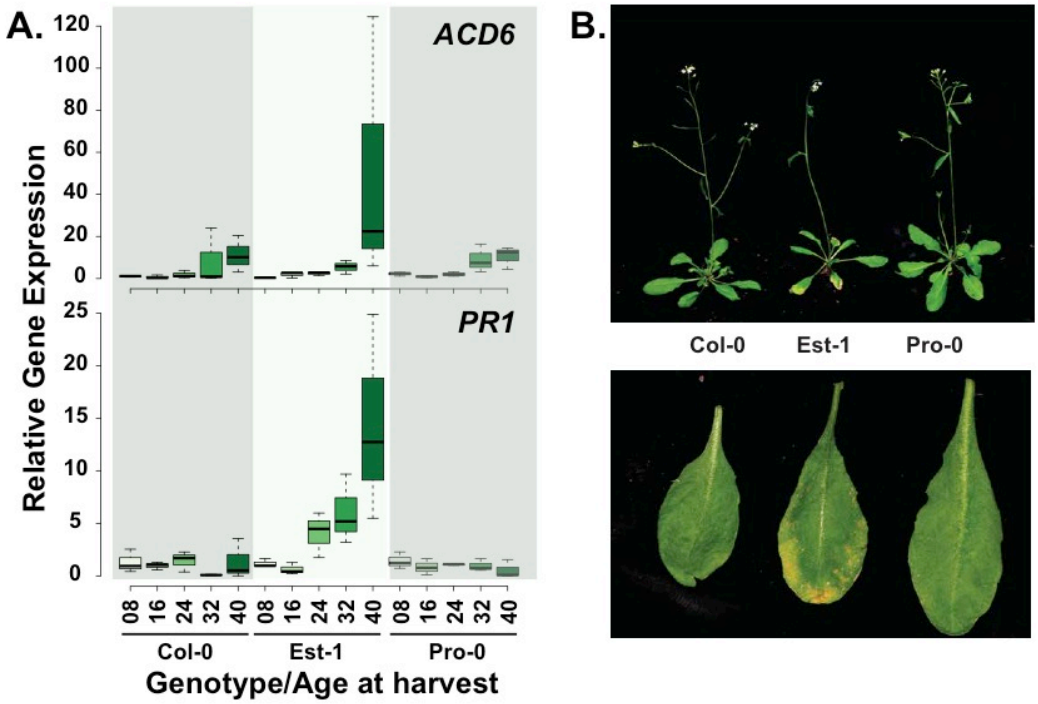

Figure 4.2 ACD6 hyperactivity phenotypes are suppressed in Pro-0. A) Whole plant gene expression kinetics of ACD6 and PR1 from 6 to 40 days after sowing. B) Characteristic phenotypes of Col-0, Est-1 and Pro-0 at data collection endpoint (40 days after sowing). Below each plant are 6th leaf representatives corresponding to the accession shown above it.

In order to test whether the *ACD6*-Pro-0 allele was suppressed due to an intragenic or extragenic mutation, I cloned the *ACD6*-Pro-0 allele and transferred it to either *acd6-2* (an *ACD6* T-DNA knockdown mutant) or Col-0 (accession with a standard non-hyperactive *ACD6* allele). The resulting transgenics had small rosette size, exhibited late-onset necrosis and had *PR1* levels comparable to Est-1 (Figure 4.3). Moreover, the transgenics had a higher *PR1* gene expression compared to the wild type counterparts. I also cloned the *ACD6*-Rmx-A180 allele and had the same results as with the *ACD6*-Pro-0 allele (Figure 4.3). Both results show that when Est-like *ACD6* alleles from Pro-0 and Rmx-A180 that do not show phenotypic signs of *ACD6*

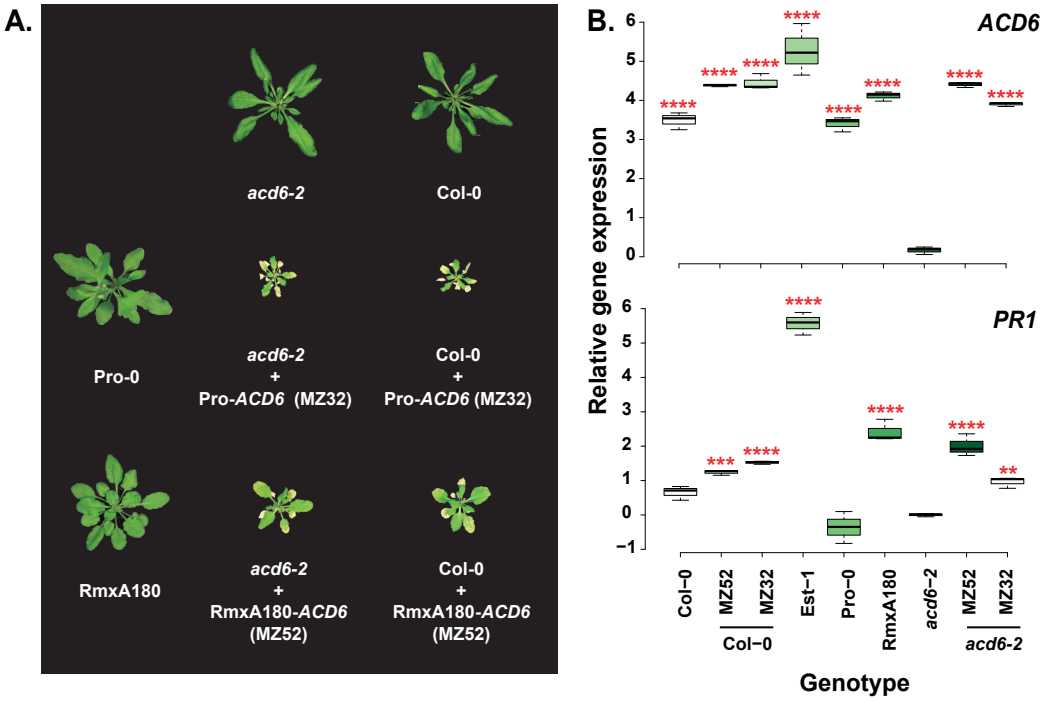

Figure 4.3 Est-like *ACD6* alleles from Pro-0 and Rmx-A180 are functional. Transformation into accession containing a non-hyperactive *ACD6* allele (Col-0) and *ACD6* T-DNA knockdown mutant (*acd6*-2) background unmasked suppression of the Pro-0 and Rmx-A180 *ACD6* alleles. A) Characteristic phenotype of the transgenics. B) Whole plant *ACD6* and *PR1* relative gene expression in representative transgenics and the reference wild-type genotypes grown at 23°C at 40 DAS.

Gene expression data for each genotype is from 3 biological replicates. Red asterisks indicate pairwise comparisons using t-tests with pooled SD, significant difference relative to *acd6*-2; p-value: **** < 0.0001 , *** < 0.001, ** < 0.005, *< 0.05.

hyperactivation are transferred into a different genetic background, the hyperactivity of the cloned *ACD6* alleles does not seem to be blocked.

I checked for sequence differences between *ACD6*-Est-1 and *ACD6*-Pro-0 and found that *ACD6*-Pro-0 had a 957bp shorter 5' UTR region (which included the promoter) than *ACD6*-Est-1 (Table 4.1, Figure 4.4A). To confirm that the differences in *ACD6* activity in Est-1 and Pro-0 were not due to promoter differences, I made chimeras of the *ACD6*-Pro-0 and *ACD6*-Est-1 alleles where 5' region including the promoter were swapped. Exact details on the construction of the chimeras are shown in Table 4.2. The first half of the *ACD6*-chimera 1 (MZ34) included *ACD6*-Pro-0 genomic DNA sequence from 1 bp - 4,073 bp (including the promoter region). The second half was composed of *ACD6*-Est-1 genomic DNA sequence 4,031 bp – 7986 bp.

ACD6-chimera 2 (MZ36) had the first part from *ACD6*-Est-1 genomic DNA truncated. The second half of *ACD6*-chimera 2 (MZ36) was from *ACD6*-Pro-0 genomic DNA sequence 4,773 bp – 7030 bp (Figure 4.4A). Either chimera was functional in the T-DNA *ACD6* knockdown mutant (*acd6*-2) and in Col-0, which has a standard *ACD6* allele that does not cause lesions (Figure 4.4B and 4.4C). This showed that the despite being shorter the *ACD6*-Pro-0 promoter region functioned similar to the Est-1 promoter region. The 3' segment of *ACD6*-Pro-0 that contained the Est-like *ACD6* hyperactivity causal amino acid changes, also worked the same as the *ACD6*-Est-1 3' segment.

Table 4.1 Pro-0 and Est-1 *ACD6* genomic feature annotation

Genomic DNA (gDNA)	Coordinates (bp)			Total Length (bp)
	5' UTR (Promoter region)	Gene body	3' UTR	
ACD6-Pro-0	1-2585	2586-6271	6272-7030	7030
ACD6-Est-1	1-3542	3543-7229	7230-7986	7986

Table 4.2 Constructed *ACD6*-chimera's genomic feature annotation

Chimera	1st half		2nd half		Total Length (bp)
	Source genomic DNA	Coordinates (bp)	Source genomic DNA	Coordinates (bp)	
ACD6-Chimera 1 (MZ34)	*ACD6*-Pro-0	1-4073	*ACD6*-Est-1	4031-7986	8028
ACD6-Chimera 2 (MZ36)	*ACD6*-Est-1	1-5729	*ACD6*-Pro-0	4773-7030	7986

Additional evidence supporting the functionality of *ACD6*-Pro-0 allele came from genotyping F_2 individuals derived from a cross between Est-1 and Pro-0. At 4 weeks after sowing, the late-onset necrosis phenotype segregated in a 3:1 ratio in this F_2 population, irrespective of the *ACD6* allele type (Figure 4.5). The extragenic nature of the *ACD6* modulator could be inferred from the observation that some F_2 individuals that had *ACD6*-Pro-0 allele exhibited marked late onset necrosis. Likewise, there were F_2 individuals with a homozygous Est-1 *ACD6* allele that did not show symptom of late-onset necrosis, even at 40 days after sowing.

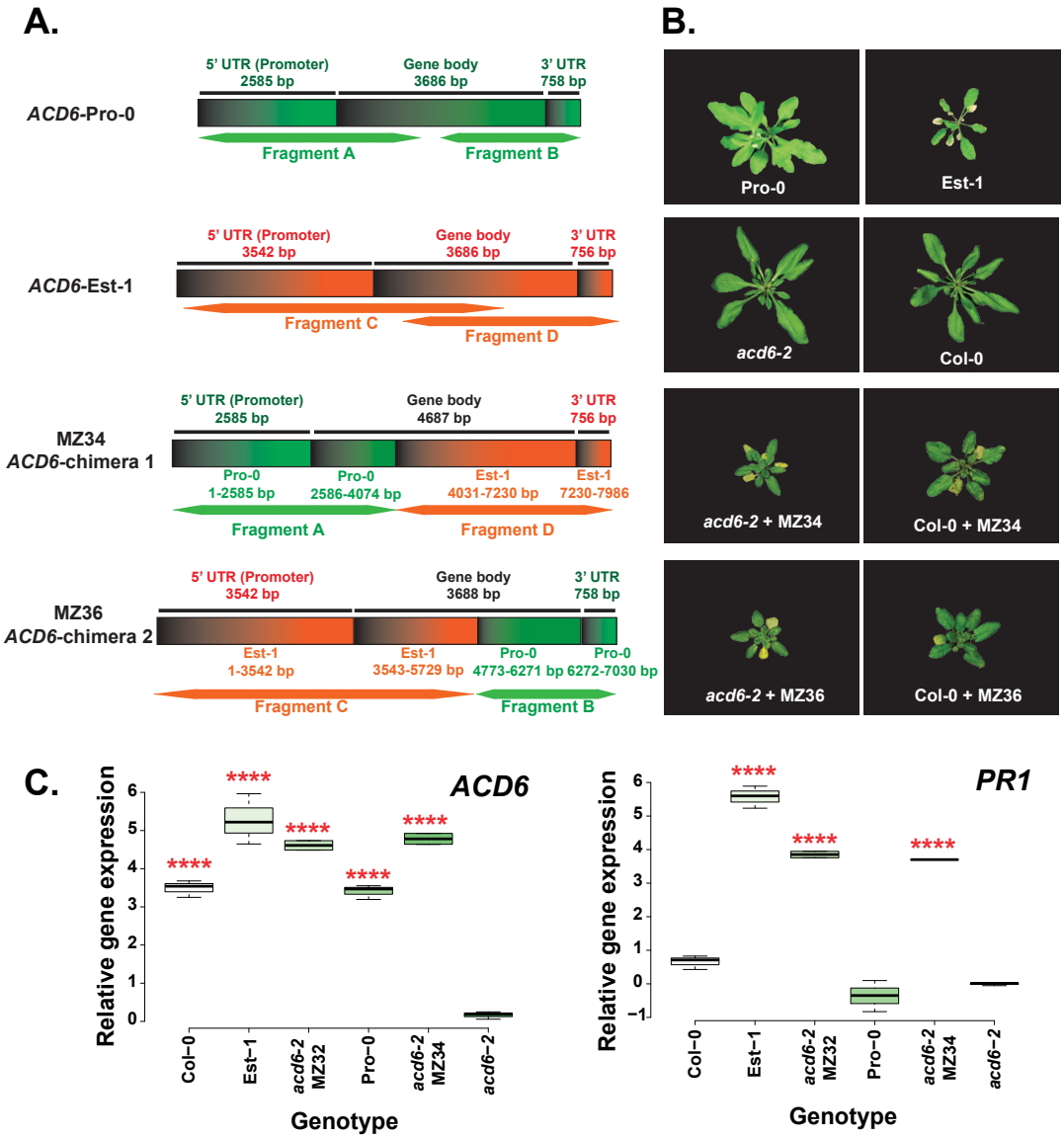

Figure 4.4 The Pro-0 *ACD6* allele is similar to the hyperactive Est-1 *ACD6* allele with respect to production of *ACD6*-dependent phenotypes: late-onset necrosis and reduction in rosette size. Domain swaps between Est-1 *ACD6* and Pro-0 *ACD6* and transformation into *ACD6* null (Col-0) and knockdown (*acd6*-2) background unmasked suppression of the Pro-0 *ACD6* allele. A) Schematic representation of *ACD6*-Pro-0, *ACD6*-Est-1 and *ACD6*-chimera constructs genomic feature annotation. B) Characteristic phenotypes of Pro-0, Est-1, *acd6-2* and Col-0 compared to the *ACD6*-chimera transgenics. C) *ACD6* and *PR1* relative gene expression at 40 DAS in *ACD6*-chimera transgenics and the reference wild-type genotypes.

Gene expression data for each genotype from 3 biological replicates. Red asterisks indicate pairwise comparisons using t-tests with pooled SD, significant difference relative to *acd6*-2; p.value: **** < 0.0001 , *** < 0.001, ** < 0.005, *< 0.05.

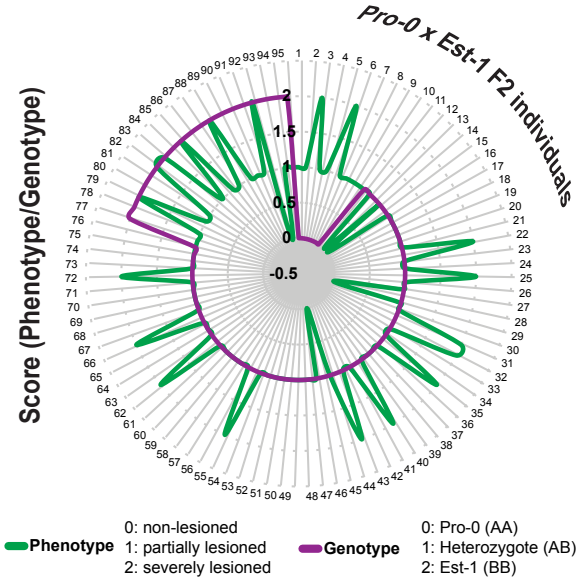

Figure 4.5 Phenotypic and genotypic distribution in a subset of Pro-0 x Est-1 F_2 individuals. *ACD6* allele type and the late-onset necrosis phenotype do not co-segregate.

Furthermore, analysis of full length genomic Sanger sequencing results from both the Pro-0 and the Rmx-A180 *ACD6* alleles did not reveal any SNPs that could cause the protein to be sufficient to block Est-1 *ACD6* hyperactivity, moving Est-1 *ACD6* into Pro-0 and Rmx-A180 background suggested the opposite (Figure 4.6). When transformed with Est-1 *ACD6*, primary Pro-0 and Rmx-A180 transformants (T_1s) exhibited strong late-onset necrosis/lesions. Previous results by Rate et al. (1999) showed that *ACD6*-related phenotypes are dosage dependent. It is possible that transgene copy-number influenced the *ACD6* phenotypes but this remains to be tested. It has been a recurring finding that expression levels of *ACD6* are higher in transgenic lines, possibly independent from copy-number (Todesco, Balasubramanian et al. 2010). Taken together, these results show that Est-like *ACD6* alleles in natural accessions are functional but do not result in Est-like late-onset necrosis due to the presence of extragenic modifiers.

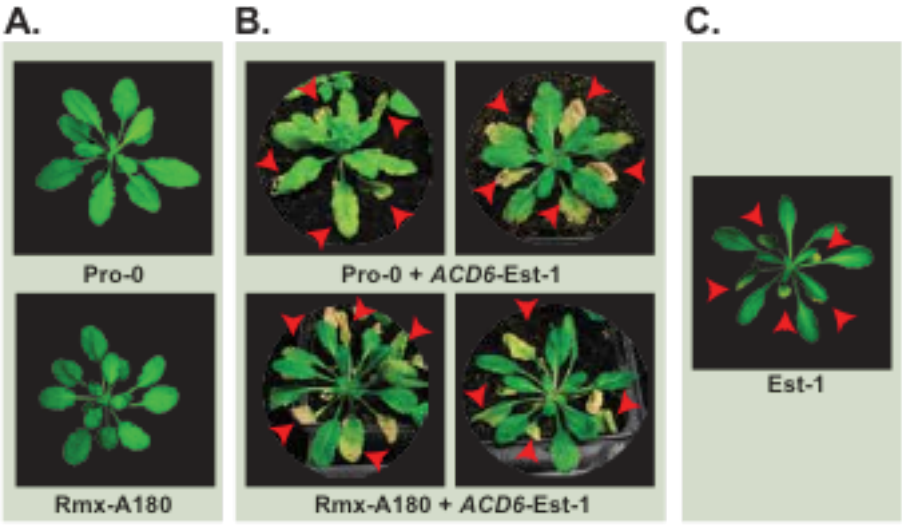

Figure 4.6 Supplementing Rmx-A180 and Pro-0 with *ACD6*-Est-1 resulted in severely lesioned transgenic lines. A) Wildtype Rmx-A180 and Pro-0, B) T_1 Rmx-A180 and Pro-0 supplemented with *ACD6*-Est-1 and C) Wildtype Est-1. Plants were grown at 23°C short day conditions. Photograph was taken 40 days after sowing, Red arrows indicate leaves with HR-like lesions.

4.2 Phenotypic differences between Pro-0 and Rmx-A180

After determining the modulators of *ACD6* hyperactivity are extragenic, I proceeded to describe the phenotypic differences among the reference accession Col-0, the accessions having *ACD6* suppressors (Pro-0 and Rmx-A180) and the accessions with highly active *ACD6* (Est-1 and *acd6*-1). As previously mentioned, the pronounced expression of defense responses conferred by a hyperactive *ACD6* allele is associated with reduced growth. Phenotypes that were scrutinized were biomass (fresh weight), rosette diameter, rosette area, and the occurrence of late-onset necrosis/lesions.

The gain-of-function *acd6*-1 line (Rate, Cuenca et al. 1999) was smaller than its background line, Col-0 (Figure 4.7). Moreover, knocking down *ACD6* in Est-1 increased plant size, as also previously shown by Todesco and colleagues (2010). While Pro-0 rosette size and weight were not altered when knocking down *ACD6,* amiR-*ACD6* expression in Rmx-A180 increased plant size (Figure 4.7). These findings suggested that *ACD6* activity in Pro-0 was differently modulated compared to Rmx-A180.

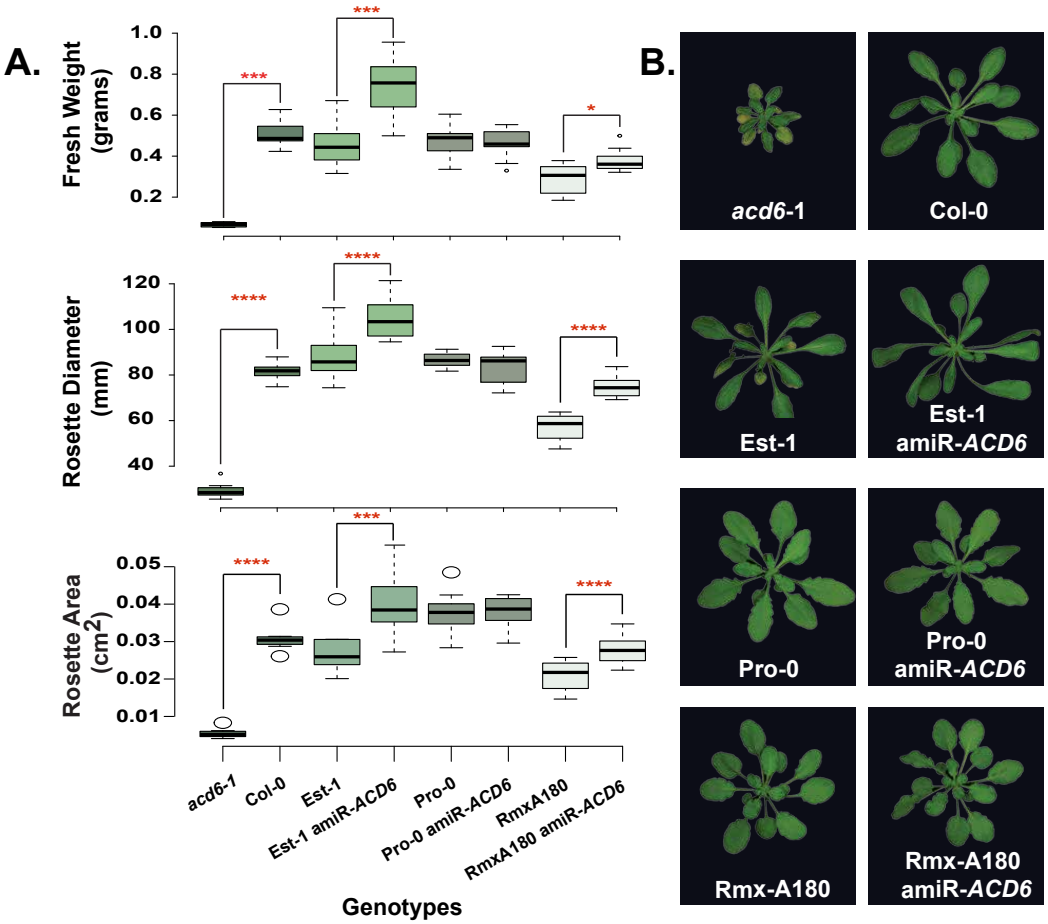

Figure 4.7 *ACD6*-dependence of plant size in accessions with variable *ACD6* activity. A) Fresh weight, rosette diameter and, rosette area in natural accessions and corresponding amiR-*ACD6* transgenics. B) Representative 40 DAS rosette samples for each genotype grown at 23°C short-day conditions for the experiment.

Data point for each genotype is from 8 biological replicates. Red asterisks indicate p-value from pairwise comparisons using t-tests, significant difference relative to the corresponding wild type; p-value: **** < 0.0001 , *** < 0.001, ** < 0.005, *< 0.05.

As late-onset necrosis/appearance of lesions has been used in previous studies as a phenotypic proxy for *ACD6* hyperactivity, I examined the presence of such microscopic cell death on mature leaves of each of the lines exhibiting variable *ACD6* hyperactivity. Trypan blue, a diazo dye that preferentially stains dead cells blue, was used to assess the amount of spontaneous cell death in Col-0, Est-1, Pro-0 and Rmx-A180, with or without amiR-*ACD6*. Other than Est-1, none of the other genotypes showed visible signs of lesions in their leaves (Figure 4.8). While Pro-0 and Rmx-A180 did not show macroscopically visible cell death patches, some leaves (usually the

older ones) exhibited microscopical patches of stained cells. I could therefore confirm that knocking down *ACD6* in Est-1 abolished late-onset necrosis/cell-death (Todesco, Balasubramanian et al. 2010), and that accessions with modulated *ACD6* activity (Pro-0 and Rmx-A180) did not show the same leaf necrosis-related cell death (Figure 4.8). The Pro-0 amiR-*ACD6* Trypan blue staining results support the inferences from macroscopic phenotyping.

4.3 Pro-0 and Rmx-A180 differ in pathogen defense responses

To elucidate how the balance between growth and defense is shifted in accessions with modulated *ACD6* activity, I monitored characteristic defense activation features in Pro-0 and Rmx-A180. I investigated: 1) SA accumulation; 2) PAMP-induced (flg22) ROS response; 3) PTI and ETI as assayed by bacterial infection with a type-III secretion mutant *Pseudomonas syringae pv. tomato DC3000* (*Pst HrcC-*) and *Pseudomonas syringae p.v. maculicola ES4326*, respectively; and 4) defense gene expression.

4.3.1 SA accumulation in Pro-0 and Rmx-A180

To start-off with the assessment of the defense aspect of the trade-off in accessions with modulated *ACD6*, I quantified free salicylic acid (SA) and conjugated SA (measurements were done and made by University of Tübingen, ZMBP Analytics unit) from rosette samples of *acd6*-1, Col-0, Col-0 amiR-*ACD6*, Est-1, Est-1 amiR-*ACD6*, Pro-0, Pro-0 amiR-*ACD6*, Rmx-A180 and Rmx-A180 amiR-*ACD6*.

High SA-containing genotypes usually can mount a robust baseline defense (Yang, Ahammed et al. 2015, Chandra-Shekara, 2006 #1772). The total amount of SA of each of the tested genotypes differed significantly from each other. Similar to the Todesco et al. (2010) results, the gain-of-function mutant *acd6*-1 and hyperactive Est-1 had significantly higher levels of SA than the isogenic Col-0 or Est-1 amiR-*ACD6*.

Compared to the other genotypes tested in this study, the hyperactive genotypes Est-1 and *acd6*-1 had the highest recorded free SA levels, which average at 40,000 ng SA / mg tissue (Figure 4.9A). Pro-0 had a very low

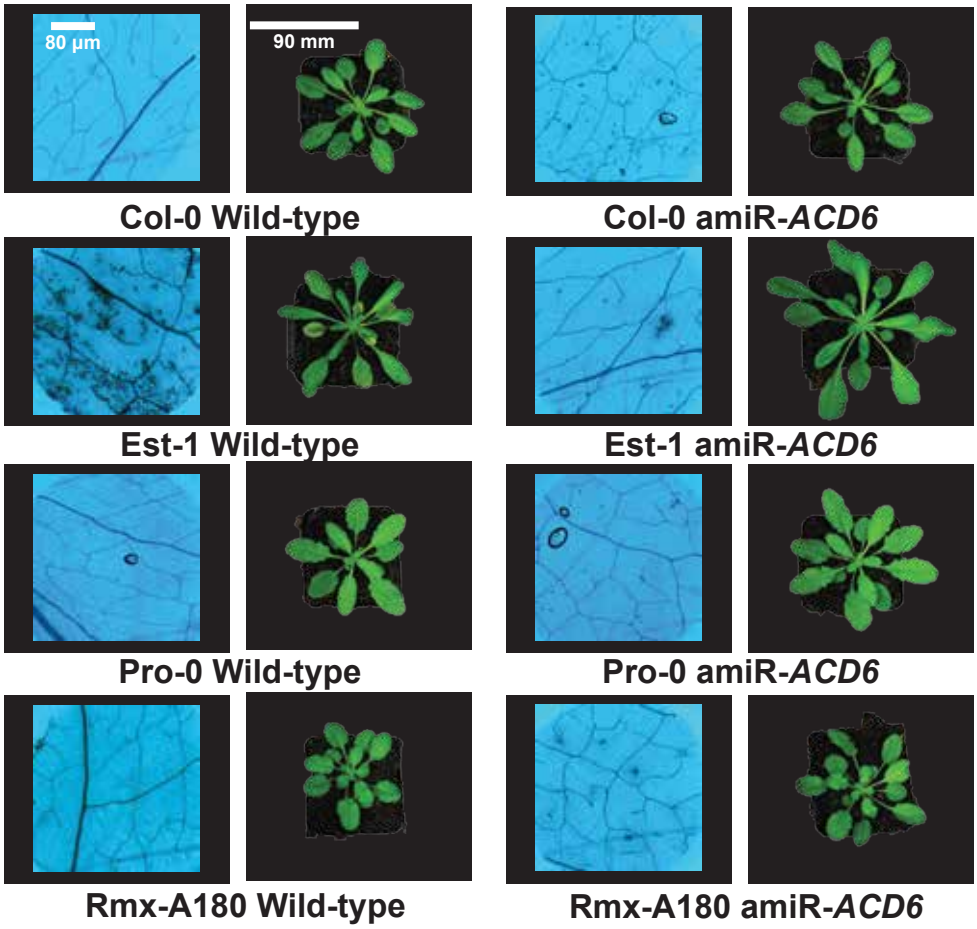

Figure 4.8 *ACD6*-dependent necrotic lesions in the hyperactive *ACD6* containing accession Est-1, but not in Pro-0 and Rmx-A180.

baseline SA content and knocking-down *ACD6* did not significantly alter the SA content. On the other hand, total SA content increased when *ACD6* was knocked down in Rmx-A180 (Figure 4.9).Although the SA content of amiR-*ACD6* Rmx-A180 was still only as much as Est-1 amiR-*ACD6*, removing *ACD6* seemed to either alleviate suppression or activate SA production. Overall, these data suggest that *ACD6* Est-like alleles affected SA accumulation differently depending on the genetic background. A strong effect of modulators on observed phenotypes are suggested by these results.

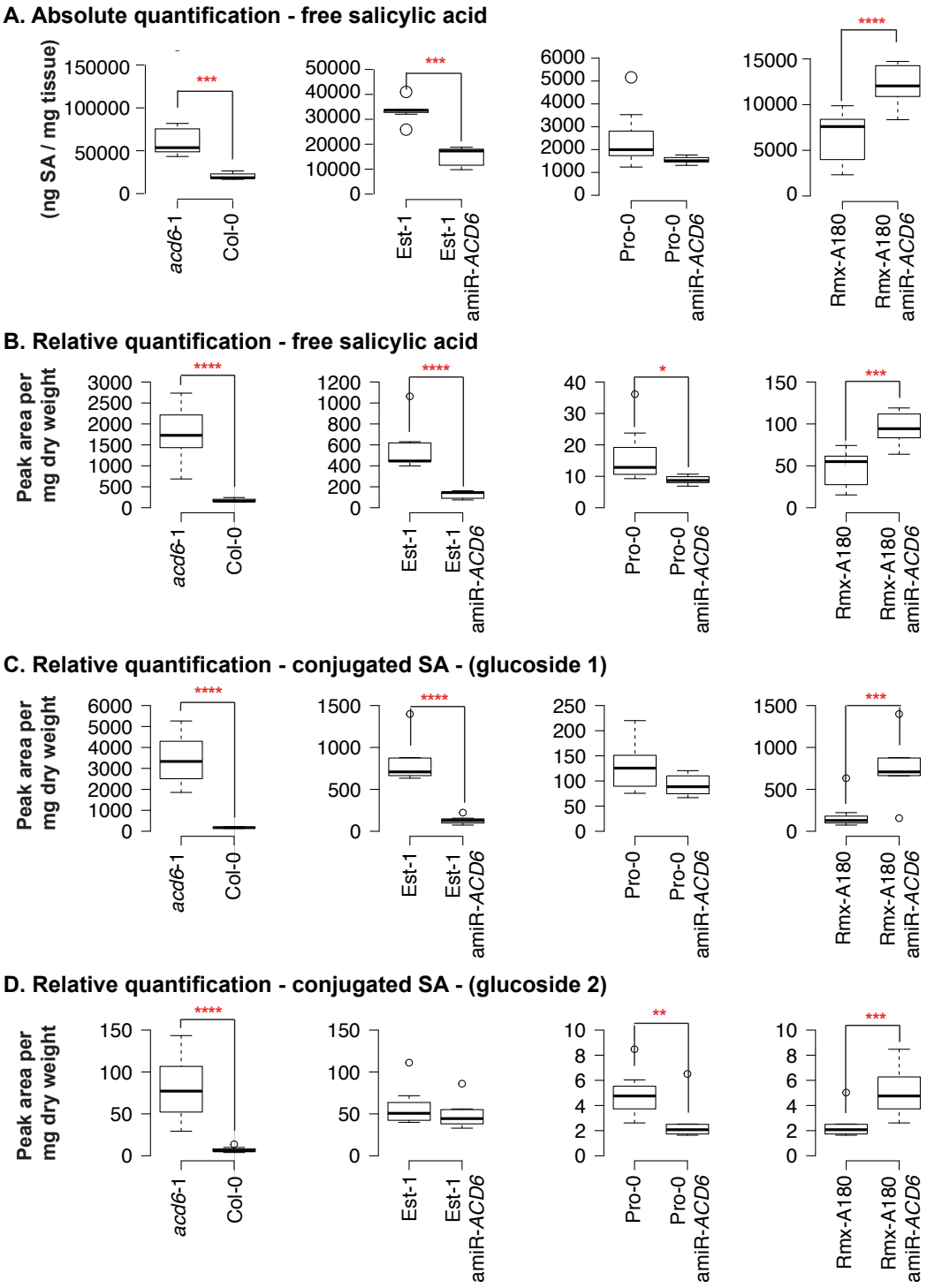

Figure 4.9 *ACD6*-dependence of SA content in unchallenged plants. A) Absolute and B) relative quantities of free SA. Relative quantities of conjugated SA C) glucoside 1 and D) glucoside 2.

Data are from 10 biological replicates. Red asterisks indicate p-value from pairwise comparisons using t-tests, significant difference relative to the corresponding wild type; p-value: **** < 0.0001 , *** < 0.001, ** < 0.005, *< 0.05.

4.3.2 flg22-induced ROS production and growth inhibition

ROS production is an indicator of immune responses. ROS accumulates when the PRR FLS2 detects the PAMP flg22 (Yi and Kwon 2014). Relevant to my work, a recent study has shown that there is natural variation in ROS production in response to flg22 (Vetter, Kronholm et al. 2012).

I used a flg22-induced ROS assay and flg22-induced seedling growth inhibition to quantify each genotype's competence for mounting an immune response. Supporting previous results by Vetter et al. (Vetter, Kronholm et al. 2012), I found natural variation in flg22-induced ROS production across accessions. For the flg22-induced ROS production assay, I also included other accessions with putative *ACD6* modifiers, Br-0 and Bs-5, and *acd6*-2. The speed and magnitude of the elicited response varied (Figure 4.10A). Clear patterns can be observed, namely *acd6*-2 had the least flg22-induced ROS produced and Rmx-A180 had a higher flg22-induced ROS response than Est-1 and *acd6*-1. Pro-0 had the lowest and slower response to flg22 among all the accessions tested, except for the loss-of-function mutant *acd6*-2.

I tested *ACD6*-dependent flg22-induced ROS production by testing wild type and the corresponding amiR-*ACD6* lines of Col-0, Est-, Pro-0 and Rmx-A180 (Figure 4.10B, 4.10C, 4.10D, and 4.10E). These additional experiments confirmed that ROS production, in response to flg22, was suppressed upon *ACD6* knockdown, except for Rmx-A180, which, similar to SA content, showed the opposite pattern of greater ROS production in the *ACD6* knockdown lines (Figure 4.10E). Measuring immediate ROS production after flg22 exposure provides a snap shot of early responses to PAMPs. I extended this experiment further by measuring the extent of growth inhibition upon prolonged flg22 exposure. For this assay, I included a flg22-insensitive mutant in Col-0 background, *bak1*-5 (Roux, Schwessinger et al. 2011, Schwessinger, Roux et al. 2011). This phosphorylation-impaired mutant cannot recruit specific phosphosites to activate flg22 recognition signaling components (Roux, Schwessinger et al. 2011). Growth inhibition differences between the

treated and un-treated samples were most obvious in the genotypes: *bak1-5*, Col-0, and Rmx-A180 (Figure 4.11).

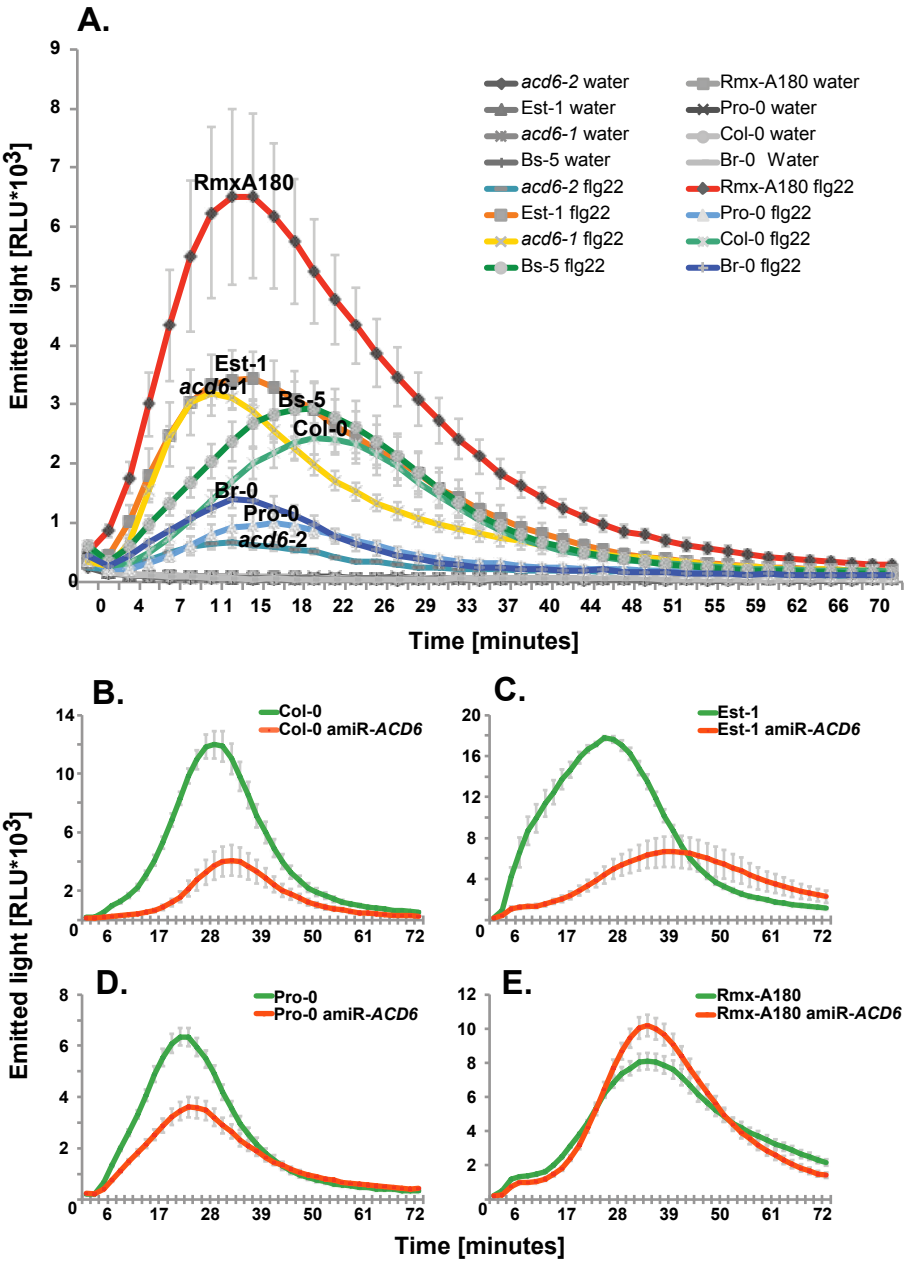

Figure 4.10 Production of reactive oxygen species (ROS) in response to flg22. A) Differences among flg22-induced ROS production in wild type accessions and the Col-0 mutants *acd6-1* and *acd6-2*. *ACD6*-dependent production of reactive oxygen species (ROS) in response to flg22 in B) Col-0, C) Est-1, D) Pro-0 and Rmx-A180.

Data are from 4 biological replicates. Error bars represent standard errors. The experiments were repeated 4 times with similar results.

4.3.3 PTI and ETI of representative genotypes with different ACD6 activities

I used *Pseudomonas syringae* to determine PTI and ETI responses. Two virulent strains commonly used for research are *Pseudomonas syringae pv. tomato* DC3000 (*Pst*) and the *Pseudomonas syringae pv. maculicola ES4326* (*Psm*), which will readily infect *A. thaliana* when infiltrated into intercellular space or applied to the leaf surface (Katagiri, Thilmony et al. 2002, Staphnill 2009). The type-III secretion mutant *Pseudomonas syringae pv. tomato DC3000* (*Pst HrcC-*) cannot deliver effectors, and is therefore useful for measuring PTI. I used *Pseudomonas syringae p.v. maculicola ES4326* (*Psm*) to determine ETI. I favored using *Psm* over *Pst* since previous studies on *ACD6* and disease resistance also used *Psm* (Ausubel, Glazebrook et al. 1993, Rate, Cuenca et al. 1999, Lu, Rate et al. 2003, Lu, Salimian et al. 2009, Wang, Seabolt et al. 2011). At the same time, *Psm* is a stronger inducer of the SA network sector than *Pst* (Wang, Mitra et al. 2008). *A. thaliana* R genes that have been shown to confer resistance to *Psm* include: RPM1, AT3G04210 and AT3G04220 (Ritter and Dangl 1995, Nimchuk, Marois et al. 2000, Preston 2000, Rant, Arraiano et al. 2013).

I measured the progression of bacterial growth in genotypes inoculated with *Psm* from 12 to 72 hours after inoculation (Figure 4.12). For most of the genotype pairs tested, bacteria grew better on the amiR-*ACD6* lines, confirming that *ACD6* has a major role in controlling defense responses (Rate, Cuenca et al. 1999, Lu, Rate et al. 2003). The difference in *ACD6*-dependent bacterial growth was most significant in *acd6*-1, Est-1 and Pro-0. The difference in Pro-0 was like Est-1 and the hyperactive *acd6*-1 wherein silencing *ACD6* increased pathogen growth. This shows that modulation of autoimmune symptoms in Pro-0 did not influence its capability to fight a pathogen attack.

Psm growth in Rmx-A180, however, was only mildly affected by reduced *ACD6* levels. This again pointed to Pro-0 and Rmx-A180 being affected by different modulators. The amiR-*ACD6* had little effect in both Col-0 and Rmx-A180 (Figure 4.12). This could either mean that the *ACD6* pathway has reduced activity in both accessions, or that they can mount an incompatible

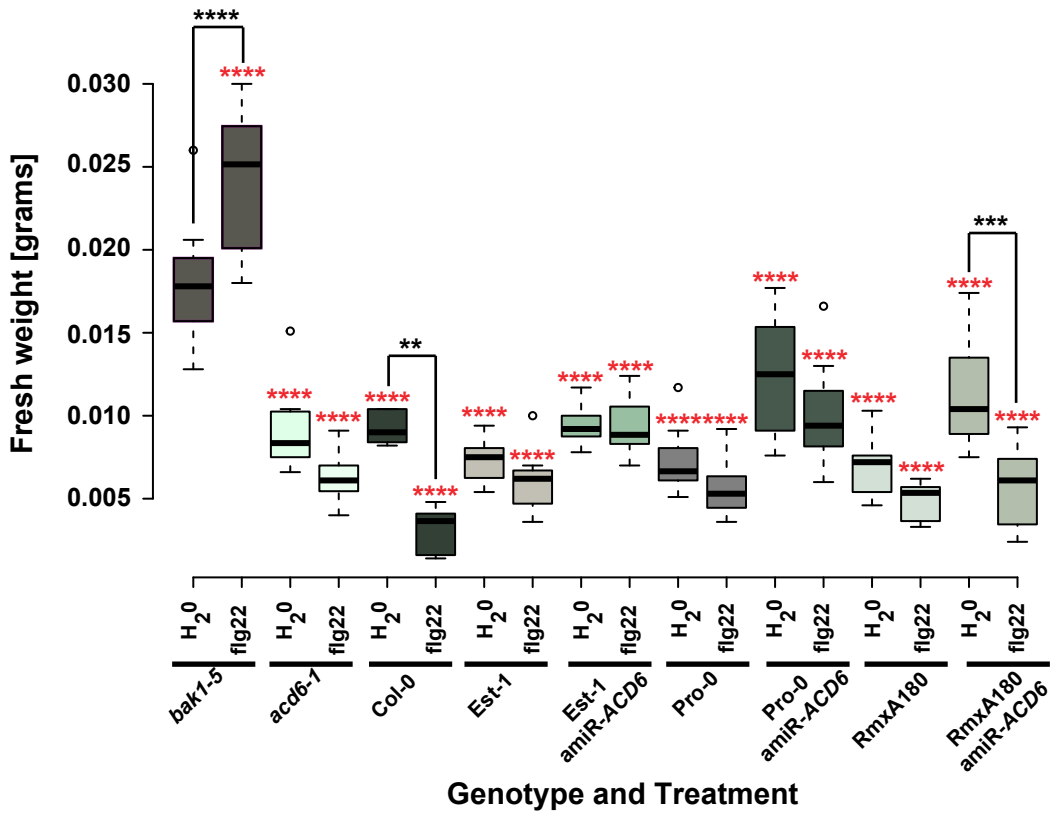

Figure 4.11 flg22-induced growth inhibition.

Data are from 8 biological replicates. Error bars represent standard error. The experiment was repeated twice with similar results. Red asterisks indicate p-value from pairwise comparisons using t-tests, significant difference relative to *bak1-5*; black asterisks indicate significant difference from pairwise comparison between the wild type and the corresponding amiR-*ACD6* transgenic line. p.value: **** <0.0001 , *** < 0.001, ** < 0.005, *< 0.05.

interaction that is not affected by the *ACD6* pathway. In particular, Rmx-A180 may have specific functional R-genes that could recognize specific effectors employed by *Psm* that are not found or do not function in the same way in the other genotypes I tested.

A hypersensitive response (HR) characterized by localized cell death at the bacterial point of entry is another marker for the severity of infection. To support the bacterial colony counting results, I looked at 6th leaf HR severity 72 hrs after infiltration in all the genotypes included in the *Psm* infection. I also utilized whole plant chlorophyll fluorescence imaging (CFI) for these plants, which provides a fast, precise and visual information on plant stress (Gorbe and Calatayud 2012). CFI at most detected patches of cells with compromised photosynthetic capacity (Figure 4.13). For the purpose of my

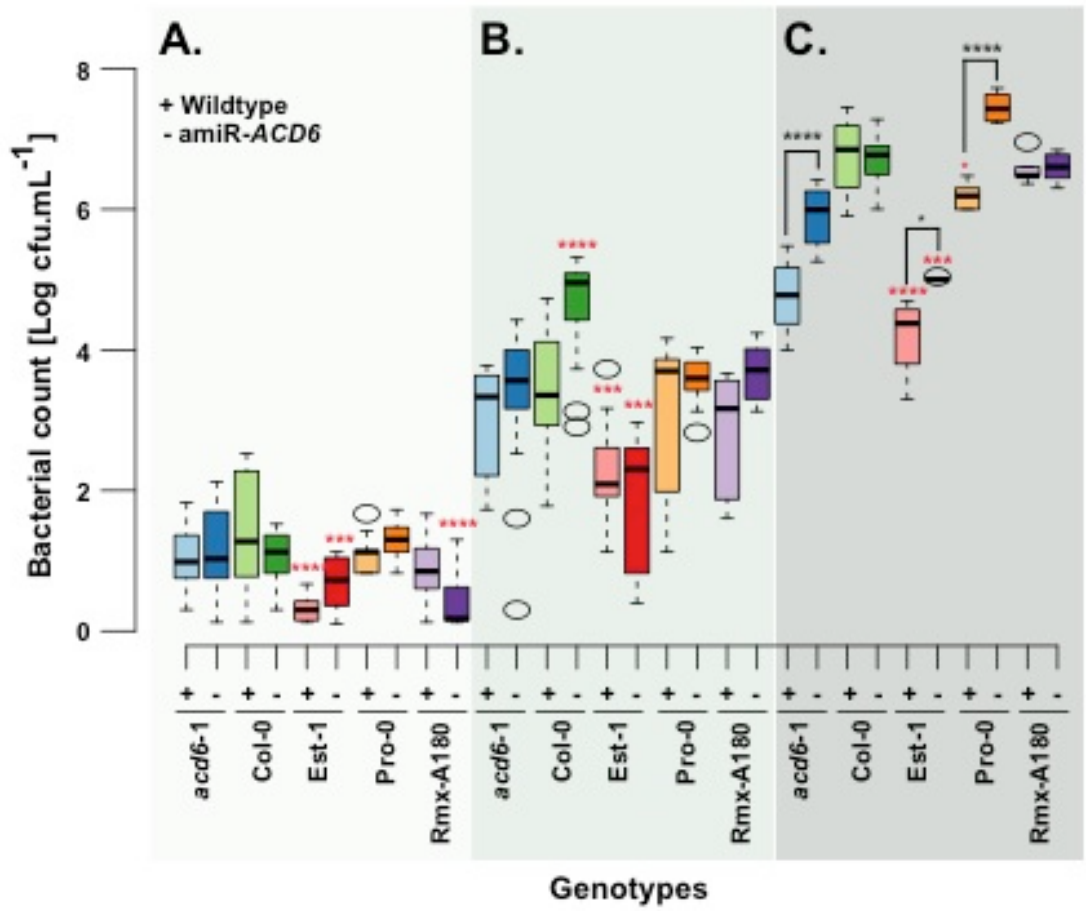

Figure 4.12 *Psm* pathogenicity test. A) Bacterial colony counts at 24 hrs, B) 48 hrs, C) 72 hrs after infiltration.

Data are from 4 biological replicates. The experiment was repeated 2 times with similar results. Red asterisks indicate p-value from pairwise comparisons using t-tests, significant difference relative to Col-0; black asterisks indicates significant difference from pairwise comparison between the wild type and the corresponding amiR-*ACD6* transgenic line. p.value: **** <0.0001 , *** < 0.001, ** < 0.005, *< 0.05.

experiment the superior method was Trypan blue staining which, as mentioned earlier, differentially stains collapsed dead cells blue. Overall Trypan blue results show that all the infected genotypes developed HR. Col-0, Rmx-A180 and their transgenic amiR-*ACD6* counterparts had the least amount of dead cell patches. Knocking-down *ACD6* dampened the HR response to bacterial infection, as seen in the decrease of dead cell patches of infected amiR-*ACD6* lines (Figure 4.13B). Whilst Pro-0 and Rmx-A180 have modulated *ACD6* responses, HR was still apparent after *Psm* infection.

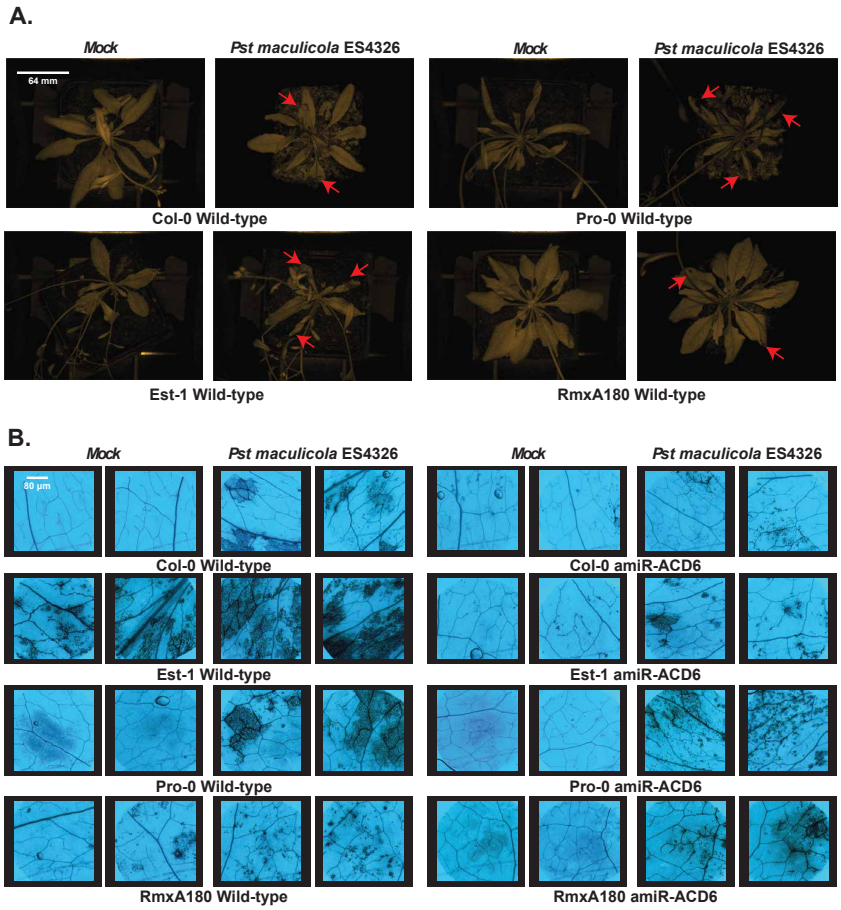

Figure 4.13 *Psm* induces *ACD6*-dependent lesions. A) Chlorophyll fluorescence images of mock and *Psm* sprayed plants with varying *ACD6* hyperactivity; red arrows indicate patches of dead cells; B) Representative Trypan blue stained 6th leaf of mock and *Psm* infiltrated plants.

This suggested that despite the modulated *ACD6* responses, Pro-0 and Rmx-A180 could maintain defense responses during bacterial infection.In addition, HR was more severe in Pro-0 amiR-*ACD6* and Rmx-A180 amiR-*ACD6* than Est-1 amiR-*ACD6*, pointing to a non-*ACD6* factor present in Pro-0 and Rmx-A180 that is causal for HR response during bacterial infection. A hypersensitive response (HR) characterized by localized cell death at the bacterial point of entry is another marker for the severity of infection. To support the bacterial colony counting results, I looked at 6th leaf HR severity 72 hrs after infiltration in all the genotypes included in the *Psm* infection. I also utilized whole plant chlorophyll fluorescence imaging (CFI) for these plants, which provides a fast, precise and visual information on plant stress (Gorbe and Calatayud 2012).

CFI at most detected patches of cells with compromised photosynthetic capacity (Figure 4.13). For the purpose of my experiment the superior method was Trypan blue staining which, as mentioned earlier, differentially stains collapsed dead cells blue. Overall Trypan blue results show that all the infected genotypes developed HR. Col-0, Rmx-A180 and their transgenic amiR-*ACD6* counterparts had the least amount of dead cell patches. Knocking-down *ACD6* dampened the HR response to bacterial infection, as seen in the decrease of dead cell patches of infected amiR-*ACD6* lines (Figure 4.13B). Whilst Pro-0 and Rmx-A180 have modulated *ACD6* responses, HR was still apparent after *Psm* infection. This suggested that despite the modulated *ACD6* responses, Pro-0 and Rmx-A180 could maintain defense responses during bacterial infection. In addition, HR was more severe in Pro-0 amiR-*ACD6* and Rmx-A180 amiR-*ACD6* than Est-1 amiR-*ACD6* pointing to a non-*ACD6* factor present in Pro-0 and Rmx-A180 that is causal for HR response during bacterial infection.

I tested PTI capacity using *Pst HrcC-*. Compared to *Psm*, bacterial growth of *Pst HrcC-,* on average, stayed at a low bacterial titer of 1.5 Log cfu mL-1 (Figure 4.14). These lower bacterial titers suggest that all the genotypes tested have the necessary factors to mount *Pseudomonas*-associated PTI. Knocking-down *ACD6* in Rmx-A180 resulted in a significant increase in PTI (Figure 4.14). This reinforces the results from the flg22-induced ROS production assay, and SA quantification results. Knocking down *ACD6* in Rmx-A180 induced parts of the pathogen response pathway. Another notable result is the strong *ACD6*-dependency of PTI response in Pro-0 (Figure 4.14).

4.3.4 ACD6-dependent marker gene expression

Through assaying changes in gene expression of these genes I aimed to determine which sections of the *ACD6* pathway were blocked in Pro-0 and Rmx-A180. Different genes of the known immune response pathways (Feys and Parker 2000, Asai, Tena et al. 2002, Azevedo, Betsuyaku et al. 2006, Lu, Salimian et al. 2009, Ng, Seabolt et al. 2011, van Verk, Bol et al. 2011, Seyfferth and Tsuda 2014, Herrera-Vasquez, Salinas et al. 2015), as consolidated in Figure 4.15, were tested for gene expression differences

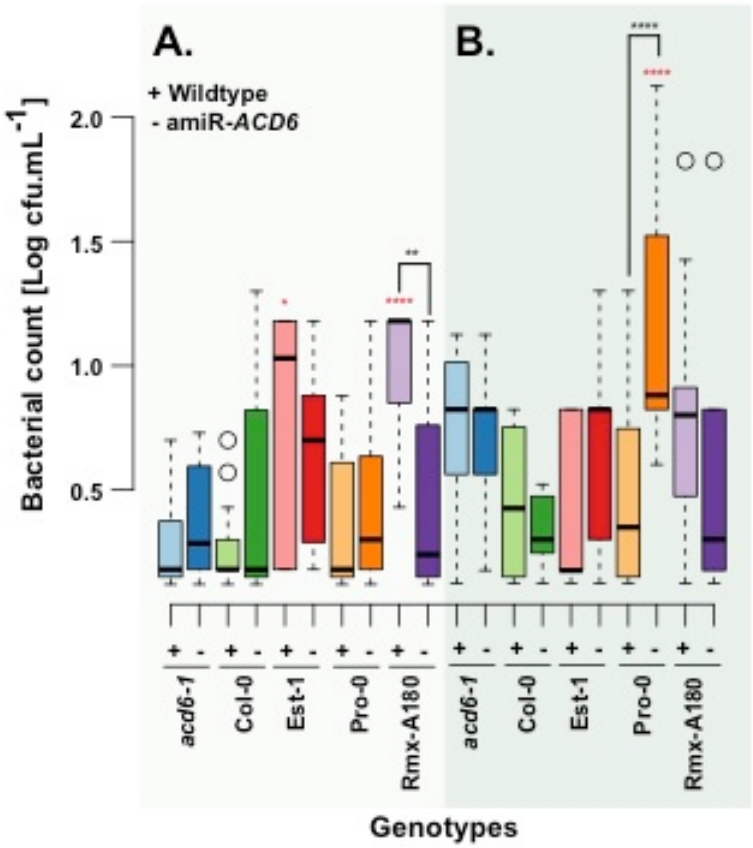

Figure 4.14 PTI response after infection with *Pst HrcC*-. A) Bacterial colony counts at 24 hrs, B) 48 hrs after infiltration.

Data are from 4 biological replicates. The experiment was repeated 2 times with similar results. Red asterisks indicate p-value from pairwise comparisons using t-tests, significant difference relative to Col-0; black asterisks indicates significant difference from pairwise comparison between the wild type and the corresponding amiR-*ACD6* transgenic line. p.value: **** <0.0001 , *** < 0.001, ** < 0.005, *< 0.05.

among the accessions and two mutants, *acd6*-1 (Col-0) and *eds1-5* (Ws-0) using reverse transcription of mRNAs followed by quantitative real-time PCR (qRT-PCR). *eds1-5* is an *EDS1* (lipase-like protein positively regulating SA accumulation and R-gene mediated defense responses) mutant, in the background of the Ws-0 accession (Falk, Feys et al. 1999). This mutant is hypersusceptible to pathogens, has very low *PR1* expression and accumulates low SA amounts (Falk, Feys et al. 1999). Parts of the overall pathway I tested can be divided in to four sets:

- Set A included *ACD6* (Todesco, Balasubramanian et al. 2010) and known *ACD6*-related marker genes, *PR1* (Lu, Rate et al. 2003), FLG22-INDUCED RECEPTOR-LIKE KINASE 1/ *SENESCENCE*-

INDUCED RECEPTOR-LIKE KINASE (FRK1/*SIRK1*) (Zhang, Shrestha et al. 2014, Zheng, McLellan et al. 2014) and SENESCENCE-ASSOCIATED GENE 12 (Morris, Mackerness et al. 2000, Todesco, Balasubramanian et al. 2010);

- Set B contained signal-transduction genes: *WRKY TRANSCRIPTION FACTOR 29* (Yi, Shirasu et al. 2014), *WRKY TRANSCRIPTION FACTOR 46* (*WRKY46*) (van Verk, Bol et al. 2011), and *NONEXPRESSOR OF PR GENES 1* (*NPR1*) (Vanacker, Lu et al. 2001, Wang, Amornsiripanitch et al. 2006, Hu, Dong et al. 2012)
- Set C included type II SA accumulation genes *ENHANCED DISEASE SUSCEPTIBILITY 1 PROTEIN* (*EDS1*), *PHYTOALEXIN DEFICIENT 4* (*PAD4*), (Aarts, Metz et al. 1998, Feys and Parker, #200, Dong 2001, Shapiro and Zhang 2001, Lu, Rate et al. 2003, Venugopal, Jeong et al. 2009, Ng, Seabolt et al. 2011). Type II SA genes encode proteins that do not act directly as SA biosynthetic enzymes but directly feed to the SA pathway (Ng, Seabolt et al. 2011).
- Set D was composed of genes contributing to resistance protein accumulation, namely: *NONRACE-SPECIFIC FOR DISEASE RESISTANCE 1* (*NDR1*) (Aarts, Metz et al. 1998) and *PROTEIN SGT1 HOMOLOG B*/ *ENHANCED DOWNY MILDEW 1 / ENHANCER OF TIR-1 AUXIN RESISTANCE 3 / SUPPRESSOR OF G2 ALELLE OF SKP1 HOMOLOG B* (*AtSGT1b/ EDM1/ETA3/RPR1*) (Azevedo, Betsuyaku et al. 2006).

Assayed gene expression levels for set A is shown in Figure 4.16. At 4 weeks after sowing, *ACD6* was expressed in the whole rosette of most of the genotypes tested at a level comparable to Est-1, except in Col-0 and *eds1*-5. The highest amount of transcript was measured in *acd6*-1. This experiment also confirmed that the transgenics I used for the experiment had *ACD6* expression knocked down as expected. *ACD6* expression in *eds1*-5 was similarly low as in the *ACD6* knockdown plants. *PR1* expression was high only

in Est-1 and *acd6*-1. As discussed earlier, high *ACD6* expression does not necessarily translate into high *PR1* expression. *SAG12* was only elevated in *acd6*-1 and Est-1. This indicated that the part of the lesion phenotype observed in both these genotypes could be due to age-dependent senescence (Gan and Amasino 1997).

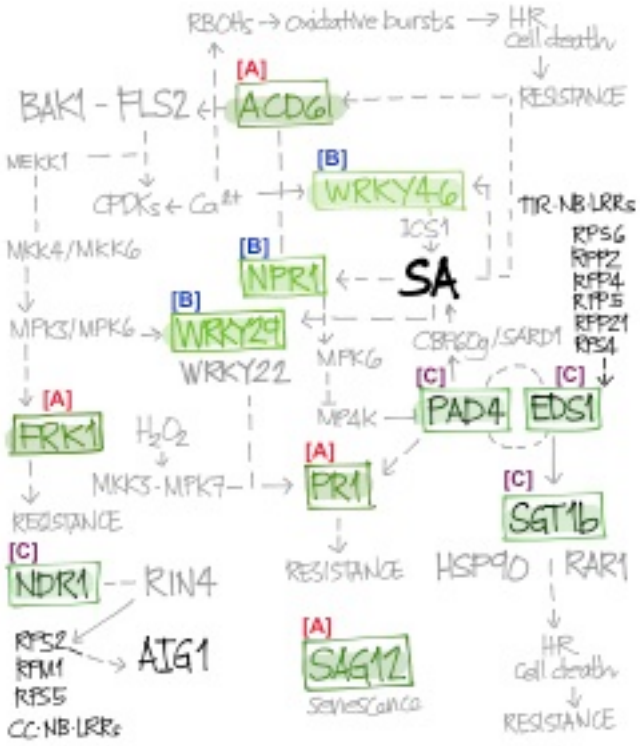

Figure 4.15 Interconnections of genes implicated in the *ACD6* immune response pathway. Highlighted are selected genes that were tested for relative gene expression and can be classified as: [A] key marker genes (including *ACD6*), [B] signal transducers, and [C] type II SA accumulation genes.

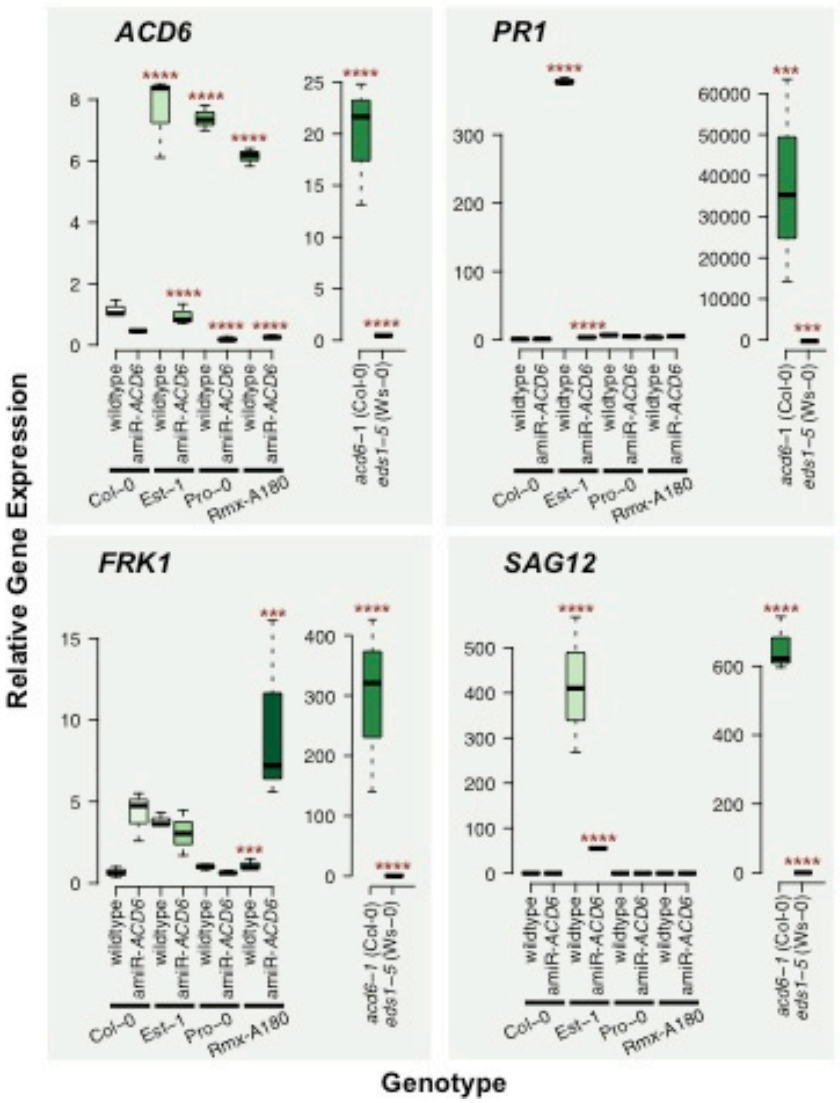

Figure 4.16 Relative expression of key marker genes in accessions with varying *ACD6* activity and mutant genotypes, *acd6-1* (Col-0) and *eds1-5* (Ws-0), as measured by qRT-PCR.

Data are from 4 biological replicates, normalized to the Col-0 values. For transgenics, biological replicates are from four different individuals of the T_1 generation. Red asterisks indicate p-value from pairwise comparisons using t-tests, significant difference from pairwise comparison between the wild type and the corresponding amiR-*ACD6* transgenic line. p.value: **** <0.0001 , *** < 0.001, ** < 0.005, *< 0.05.

Considering these known functions, the significantly higher *FRK1* expression in the Rmx-A180 amiR-*ACD6* plants suggests that down-regulation of *ACD6* in Rmx-A180 mimics flg22 activated defense responses. The opposite *SAG12* and *FRK1* profiles imply that the developmental senescence signal through *WRKY6* for *FRK1* expression was likely blocked (Figure 4.16).

WRKY transcription factors are involved in plant defense responses to biotrophic and necrotrophic pathogens. The activation of MAP kinase

pathways upon recognition of the PAMP flg22 by its cognate receptor FLS2 leads to the transcription of defense-related genes through WRKY transcription factors like *WRKY22/29* (Cheng, Gao et al. 2013). *WRKY46* was shown to specifically induce salicylic acid and pathogen defense in such a way that plants over-expressing *WRKY46* were more resistant to *Pseudomonas syringae* (Hu, Dong et al. 2012). *NPR1* is central for SA-dependent activation of defense response genes, encoding an SA receptor (Wu, Zhang et al. 2012). In all backgrounds, *ACD6* knockdown led to increased expression of *WRKY29* (Figure 4.17). In contrast, *ACD6* knockdown reduced *WRKY46* expression in Col-0, Est-1 and Pro-0, but induced it in Rmx-A180 (Figure 4.17). *NPR1* expression was low and highly variable, and therefore difficult to assess. A trend could be seen, with Col-0 behaving opposite of Est-1 when *ACD6* was knocked down.

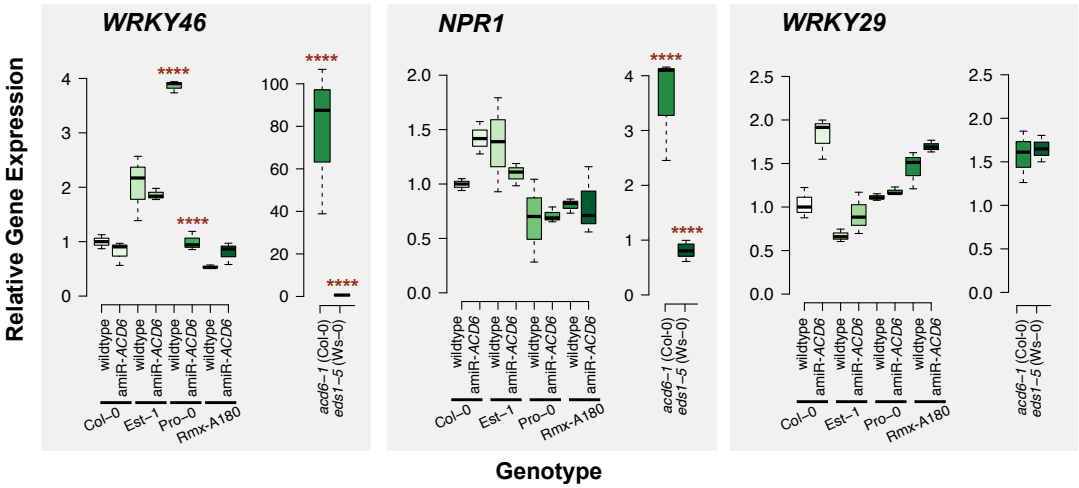

Figure 4.17 Relative expression of defense signal transduction genes in accessions with varying *ACD6* activity and mutant genotypes *acd6-1* (Col-0) and *eds1-5* (Ws-0), as measured by qRT-PCR.

Data are from 4 biological replicates, normalized to the Col-0 values. For transgenics, biological replicates are from four different individuals of the T_1 generation. Red asterisks indicate p-value from pairwise comparisons using t-tests, significant difference from pairwise comparison between the wild type and the corresponding amiR-*ACD6* transgenic line. p.value: **** <0.0001 , *** < 0.001, ** < 0.005, *< 0.05.

The set C gene expression levels are shown in Figure 4.18. I separated them from the transcription factor gens owing to their more diverse functional roles. Both *PAD4* and *EDS1* function in resistance (R) gene-

The set C gene expression levels are shown in Figure 4.18. I separated them from the transcription factor gens owing to their more diverse functional roles. Both *PAD4* and *EDS1* function in resistance (R) gene-mediated and basal plant disease resistance. Association of these two lipase-like proteins has been shown to be necessary for SA accumulation (Rietz, Stamm et al. 2011). On the other hand, even though both proteins are required by the same set of R-genes, they fulfill distinct roles in mounting a defense response (Feys and Parker 2000). Between *EDS1* and *PAD4*, only *EDS1* is essential for amplification of the hypersensitive response. *PAD4* is recruited later in the amplification of plant defense responses (Rietz, Stamm et al. 2011).

Opposite to what I expected, *ACD6* knockdown primarily affected expression of *PAD4* and not *EDS1* (Figure 4.18). *PAD4* levels were increased in Col-0 amiR-*ACD6* and Rmx-A180 amiR-*ACD6*. The pattern was opposite for Est-1 and Pro-0. An obvious effect on *EDS1* expression could only be seen in the controls *acd6*-1 and *eds1*-5. *EDS1* expression was highly variable, making it harder to infer much from *EDS1* expression differences.

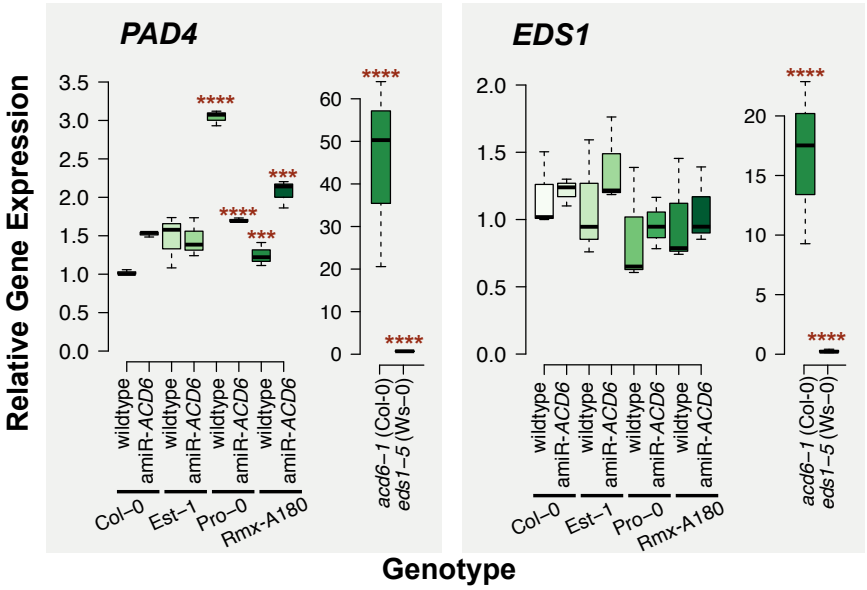

Figure 4.18 Relative expression of type II SA accumulation genes in accessions with varying ACD6 activity and mutant genotypes acd6-1 (Col-0) and eds1-5 (Ws-0), as measured by qRT-PCR.

Data are from 4 biological replicates, normalized to the Col-0 values. For transgenics, biological replicates are from four different individuals of the T1 generation. Red asterisks indicate p-value from pairwise comparisons using t-tests, significant difference from pairwise comparison between the wild type and the corresponding amiR-ACD6 transgenic line. p.value: **** <0.0001 , *** < 0.001, ** < 0.005, *< 0.05.

NDR1, shown by Shapiro and Zhang (Shapiro and Zhang 2001) to mediate the induction of SA through the production of reactive oxygen species (ROS), is responsive to a different set of R-genes than *EDS1*. *RPS2*, *RPM1* and *RPS2*, all R-loci that require *NDR1*, operate independently of *EDS1* (Aarts, Metz et al. 1998). Consistent with different upstream inputs, trends of *NDR1* and *EDS1* levels differed among the genotypes I tested. Knocking down *ACD6* increased *NDR1* expression in Col-0 and Rmx-A180 and lowered it in Est-1 and Pro-0 (Figure 4.19). The opposite changes in Pro-0 and Rmx-A180 further reinforce the hypothesis that *ACD6* response is differently modulated in these two genotypes. Moreover, given there is a strong distinction in the effect of *ACD6* knockdown on *NDR1* transcript levels makes it possible that CC-NBS-LRR's could be a point of modulation in these two genotypes.

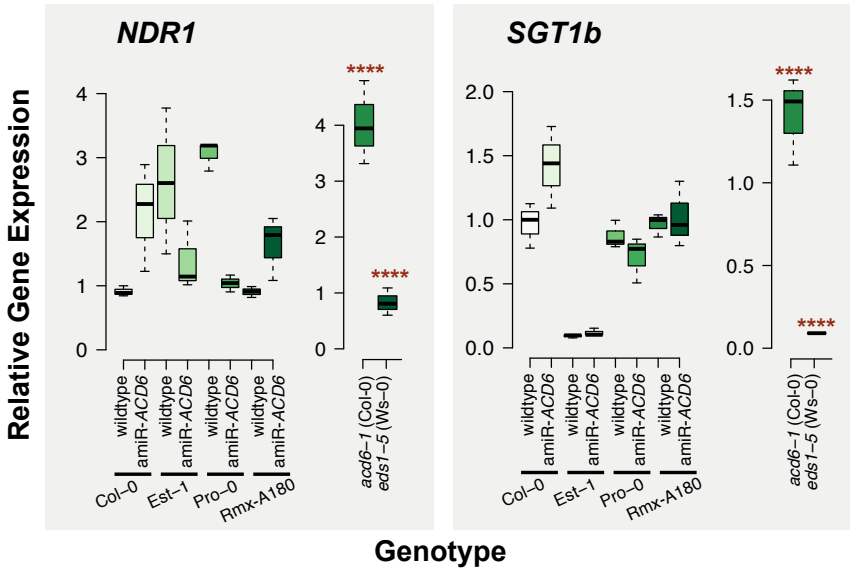

Figure 4.19 Relative expression of genes contributing to resistance protein accumulation in accessions with varying *ACD6* activity and mutant genotypes *acd6-1* (Col-0) and *eds1-5* (Ws-0), as measured by qRT-PCR.

Data are from 4 biological replicates, normalized to the Col-0 values. For transgenics, biological replicates are from four different individuals of the T_1 generation. Red asterisks indicate p-value from pairwise comparisons using t-tests, significant difference from pairwise comparison between the wild type and the corresponding amiR-*ACD6* transgenic line. p.value: **** <0.0001 , *** < 0.001, ** < 0.005, *< 0.05.

Although not highly significant, there were indications, at least in Col-0 and Est-1 that gene expression of *SGT1b* was upregulated upon *ACD6* knockdown (Figure 4.19). Rmx-A180 amiR-*ACD6* showed a predisposition to

reduced *SGT1b* expression in Pro-0 amiR-*ACD6* may have been due to the difference in the modulation factor that perturbed the usual *ACD6* defense response pathway.

In *acd6*-1, most of the marker genes were significantly higher expressed compared to any of the other genotypes analyzed (Figures 4.17, 4.18 and 4.19). On the other hand, the hypersusceptible mutant, *eds1*-1, had the lowest transcript levels for most the genes tested except *WRKY29*.

From all these results I infer some key generalizations for the reaction cascade contributing to *ACD6* activity. Upon *ACD6* knockdown, a general de-repression of key markers for the plant immune reactions was observed in Col-0 and Rmx-A180. The opposite was noticeable in Est-1 and Pro-0 (except for *WRKY29*). I hypothesize that in certain situations (i.e. upon pathogen challenge of Rmx-A180), *ACD6* can act as a sensor for immune activity, bringing about activation of key response pathways.

4.4 Conclusions regarding differences between Pro-0 and Rmx-A180

The phenotypic assays and gene expression assays showed that Pro-0 and Rmx-A180 are equipped with different defense repertoires that result in varying responses to induced pathogen attacks.

Pro-0 partly resembled Est-1-type immune response without the adverse negative effects of an autoimmune version of *ACD6*. This pushes forward the idea that an extragenic factor, which could be the Pro-0 modulator, is partly balancing the negative effect of having a hyperactive *ACD6* allele. Pro-0 does not exhibit unregulated cell death, and dwarfism. Despite being suppressed, not having high basal SA levels and strong flg22-induced ROS production, *ACD6*-Pro-0 does not seem to be completely inactive as shown by *Psm* and *Pst HrcC*- infection results. Rmx-A180 presented unconventional defense and growth response changes upon *ACD6* knockdown. These peculiarities included up-regulated SA production, elevated PAMP-induced ROS production and up-regulated *FRK1*, *PAD4*, *WRKY46* and *NDR1* gene expression. This further supports the idea that RmxA-180 *ACD6*-dependent responses are modulated differently compared to Pro-0. Rmx-A180 may be equipped for a specific induced defense response that could be activated and

is detected by a modification or down-regulation of *ACD6*. These results can also fit in a hypothesis that the modifier guards *ACD6*, in accordance with the guard-guardee/decoy model (van der Hoorn and Kamoun 2008); without the functional removal (as in knocking down) of *ACD6*, the modifier could be inactive, therefore completely suppressing hyperactive *ACD6* effects. Either the “activated” modifier itself or another component that is activated by the modifier could be causal for activation of downstream Rmx-A180 defense responses and only activated when the modifier detects *ACD6* degradation or modification.

A more straightforward answer to what happens in Rmx-A180 or Pro-0 during defense response could be obtained once the modifier has been identified. Efforts to identify and pinpoint the modifier gene/s present in accessions with modulated *ACD6*-dependent phenotypes are discussed in Chapter 5. All in all, the results of this chapter depict that hyperactivated defense responses can be modulated to minimize the compromise made towards growth.

5 A diverse set of genetic modifiers of *ACD6* responses

"Certain students of genetics inferred that the Mendelian units responsible for the selected character were genes producing only a single effect. This was careless logic. It took a good deal of hammering to get rid of this erroneous idea. As facts accumulated it became evident that each gene produces not a single effect, but in some cases a multitude of effects on the characters of the individual. It is true that in most genetic work only one of these character-effects is selected for study—the one that is most sharply defined and separable from its contrasted character—but in most cases minor differences also are recognizable that are just as much the product of the same gene as is the major effect."

-Thomas Hunt Morgan, 1935

Plants of the same species vary in both distinct and subtle ways. This difference in the manifested trait (phenotype) is due to an environmental influence and the concomitant underlying genetic basis (genotype). Based on our understanding of genetics and inheritance, the complexity of these phenotypes can arise from a single gene variation or from the segregation of alleles at many interacting loci (quantitative trait loci). To identify loci and specific alleles that control the apparent phenotypic variation, a forward genetic approach like quantitative trait loci (QTL) analysis can be utilized. In this approach parents characterized by opposite phenotypes are crossed and their offspring is self-fertilized; resulting generation (mapping population; F_2) is genotyped and phenotyped. Statistical methods are applied to uncover association between phenotype and genotypes of molecular markers across genome.

Usually the probability of observing a particular allele in a given locus is independent of an allele observed at another locus. That simplifies finding an

association between a single genetic marker and a phenotype. There are also cases however, when a specific trait results from a corresponding interaction between alleles and the magnitude of their respective effects contributes to the phenotype observed. These interacting alleles can be at different regions of the genome or be at direct physical linkage. As long as there are reliable genetic markers for each locus that co-segregates with the trait being measured, a probable chromosomal location of the allele governing the phenotype can be identified. One can use either simple or more elaborate statistical techniques for the calculations, depending on the complexity of a trait being studied. It is also prudent to note that the manifestation of a trait is not purely based on the genetic component. Phenotypes are dependent on environmental condition. It is therefore important to measure the phenotype in mapping population in the condition conducive for exposing relevant traits and to keep these conditions constant.

Once a localized chromosomal region is identified, fine mapping that involves genotyping recombinants of the mapping population can be used for the analysis to narrow down the list of candidate genes controlling the trait. One can directly employ reverse genetics approaches when a reasonably narrow mapping interval is attained. Reverse genetic approaches like transgenic techniques in a reciprocal background can be employed to confirm candidate genes. With these techniques, sufficiency and necessity tests can be conducted to pinpoint causality and feasible mechanisms of genes controlling the trait/s being studied.

This Chapter of the thesis presents the results from the efforts to find genes that modify the expression of Est-like *ACD6* alleles. I focused on four accessions, Pro-0, Rmx-A180, Bs-5 and Br-0, that have Est-like *ACD6* alleles but do not show the *ACD6*-dependent lesion phenotype.

5.1 The genetic basis of *ACD6* modulation

5.1.1 Dominance behavior of ACD6 modifier loci

The response to various pathogen type challenges had suggested different causes for the modification of the *ACD6*-Est effect in Pro-0 and Rmx-

A180. To determine whether this difference was genetic, I crossed Pro-0 and Rmx-A180 as well as Bs-5 and Br-0 and Est-1 to each other, and examined the F_1 progeny of each cross for the presence of lesions characteristic for Est-1 (Todesco, Balasubramanian et al. 2010). The expected outcomes in the F_1 progeny based on different dominance behavior are shown in Figure 5.1 and Figure 5.2. The F_1 progeny from crosses of the four suppressed accessions to Est-1 was intermediate in phenotype, pointing to modifiers being semi-dominant. Intercrosses among the suppressed accessions also resulted in mildly lesioned F_1 progeny (Figure 5.3), suggesting that most of the modifiers are unique to each accession.

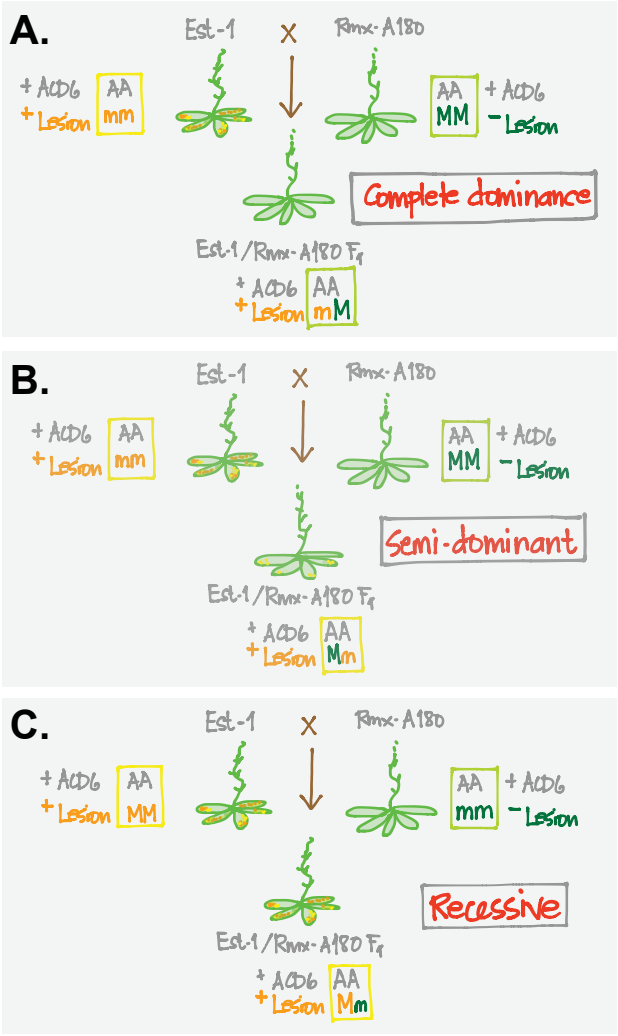

Figure 5.1 Expected phenotypes and underlying genotypes based on different dominance of modifier genes in accessions with Est-like *ACD6*. Shown are anticipated results from crosses of lesioned Est-1 and a non-lesioned accession such as Rmx-A180 when A) modifier exerts complete dominance; B) modifier is semi-dominant and; C) modifier is recessive.

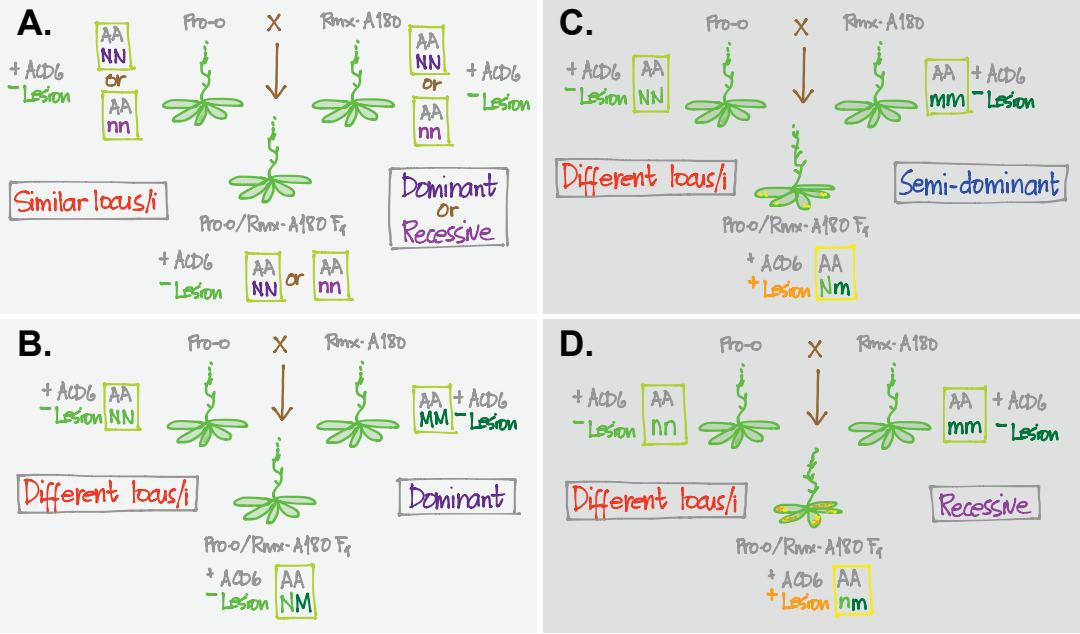

Figure 5.2 Expected phenotypes and underlying genotypes based on similarity and dominance of modifier genes in accessions with suppressed effects of Est-1-like *ACD6*, such as Pro-0 and Rmx-A180, when A) modifier is locus/i is either dominant or recessive and similar between Pro-0 and Rmx-A180; B) modifier is dominant and different between Pro-0 and Rmx-A180; C) modifier is dominant and different between Pro-0 and Rmx-A180 and D) modifier is recessive and different between Pro-0 and Rmx-A180.

5.1.2 Phenotypic segregation of ACD6 modulation

I next constructed mapping populations for each suppressed accession, by selfing F_1 progeny obtained from the crosses with Est-1. The F_2 individuals from each cross were expected to have the same Est-1 like "hyperactive" *ACD6* allele but to segregate for modifier locus/i. Segregation ratios in the F_2 mapping populations were utilized to assess the genetic architecture of modifier alleles. A total of 403 (Pro-0/Est-1), 270 (Rmx-A180/Est-1), 255 (Bs-5/Est-1) and 243 (Br-0/Est-1) F_2 individuals were phenotyped for the development of HR-like lesions at 5 weeks (Table 5.1).

The lesion phenotype was still the trait chosen for genetic mapping because it was more robust than other *ACD6*-dependent phenotypes, such as size and leaf initiation rate. Classification of HR in F_2 individuals was as follows: Est-like (severely lesioned), F_1-like (mildly lesioned) and modified (non-lesioned). Representative phenotypes from the Pro-0/Est-1 population

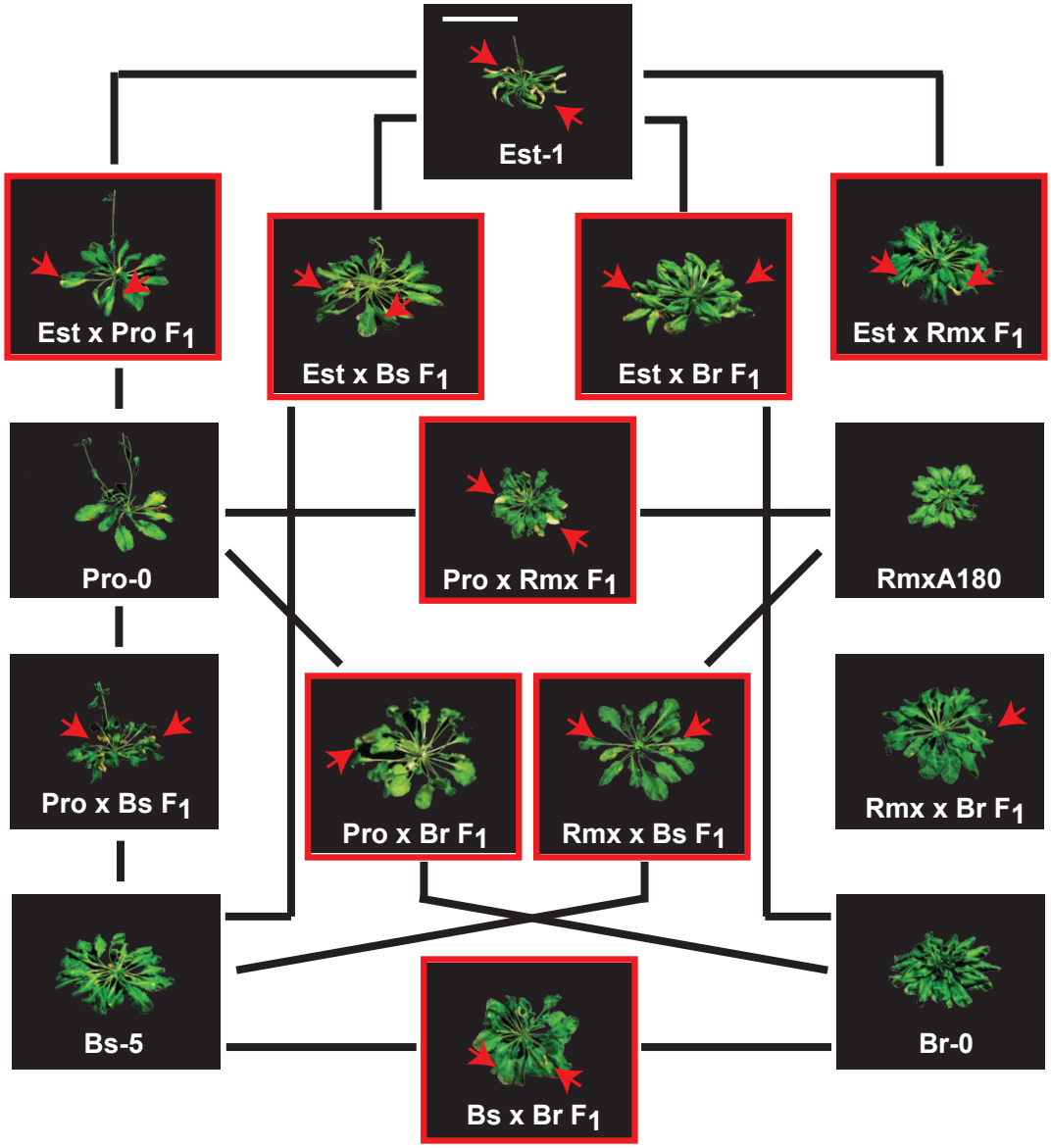

Figure 5.3 F_1 individuals from intercrossing accessions with suppressed *ACD6*-Est activity, showing that modifiers are semi-dominant and not completely shared. Orange boxes indicate F_1 progeny and red arrows late-onset necrosis symptoms.

are shown in Figure 5.4. Assuming that the Est-like *ACD6* alleles in the modulated accessions are not genetically distinct from *ACD6*-Est-1, the lesion phenotype segregation in the F_2 populations analyzed should be due to segregation of modifier locus/i in the F_2 individuals. The phenotypic segregation would remain the same if the modifier locus/i is linked to *ACD6* and therefore both modifier and *ACD6* would segregate together. With these scenarios a semi-dominant lesion phenotype controlled by a single gene predicts a segregation ratio of 1:2:1 of lesioned, mildly lesioned and non-

are shown in Figure 5.4. Assuming that the Est-like *ACD6* alleles in the modulated accessions are not genetically distinct from *ACD6*-Est-1, the lesion phenotype segregation in the F_2 populations analyzed should be due to segregation of modifier locus/i in the F_2 individuals. The phenotypic segregation would remain the same if the modifier locus/i is linked to *ACD6* and therefore both modifier and *ACD6* would segregate together. With these scenarios a semi-dominant lesion phenotype controlled by a single gene predicts a segregation ratio of 1:2:1 of lesioned, mildly lesioned and non-lesioned individuals. This proposed segregation ratio did not fit the Pro-0/Est-1, Rmx-A180/Est-1 or Bs-5/Est-1 F_2 populations (Table 5.1). The phenotypic scoring adapted was only semi-quantitative and prone to bias of the person doing the scoring. Using a quantitative assay such as ion leakage could in future potentially circumvent this problem.

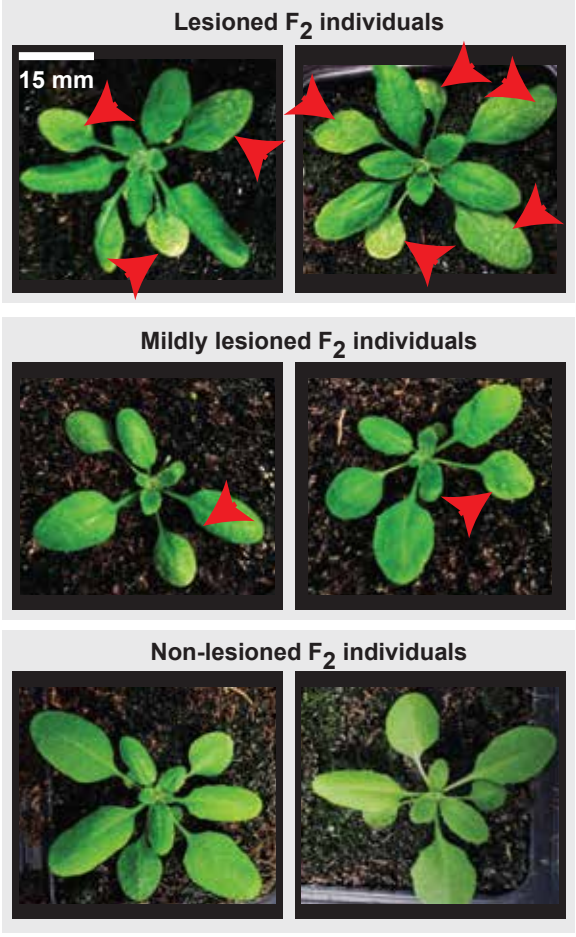

Figure 5.4 Phenotypic scale adapted for grouping F_2 individuals from the F_2 populations used in the study. Shown are representative F_2 individuals from the Pro-0/Est-1 population. Red arrows indicate leaves that showed late-onset necrosis symptoms.

Table 5.1 Phenotypic segregation of Est-like *ACD6* modifier-loci mapping populations phenotyped at 40 days after sowing and the corresponding goodness-of-fit to 1:2:1 segregation ratio.

F_2 population	*N*[1]	Observed			Expected ratio			χ2 Test Statistic	P-value	χ2 Crit	Sig
		Est-like	F_1-like	Non-lesioned	Est-like	F_1-like	Non-lesioned				
Pro-0/Est-1	403	238	86	79	100	203	100	262.28	1.11^{-57}	5.99	yes
Rmx-A180/Est-1	270	71	161	38	68	137	68	17.57	1.53^{-4}	5.99	yes
Bs-5/Est-1	255	160	77	18	63	129	63	202.45	1.09^{-44}	5.99	yes
Br-0/Est-1	243	87	94	62	61	121	61	17.12	1.91^{-4}	5.99	yes

[1] Number of individuals analyzed for the F_2 population

Table 5.2 Phenotypic segregation of Est-like *ACD6* modifier-loci mapping populations phenotyped at 40 days after sowing and the corresponding goodness-of-fit to 3:1 segregation ratio.

F_2 population	*N*[1]	Observed		Expected		χ2 Test Statistic (df=1)	P-value	χ2 Crit	Sig
		Lesioned	Non-lesioned	Lesioned	Non-lesioned				
Pro-0/Est-1	403	324	79	303	100	5.87	1.54^{-02}	3.84	yes
Rmx-A180/Est-1	270	232	38	205	68	16.79	4.17^{-05}	3.84	yes
Bs-5/Est-1	255	237	18	192	63	42.69	6.41^{-11}	3.84	yes
Br-0/Est-1	243	181	62	182	61	0.02	8.82^{-01}	3.84	no

[1] Number of individuals analyzed for the F_2 population

There also seemed to be an age-related progression of the lesion phenotype such that at around week 6 after sowing previously non-lesioned F_2 individuals developed mild lesions. An example of age-related progression of the lesion phenotype that affected phenotypic segregation in representative F_2 individuals from the Pro-0/Est-1 F_2 population is shown in Figure 5.5. With these discrepancies, I was not confident in the distinction between severely lesioned and mildly lesioned F_2 individuals. I then opted to target causal locus responsible for lesion suppression by the 5th week of growth. I did a second goodness-of-fit test for a 3:1 lesioned and non-lesioned segregation ratio. For this I bulked the severely lesioned and mildly lesioned into one lesioned phenotypic class. A 3:1 segregation ratio still did not fit the Pro-0/Est-1, Rmx-A180/Est-1 or Bs-5/Est-1 F_2 populations (Table 5.2). Only Br-0/Est-1 F_2 observed segregation ratios fit the expected 3:1 segregation ratio. This implied that there is possibly more than one locus responsible for suppression of HR-like lesions in the accessions with modified *ACD6* activity.

Figure 5.5 Age-dependent progression of the *ACD6*-dependent lesion phenotype in the Pro-0/Est-1 F_2 population used in the study.

5.1.3 QTL mapping of ACD6 modifiers

I mapped causal loci for *ACD6*-Est modifiers through RAD-Seq genotyping of F_2 individuals. I used Pst-1/Mse-1 restriction enzymes to

5.1.3 QTL mapping of ACD6 modifiers

I mapped causal loci for *ACD6*-Est modifiers through RAD-Seq genotyping of F_2 individuals. I used Pst-1/Mse-1 restriction enzymes to generate fragments for a reduced representation of the genome. An in silico digest of the reference genome, generates 40,244 Pst-1/Mse-fragments, of those, 8,444 fragments were 400 bp long or shorter. My DNA libraries were size selected to include only fragments shorter than 400 bp. I multiplexed 96 libraries in a single sequencing lane of Illumina HiSeq 2000 flow cell and expected 90X coverage. The observed coverage was uneven but on average I obtained 30X coverage across all the samples that were sequenced. Uneven coverage may have been due to uneven starting DNA qualities and concentrations, efficiency of restriction digest and adaptor ligation.

From sequenced short reads I called ~2,000 SNPs that could be used for QTL mapping, however, I filtered them based on: 1) high sequence quality in individuals of the F_2 population, 2) presence in at least 80% of the individuals in the F_2 population, and 3) being polymorphic in F_2 population. Additional marker and F_2 individual filtering was done using R/qtl for redundant markers, genotyping errors, and redundant individuals.

I ended up with a 304 (Pro-0/Est-1), 209 (Rmx-A180/Est-1), 256 (Bs-5/Est-1) and 243 (Br-0/Est-1) individual, respectively, for QTL mapping (Table 5.3). These individuals were genotyped with 285 (Pro-0/Est-1), 547 (Rmx-A180/Est-1), 396 (Bs-5/Est-1) and 328 (Br-0/Est-1) reliable and high-quality markers, respectively (Table 5.3). The markers were evenly spaced throughout the genomes, with an average of 1 marker per cM (Table 5.3). For QTL mapping, lesion appearance at 5 weeks of growth was used as phenotype. At least one significant QTL was found in each population (Table 5.4, Figure 5.6).

Same as Pro-0, Bs-5 also had two *ACD6* modifier loci. The first *ACD6*-Bs-5 modifier locus was also in chromosome 1 (4.27 Mb interval) with a significant LOD score of 3.52 (Table 5.4, Figure 5.6). The second *ACD6*-Bs-5 modifier locus was on chromosome 4 (2.33 Mb interval) with a significant LOD score of 5.55 (Table 5.4, Figure 5.6). Br-0 had only one significant *ACD6*

modifier locus, which had a LOD score of 5.13 at chromosome 5 (2.44 Mb interval) (Table 5.4, Figure 5.6). There were two distinct patterns, two accessions (Pro-0 and Bs-5) with two significant modifier loci and two accessions (Rmx-A180 and Br-0) with only one significant modifier locus. Pro-0 and Bs-5 had QTL at close positions on chromosome 4, and in addition had individual QTL on chromosome 1. Rmx-A180 and Br-0 could each have more *ACD6* modifier loci, however the LOD scores did not pass the significant threshold (Figure 5.6). A non-significant chromosome 3 *ACD6*-Br-0 modifier locus could be the same as the significant chromosome 3 *ACD6*-Rmx-A180 modifier locus. On the other hand the significant chromosome 5 *ACD6*-Br-0 modifier locus was similar to an insignificant chromosome 5 *ACD6*-Rmx-A180 modifier locus. To check this possibility, screening more F_2 individuals from the same F_2 populations or from an advanced mapping population with more precise phenotyping be done.

LOD scores tell us how significant an association of the phenotype with genetic markers is, but it does not provide information regarding the effects of these QTL. For the markers nearest to the highest LOD score value at each QTL, I calculated effect sizes of the three different allelic configurations, both for individual loci (Figure 5.7 A), and for potential interaction between the two loci found in the mapping populations (Figure 5.7 B). The QTL showed a range of different behaviors in their effects.

Pro-0 alleles at the chromosome 4 locus, near *ACD6*, were associated with weak lesioning, as expected, but in this case heterozygotes had a more intermediate phenotype than what was seen for Bs-5 at the chromosome 4 locus (Figure 5.7 A2 and A4). Unexpected was an opposite effect of Pro-0 alleles on chromosome 1, which enhanced lesioning (Figure 5.7 A1). The enhancement was strongly dependent, however, on the chromosome 4 locus, and not seen when the chromosome 4 locus was homozygous for the Pro-0 allele, consistent with the parental Pro-0 accession not being lesioned (Figure 5.7 B1).

In the Bs-5 cross, the Bs-5 alleles at the chromosome 1 locus were almost completely recessive (Figure 5.7 A3), while alleles at the chromosome 4 locus were semi-dominant (Figure 5.7 A4), with similar effect sizes of the homozygous configurations at both loci. Thus, the fewest lesions were seen in

plants doubly homozygous for Bs-5 alleles on chromosomes 1 and 4, and the most in plants doubly homozygous for Est-1 alleles at both QTL (Figure 5.7 B2).

The Rmx-A180 locus on chromosome 3 showed an overdominant behavior, with heterozygotes being much more lesioned than either Rmx-A180 or Est-1 homozygotes (Figure 5.7 A6). Br-0 turned out to be quite different from the expectations based on phenotypic segregation (Table 5.1 and Table 5.2).

The Br-0 alleles on chromosome 5 were dominant, with Br-0 homozygotes and heterozygotes having similarly low levels of lesioning (Figure 5.7 A6).

I also estimated the amount of phenotypic variance in each population explained by the QTL, both individually and in combination. A full genetic model (Lesion ~ Locus1 + Locus2 + Locus1:Locus2**)** accounting for both additive and epistatic interactions between the two candidate loci could explain between 2.3 and 23% of the variance (Table 5.5). The chromosome 4 QTL in the Pro-0/Est-1 cross was the clearest and explained 18% of the variance in the lesion phenotype observed in the F_2 individuals (Table 5.6). The other Pro-0 QTL in chromosome 1 explained 5.29% of the variation. The additive effect of these two QTLs explained the bulk (23.14%) of the variationobserved in the Pro-0/Est-1 F_2 population. On the other hand, the QTL from the Br-0/Est-1 cross explained just a little more than 2% of the variation (Table 5.5 and Table 5.6).

Table 5.3 Summary of markers used per chromosome of each mapping population used for QTL analysis.

F_2 population	*N*[1]	Markers on chromosomes					
		1	2	3	4	5	Total
Pro-0/Est-1	304						
Number of markers		67	43	60	42	73	285
Average spacing (cM)		1.1	1.1	1.0	1.1	0.9	1.0
Max spacing (cM)		4.1	3.9	3.3	8.9	3.9	8.9
Rmx-A180/Est-1	209						
Number of markers		157	75	80	94	141	547
Average spacing (cM)		0.4	0.6	0.6	0.4	0.4	0.5
Max spacing (cM)		3.7	3.2	5.4	5.1	1.8	5.4
Bs-5/Est-1	256						
Number of markers		110	59	86	86	58	396
Average spacing (cM)		0.6	0.7	0.6	0.5	1.0	0.7
Max spacing (cM)		4.8	4.4	5.2	3.9	4.9	5.2
Br-0/Est-1	243						
Number of markers		63	57	82	50	76	328
Average spacing (cM)		1.0	0.7	0.6	0.8	0.8	0.8
Max spacing (cM)		6.7	4.8	5.2	4.4	3.9	6.7

[1] Number of individuals analyzed for the F_2 population

Table 5.4 Summary of mapped loci by QTL analysis for each mapping population.

F_2 population	Locus 1 Interval (Mb)				Locus 2 Interval (Mb)				Threshold (α =0.05) 10,000 permutations
	Chr	Bayesint[a] (Genome location)	Size	LOD Score	Chr	Bayesint[a] (Genome location)	Size	LOD Score	
Pro-0/Est-1	1	13.92 – 23.62	9.69	3.59	4	7.48-9.69	2.21	13.14	3.09
Rmx-A180/Est-1	3	10.47 – 16.67	6.2	4.12	NA[b]	NA[b]	NA[b]	NA[b]	3.30
Bs-5/Est-1	1	25.91 – 30.28	4.27	3.52	4	9.70 – 12.03	2.33	5.55	3.23
Br-0/Est-1	5	21.88 – 24.32	2.44	5.43	NA[b]	NA[b]	NA[b]	NA[b]	3.62[c]

[a] Bayesint - approximate Bayesian credible interval for a particular chromosome; [b] NA – not applicable; [c] Threshold α =0.10 with 10,000 permutations

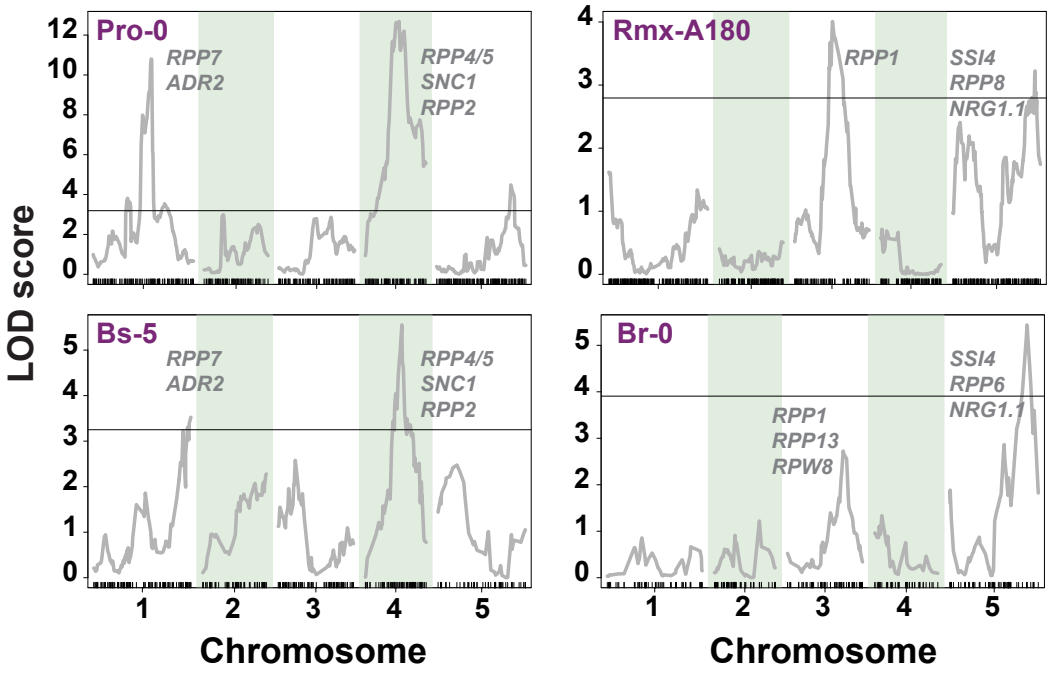

Figure 5.6 QTL maps for lesioning. Immune genes with known major phenotypic effects that fall within the QTL intervals are indicated in italics. Vertical tick marks indicate RAD-seq markers. LOD thresholds at alpha=0.05 for each population mapped are indicated by solid horizontal lines.

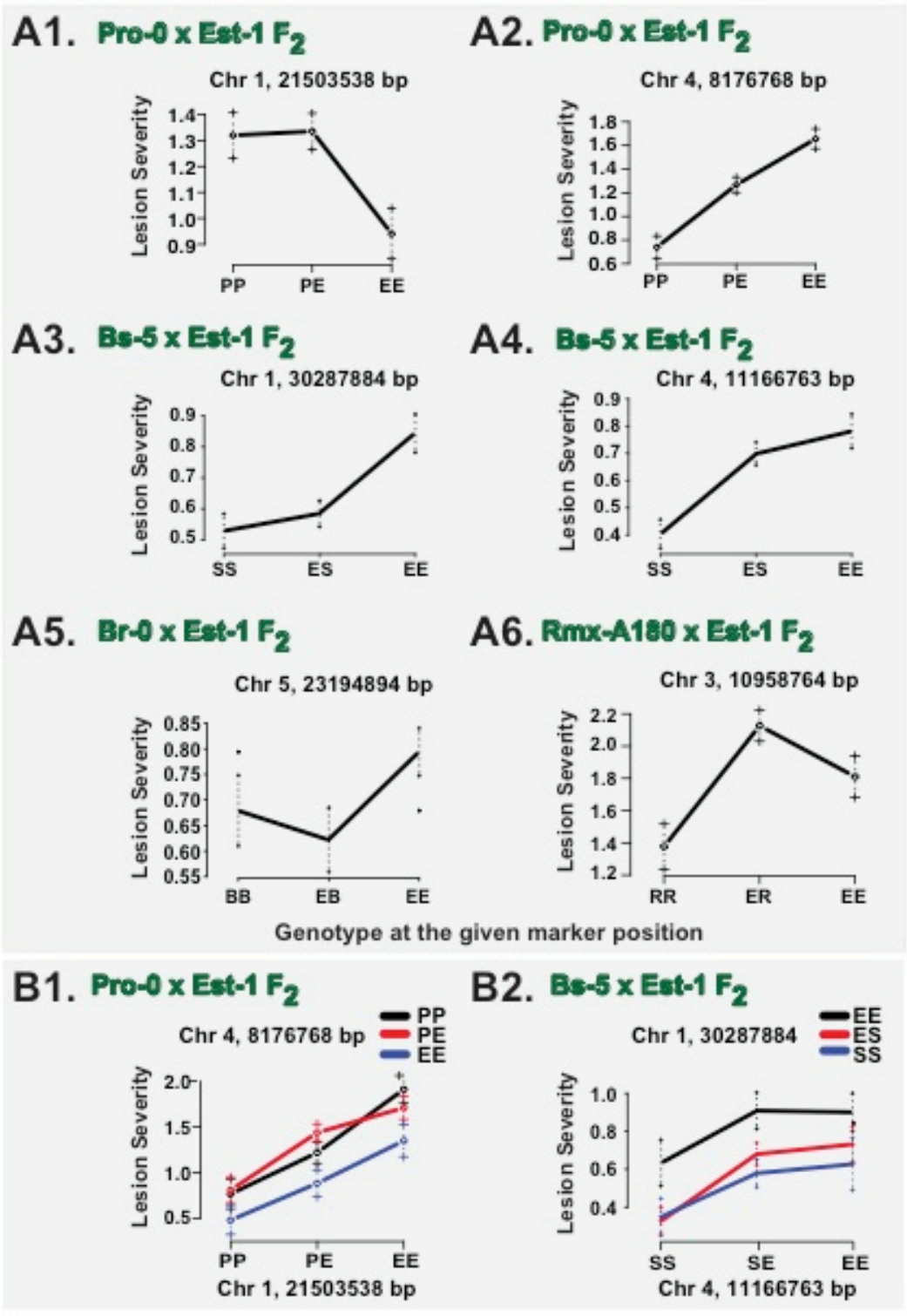

Figure 5.7 A) Effect size and B) interaction plots for markers closest to the highest LOD score for each QTL. The x-axis depicts the three genotypes at each marker. EE stands for F_2 individuals that are homozygous for Est-1 alleles, and the other letters indicate the alternative alleles.

Table 5.5 Summary of phenotypic variance explained given a full, additive and interaction model between QTL 1 and QTL 2 of each mapping population used for QTL mapping.

F_2 Population	Variance Explained by each QTL								
	Full (y ~ Q1 + Q2 + Q1:Q2) or Full (y ~ Q1)			Additive (y ~ Q1 + Q2)			Interaction (y ~ Q1:Q2)		
	LOD	% Var	X^2	LOD	% Var	X^2	LOD	% Var	X^2
Pro-0/Est-1	17.37	23.14	4.88^{-14}	16.7632	22.43	6.66^{-16}	0.695	0.71	0.59
RmxA180/Est-1	4.12	8.68	8.69^{-05}	NA	NA	NA	NA	NA	NA
Bs-5/Est-1	8.97	14.96	1.82^{-06}	8.75	14.62	3.71^{-08}	0.330	0.24	0.91
Br-0/Est-1	1.23	2.30	0.05	NA	NA	NA	NA	NA	NA

Table 5.6 Summary of phenotypic variance explained taking individual QTLs separately for each mapping population used for QTL mapping.

F_2 Population	(y ~ Q1)				(y ~ Q2)			
	Chr	LOD	% Var	X^2	Chr	LOD	% Var	X^2
Pro-0/Est-1	1	3.58	5.29	2.59^{-14}	4	13.1	18.01	7.85^{-14}
RmxA180/Est-1	3	4.12	8.68	7.59^{-05}	NA	NA	NA	NA
Bs-5/Est-1	1	2.79	5.94	1.61^{-03}	4	4.27	8.95	5.631^{-05}
Br-0/Est-1	5	1.38	2.59	0.04	NA	NA	NA	NA

5.1.4 Identification of genes underlying modifier QTLs

Several of the QTLs I mapped are near regions with NLR genes (Nemri, Atwell et al. 2010). Overexpression of several NLR genes, their truncation or point mutations can all lead to autoimmune phenotypes (Bi, Johnson et al. 2011, Xia, Cheng et al. 2013, Chae, Bomblies et al. 2014) and hence I speculated that NLR genes might be causal for modification of *ACD6* activity. I therefore knocked down members of NLR clusters using artificial microRNAs (amiRNAs) (Schwab, Ossowski et al. 2006). AmiRNAs were designed based on the reference accession Col-0 NLR annotation, with several amiRNAs per cluster. Where possible amiRNAs that can target individual genes in a cluster were designed, but most amiRNAs targeted several genes in a cluster. A list of all the NLR candidates for which amiRNAs were transformed into the corresponding accessions is presented in Table 5.7.

NLR genes were knocked down in Est-1, in all tested accessions having an Est-like *ACD6* allele, but with reduced late-onset necrosis, and Col-0 as control. Because the modifiers seemed to be dominant, semi-dominant or recessive, I constructed a range of scenarios for the outcome of the experiments (Figure 5.9). In case of a loss-of-function modifier, the Est-1 knockdown was expected to show reduced lesions and improved growth resulting in a bigger plant (larger and heavier), while in case of a gain-of-function modifier; the non-lesioned accession was expected to now show lesions and reduced growth. Col-0 was not expected to be affected by amiRNAs, for an ACD6 dependent effect of either a gain-of- function or a loss-of-function modifier. If Col-0 also gained lesions, it would indicate that the knockdown in one of the non-lesioned accessions did not require *ACD6*-Est for its effect.

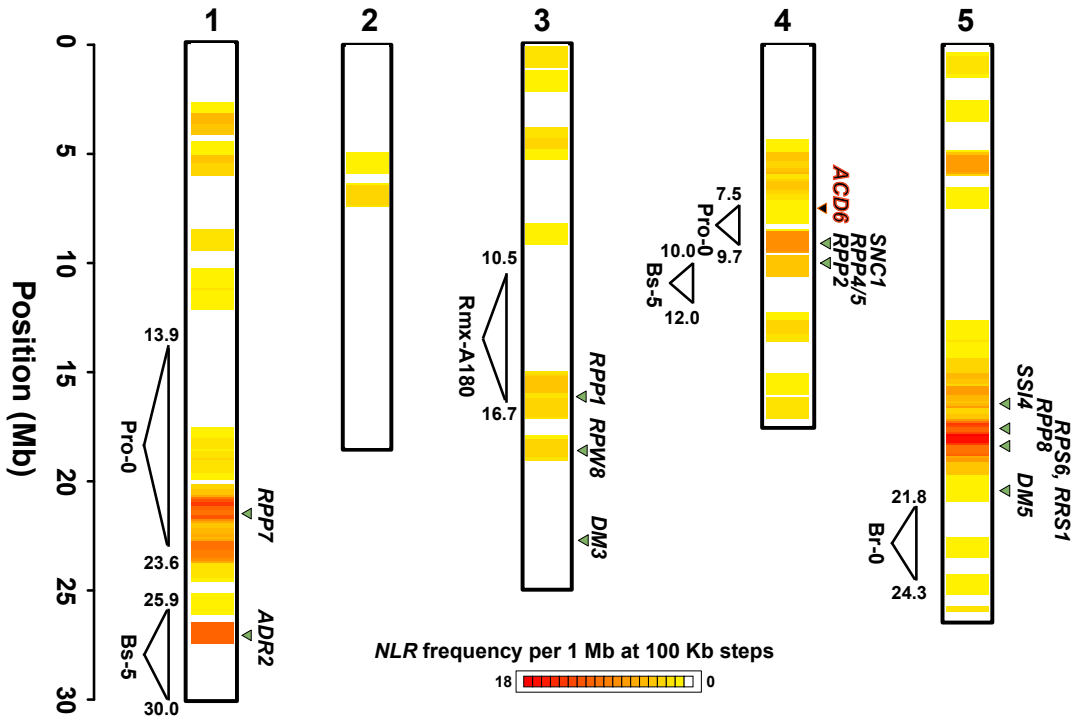

Figure 5.8 Location of *ACD6* modifier QTL compared with that of NLR genes. QTL intervals are indicated by unfilled triangles. NLR density after Chae et al. (Chae, Bomblies et al.).

Table 5.7 AmiRNAs to identify *ACD6* modifiers.

Target Accession	Target Gene(s)	amiRNA name	amiRNA sequence	Transcript Library/ Reference
RmxA180, Br-0	AT1G58602	NB-ARC (2)	GGGCGATACGACGAACATTTA	TAIR9_cdna_20090619
Pro-0, Bs-5	AT1G58410	NB-LRR (7)	TCATAAATCTGGGTAGTTCAT	TAIR9_cdna_20090619
Pro-0	AT1G62630.1, AT1G63350.1, AT1G63360.1	CC-NBS-LRR (2)	TAATTCTTAGAGCAAAACCGG	TAIR9_cdna_20090619
RmxA180, Br-0	AT3G46530.1, AT3G46710.1, AT3G46730.1	RPP13 (1)	CAACCCAACTTTGAAAACGTT	TAIR9_cdna_20090619
RmxA180, Br-0	AT3G46530.1, AT3G46710.1, AT3G46730.1	RPP13 (2)	AAACTAGTTCGAGAGCTTAAT	TAIR9_cdna_20090619
RmxA180, Br-0	AT3G46530.1, AT3G46710.1, AT3G46730.1	RPP13 (3)	GAACTGAACTTTGAAAACGTT	TAIR9_cdna_20090619
RmxA180, Br-0	AT5G58120.1	ADR2-x5 (1)	TCTACGCAATATACCTTCCGA	TAIR9_cdna_20090619
RmxA180, Br-0	AT5G58120.1	ADR2-x5 (2)	TCACTCCGGCTATAATCTAAT	TAIR9_cdna_20090619
RmxA180, Br-0	AT5G58120.1	ADR2-x5 (3)	GAAACGTTTCGAAGAAACTAT	TAIR9_cdna_20090619
Pro-0	AT1G58602	RPP7 (19)	TAAATGACCATATTCCTGCTC	TAIR9_cdna_20090619
Pro-0	AT1G58602 -- RPP7 cluster2	RPP7 (20)	TTTTCCAGGTATTTCAGTCAA	TAIR9_cdna_20090619
Pro-0	AT1G58602	RPP7 (21)	TCGAGGTATTTCAATCCGCTT	TAIR9_cdna_20090619
Pro-0	AT1G58602	RPP7 (22)	TAAAGTTAGTTCTTGCTCCCA	TAIR9_cdna_20090619
Pro-0	AT1G58390	RPP7 (26)	TTAGATCACGTTTTAGCCCAG	TAIR9_cdna_20090619
Pro-0	AT1G58400	RPP7 (27)	TATGTCTAGATAGATCGGCAA	TAIR9_cdna_20090619
Pro-0	AT1G58400	RPP7 (28)	TAAGTTAGTTTTGTGATGCGC	TAIR9_cdna_20090619
Pro-0	AT1G58390	RPP7 (29)	TCTTAATTCATGCATCCGCAT	TAIR9_cdna_20090619
Pro-0	AT1G58410	RPP7 (30)	TATATCAGACGCAAGTTCCCT	TAIR9_cdna_20090619
Pro-0, Bs-5	AT4g16860, AT4g16890, AT4g16900, AT4g16920, AT4g16940, AT4g16950, AT4g16960	RPP4/5 (EC290)	TAGATGACAAGTTGACGTCGA	TAIR9_cdna_20090619
Pro-0, Bs-5	AT4g16860, AT4g16920	RPP4/5 (EC292)	CTACGACGATAGGATAAATAT	TAIR9_cdna_20090619
Pro-0, Bs-5	AT4g16860, AT4g16920	RPP4/5 (EC293)	TATCTATTAATAGCCCCCCCG	TAIR9_cdna_20090619
Pro-0, Bs-5	AT4g16860, AT4g16920	RPP4/5 (EC294)	TGTCCGCTACAATTCGGCCGT	TAIR9_cdna_20090619
Pro-0, Bs-5	AT4g16860, AT4g16920	RPP4/5 (EC295)	TGAATGGCAAACGTATTGCAC	TAIR9_cdna_20090619
RmxA180, Br-0	AT3G44400, AT3G44480, AT3G44630, AT3G44670	RPP1 (209)	UGACACAUAAACUCCAUCGGU	Chae et al., 2014
RmxA180, Br-0	AT3G44400, AT3G44480, AT3G44630, AT3G44670	RPP1 (210)	TAGTTGGAAAATCTCACGCAT	Chae et al., 2014
RmxA180, Br-0	AT3G44400, AT3G44480, AT3G44630, AT3G44670	RPP1 (211)	UGUUGGCACAUAAACUCGGAG	Chae et al., 2014
RmxA180, Br-0	AT3G44400, AT3G44480, AT3G44630, AT3G44670	RPP1 (212)	UACAUUUCAACUGCGAGCGUC	Chae et al., 2014
RmxA180, Br-0	AT3G44400, AT3G44480, AT3G44630, AT3G44670	RPP1 (217)	TAATAATCGAATGACTCGAGG	Chae et al., 2014
RmxA180, Br-0	AT3G44400, AT3G44480, AT3G44630, AT3G44670	RPP1 (226)	UUCUUACCGAUCCCAGGCGGU	Chae et al., 2014
RmxA180, Br-0	AT3G44400, AT3G44480, AT3G44630, AT3G44670	RPP1 (228)	UAUAUCCGUAAUGAUUGCGGC	Chae et al., 2014
Br-0	AT3G26450, AT3G26460, AT3G26470, AT3G26480	RPW8 (110)	TTCAAGGAAACACGTGAGACG	TAIR9_cdna_20090619
Br-0	AT3G26450, AT3G26460, AT3G26470, AT3G26480	RPW8 (140)	TCAGAACGTAAATCGGATCGC	TAIR9_cdna_20090619

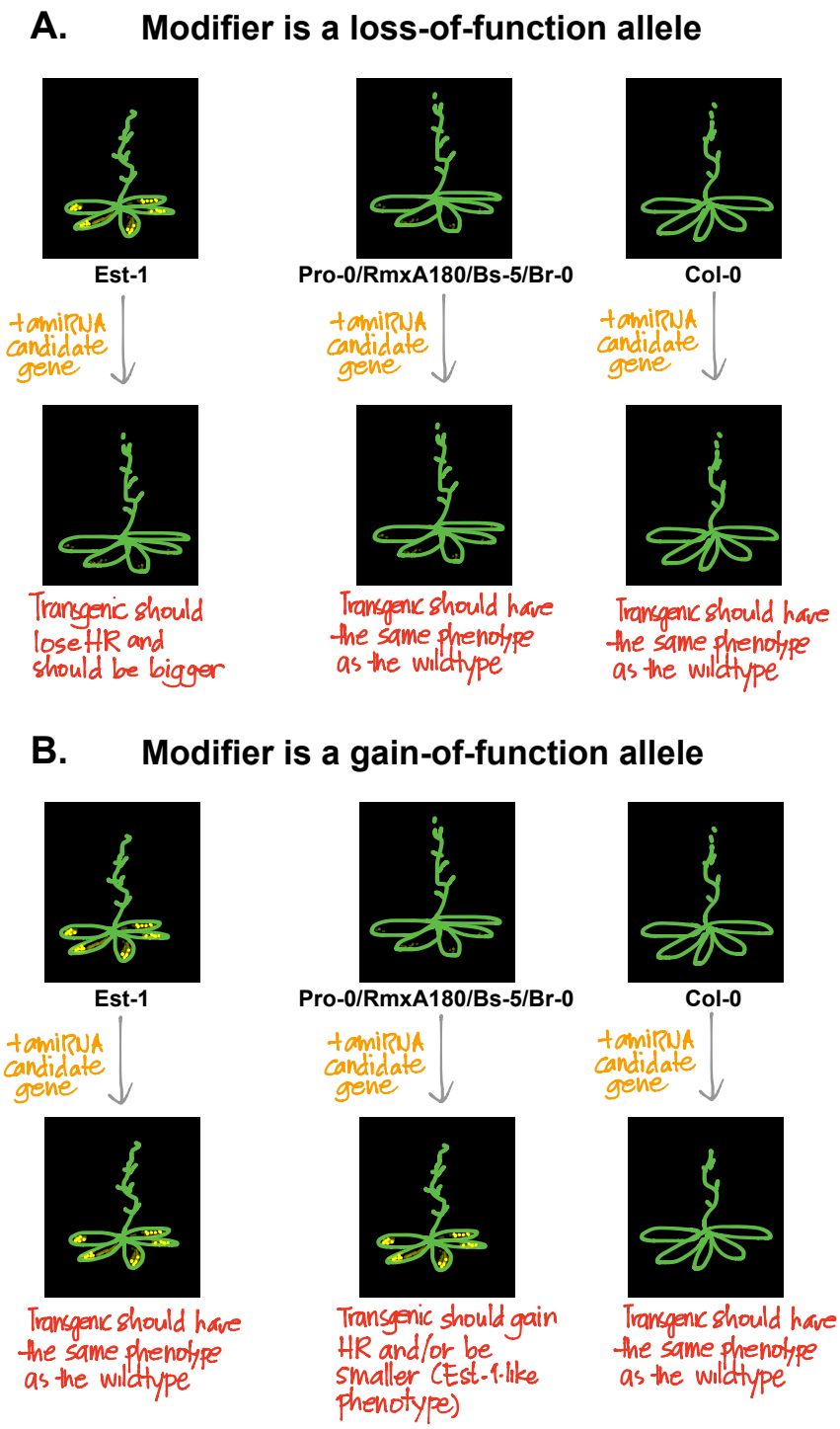

Figure 5.9 Expected phenotypes upon candidate gene knockdown in Est-1, the accession with the modifier, and Col-0

5.1.4.1 RPP4/5 *as a candidate modifier of* ACD6 *hyperactivity*

Similar to knocking down *ACD6* itself in Est-1, knocking down genes of the *RPP4/5* cluster in Est-1 abolished autoimmunity-related late-onset necrosis (Figure 5.10, Figure 5.11). This was only seen when a black Moosgummi cover isolated plants from soil, presumably reducing microbial stimuli emanating from the soil, which otherwise could cause HR-like lesions. At 23°C, the amiRNA EC290, which targeted most genes in the *RPP4/5* cluster completely suppressed lesion formation until around 8 weeks after sowing (Figure 5.10). For comparison, knocking down *ACD6* with an amiRNA suppressed lesions even at 10 weeks of growth, and also on soil (Figure 5.10). Trypan blue staining confirmed the suppression of cell death (Figure 5.11). Two other amiRNAs, EC292 and EC294, were similarly effective as amiRNA EC290, while EC293 and EC295 were less effective, with transgenic plants having collapsed dead cells at the leaf tips (Figure 5.11). No phenotypic lesion effects were apparent in Pro-0 and Col-0 (Figure 5.10, Figure 5.11).

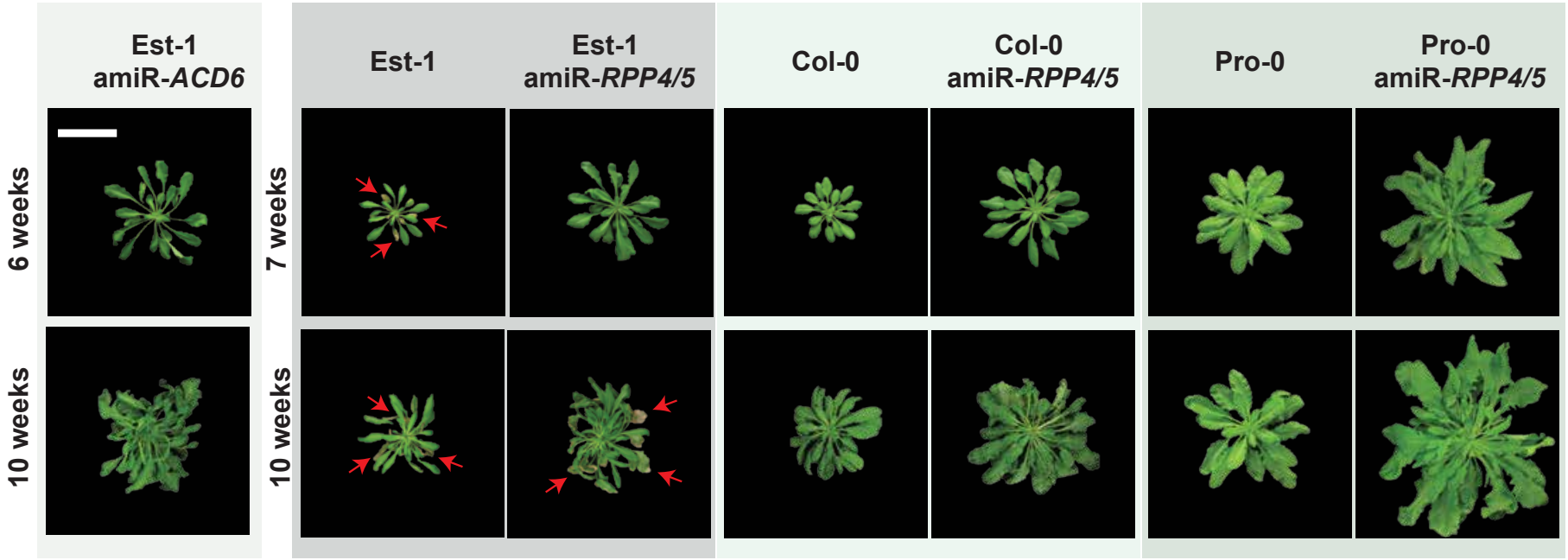

Figure 5.10 Representative amiR-*ACD6* (6 WAS and 10 WAS) and amiR-*RPP4/5* (7 WAS and 10 WAS) Col-0, Est-1 and Pro-0 transgenics.

Note: Est-1 amiR-ACD6 transgenics were generated by Dr. Marco Todesco; Est-1, Col-0 and Pro-0 amiR-RPP4/5 transgenics were generated by either Maricris Zaidem or Dr. Wangsheng Zhu. Growing the transgenic lines for phenotyping was spear-headed by Dr. Wangsheng Zhu.

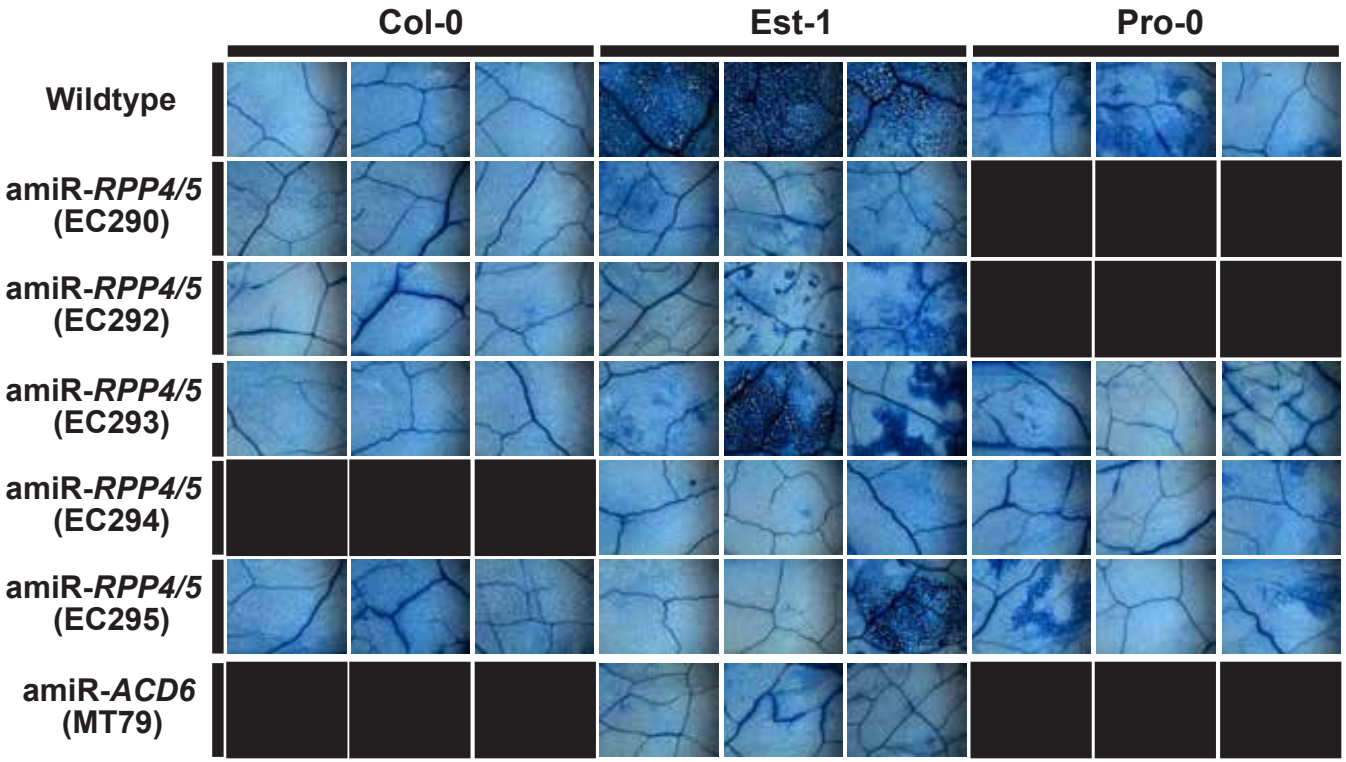

Figure 5.11 Trypan blue staining of representative amiR-*ACD6* (42 DAS) and amiR-*RPP4/5* (56 DAS) Est-1 and Pro-0 transgenics. Black squares indicate that the corresponding transgenic lines were not available.

Note: Est-1 amiR-ACD6 transgenics were generated by Dr. Marco Todesco; Est-1, Col-0 and Pro-0 amiR-RPP4/5 transgenics were generated by either Maricris Zaidem or Dr. Wangsheng Zhu. Trypan blue staining of the transgenic lines for phenotyping was spear-headed by Maricris Zaidem.

The *RPP4/5* cluster is highly variable in organization and sequence between accessions (Guo, Fitz et al. 2011, Tsuchiya and Eulgem 2013, Chae, Bomblies et al. 2014), and the Pro-0 and Est-1 sequences are unknown. That amiRNAs predicted to target the same genes in Col-0 (EC292, EC293, EC294 and EC295) gave different results in Est-1 points to Est-1 genes differing from those in Pro-0.

The *ACD6*-Est allele not only induces late-onset necrosis, but also reduces growth and thus biomass (Todesco, Balasubramanian et al. 2010). There was a trend for several amiR-*RPP4/5* to increase biomass specifically in Est-1, but not Pro-0, although a similar trend was observed also in Col-0 (Figure 5.12).

In summary, these results, while preliminary, point to a potential role of genes in the *RPP4/5* cluster of Est-1 contributing to the lesions caused by the hyperactive *ACD6*-Est allele. I note that the effects are not unexpected, since the QTL explained only ~18.01% of phenotypic variance (Table 5.5), and because I had found multiple independent QTL in the four crosses examined.

5.1.5 General conclusions about Est-like ACD6 modulators

The evidence presented in this chapter indicates that modifiers of the hyperactive *ACD6*-Est are surprisingly diverse. This can be concluded from the different genomic locations of QTL in different crosses, their dominance behavior, and their genetic interactions (additive versus epistatic). It will be interesting to construct strains in which modifiers from different accessions are combined, to test whether they further enhance the suppression of the *ACD6*-Est lesioning phenotype.

The possibility that NLRs might contribute to *ACD6* hyperactivity, as deduced from the *RPP4/5* knockdowns in Est-1, is particularly exciting, since NLRs have so far not been linked directly to *ACD6* function.

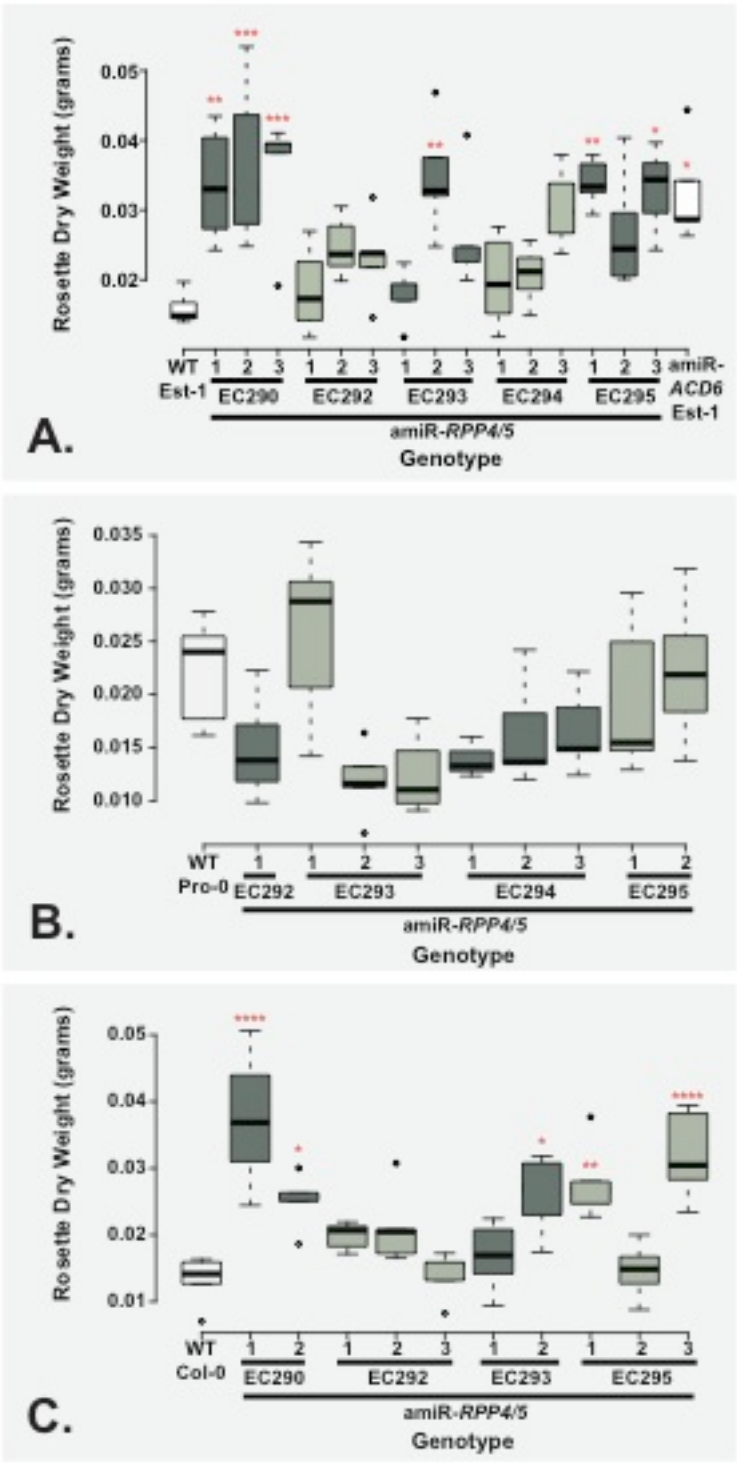

Figure 5.12 Biomass of representative A) Est-1, B) Pro-0 and C) Col-0 amiR-*RPP4/5* transgenics. Data are from 5 biological replicates each, with three independent lines for most transgenes. Pairwise comparisons using t-tests with pooled SD, significant difference relative to the wildtype (Est-1, Pro-0 or Col-0); p-value: **** < 0.0001 , *** < 0.001, ** < 0.005, *< 0.05.

Note: Est-1 amiR-ACD6 transgenics were generated by Dr. Marco Todesco; Est-1, Col-0 and Pro-0 amiR-RPP4/5 transgenics were generated by either Maricris Zaidem or Dr. Wangsheng Zhu. Weighing of the transgenic lines for phenotyping was spear-headed by Dr. Wangsheng Zhu.

6 Discussion

Darwinian fitness is defined as the number of fertile offspring an individual has. Maximizing Darwinian fitness means to find the right balance between investments in growth, reproduction and in defense against pathogens and other environmental challenges. My thesis work built on the finding of a special allele at the *A. thaliana ACD6* locus that shifted the balance from growth to defense (Todesco, Balasubramanian et al. 2010). However, not all accessions that appeared to have this special allele showed an obviously increased activity of the immune system (Todesco, Balasubramanian et al. 2010).

Specifically, my work had three interrelated objectives. The first major objective was to better understand the worldwide distribution of hyperactive *ACD6* alleles. The second objective was to extend our knowledge of the relationship between *ACD6* activity and plant defense. The third objective was to identify natural modifiers of the hyperactive *ACD6* allele.

6.1 Variation in the hyperactive *ACD6* allele

6.1.1 Est-like ACD6 in A. thaliana accessions

Hyperactivity of the *ACD6*-Est-1 allele has been attributed to two amino acid changes in the transmembrane domain of the protein (Todesco, Balasubramanian et al. 2010). That just several or one amino acid change in a protein is enough to confer phenotypic variation is not new. Several examples of *Arabidopsis* proteins that have altered function due to a single amino acid change include ATMYC1, PHYB, PHYA, CRY2, APR2, HUA2, TFL and FT (El-Assal, Alonso-Blanco et al. 2001, Maloof, Borevitz et al. 2001, Hanzawa, Money et al. 2005, Loudet, Saliba-Colombani et al. 2007, Wang, Sajja et al. 2007, Filiault, Wessinger et al. 2008, Symonds, Hatlestad et al. 2011). Amino acid changes in these proteins caused altered protein-protein

interactions, altered activity of activator or repressor, or altered protein stability. For *ACD6*, as with *HUA2*, the SNPs causal for these amino acid changes are thought to result in a hypermorphic allele (enhancing functionality). ACD6 have two major domains: 1) ankyrin domain which mediates protein-protein interactions and 2) transmembrane domain, which anchors ACD6 in the membrane. The fact that the two causal SNPs confering hypermorphism are located in region coding trans membrane domain points to the relevance of the transmembrane region for ACD6 function. Non-hyperactive ACD6 anchors to the plasma membrane upon elevated SA concentration in the cytosol (Zhang, Shrestha et al.). In *acd6-1,* with an activated *ACD6* version similar to Est-like allele, ACD6 was found to localize in the plasma membrane, irrespective of SA or BTH concentration (Zhang, Shrestha et al. 2014).

Among the *ACD6* alleles discovered in natural Arabidopsis accessions so far (Todesco, Balasubramanian et al. 2010, Todesco, Kim et al. 2014), only Est-like alleles confer autoimmunity. In my study, ~12% of Arabidopsis natural accessions contained Est-like *ACD6* alleles, within those 88% exhibited the HR-like lesions similar to autoimmune mutants or accessions. The rest could either contain other SNPs that render *ACD6*-Est-1 non-hyperactive or have extragenic modulators of ACD6 similarly to studied cases of Pro-0 and Rmx-A180.

GWAS on 96 Arabidopsis accessions conducted by Todesco and colleagues (2010) confirmed *ACD6* association with necrosis. Est-like *ACD6* allele has a clear impact on the phenotype and segregates at low frequency in population, which suggests that either it is a relatively young allele or is only advantageous at specific conditions (Memon, Jia et al. 2016). Data I generated from my study could be used to conduct analyses to estimate allele age (Slatkin and Rannala 2000). Accessions that I identified to contain Est-like *ACD6* alleles could be used to determine the conditions that influence *ACD6* hyperactivity. Moreover, I hypothesize that natural modulators are relevant for tempering and keeping the hyperactive *ACD6* allele type in the population.

6.1.2 Maintenance of ACD6 allelic diversity

Genetic variation observed in *ACD6* can be maintained within populations or species through balancing selection by mechanisms such as heterozygote advantage or overdominance, epistatic selection, frequency-dependent selection, spatial or temporal selection, local adaptation to different environments (Charlesworth and Awadalla 1998, Tian, Araki et al. 2002, Charbonnel and Pemberton 2005, Kroymann and Mitchell-Olds 2005, Tellier and Brown 2011). Although differing in the specifics, these mechanisms are all built on the precondition that having a particular allele is beneficial (advantageous) or deleterious (detrimental) in some way depending on a associated condition. For instance, in a spatial-temporal selection scenario, balancing selection can occur when different alleles are favored in different environments over time or geography (Hedrick, Ginevan et al. 1976, Wardlaw and Agrawal 2012). Given these particulars, prerequisites for the *ACD6* locus to be under balancing selection can be envisioned. Co-occurrence of diverse *ACD6* allele types in local (Todesco, Kim et al. 2014) and global populations (this work and Todesco et al., 2010) and the pattern of diversity I observed in *ACD6* locus (divergence between major allelic clusters) supports that this locus is under balancing selection.

Other than the fact that functionally distinct *ACD6* allele types are found interspersed with each other across the global range of Arabidopsis occurrence, the expressivity of the *ACD6*-Est-1 allele seem to follow a geographic latitudinal gradient. The trend was that suppressed or non-lesioned accessions with Est-like *ACD6* alleles are more often found in lower latitudes of the Arabidopsis geographical range of growth. While the *ACD6* allele type explained 30% of the lesion severity variation, a further 10% could be explained by latitudinal location alone in the subset of accessions analyzed. The observed gradient might be a result of lower mean annual temperature with higher latitude. Lines carrying Est-like *ACD6* alleles are expected to produce more SA and like *acd6-1* be small, lesioned and have reduced fitness at lower temperatures (Todesco, Kim et al. 2014). Testing temperature or SA gradients explicitly in relation to *ACD6* allele occurrence in the global populations should give more information.

There has been an attempt to test this on a local scale. In a set of four Iberian populations, *ACD6*-Est-like alleles were more common at lower elevations where the annual mean temperature is at 14.6°C than at higher elevations where annual mean temperatures are around 6.8°C (Zhang, Lariviere et al. 2014). In addition, Zhang and colleagues (Zhang, Tonsor et al. 2015) found that in these Iberian populations, there was a cline in SA concentration with increasing elevation. This trend is contradictory to our expectations based on effect of temperature on *acd6-1*. Local adaptation offers a plausible explanation for the patterns surveyed from the aforementioned study's Iberian Peninsula populations.

I propose that further experiments be conducted to test for a role of *ACD6* in local adaptation such as: identification of *ACD6* allele frequencies in relation to local conditions (Gunther and Coop 2013); genomic comparisons of locally heterogenous *ACD6* stands (Kubota, Iwasaki et al. 2015); and common garden experiments combined with reciprocal transplantation experiments (Rutter and Fenster 2007).

6.2 Hyperactive ACD6 alleles, growth, late-onset necrosis and immunity

A hyperactive *ACD6* allele while exhibiting HR-like lesions and stunted growth confers elevated immunity, which results in better pathogen response (Lu, Salimian et al. 2009, Todesco, Balasubramanian et al. 2010). Therefore an accession with a modulated hyperactive *ACD6* allele exhibiting suppressed HR-like lesions and normal growth is expected to have lessened immunity and inadequate pathogen response. I tested this hypothesis using Pro-0 and Rmx-A180. What was assumed as a simple relationship between ACD6 allele type, growth, necrosis and pathogen response was more complex in reality.

Taking the growth and pathogen challenge results together, I conclude that: 1) The Pro-0 and Rmx-A180 *ACD6* modifiers could positively uncouple *ACD6*-dependent growth and defense trade-off and 2) Pro-0 and Rmx-A180 have different *ACD6* modifiers. The fact that silencing *ACD6*-Pro-0 did not have an effect on growth but had an effect on defense was the first evidence that *ACD6*-Pro-0 could possibly uncouple the Est-like *ACD6* effect on growth

and defense. The hypothesis of Pro-0 and Rmx-A180 having different *ACD6* modifiers was supported by the opposite responses exhibited by these two accessions upon *ACD6* knockdown.

6.2.1 SA accumulation and ROS production

ACD6 is a positive regulator of cell death, defense, and its down-regulation decreases SA accumulation (Lu, Rate et al. 2003, Tateda, Zhang et al. 2014, Zhang, Shrestha et al. 2014). This concomitantly dampens flg22-elicited ROS response (Yi and Kwon 2014, Yi, Shirasu et al. 2014). Pro-0 exhibits the same pattern of SA accumulation and flg-22 induced ROS response as Est-1. On the other hand, Rmx-A180 responses were atypical compared to Est-1. For this atypical Rmx-A180 response upon *ACD6* knockdown to be explained, it would be best to first discuss the nature of the SA accumulation difference among the control (Est-1 and *acd6-1*) and the *ACD6* modulated (Pro-0 and Rmx-A180) genotypes. The growth challenged genotypes, Est-1 and *acd6-1*, had SA concentrations almost at scale with each other. The accessions with modulated *ACD6* function, Rmx-A180 and Pro-0 had 4-fold less and 10–fold less SA than Est-1, respectively.

My findings raise the following questions:

- Is there a significant threshold for physiological SA concentrations that can set-off the defense reaction cascade and the appearance of HR-like lesions?
- Is there a preferred form of SA to induce downstream immune responses?
- Are there known hormones or proteins that can titrate or offset the effect of SA (without changing the levels of SA)?

A study from Kliebenstein and colleagues (Kliebenstein, West et al. 2006) included a side experiment with seven *A. thaliana* accessions, including Col-0 and Est-1, to test variation in response to SA application. Their report suggested that concentrations higher than 0.30 mM SA were phytotoxic in some of the accessions they tested, although they did not show the actual data in the paper. On the other hand, a study conducted 20 years ago on the ability of the synthetic SA analog abenzo-(1,2,3)-thiadiazole-7-carbothioic acid

S-methyl ester (BTH) to activate resistance transduction pathway showed that concentrations lower than 0.12 mM of BTH are insufficient to activate *PR1* (Lawton, Friedrich et al. 1996). Furthermore, Lu and colleagues (Lu, Rate et al. 2003) found that *ACD6* is consistently expressed even without BTH induction, but both studies concur that as much as 100 µM (0.1 mM) BTH is needed to induce *PR1* protein expression. Albeit through experiments using the SA analog, this indicates that there is a threshold level concentration needed for activating *ACD6* and SA-dependent resistance. The Pro-0 and Rmx-A180 examples suggested that the concentration level needed to induce *PR1* expression and HR-like lesions are non-uniform. Consistent with this, two other accessions, KZ1 and Got22, when treated with as much as 300 µM SA failed to accumulate *PR1* protein (Gangadharan 2014). In parallel with results from my experiments, results from Gangadharan (Gangadharan 2014) not only show that there might be a different threshold level for SA to activate downstream immune responses, but also indicates that other accessions contain modulators that suppresses SA accumulation or titrate the effects of SA upon bacterial (*Pseudomonas syringae* pv. *phaseolicola*) infection.

SA function during resistance to infection lies predominantly in its ability to activate defense genes (Blanco, Salinas et al. 2009). van Leeuwen and colleagues (van Leeuwen, Kliebenstein et al. 2007) found that there is significant natural variation in transcriptional responses to exogenous SA. In the case of Rmx-A180, SA accumulation might bring about a concomitant transcriptional response that is not as intense as Est-1. To prove *ACD6*-dependency and narrow down candidate *ACD6*-Rmx-A180 modulators, transcriptome comparison between wild-type Rmx-A180 and Est-1 and the corresponding amiR-*ACD6* lines can be conducted.

The accumulation of SA in leaves following pathogen infection coincides with the appearance of salicylic acid β-glucoside (Wang, Sager et al. 2013) (Delaney 1994). Although free SA is considered the biologically active form of SA, elevated SAG concentration was also observed during activation of plant defenses (Enyedi, Yalpani et al. 1992). SAG function is not well established but several studies have proposed that it may serve to blunting potentially toxic effects of high SA concentrations through vacuolar sequestration (Enyedi and Raskin 1993, Chen, Malamy et al. 1995, Seo,

Ishizuka et al. 1995, Dean and Delaney 2008). In the assays I conducted, conjugated SA (glucoside 1) was always more abundant than free SA. The difference is more striking in Pro-0 and Rmx-A180 where the conjugated SA (glucoside 1) level was as much as 10 times higher than the free SA. It is conceivable that the SA signal is not being relayed efficiently because either SA is mostly present in its conjugated form or low expression of the SA transducer, *NPR1*.

Although SA and JA are the main hormones implicated in disease resistance pathways, other hormones such as gibberellic acid may affect the SA-JA equilibrium (Robert-Seilaniantz, Navarro et al. 2007). Relevant to my study, ABA-dependent repression of BTH-induced resistance and *PR1* expression has been demonstrated (Yasuda, Ishikawa et al. 2008). This repression is affected by the *NPR1* protein or signaling downstream of *NPR1*. Inspection of hormone concentrations, other than SA, could help clarify the reason for the SA block in accessions with modulated *ACD6* phenotypes.

There are several ways by which ROS is produced by the plant. An *ACD6*-relevant mechanism is that SA or SAG build-up blocks catalase from converting toxic H_2O_2 into H_2O and singlet $O^{\cdot}$ (Chen, Malamy et al. 1995, Noctor, Lelarge-Trouverie et al. 2015). Further, FLS2 activation by flg22 transiently elevates cytosolic calcium, production of ROS and other signaling particles to coordinate bacterial defenses (Li, Li et al. 2014). In numerous experiments, ROS production after flg22 treatment has been used as a key assay to assess PTI responses (Zhang, Shao et al. 2007, Chakravarthy, Velasquez et al. 2010, Segonzac and Zipfel 2011, Daudi, Cheng et al. 2012, Vetter, Kronholm et al. 2012, Smith and Heese 2014). Similar to SA, flg22-induced ROS production varied among the accessions I tested. While I saw parallel trends, as expected, in Est-1 and Pro-0 (and the *acd*6-1 control), this was not the case for Rmx-A180. My inspection of *FLS2* sequences did not reveal obvious mutations that might be responsible for the observed differential flg22 responses. The *ACD6*-Rmx-A180 extragenic modulator might be a component protein in the response pathway that affects:

- Mechanisms for titrating H_2O_2 accumulation, i.e. peroxidase activity or,

- Mechanisms that directly increase H_2O_2 accumulation (i.e. photorespiration, fatty acid β-oxidation, superoxide dismutase accumulation) or,
- FLS2 co-activators and interactors and downstream reaction components.

One peroxidase superfamily protein, AT3G28200, was actually included in the candidate genes from the Bayesian credible interval of the QTL mapping for *ACD6*-Rmx-A180 modifier.

While high SA accumulation has generally been pinpointed as a causal prerequisite for the formation of HR/cell-death lesions in plants, there are exceptions. For instance, SA sequestration by bacterial SA hydroxylase (*nahG*) expression did not suppress lesion formation in *lsd2* and *lsd4* mutants (Hunt, Delaney et al. 1997). Additionally, *sid1* and *sid2* mutants whilst unable to accumulate SA developed HR following inoculation with a high titer of *P. syringae* (Nawrath and Metraux 1999). Pertinent to the Rmx-A180 situation are cases where high SA levels coupled with elevated broad-spectrum resistance did not result in severe HR or at most resulted in a severely reduced HR. Examples of such mutants are *defense, no death 1* (*dnd1*), and *defense, no death 2*/*HR-like lesion mimic* (*dnd2*/*hlm1*) (Clough, Fengler et al. 2000, Balague, Lin et al. 2003, Jurkowski, Smith et al. 2004). Research from Lorrain and colleagues (Lorrain, Vailleau et al. 2003) using these mutants show that cell death may be SA-dependent but SA by itself is not the only thing needed for HR production. They assert that another signaling molecule is required in addition to SA to induce cell death after pathogen recognition. *DND1* and *DND2* encode cyclic nucleotide-gated ion channels (Genger, Jurkowski et al. 2008). These channels can mediate transport of K+ and Na+ that is activated by both cyclic GMP and cyclic AMP50. It is important to note that *DND2*/*HLM1* was included in the candidate genes from the Bayesian credible interval of the QTL mapping for *ACD6*-Br-0 modifier.

The *hypersensitive response like lesions 1* (*hrl1*) experiments by Devadas and Raina (Devadas and Raina 2002) showed that pre-treating Arabidopsis with SA or BTH suppressed HR development; such that a constitutively active SAR negatively regulates cell death. Further, research

using *hrl1* show that synergistic overlapping roles for SA, JA and ethylene signaling fine-tune the cell death and defense response against pathogens. A relevant point is the finding that inhibition of JA responses resulted in exaggerated cell death and severe stunting of plants (Devadas, Enyedi et al. 2002). It would therefore be of interest to monitor JA levels in wild-type and amiR-*ACD6* Rmx-A180 plants.

6.2.2 Gene expression differences

In Rmx-A180, it was expected that *PR1* levels would also be high, given the high levels of *FRK1* (Robatzek and Somssich 2002), yet this was not what I observed. There appears to be a disconnection between the known strong developmentally induced expression of *FRK1* during leaf senescence (Robatzek and Somssich 2002) and *PR1* up-regulation in RmxA180 amiR-*ACD6* lines. Pinpointing the gene function for *ACD6*-RmxA180 modifier could help clarify this unexplained pattern.

In the *ACD6*-dependent pathway, *PAD4-EDS1* participates in a positive regulatory loop that increases SA levels (Dong 2004). *PAD4* (Wagner, Stuttmann et al. 2013) has been shown to be essential for defense against green peach aphid (GPA; *Myzus persicae*), and the pathogens *Pseudomonas syringae* and *Hyaloperonospora arabidopsidis* (Louis, Gobbato et al. 2012). It has been demonstrated to be required for multiple defense response including camalexin synthesis and *PR1* gene expression in response to *Pma* but not in response to the avirulent bacterial pathogen *Pst* DC3000/*avrRpt2* (Zhou, Tootle et al. 1998). These results show that there are exceptions and prerequisites for *PAD4* participation in specific defense responses. In Pro-0, *ACD6*-Pro-0 knockdown resulted in reduction of *PAD4* expression. Parallel with Rmx-A180 amiR-*ACD6* responses, a *pad4* mutation only partially suppressed SA accumulation and disease resistance in *acd6-1* (Lu, Rate et al. 2003). Additionally, *pad4* itself is not sufficient to abolish *PR1* expression except in conjunction with *eds1* for the *acd6-1* mutant (Ng, Seabolt et al. 2011). The same circumstances may apply to Rmx-A180 given that *EDS1* expression levels were the same in Rmx-A180 wild-type and Rmx-A180 amiR-*ACD6* transgenic lines. Rustérucci and colleagues (Rusterucci, Aviv et

al. 2001) have proposed that *an EDS1-PAD4* effect on ROS/SA-dependent signaling is modulated by *LSD1*. *LSD1* was included in the candidate genes from the Bayesian credible interval of the QTL mapping for *ACD6*-Pro-0 modifier. It might also be worthwhile to investigate the role of *LESION STIMULATING DISEASE RESISTANCE 1 (LSD1)* in conjunction with *PAD4* and *EDS1* function.

A number of mutants constitutively accumulate high levels of SA. Like Est-1, these mutants show increased disease resistance that requires SA, *PAD4*, *EDS1*, and/or *NDR1* (Lu, Rate et al. 2003). Therefore, another protein that might have implications for *ACD6*-dependent responses in Pro-0 and Rmx-A180 is the plasma membrane-localized integrin-like *NDR1*. Reflecting *NDR1* effect on SA accumulation, *ACD6* knockdown led to decreased *NDR1* expression in Pro-0 but increased *NDR1* expression in Rmx-A180.

Defense signaling mediated by TIR-NLR proteins seems to be largely dependent on *EDS1* (Aarts, Metz et al. 1998, Hu, deHart et al. 2005), while *NDR1* has an equivalent role for CC-NLRs (Century, Holub et al. 1995, Aarts, Metz et al. 1998, Bittner-Eddy and Beynon 2001, Venugopal, Jeong et al. 2009). Several exceptions to this proposed dichotomy include CC-NLRs RPP8, RPP13-Nd, HRT, and RPP7, all of which appear to function independently of *NDR1* (Aarts, Metz et al. 1998, McDowell, Cuzick et al. 2000, Bittner-Eddy and Beynon 2001). My results suggest that an *NDR1* controlled pathway is perturbed upon *ACD6* knockdown in Pro-0 and RmxA180. The higher *NDR1* levels upon amiR-*ACD6* knockdown in Rmx-A180 could be responsible for titration of SA-induced effects such as ROS production that result in necrosis.

In summary, the gene expression assays further support that in Pro-0, a general *ACD6*-dependent dampening of defense responses that happens upon *ACD6* silencing. On the other hand, silencing of *ACD6*-Rmx-A180 results in a general up-regulation of defense responses that culminated with an increased accumulation of SA.

6.2.3 Uncoupled ACD6-dependent growth and defense responses

ACD6 mode of action in Pro-0 and Rmx-A180 accessions is different. *ACD6*-Pro-0 behaved like a suppressed *ACD6*-Est-1. On the other hand the Rmx-A180 atypical responses implied a subduing role of *ACD6*-RmxA180 in defense responses. *ACD6* hyperactivity relies heavily on its maturation and localization in the plasma membrane as controlled by SA levels (Zhang, Shrestha et al. 2014). Despite having a hyperactive *ACD6* allele, Pro-0 does not accumulate SA. Due to this blockage, *ACD6*-Pro-0 was rendered functionally analogous to a non-hyperactive *ACD6* allele like Col-0. Similar to knocking down *ACD6*-Col-0 wherein no apparent biomass change was evident (Todesco, Balasubramanian et al. 2010), knocking down *ACD6*-Pro-0 did not show any biomass/growth changes. Candidate modulators of *ACD6*-Pro-0 would probably have a role in SA accumulation. The Rmx-A180 case is more complicated because even with relatively high SA levels, hyperactive *ACD6*-dependent phenotypes were not apparent. *ACD6*-Rmx-A180 seemed to be functioning as a hyperactive *ACD6* allele but in a tempered capacity. Candidate modulators of *ACD6*-Rmx-A180 could be proteins it forms complex with, including PRRs such as FLS2, EFR and CERK1 (Zhang, Shrestha et al. 2014). ACD6 complexes increase in size during SA signaling (Zhang, Shrestha et al. 2014). The size of the protein complex formed in Col-0 and *acd6-1* was the same, but *acd6-1* contained more of the protein complex at the membrane (Zhang, Shrestha et al. 2014). When *ACD6*-Rmx-A180 was knocked down complex formation may have been altered which could possibly activate or liberate a protein responsible for the higher amplitude of defense responses. Given that *ACD6*-Rmx-A180 knockdown resulted in a bigger and heavier rosette, the “activated” protein’s function could possible not rely on the amplification of SA responses but instead spurs growth-promoting hormones such as auxins, brassinosteroids, gibberellins or cytokinins (Huot, Yao et al. 2014). Quantification of these hormones in Rmx-A180 and Rmx-A180 amiR-*ACD6* lines could substantiate this claim.

6.3 Genetic basis of extragenic *ACD6* modifiers

To ultimately understand potential uncoupling of *ACD6* downstream responses in the accessions that have the hyperactive *ACD6*-Est-like allele, but do not show necrosis, it is necessary to learn the identity of the genes that suppress necrosis in these accessions. Consistent with different pathogen responses in the accessions, crosses between the accessions already pointed to different genes modifying *ACD6* effects in these accessions.

I conducted QTL analyses in four accessions. These confirmed that the different accessions mostly have different modifiers, as they map to different regions of the genome and interact in different ways with each other. From all previously described *ACD6* suppressors identified in *acd6-1* suppressor screens (Lu, Salimian et al. 2009, Wang, Shi et al. 2011, Wang, Zhang et al. 2014), the mapping intervals overlap only with *NPR1, SA INDUCTION DEFICIENT 2* (*SID2*), *EDS1*, *PAD4*, and *FLS2* (Table 8.1). Other known suppressors such as *PHOSPHATE TRANSPORTER 4;1* (*PHT4;1*), *HOPW1-1-INTERACTING3* (Wang, Seabolt et al. 2011), and an uncharacterized putative metalloprotease (AT5G20660) were not included in studied mapping intervals. Based on previous genetic studies *NPR1* definitely plays a part in the *ACD6* reaction cascade (Vanacker, Lu et al. 2001, Lu, Salimian et al. 2009). *NPR1* was just at the edge of the mapping interval for the *ACD6*-Pro-0 chromosome 1 modifier. It was an appealing candidate as an *ACD6*-Pro-0 modifier given its known function in SA accumulation. However, comparison of the reference, Est-1, and Pro-0 NPR1 amino acid sequence does not show any non-synonymous changes that could result in an altered *NPR1* function (Appendix Figure 1). *EDS1-PAD4*, *SID2* and *FLS2* were included in Bayesian credible mapping intervals for modifier loci from Br-0, Bs-5 and Rmx-A180, respectively. *FLS2* function in Rmx-A180 should definitely be studied further given the amplified flg22-induced ROS responses observed upon *ACD6* knockdown. At the same time, FLS2-Rmx-A180 contains several possibly non-synonymous amino acid changes that could be implicated in an altered FLS2 function (Appendix Figure 2). Br-0 definitely has several possible non-synonymous amino acid changes in EDS1 and PAD4 compared to Col-0 and Est-1 (Appendix Figure 3 and Appendix Figure 4) that can cause a differential

function. SID2-Bs-5 does not seem to have possible non-synonymous amino acid changes compared to Col-0 and Est-1 (Appendix Figure 5). Assays to determine *ACD6* hyperactivity, similar to those conducted with Pro-0 and Rmx-A180, should be done for Bs-5 and Br-0. Fine-mapping to narrow down the mapping intervals are currently underway. However some stumbling blocks, i.e. genomic locations of mapping intervals, insufficiency of quantitative phenotypic scale used for characterization of *ACD6*-dependent responses, are still being overcome.

Some *ACD6* modifier QTLs I mapped appear to include NLR genes based on Bayesian credible intervals. *RPP13* is close to one of the QTL intervals, and it is a candidate for being one of the Rmx-A180 modifier loci because comparable to Rmx-A180 responses, *RPP13* function does not necessarily depend on just SA accumulation (Bittner-Eddy and Beynon 2001). A natural variant, *RPP13*-Nd, functions independently of SA and its activity is not changed in *ndr1* and *eds1* mutants (Bittner-Eddy and Beynon 2001). There is considerable functional variation at the *RPP13* locus in *A. thaliana* accessions (Bittner-Eddy and Beynon 2001, Rose, Bittner-Eddy et al. 2004), consistent with a rare *RPP13* allele affecting *ACD6* responses in Rmx-A180.

Table 6.1 Suppressors of *acd6*-1 and their genomic locations

Gene	Other Names	TAIR10 coordinates (bp)	Accession for which gene may be included in mapping interval
AT2G29650	PHT4;1	12673383 - 12676049	None
AT5G13320	WIN3	4267510 - 4271051	None
AT5G20660	Zn-dependent exopeptidase	6986235 - 6991043	None
AT1G64280	NPR1	23852748 - 23855566	Pro-0
AT1G74710	SID2	28070296 - 28074118	Bs-5
AT3G48090	EDS1	17755373 - 17757780	Br-0[1]
AT3G52430	PAD4	19431371 - 19434401	Br-0[1]
AT5G46330	FLS2	18791736 - 18795546	Rmx-A180[1]

[1] QTL did not cross the significance threshold but LOD score value spanning the specified interval was higher than other genomic regions

I have more direct evidence for an NLR modifying *ACD6*-dependent responses in Pro-0 from amiRNA-mediated knockdown of genes in the *RPP4/5* cluster. *RPP4/5* activity is SA and *NDR1* dependent (van der Biezen, Freddie et al. 2002), consistent with the hypothesized *ACD6*-Pro-0 modifier function. In particular, *SUPPRESSOR OF NPR1, CONSTITUTIVE 1* (*SNC1*), part of the *RPP4/5* cluster, has been implicated in constitutive resistance to *Psm* and *Hyaloperonospora arabidopsidis* pv. Noco (Li, Clarke et al. 2001). Specifically, *PAD4* and SA mediate enhanced *SNC1*-dependent resistance (Yang, Li et al. 2006), similar to *ACD6*. Moreover, feedback amplification in disease resistance involves SA and is linked to growth and defense trade-off subject to temperature conditions (Yang and Hua 2004). Deletions of an *RPP4* NLR gene in *snc1* reverted the plants to wild-type morphology and completely abolished constitutive *PR1* expression and disease resistance (Zhang, Goritschnig et al. 2003). All these features make *SNC1* or other gene in the *RPP4/5* cluster a likely candidate as the *ACD6*-Pro-0 modifier in chromosome 4. Cloning of Est-1 and Pro-0 *SNC1* and *RPP4/5* genes and transformation into Col-0 and *acd6-2* should further support this hypothesis.

A screen for *SNC1* suppressors has identified *MODIFIER OF SNC1, 3* (*MOS3*), mutations in which suppress *snc1* autoimmune phenotypes (Zhang and Li 2005). *SNC1* could be the shared modifier loci between Pro-0 and Bs-5. In addition, *MOS3* was included in the Bayesian credible interval of the chromosome 1 *ACD6*-Bs-5 modifier. Non-synonymous amino acid changes could be seen when Col-0, Est-1 and Bs-1 *MOS3* amino acid sequences were compared (Appendix Figure 6).

There has been speculation on NLRs having a link to *ACD6* responses (Dong 2004). However a direct NLR-ACD6 interaction has yet to be shown. ACD6 is a very low abundance protein for which cell biological approaches (e.g. imaging of fluorescent fusion proteins) have not been possible (Zhang, Shrestha et al. 2014). Biochemical approaches such as co-immunoprecipitation of complexes are very tedious since tagging ACD6 seems to often disrupt protein function as seen from attempts from myself, Dr. Marco Todesco (pers. communication) and Shrestha (2010). Taking results from my study, it is possible that *NLR* and *ACD6* function are linked via SA or genes that are involved in the SA-dependent immune response. Some of

these genes that could link *NLR*s and *ACD6* include *EDS1*, *PAD4, NPR1* and *NDR1* (Century, Holub et al. 1995, Aarts, Metz et al. 1998, Bittner-Eddy and Beynon 2001, Lu, Rate et al. 2003, Hu, deHart et al. 2005, Venugopal, Jeong et al. 2009, Ng, Seabolt et al. 2011).

6.4 Summary

Based on my results, I propose that 1) Pro-0 has suppressors of *ACD6* hyperactivity that dampen Pro-0 immune responses, but do not increase growth, and 2) Rmx-A180 has modulators of *ACD6* hyperactivity that moderate hyperactive *ACD6* constitutive activation of immune responses to be inducible instead (Figure 6.1). Rmx-A180 tempered immune responses seem to uncouple hyperactive *ACD6* effects on growth and overt necrosis from those on immunity. At least in Rmx-A180, my results are consistent with the speculative idea that *ACD6* may function like a guardee or decoy. Removal or modification of the guardee results in R signaling and activation of

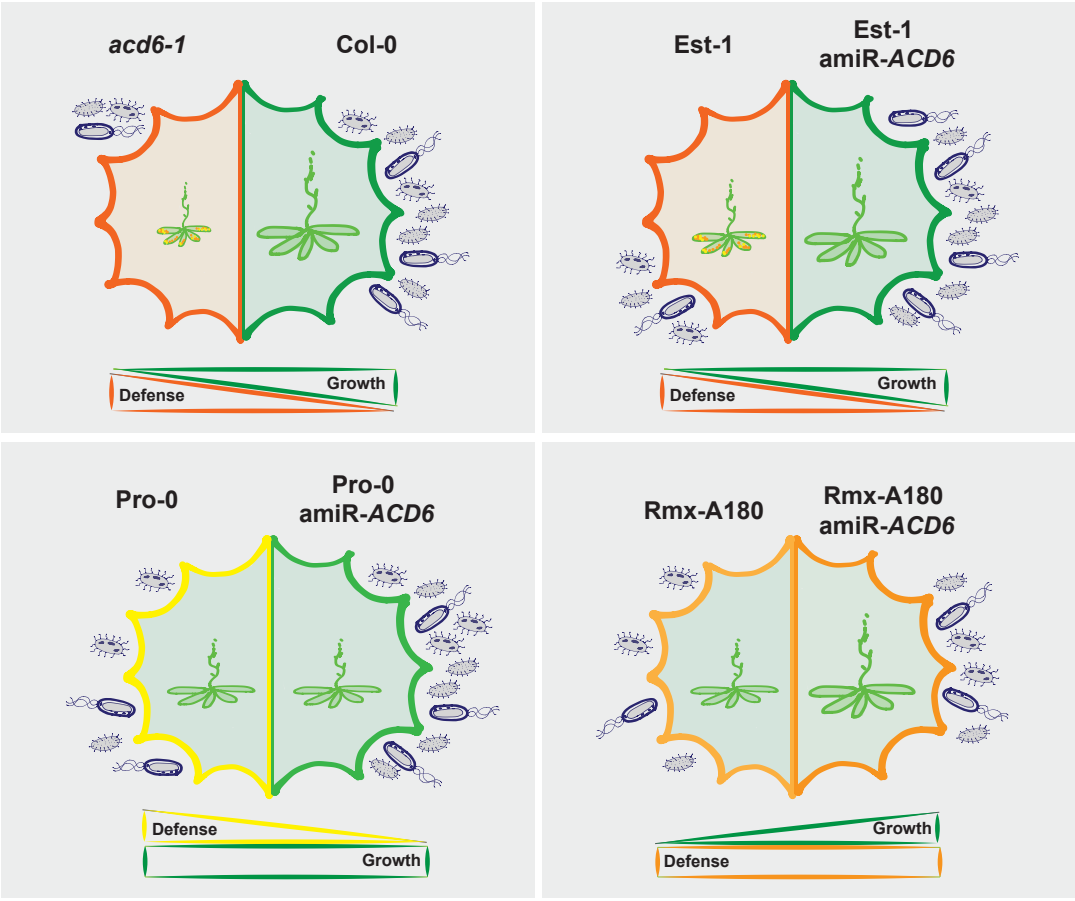

Figure 6.1 The hyperactive *ACD6* allele trade-off effect on growth and defense can be uncoupled as exemplified by accessions with modifiers of the effects of Est-like *ACD6* alleles.

resistance (Van der Biezen and Jones 1998, Dangl and Jones 2001, van der Hoorn and Kamoun 2008). Without the functional removal (as in knocking down) of *ACD6*, the modifier could be inactive, therefore completely suppressing hyperactive *ACD6* effects. Either the "activated" modifier itself or another component that is switched on by the modifier could be causal for inducing downstream Rmx-A180 defense responses and only be activated when the modifier detects *ACD6* degradation or modification. Further experiments are needed to support this hypothesis and are thus currently underway.

6.5 Outlook

My work furthers our understanding of how *ACD6* affects the trade-off between plant growth and defense. My work also brings us closer to understanding why a hyperactive *ACD6* allele is maintained in natural populations. On the basis of natural variation, I have been able to showcase 1) the diversity in *ACD6* allele types, and 2) diversification of *ACD6*-downstream signaling through the action of extragenic modifiers. The study of accessions with a hyperactive *ACD6* allele showed that *ACD6* has variable effects on the growth and defense phenotypes of specific accessions, which can be due to extragenic modulators of *ACD6* activity.

Defense signaling in plants is a product of multiple, sometimes bifurcated and complex pathways with significant crosstalk. The proper activation of these responses relies on numerous defenses repertoires inclusive of preformed defense responses, molecular and biochemical cascades, hormonal regulation and the initiation of gene-for-gene resistance (Knepper and Day 2010). These immune responses must be modulated such that constitutive activation costs are minimized. The pleiotropic *ACD6* trade-off on growth and defense is not an exception. It will be important to identify these modifiers, and investigate whether they evolved only on the background of the hyperactive *ACD6* allele, or segregate independently in the global *A. thaliana* population, and whether they have effects on their own on growth and defense.

7 References

. "Arabidopsis Biological Resource Center." 2010, from https://abrc.osu.edu.

. "R." from http://www.R-project.org.

(2013). "SHORE." from https://sourceforge.net/projects/shore/files/.

Aarts, N., M. Metz, E. Holub, B. J. Staskawicz, M. J. Daniels and J. E. Parker (1998). "Different requirements for EDS1 and NDR1 by disease resistance genes define at least two R gene-mediated signaling pathways in Arabidopsis." Proc Natl Acad Sci U S A **95**(17): 10306-10311.

Abramovitch, R. B., J. C. Anderson and G. B. Martin (2006). "Bacterial elicitation and evasion of plant innate immunity." Nat Rev Mol Cell Biol **7**(8): 601-611.

Alba, C., M. D. Bowers and R. Hufbauer (2012). "Combining optimal defense theory and the evolutionary dilemma model to refine predictions regarding plant invasion." Ecology **93**(8): 1912-1921.

Alfano, J. R. and A. Collmer (1996). "Bacterial pathogens in plants: Life up against the wall." Plant Cell **8**(10): 1683-1698.

Allen, R. L., P. D. Bittner-Eddy, L. J. Grenville-Briggs, J. C. Meitz, A. P. Rehmany, L. E. Rose and J. L. Beynon (2004). "Host-parasite coevolutionary conflict between Arabidopsis and downy mildew." Science **306**(5703): 1957-1960.

Alonso-Blanco, C., M. G. Aarts, L. Bentsink, J. J. Keurentjes, M. Reymond, D. Vreugdenhil and M. Koornneef (2009). "What has natural variation taught us about plant development, physiology, and adaptation?" Plant Cell **21**(7): 1877-1896.

Alonso-Blanco, C. and M. Koornneef (2000). "Naturally occurring variation in Arabidopsis: an underexploited resource for plant genetics." Trends in Plant Science **5**(1): 22-29.

Arber, W. (2011). "Molecular Darwinism: the contingency of spontaneous genetic variation." Genome Biol Evol **3**: 1090-1092.

Asai, T., G. Tena, J. Plotnikova, M. R. Willmann, W. L. Chiu, L. Gomez-Gomez, T. Boller, F. M. Ausubel and J. Sheen (2002). "MAP kinase signalling cascade in Arabidopsis innate immunity." Nature **415**(6875): 977-983.

Asselbergh, B., K. Curvers, S. C. Franca, K. Audenaert, M. Vuylsteke, F. Van Breusegem and M. Hofte (2007). "Resistance to Botrytis cinerea in sitiens, an abscisic acid-deficient tomato mutant, involves timely production of hydrogen peroxide and cell wall modifications in the epidermis." Plant Physiol **144**(4): 1863-1877.

Ausubel, F. M., J. Glazebrook, J. Greenberg, F. Katagiri, M. Mindrinos and G. L. Yu (1993). "Analysis of the Arabidopsis Defense Response to Pseudomonas Pathogens." Journal of Cellular Biochemistry: 129-129.

Azevedo, C., S. Betsuyaku, J. Peart, A. Takahashi, L. Noel, A. Sadanandom, C. Casais, J. Parker and K. Shirasu (2006). "Role of SGT1 in resistance protein accumulation in plant immunity." EMBO J **25**(9): 2007-2016.

Balague, C., B. Lin, C. Alcon, G. Flottes, S. Malmstrom, C. Kohler, G. Neuhaus, G. Pelletier, F. Gaymard and D. Roby (2003). "HLM1, an essential signaling component in the

hypersensitive response, is a member of the cyclic nucleotide-gated channel ion channel family." Plant Cell **15**(2): 365-379.

Baltrus, D. A., M. T. Nishimura, A. Romanchuk, J. H. Chang, M. S. Mukhtar, K. Cherkis, J. Roach, S. R. Grant, C. D. Jones and J. L. Dangl (2011). "Dynamic evolution of pathogenicity revealed by sequencing and comparative genomics of 19 Pseudomonas syringae isolates." PLoS Pathog **7**(7): e1002132.

Bari, R. and J. D. Jones (2009). "Role of plant hormones in plant defence responses." Plant Mol Biol **69**(4): 473-488.

Barto, E. K. and D. Cipollini (2005). "Testing the optimal defense theory and the growth-differentiation balance hypothesis in Arabidopsis thaliana." Oecologia **146**(2): 169-178.

Bednarek, P. and A. Osbourn (2009). "Plant-microbe interactions: chemical diversity in plant defense." Science **324**(5928): 746-748.

Bestwick, C. S., M. H. Bennett and J. W. Mansfield (1995). "Hrp Mutant of Pseudomonas syringae pv phaseolicola Induces Cell Wall Alterations but Not Membrane Damage Leading to the Hypersensitive Reaction in Lettuce." Plant Physiol **108**(2): 503-516.

Bi, D. L., K. C. M. Johnson, Z. H. Zhu, Y. Huang, F. Chen, Y. L. Zhang and X. Li (2011). "Mutations in an atypical TIR-NB-LRR-LIM resistance protein confer autoimmunity." Frontiers in Plant Science **2**.

Bittner-Eddy, P. D. and J. L. Beynon (2001). "The Arabidopsis downy mildew resistance gene, RPP13-Nd, functions independently of NDR1 and EDS1 and does not require the accumulation of salicylic acid." Molecular Plant-Microbe Interactions **14**(3): 416-421.

Blanco, F., P. Salinas, N. M. Cecchini, X. Jordana, P. Van Hummelen, M. E. Alvarez and L. Holuigue (2009). "Early genomic responses to salicylic acid in Arabidopsis." Plant Molecular Biology **70**(1-2): 79-102.

Block, A., G. Li, Z. Q. Fu and J. R. Alfano (2008). "Phytopathogen type III effector weaponry and their plant targets." Curr Opin Plant Biol **11**(4): 396-403.

Boch, J. and U. Bonas (2010). "Xanthomonas AvrBs3 Family-Type III Effectors: Discovery and Function." Annual Review of Phytopathology, Vol 48 **48**: 419-436.

Boller, T. and G. Felix (2009). "A renaissance of elicitors: perception of microbe-associated molecular patterns and danger signals by pattern-recognition receptors." Annu Rev Plant Biol **60**: 379-406.

Bolwell, G. P. (1995). "Cyclic-Amp, the Reluctant Messenger in Plants." Trends in Biochemical Sciences **20**(12): 492-495.

Boots, M. (2011). "The Evolution of Resistance to a Parasite Is Determined by Resources." American Naturalist **178**(2): 214-220.

Bos, J. I., M. R. Armstrong, E. M. Gilroy, P. C. Boevink, I. Hein, R. M. Taylor, T. Zhendong, S. Engelhardt, R. R. Vetukuri, B. Harrower, C. Dixelius, G. Bryan, A. Sadanandom, S. C. Whisson, S. Kamoun and P. R. Birch (2010). "Phytophthora infestans effector AVR3a is essential for virulence and manipulates plant immunity by stabilizing host E3 ligase CMPG1." Proc Natl Acad Sci U S A **107**(21): 9909-9914.

Bowling, S. A., A. Guo, H. Cao, A. S. Gordon, D. F. Klessig and X. I. Dong (1994). "A Mutation in Arabidopsis That Leads to Constitutive Expression of Systemic Acquired-Resistance." Plant Cell **6**(12): 1845-1857.

Bruggeman, Q., C. Raynaud, M. Benhamed and M. Delarue (2015). "To die or not to die? Lessons from lesion mimic mutants." Frontiers in Plant Science **6**.

Brutus, A., F. Sicilia, A. Macone, F. Cervone and G. De Lorenzo (2010). "A domain swap approach reveals a role of the plant wall-associated kinase 1 (WAK1) as a receptor of oligogalacturonides." Proceedings of the National Academy of Sciences of the United States of America **107**(20): 9452-9457.

Burdon, J. J. and P. H. Thrall (2009). "Coevolution of Plants and Their Pathogens in Natural Habitats." Science **324**(5928): 755-756.

Cambronne, E. D. and C. R. Roy (2006). "Recognition and delivery of effector proteins into eukaryotic cells by bacterial secretion systems." Traffic **7**(8): 929-939.

Canonne, J., D. Marino, A. Jauneau, C. Pouzet, C. Briere, D. Roby and S. Rivas (2011). "The Xanthomonas type III effector XopD targets the Arabidopsis transcription factor MYB30 to suppress plant defense." Plant Cell **23**(9): 3498-3511.

Cao, J., K. Schneeberger, S. Ossowski, T. Gunther, S. Bender, J. Fitz, D. Koenig, C. Lanz, O. Stegle, C. Lippert, X. Wang, F. Ott, J. Muller, C. Alonso-Blanco, K. Borgwardt, K. J. Schmid and D. Weigel (2011). "Whole-genome sequencing of multiple Arabidopsis thaliana populations." Nat Genet **43**(10): 956-963.

Cao, Y., Y. Liang, K. Tanaka, C. T. Nguyen, R. P. Jedrzejczak, A. Joachimiak and G. Stacey (2014). "The kinase LYK5 is a major chitin receptor in Arabidopsis and forms a chitin-induced complex with related kinase CERK1." Elife **3**.

Century, K. S., E. B. Holub and B. J. Staskawicz (1995). "Ndr1, a Locus of Arabidopsis-Thaliana That Is Required for Disease Resistance to Both a Bacterial and a Fungal Pathogen." Proceedings of the National Academy of Sciences of the United States of America **92**(14): 6597-6601.

Chae, E., K. Bomblies, S. T. Kim, D. Karelina, M. Zaidem, S. Ossowski, C. Martin-Pizarro, R. A. Laitinen, B. A. Rowan, H. Tenenboim, S. Lechner, M. Demar, A. Habring-Muller, C. Lanz, G. Ratsch and D. Weigel (2014). "Species-wide Genetic Incompatibility Analysis Identifies Immune Genes as Hot Spots of Deleterious Epistasis." Cell **159**(6): 1341-1351.

Chakravarthy, S., A. C. Velasquez, S. K. Ekengren, A. Collmer and G. B. Martini (2010). "Identification of Nicotiana benthamiana Genes Involved in Pathogen-Associated Molecular Pattern-Triggered Immunity." Molecular Plant-Microbe Interactions **23**(6): 715-726.

Charbonnel, N. and J. Pemberton (2005). "A long-term genetic survey of an ungulate population reveals balancing selection acting on MHC through spatial and temporal fluctuations in selection." Heredity **95**(5): 377-388.

Charlesworth, D. and P. Awadalla (1998). "Flowering plant self-incompatibility: the molecular population genetics of Brassica S-loci." Heredity **81**: 1-9.

Chen, Z. X., J. Malamy, J. Henning, U. Conrath, P. Sanchezcasas, H. Silva, J. Ricigliano and D. F. Klessig (1995). "Induction, Modification, and Transduction of the Salicylic-Acid Signal in Plant Defense Responses." Proceedings of the National Academy of Sciences of the United States of America **92**(10): 4134-4137.

Cheng, C., X. Q. Gao, B. M. Feng, J. Sheen, L. B. Shan and P. He (2013). "Plant immune response to pathogens differs with changing temperatures." Nature Communications **4**.

Chinchilla, D., Z. Bauer, M. Regenass, T. Boller and G. Felix (2006). "The Arabidopsis receptor kinase FLS2 binds flg22 and determines the specificity of flagellin perception." Plant Cell **18**(2): 465-476.

Clay, K. and P. X. Kover (1996). "The Red Queen Hypothesis and plant/pathogen interactions." Annu Rev Phytopathol **34**: 29-50.

Clay, N. K., A. M. Adio, C. Denoux, G. Jander and F. M. Ausubel (2009). "Glucosinolate metabolites required for an Arabidopsis innate immune response." Science **323**(5910): 95-101.

Clough, S. J., K. A. Fengler, I. C. Yu, B. Lippok, R. K. Smith and A. F. Bent (2000). "The Arabidopsis dnd1 "defense, no death" gene encodes a mutated cyclic nucleotide-gated ion channel." Proceedings of the National Academy of Sciences of the United States of America **97**(16): 9323-9328.

Coley, P. D., J. P. Bryant and F. S. Chapin (1985). "Resource Availability and Plant Antiherbivore Defense." Science **230**(4728): 895-899.

Cook, D. E., C. H. Mesarich and B. P. H. J. Thomma (2015). "Understanding Plant Immunity as a Surveillance System to Detect Invasion." Annual Review of Phytopathology, Vol 53 **53**: 541-563.

Dangl, J. L. and J. D. Jones (2001). "Plant pathogens and integrated defence responses to infection." Nature **411**(6839): 826-833.

Daudi, A., Z. Y. Cheng, J. A. O'Brien, N. Mammarella, S. Khan, F. M. Ausubel and G. P. Bolwell (2012). "The Apoplastic Oxidative Burst Peroxidase in Arabidopsis Is a Major Component of Pattern-Triggered Immunity." Plant Cell **24**(1): 275-287.

Day, B., D. Dahlbeck, J. Huang, S. T. Chisholm, D. Li and B. J. Staskawicz (2005). "Molecular basis for the RIN4 negative regulation of RPS2 disease resistance." Plant Cell **17**(4): 1292-1305.

de Jonge, R., H. P. van Esse, K. Maruthachalam, M. D. Bolton, P. Santhanam, M. K. Saber, Z. Zhang, T. Usami, B. Lievens, K. V. Subbarao and B. P. H. J. Thomma (2012). "Tomato immune receptor Ve1 recognizes effector of multiple fungal pathogens uncovered by genome and RNA sequencing." Proceedings of the National Academy of Sciences of the United States of America **109**(13): 5110-5115.

de Torres, M., J. W. Mansfield, N. Grabov, I. R. Brown, H. Ammouneh, G. Tsiamis, A. Forsyth, S. Robatzek, M. Grant and J. Boch (2006). "Pseudomonas syringae effector AvrPtoB suppresses basal defence in Arabidopsis." Plant J **47**(3): 368-382.

De Vos, M., V. R. Van Oosten, R. M. Van Poecke, J. A. Van Pelt, M. J. Pozo, M. J. Mueller, A. J. Buchala, J. P. Metraux, L. C. Van Loon, M. Dicke and C. M. Pieterse (2005). "Signal signature and transcriptome changes of Arabidopsis during pathogen and insect attack." Mol Plant Microbe Interact **18**(9): 923-937.

de Wit, P. J. (2007). "How plants recognize pathogens and defend themselves." Cell Mol Life Sci **64**(21): 2726-2732.

Dean, J. V. and S. P. Delaney (2008). "Metabolism of salicylic acid in wild-type, ugt74f1 and ugt74f2 glucosyltransferase mutants of Arabidopsis thaliana." Physiologia Plantarum **132**(4): 417-425.

Delaney, T. P. (1994). "A Central Role of Salicylic-Acid in Plant-Disease Resistance (Vol 266, Pg 1247, 1994)." Science **266**(5192): 1793-1793.

Dempsey, D. A., A. C. Vlot, M. C. Wildermuth and D. F. Klessig (2011). "Salicylic Acid biosynthesis and metabolism." Arabidopsis Book **9**: e0156.

Deslandes, L., J. Olivier, N. Peeters, D. X. Feng, M. Khounlotham, C. Boucher, I. Somssich, S. Genin and Y. Marco (2003). "Physical interaction between RRS1-R, a protein conferring

resistance to bacterial wilt, and PopP2, a type III effector targeted to the plant nucleus." Proc Natl Acad Sci U S A **100**(13): 8024-8029.

Devadas, S. K., A. Enyedi and R. Raina (2002). "The Arabidopsis hrl1 mutation reveals novel overlapping roles for salicylic acid, jasmonic acid and ethylene signalling in cell death and defence against pathogens." Plant Journal **30**(4): 467-480.

Devadas, S. K. and R. Raina (2002). "Preexisting systemic acquired resistance suppresses hypersensitive response-associated cell death in Arabidopsis hrl1 mutant." Plant Physiology **128**(4): 1234-1244.

Dietrich, R. A., T. P. Delaney, S. J. Uknes, E. R. Ward, J. A. Ryals and J. L. Dangl (1994). "Arabidopsis mutants simulating disease resistance response." Cell **77**(4): 565-577.

Dong, X. (2001). "Genetic dissection of systemic acquired resistance." Curr Opin Plant Biol **4**(4): 309-314.

Dong, X. (2004). "The role of membrane-bound ankyrin-repeat protein ACD6 in programmed cell death and plant defense." Sci STKE **2004**(221): pe6.

Doyle, J. J. and E. E. Dickson (1987). "Preservation of Plant-Samples for DNA Restriction Endonuclease Analysis." Taxon **36**(4): 715-722.

El-Assal, S. E. D., C. Alonso-Blanco, A. J. M. Peeters, V. Raz and M. Koornneef (2001). "A QTL for flowering time in Arabidopsis reveals a novel allele of CRY2." Nature Genetics **29**(4): 435-440.

Endara, M. J. and P. D. Coley (2011). "The resource availability hypothesis revisited: a meta-analysis." Functional Ecology **25**(2): 389-398.

Enyedi, A. J. and I. Raskin (1993). "Induction of Udp-Glucose - Salicylic-Acid Glucosyltransferase Activity in Tobacco Mosaic Virus-Inoculated Tobacco (Nicotiana-Tabacum) Leaves." Plant Physiology **101**(4): 1375-1380.

Enyedi, A. J., N. Yalpani, P. Silverman and I. Raskin (1992). "Localization, Conjugation, and Function of Salicylic-Acid in Tobacco during the Hypersensitive Reaction to Tobacco Mosaic-Virus." Proceedings of the National Academy of Sciences of the United States of America **89**(6): 2480-2484.

Falk, A., B. J. Feys, L. N. Frost, J. D. G. Jones, M. J. Daniels and J. E. Parker (1999). "EDS1, an essential component of R gene-mediated disease resistance in Arabidopsis has homology to eukaryotic lipases." Proceedings of the National Academy of Sciences of the United States of America **96**(6): 3292-3297.

Feys, B. J. and J. E. Parker (2000). "Interplay of signaling pathways in plant disease resistance." Trends Genet **16**(10): 449-455.

Filiault, D. L., C. A. Wessinger, J. R. Dinneny, J. Lutes, J. O. Borevitz, D. Weigel, J. Chory and J. N. Maloof (2008). "Amino acid polymorphisms in Arabidopsis phytochrome B cause differential responses to light." Proceedings of the National Academy of Sciences of the United States of America **105**(8): 3157-3162.

Fine, P. V. A., Z. J. Miller, I. Mesones, S. Irazuzta, H. M. Appel, M. H. H. Stevens, I. Saaksjarvi, L. C. Schultz and P. D. Coley (2006). "The growth-defense trade-off and habitat specialization by plants in Amazonian forests." Ecology **87**(7): S150-S162.

Flor, H. H. (1955). "Host-Parasite Interaction in Flax Rust - Its Genetics and Other Implications." Phytopathology **45**(12): 680-685.

Fu, Y., S. J. Emrich, L. Guo, T. J. Wen, D. A. Ashlock, S. Aluru and P. S. Schnable (2005). "Quality assessment of maize assembled genomic islands (MAGIs) and large-scale experimental verification of predicted genes." Proc Natl Acad Sci U S A **102**(34): 12282-12287.

Fu, Z. Q., M. Guo, B. R. Jeong, F. Tian, T. E. Elthon, R. L. Cerny, D. Staiger and J. R. Alfano (2007). "A type III effector ADP-ribosylates RNA-binding proteins and quells plant immunity." Nature **447**(7142): 284-288.

Gaffney, T., L. Friedrich, B. Vernooij, D. Negrotto, G. Nye, S. Uknes, E. Ward, H. Kessmann and J. Ryals (1993). "Requirement of salicylic Acid for the induction of systemic acquired resistance." Science **261**(5122): 754-756.

Gan, S. S. and R. M. Amasino (1997). "Making sense of senescence - Molecular genetic regulation and manipulation of leaf senescence." Plant Physiology **113**(2): 313-319.

Gangadharan, A. (2014). Characterization of defense pathways and genes involved in host-pathovar level resistance using Arabidopsis-Pseudomonas Electroni Thesis or Dissertation, The Ohio State University.

Garnica, D. P., A. Nemri, N. M. Upadhyaya, J. P. Rathjen and P. N. Dodds (2014). "The Ins and Outs of Rust Haustoria." Plos Pathogens **10**(9).

Genger, R. K., G. I. Jurkowski, J. M. McDowell, H. Lu, H. W. Jung, J. T. Greenberg and A. F. Bent (2008). "Signaling pathways that regulate the enhanced disease resistance of Arabidopsis "defense, no death" mutants." Mol Plant Microbe Interact **21**(10): 1285-1296.

Genomes Consortium. Electronic address, m. n. g. o. a. a. and C. Genomes (2016). "1,135 Genomes Reveal the Global Pattern of Polymorphism in Arabidopsis thaliana." Cell.

Glazebrook, J. (2005). "Contrasting mechanisms of defense against biotrophic and necrotrophic pathogens." Annu Rev Phytopathol **43**: 205-227.

Gomez-Gomez, L. and T. Boller (2000). "FLS2: an LRR receptor-like kinase involved in the perception of the bacterial elicitor flagellin in Arabidopsis." Mol Cell **5**(6): 1003-1011.

Gorbe, E. and A. Calatayud (2012). "Applications of chlorophyll fluorescence imaging technique in horticultural research: A review." Scientia Horticulturae **138**: 24-35.

Gorlach, J., S. Volrath, G. Knauf-Beiter, G. Hengy, U. Beckhove, K. H. Kogel, M. Oostendorp, T. Staub, E. Ward, H. Kessmann and J. Ryals (1996). "Benzothiadiazole, a novel class of inducers of systemic acquired resistance, activates gene expression and disease resistance in wheat." Plant Cell **8**(4): 629-643.

Greenberg, J. T. (2000). "Positive and negative regulation of salicylic acid-dependent cell death and pathogen resistance in arabidopsis lsd6 and ssi1 mutants." Molecular Plant-Microbe Interactions **13**(8): 877-+.

Greenberg, J. T. and N. Yao (2004). "The role and regulation of programmed cell death in plant-pathogen interactions." Cell Microbiol **6**(3): 201-211.

Grennan, A. K. (2006). "Plant response to bacterial pathogens. Overlap between innate and gene-for-gene defense response." Plant Physiol **142**(3): 809-811.

group, C. B. (2016). "nextflow." 2016, from http://www.nextflow.io/about-us.html.

Gunther, T. and G. Coop (2013). "Robust identification of local adaptation from allele frequencies." Genetics **195**(1): 205-220.

Guo, Y. L., J. Fitz, K. Schneeberger, S. Ossowski, J. Cao and D. Weigel (2011). "Genome-wide comparison of nucleotide-binding site-leucine-rich repeat-encoding genes in Arabidopsis." Plant Physiol **157**(2): 757-769.

Haas, B. J., S. Kamoun, M. C. Zody, R. H. Jiang, R. E. Handsaker, L. M. Cano, M. Grabherr, C. D. Kodira, S. Raffaele, T. Torto-Alalibo, T. O. Bozkurt, A. M. Ah-Fong, L. Alvarado, V. L. Anderson, M. R. Armstrong, A. Avrova, L. Baxter, J. Beynon, P. C. Boevink, S. R. Bollmann, J. I. Bos, V. Bulone, G. Cai, C. Cakir, J. C. Carrington, M. Chawner, L. Conti, S. Costanzo, R. Ewan, N. Fahlgren, M. A. Fischbach, J. Fugelstad, E. M. Gilroy, S. Gnerre, P. J. Green, L. J. Grenville-Briggs, J. Griffith, N. J. Grunwald, K. Horn, N. R. Horner, C. H. Hu, E. Huitema, D. H. Jeong, A. M. Jones, J. D. Jones, R. W. Jones, E. K. Karlsson, S. G. Kunjeti, K. Lamour, Z. Liu, L. Ma, D. Maclean, M. C. Chibucos, H. McDonald, J. McWalters, H. J. Meijer, W. Morgan, P. F. Morris, C. A. Munro, K. O'Neill, M. Ospina-Giraldo, A. Pinzon, L. Pritchard, B. Ramsahoye, Q. Ren, S. Restrepo, S. Roy, A. Sadanandom, A. Savidor, S. Schornack, D. C. Schwartz, U. D. Schumann, B. Schwessinger, L. Seyer, T. Sharpe, C. Silvar, J. Song, D. J. Studholme, S. Sykes, M. Thines, P. J. van de Vondervoort, V. Phuntumart, S. Wawra, R. Weide, J. Win, C. Young, S. Zhou, W. Fry, B. C. Meyers, P. van West, J. Ristaino, F. Govers, P. R. Birch, S. C. Whisson, H. S. Judelson and C. Nusbaum (2009). "Genome sequence and analysis of the Irish potato famine pathogen Phytophthora infestans." Nature **461**(7262): 393-398.

Hamdoun, S., Z. Liu, M. Gill, N. Yao and H. Lu (2013). "Dynamics of defense responses and cell fate change during Arabidopsis-Pseudomonas syringae interactions." PLoS One **8**(12): e83219.

Hamilton, J. G., A. R. Zangerl, E. H. DeLucia and M. R. Berenbaum (2001). "The carbon-nutrient balance hypothesis: its rise and fall." Ecology Letters **4**(1): 86-95.

Hammond-Kosack, K. E. and J. D. Jones (1996). "Resistance gene-dependent plant defense responses." Plant Cell **8**(10): 1773-1791.

Hanzawa, Y., T. Money and D. Bradley (2005). "A single amino acid converts a repressor to an activator of flowering." Proceedings of the National Academy of Sciences of the United States of America **102**(21): 7748-7753.

Hauck, P., R. Thilmony and S. Y. He (2003). "A Pseudomonas syringae type III effector suppresses cell wall-based extracellular defense in susceptible Arabidopsis plants." Proc Natl Acad Sci U S A **100**(14): 8577-8582.

Hayashi, F., K. D. Smith, A. Ozinsky, T. R. Hawn, E. C. Yi, D. R. Goodlett, J. K. Eng, S. Akira, D. M. Underhill and A. Aderem (2001). "The innate immune response to bacterial flagellin is mediated by Toll-like receptor 5." Nature **410**(6832): 1099-1103.

Hedrick, P. W., M. E. Ginevan and E. P. Ewing (1976). "Genetic-Polymorphism in Heterogeneous Environments." Annual Review of Ecology and Systematics **7**: 1-32.

Hellens, R. P., E. A. Edwards, N. R. Leyland, S. Bean and P. M. Mullineaux (2000). "pGreen: a versatile and flexible binary Ti vector for Agrobacterium-mediated plant transformation." Plant Molecular Biology **42**(6): 819-832.

Herrera-Vasquez, A., P. Salinas and L. Holuigue (2015). "Salicylic acid and reactive oxygen species interplay in the transcriptional control of defense genes expression." Frontiers in Plant Science **6**.

Hillebrand, H. (2004). "On the generality of the latitudinal diversity gradient." Am Nat **163**(2): 192-211.

Holub, E. B. (2001). "The arms race is ancient history in Arabidopsis, the wildflower." Nat Rev Genet **2**(7): 516-527.

Horger, A. C., M. Ilyas, W. Stephan, A. Tellier, R. A. van der Hoorn and L. E. Rose (2012). "Balancing selection at the tomato RCR3 Guardee gene family maintains variation in strength of pathogen defense." PLoS Genet **8**(7): e1002813.

Houterman, P. M., B. J. C. Cornelissen and M. Rep (2008). "Suppression of plant resistance gene-based immunity by a fungal effector." Plos Pathogens **4**(5).

Hu, G. S., A. K. A. deHart, Y. S. Li, C. Ustach, V. Handley, R. Navarre, C. F. Hwang, B. J. Aegerter, V. M. Williamson and B. Baker (2005). "EDS1 in tomato is required for resistance mediated by TIR-class R genes and the receptor-like R gene Ve." Plant Journal **42**(3): 376-391.

Hu, Y. R., Q. Y. Dong and D. Q. Yu (2012). "Arabidopsis WRKY46 coordinates with WRKY70 and WRKY53 in basal resistance against pathogen Pseudomonas syringae." Plant Science **185**: 288-297.

Huard-Chauveau, C., L. Perchepied, M. Debieu, S. Rivas, T. Kroj, I. Kars, J. Bergelson, F. Roux and D. Roby (2013). "An atypical kinase under balancing selection confers broad-spectrum disease resistance in Arabidopsis." PLoS Genet **9**(9): e1003766.

Hunt, M. D., T. P. Delaney, R. A. Dietrich, K. B. Weymann, J. L. Dangl and J. A. Ryals (1997). "Salicylate-independent lesion formation in Arabidopsis lsd mutants." Molecular Plant-Microbe Interactions **10**(5): 531-536.

Huot, B., J. Yao, B. L. Montgomery and S. Y. He (2014). "Growth-defense tradeoffs in plants: a balancing act to optimize fitness." Mol Plant **7**(8): 1267-1287.

Ingle, R. A., M. Carstens and K. J. Denby (2006). "PAMP recognition and the plant-pathogen arms race." Bioessays **28**(9): 880-889.

Institute, B. "Picard." from http://broadinstitute.github.io.picard.

Jambunathan, N., J. M. Siani and T. W. McNellis (2001). "A humidity-sensitive Arabidopsis copine mutant exhibits precocious cell death and increased disease resistance." Plant Cell **13**(10): 2225-2240.

Jehle, A. K., M. Lipschis, M. Albert, V. Fallahzadeh-Mamaghani, U. Furst, K. Mueller and G. Felix (2013). "The receptor-like protein ReMAX of Arabidopsis detects the microbe-associated molecular pattern eMax from Xanthomonas." Plant Cell **25**(6): 2330-2340.

Jelenska, J., J. A. van Hal and J. T. Greenberg (2010). "Pseudomonas syringae hijacks plant stress chaperone machinery for virulence." Proc Natl Acad Sci U S A **107**(29): 13177-13182.

Jones, J. D. and J. L. Dangl (2006). "The plant immune system." Nature **444**(7117): 323-329.

Jurkowski, G. I., R. K. Smith, I. C. Yu, J. H. Ham, S. B. Sharma, D. F. Klessig, K. A. Fengler and A. F. Bent (2004). "Arabidopsis DND2, a second cyclic nucleotide-gated ion channel gene for which mutation causes the "defense, no death" phenotype." Molecular Plant-Microbe Interactions **17**(5): 511-520.

Kachroo, A., C. R. Schopfer, M. E. Nasrallah and J. B. Nasrallah (2001). "Allele-specific receptor-ligand interactions in Brassica self-incompatibility." Science **293**(5536): 1824-1826.

Kaku, H., Y. Nishizawa, N. Ishii-Minami, C. Akimoto-Tomiyama, N. Dohmae, K. Takio, E. Minami and N. Shibuya (2006). "Plant cells recognize chitin fragments for defense signaling through a plasma membrane receptor." Proc Natl Acad Sci U S A **103**(29): 11086-11091.

Karasov, T. L., J. M. Kniskern, L. Gao, B. J. DeYoung, J. Ding, U. Dubiella, R. O. Lastra, S. Nallu, F. Roux, R. W. Innes, L. G. Barrett, R. R. Hudson and J. Bergelson (2014). "The long-

term maintenance of a resistance polymorphism through diffuse interactions." Nature **512**(7515): 436-440.

Katagiri, F., R. Thilmony and S. Y. He (2002). "The Arabidopsis thaliana-pseudomonas syringae interaction." Arabidopsis Book **1**: e0039.

Katagiri, F. and K. Tsuda (2010). "Understanding the plant immune system." Mol Plant Microbe Interact **23**(12): 1531-1536.

Kempel, A., M. Schadler, T. Chrobock, M. Fischer and M. van Kleunen (2011). "Tradeoffs associated with constitutive and induced plant resistance against herbivory." Proceedings of the National Academy of Sciences of the United States of America **108**(14): 5685-5689.

Kiani, S. P., C. Trontin, M. Andreatta, M. Simon, T. Robert, D. E. Salt and O. Loudet (2012). "Allelic Heterogeneity and Trade-Off Shape Natural Variation for Response to Soil Micronutrient." Plos Genetics **8**(7).

Kim, M. G., X. Geng, S. Y. Lee and D. Mackey (2009). "The Pseudomonas syringae type III effector AvrRpm1 induces significant defenses by activating the Arabidopsis nucleotide-binding leucine-rich repeat protein RPS2." Plant J **57**(4): 645-653.

Kim, S. H., S. I. Kwon, D. Saha, N. C. Anyanwu and W. Gassmann (2009). "Resistance to the Pseudomonas syringae effector HopA1 is governed by the TIR-NBS-LRR protein RPS6 and is enhanced by mutations in SRFR1." Plant Physiol **150**(4): 1723-1732.

Kliebenstein, D. J., J. Kroymann, P. Brown, A. Figuth, D. Pedersen, J. Gershenzon and T. Mitchell-Olds (2001). "Genetic control of natural variation in Arabidopsis glucosinolate accumulation." Plant Physiology **126**(2): 811-825.

Kliebenstein, D. J., M. A. L. West, H. van Leeuwen, K. Kim, R. W. Doerge, R. W. Michelmore and D. A. St Clair (2006). "Genomic survey of gene expression diversity in Arabidopsis thaliana." Genetics **172**(2): 1179-1189.

Knepper, C. and B. Day (2010). "From perception to activation: the molecular-genetic and biochemical landscape of disease resistance signaling in plants." Arabidopsis Book **8**: e012.

Koornneef, M., C. Alonso-Blanco and D. Vreugdenhil (2004). "Naturally occurring genetic variation in Arabidopsis thaliana." Annu Rev Plant Biol **55**: 141-172.

Kroymann, J. and T. Mitchell-Olds (2005). "Epistasis and balanced polymorphism influencing complex trait variation." Nature **435**(7038): 95-98.

Kubota, S., T. Iwasaki, K. Hanada, A. J. Nagano, A. Fujiyama, A. Toyoda, S. Sugano, Y. Suzuki, K. Hikosaka, M. Ito and S. Morinaga (2015). "A Genome Scan for Genes Underlying Microgeographic-Scale Local Adaptation in a Wild Arabidopsis Species." PLoS Genet **11**(7): e1005361.

Kunze, G., C. Zipfel, S. Robatzek, K. Niehaus, T. Boller and G. Felix (2004). "The N terminus of bacterial elongation factor Tu elicits innate immunity in Arabidopsis plants." Plant Cell **16**(12): 3496-3507.

Kwon, C., C. Neu, S. Pajonk, H. S. Yun, U. Lipka, M. Humphry, S. Bau, M. Straus, M. Kwaaitaal, H. Rampelt, F. El Kasmi, G. Jurgens, J. Parker, R. Panstruga, V. Lipka and P. Schulze-Lefert (2008). "Co-option of a default secretory pathway for plant immune responses." Nature **451**(7180): 835-840.

Laluk, K. and T. Mengiste (2010). "Necrotroph attacks on plants: wanton destruction or covert extortion?" Arabidopsis Book **8**: e0136.

Lam, E., N. Kato and M. Lawton (2001). "Programmed cell death, mitochondria and the plant hypersensitive response." Nature **411**(6839): 848-853.

Lawton, K. A., L. Friedrich, M. Hunt, K. Weymann, T. Delaney, H. Kessmann, T. Staub and J. Ryals (1996). "Benzothiadiazole induces disease resistance in Arabidopsis by activation of the systemic acquired resistance signal transduction pathway." Plant Journal **10**(1): 71-82.

Leborgne-Castel, N. and K. Bouhidel (2014). "Plasma membrane protein trafficking in plant-microbe interactions: a plant cell point of view." Frontiers in Plant Science **5**.

Lee, S. J. and J. K. Rose (2010). "Mediation of the transition from biotrophy to necrotrophy in hemibiotrophic plant pathogens by secreted effector proteins." Plant Signal Behav **5**(6): 769-772.

Lewis, J. D., R. Wu, D. S. Guttman and D. Desveaux (2010). "Allele-specific virulence attenuation of the Pseudomonas syringae HopZ1a type III effector via the Arabidopsis ZAR1 resistance protein." PLoS Genet **6**(4): e1000894.

Li, H. and R. Durbin (2009). "Fast and accurate short read alignment with Burrows-Wheeler transform." Bioinformatics **25**(14): 1754-1760.

Li, L., M. Li, L. Yu, Z. Zhou, X. Liang, Z. Liu, G. Cai, L. Gao, X. Zhang, Y. Wang, S. Chen and J. M. Zhou (2014). "The FLS2-associated kinase BIK1 directly phosphorylates the NADPH oxidase RbohD to control plant immunity." Cell Host Microbe **15**(3): 329-338.

Li, X., J. D. Clarke, Y. L. Zhang and X. N. Dong (2001). "Activation of an EDS1-mediated R-gene pathway in the snc1 mutant leads to constitutive, NPR1-independent pathogen resistance." Molecular Plant-Microbe Interactions **14**(10): 1131-1139.

Li, X., H. Lin, W. Zhang, Y. Zou, J. Zhang, X. Tang and J. M. Zhou (2005). "Flagellin induces innate immunity in nonhost interactions that is suppressed by Pseudomonas syringae effectors." Proc Natl Acad Sci U S A **102**(36): 12990-12995.

Lindeberg, M., S. Cartinhour, C. R. Myers, L. M. Schechter, D. J. Schneider and A. Collmer (2006). "Closing the circle on the discovery of genes encoding Hrp regulon members and type III secretion system effectors in the genomes of three model Pseudomonas syringae strains." Mol Plant Microbe Interact **19**(11): 1151-1158.

Liu, B., J. F. Li, Y. Ao, J. Qu, Z. Li, J. Su, Y. Zhang, J. Liu, D. Feng, K. Qi, Y. He, J. Wang and H. B. Wang (2012). "Lysin motif-containing proteins LYP4 and LYP6 play dual roles in peptidoglycan and chitin perception in rice innate immunity." Plant Cell **24**(8): 3406-3419.

Loake, G. and M. Grant (2007). "Salicylic acid in plant defence--the players and protagonists." Curr Opin Plant Biol **10**(5): 466-472.

Lorrain, S., F. Vailleau, C. Balaque and D. Roby (2003). "Lesion mimic mutants: keys for deciphering cell death and defense pathways in plants?" Trends in Plant Science **8**(6): 263-271.

Loudet, O., V. Saliba-Colombani, C. Camilleri, F. Calenge, V. Gaudon, A. Koprivova, K. A. North, S. Kopriva and F. Daniel-Vedele (2007). "Natural variation for sulfate content in Arabidopsis thaliana is highly controlled by APR2." Nature Genetics **39**(7): 896-900.

Louis, J., E. Gobbato, H. A. Mondal, B. J. Feys, J. E. Parker and J. Shah (2012). "Discrimination of Arabidopsis PAD4 Activities in Defense against Green Peach Aphid and Pathogens." Plant Physiology **158**(4): 1860-1872.

Lovell, H. C., R. W. Jackson, J. W. Mansfield, S. A. Godfrey, J. T. Hancock, R. Desikan and D. L. Arnold (2011). "In planta conditions induce genomic changes in Pseudomonas syringae pv. phaseolicola." Mol Plant Pathol **12**(2): 167-176.

Lozano-Duran, R., A. P. Macho, F. Boutrot, C. Segonzac, I. E. Somssich and C. Zipfel (2013). "The transcriptional regulator BZR1 mediates trade-off between plant innate immunity and growth." Elife **2**: e00983.

Lu, H., D. N. Rate, J. T. Song and J. T. Greenberg (2003). "ACD6, a novel ankyrin protein, is a regulator and an effector of salicylic acid signaling in the Arabidopsis defense response." Plant Cell **15**(10): 2408-2420.

Lu, H., S. Salimian, E. Gamelin, G. Wang, J. Fedorowski, W. LaCourse and J. T. Greenberg (2009). "Genetic analysis of acd6-1 reveals complex defense networks and leads to identification of novel defense genes in Arabidopsis." Plant J **58**(3): 401-412.

Luna, E., V. Pastor, J. Robert, V. Flors, B. Mauch-Mani and J. Ton (2011). "Callose deposition: a multifaceted plant defense response." Mol Plant Microbe Interact **24**(2): 183-193.

Ma, W., F. F. Dong, J. Stavrinides and D. S. Guttman (2006). "Type III effector diversification via both pathoadaptation and horizontal transfer in response to a coevolutionary arms race." PLoS Genet **2**(12): e209.

Malinovsky, F. G., J. U. Fangel and W. G. Willats (2014). "The role of the cell wall in plant immunity." Front Plant Sci **5**: 178.

Maloof, J. N., J. O. Borevitz, T. Dabi, J. Lutes, R. B. Nehring, J. L. Redfern, G. T. Trainer, J. M. Wilson, T. Asami, C. C. Berry, D. Weigel and J. Chory (2001). "Natural variation in light sensitivity of Arabidopsis." Nature Genetics **29**(4): 441-446.

Maor, R. and K. Shirasu (2005). "The arms race continues: battle strategies between plants and fungal pathogens." Curr Opin Microbiol **8**(4): 399-404.

Martin, G. B., A. J. Bogdanove and G. Sessa (2003). "Understanding the functions of plant disease resistance proteins." Annual Review of Plant Biology **54**: 23-61.

Massad, T. J., L. A. Dyer and C. G. Vega (2012). "Costs of defense and a test of the carbon-nutrient balance and growth-differentiation balance hypotheses for two co-occurring classes of plant defense." PLoS One **7**(10): e47554.

McDowell, J. M. (2011). "Genomes of obligate plant pathogens reveal adaptations for obligate parasitism." Proc Natl Acad Sci U S A **108**(22): 8921-8922.

McDowell, J. M., A. Cuzick, C. Can, J. Beynon, J. L. Dangl and E. B. Holub (2000). "Downy mildew (Peronospora parasitica) resistance genes in Arabidopsis vary in functional requirements for NDR1, EDS1, NPR1 and salicylic acid accumulation." Plant Journal **22**(6): 523-529.

McKenna, A., M. Hanna, E. Banks, A. Sivachenko, K. Cibulskis, A. Kernytsky, K. Garimella, D. Altshuler, S. Gabriel, M. Daly and M. A. DePristo (2010). "The Genome Analysis Toolkit: a MapReduce framework for analyzing next-generation DNA sequencing data." Genome Res **20**(9): 1297-1303.

Meldau, S., M. Erb and I. T. Baldwin (2012). "Defence on demand: mechanisms behind optimal defence patterns." Annals of Botany **110**(8): 1503-1514.

Memon, S., X. Q. Jia, L. J. Gu and X. H. Zhang (2016). "Genomic variations and distinct evolutionary rate of rare alleles in Arabidopsis thaliana." Bmc Evolutionary Biology **16**.

Mengiste, T. (2012). "Plant immunity to necrotrophs." Annu Rev Phytopathol **50**: 267-294.

Meyers, B. C., A. Kozik, A. Griego, H. Kuang and R. W. Michelmore (2003). "Genome-wide analysis of NBS-LRR-encoding genes in Arabidopsis." Plant Cell **15**(4): 809-834.

Michelmore, R. W. and B. C. Meyers (1998). "Clusters of resistance genes in plants evolve by divergent selection and a birth-and-death process." Genome Res **8**(11): 1113-1130.

Miya, A., P. Albert, T. Shinya, Y. Desaki, K. Ichimura, K. Shirasu, Y. Narusaka, N. Kawakami, H. Kaku and N. Shibuya (2007). "CERK1, a LysM receptor kinase, is essential for chitin elicitor signaling in Arabidopsis." Proc Natl Acad Sci U S A **104**(49): 19613-19618.

Moeder, W. and K. Yoshioka (2008). "Lesion mimic mutants: A classical, yet still fundamental approach to study programmed cell death." Plant Signal Behav **3**(10): 764-767.

Morris, K., S. A. H. Mackerness, T. Page, C. F. John, A. M. Murphy, J. P. Carr and V. Buchanan-Wollaston (2000). "Salicylic acid has a role in regulating gene expression during leaf senescence." Plant Journal **23**(5): 677-685.

Morrissey, J. P. and A. E. Osbourn (1999). "Fungal resistance to plant antibiotics as a mechanism of pathogenesis." Microbiol Mol Biol Rev **63**(3): 708-724.

Nagy, E. D. and J. L. Bennetzen (2008). "Pathogen corruption and site-directed recombination at a plant disease resistance gene cluster." Genome Res **18**(12): 1918-1923.

Nawrath, C. and J. P. Metraux (1999). "Salicylic acid induction-deficient mutants of Arabidopsis express PR-2 and PR-5 and accumulate high levels of camalexin after pathogen inoculation." Plant Cell **11**(8): 1393-1404.

Nemri, A., S. Atwell, A. M. Tarone, Y. S. Huang, K. Zhao, D. J. Studholme, M. Nordborg and J. D. G. Jones (2010). "Genome-wide survey of Arabidopsis natural variation in downy mildew resistance using combined association and linkage mapping." Proceedings of the National Academy of Sciences of the United States of America **107**(22): 10302-10307.

Ng, G., S. Seabolt, C. Zhang, S. Salimian, T. A. Watkins and H. Lu (2011). "Genetic dissection of salicylic acid-mediated defense signaling networks in Arabidopsis." Genetics **189**(3): 851-859.

Nimchuk, Z., E. Marois, S. Kjemtrup, R. T. Leister, F. Katagiri and J. L. Dangl (2000). "Eukaryotic fatty acylation drives plasma membrane targeting and enhances function of several type III effector proteins from Pseudomonas syringae." Cell **101**(4): 353-363.

Nitta, Y., P. Ding and Y. Zhang (2014). "Identification of additional MAP kinases activated upon PAMP treatment." Plant Signal Behav **9**(11): e976155.

Noctor, G., C. Lelarge-Trouverie and A. Mhamdi (2015). "The metabolomics of oxidative stress." Phytochemistry **112**: 33-53.

Nomura, K., M. Melotto and S. Y. He (2005). "Suppression of host defense in compatible plant-Pseudomonas syringae interactions." Curr Opin Plant Biol **8**(4): 361-368.

Oakley, C. G., J. Agren, R. A. Atchison and D. W. Schemske (2014). "QTL mapping of freezing tolerance: links to fitness and adaptive trade-offs." Molecular Ecology **23**(17): 4304-4315.

Ondov, B., Treangen, TJ., Mallonee, AB., Bergman, NH., Koren, S., Phillippy, AM. (2015). "Fast genome and metagenome distance estimation using MinHash." bioRxiv.

Ossowski, S., R. Schwab and D. Weigel (2008). "Gene silencing in plants using artificial microRNAs and other small RNAs." Plant Journal **53**(4): 674-690.

Partida-Martinez, L. P. and M. Heil (2011). "The microbe-free plant: fact or artifact?" Front Plant Sci **2**: 100.

Perez-Perez, J. M., J. Serrano-Cartagena and J. L. Micol (2002). "Genetic analysis of natural variations in the architecture of Arabidopsis thaliana vegetative leaves." Genetics **162**(2): 893-915.

Petutschnig, E. K., A. M. Jones, L. Serazetdinova, U. Lipka and V. Lipka (2010). "The lysin motif receptor-like kinase (LysM-RLK) CERK1 is a major chitin-binding protein in Arabidopsis thaliana and subject to chitin-induced phosphorylation." J Biol Chem **285**(37): 28902-28911.

Pfaffl, M. W. (2001). "A new mathematical model for relative quantification in real-time RT-PCR." Nucleic Acids Research **29**(9).

Pieterse, C. M., A. Leon-Reyes, S. Van der Ent and S. C. Van Wees (2009). "Networking by small-molecule hormones in plant immunity." Nat Chem Biol **5**(5): 308-316.

Platt, A., M. Horton, Y. S. Huang, Y. Li, A. E. Anastasio, N. W. Mulyati, J. Agren, O. Bossdorf, D. Byers, K. Donohue, M. Dunning, E. B. Holub, A. Hudson, V. Le Corre, O. Loudet, F. Roux, N. Warthmann, D. Weigel, L. Rivero, R. Scholl, M. Nordborg, J. Bergelson and J. O. Borevitz (2010). "The scale of population structure in Arabidopsis thaliana." PLoS Genet **6**(2): e1000843.

Poland, J. A., P. J. Brown, M. E. Sorrells and J. L. Jannink (2012). "Development of high-density genetic maps for barley and wheat using a novel two-enzyme genotyping-by-sequencing approach." PLoS One **7**(2): e32253.

Ponce de Leon, I. and M. Montesano (2013). "Activation of Defense Mechanisms against Pathogens in Mosses and Flowering Plants." Int J Mol Sci **14**(2): 3178-3200.

Pontier, D., C. Balague and D. Roby (1998). "The hypersensitive response. A programmed cell death associated with plant resistance." C R Acad Sci III **321**(9): 721-734.

Preston, G. M. (2000). "Pseudomonas syringae pv. tomato: the right pathogen, of the right plant, at the right time." Molecular Plant Pathology **1**(5): 263-275.

Qi, D., U. Dubiella, S. H. Kim, D. I. Sloss, R. H. Dowen, J. E. Dixon and R. W. Innes (2014). "Recognition of the Protein Kinase AVRPPHB SUSCEPTIBLE1 by the Disease Resistance Protein RESISTANCE TO PSEUDOMONAS SYRINGAE5 Is Dependent on S-Acylation and an Exposed Loop in AVRPPHB SUSCEPTIBLE." Plant Physiology **164**(1): 340-351.

Raberg, L., E. Alacid, E. Garces and R. Figueroa (2014). "The potential for arms race and Red Queen coevolution in a protist host-parasite system." Ecol Evol **4**(24): 4775-4785.

Rant, J. C., L. S. Arraiano, M. Chabannes and J. K. M. Brown (2013). "Quantitative trait loci for partial resistance to Pseudomonas syringae pv. maculicola in Arabidopsis thaliana." Molecular Plant Pathology **14**(8): 828-837.

Rasmann, S., E. Chassin, J. Bilat, G. Glauser and P. Reymond (2015). "Trade-off between constitutive and inducible resistance against herbivores is only partially explained by gene expression and glucosinolate production." J Exp Bot **66**(9): 2527-2534.

Rate, D. N., J. V. Cuenca, G. R. Bowman, D. S. Guttman and J. T. Greenberg (1999). "The gain-of-function Arabidopsis acd6 mutant reveals novel regulation and function of the salicylic acid signaling pathway in controlling cell death, defenses, and cell growth." Plant Cell **11**(9): 1695-1708.

Rate, D. N. and J. T. Greenberg (2001). "The Arabidopsis aberrant growth and death2 mutant shows resistance to Pseudomonas syringae and reveals a role for NPR1 in suppressing hypersensitive cell death." Plant J **27**(3): 203-211.

Rietman, H., G. Bijsterbosch, L. M. Cano, H. R. Lee, J. H. Vossen, E. Jacobsen, R. G. Visser, S. Kamoun and V. G. Vleeshouwers (2012). "Qualitative and quantitative late blight

resistance in the potato cultivar Sarpo Mira is determined by the perception of five distinct RXLR effectors." Mol Plant Microbe Interact **25**(7): 910-919.

Rietz, S., A. Stamm, S. Malonek, S. Wagner, D. Becker, N. Medina-Escobar, A. C. Vlot, B. J. Feys, K. Niefind and J. E. Parker (2011). "Different roles of Enhanced Disease Susceptibility1 (EDS1) bound to and dissociated from Phytoalexin Deficient4 (PAD4) in Arabidopsis immunity." New Phytol **191**(1): 107-119.

Ritter, C. and J. L. Dangl (1995). "The avrRpm1 gene of Pseudomonas syringae pv. maculicola is required for virulence on Arabidopsis." Mol Plant Microbe Interact **8**(3): 444-453.

Rivas-San Vicente, M. and J. Plasencia (2011). "Salicylic acid beyond defence: its role in plant growth and development." J Exp Bot **62**(10): 3321-3338.

Robatzek, S. (2007). "Vesicle trafficking in plant immune responses." Cell Microbiol **9**(1): 1-8.

Robatzek, S. and I. E. Somssich (2002). "Targets of AtWRKY6 regulation during plant senescence and pathogen defense." Genes & Development **16**(9): 1139-1149.

Robert-Seilaniantz, A., M. Grant and J. D. Jones (2011). "Hormone crosstalk in plant disease and defense: more than just jasmonate-salicylate antagonism." Annu Rev Phytopathol **49**: 317-343.

Robert-Seilaniantz, A., L. Navarro, R. Bari and J. D. Jones (2007). "Pathological hormone imbalances." Curr Opin Plant Biol **10**(4): 372-379.

Rodriguez, M. C., M. Petersen and J. Mundy (2010). "Mitogen-activated protein kinase signaling in plants." Annu Rev Plant Biol **61**: 621-649.

Rodriguez-Herva, J. J., P. Gonzalez-Melendi, R. Cuartas-Lanza, M. Antunez-Lamas, I. Rio-Alvarez, Z. Li, G. Lopez-Torrejon, I. Diaz, J. C. Del Pozo, S. Chakravarthy, A. Collmer, P. Rodriguez-Palenzuela and E. Lopez-Solanilla (2012). "A bacterial cysteine protease effector protein interferes with photosynthesis to suppress plant innate immune responses." Cell Microbiol **14**(5): 669-681.

Romer, P., S. Hahn, T. Jordan, T. Strauss, U. Bonas and T. Lahaye (2007). "Plant pathogen recognition mediated by promoter activation of the pepper Bs3 resistance gene." Science **318**(5850): 645-648.

Ron, M. and A. Avni (2004). "The receptor for the fungal elicitor ethylene-inducing xylanase is a member of a resistance-like gene family in tomato." Plant Cell **16**(6): 1604-1615.

Rose, L. E., P. D. Bittner-Eddy, C. H. Langley, E. B. Holub, R. W. Michelmore and J. L. Beynon (2004). "The maintenance of extreme amino acid diversity at the disease resistance gene, RPP13, in Arabidopsis thaliana." Genetics **166**(3): 1517-1527.

Roux, M., B. Schwessinger, C. Albrecht, D. Chinchilla, A. Jones, N. Holton, F. G. Malinovsky, M. Tor, S. de Vries and C. Zipfel (2011). "The Arabidopsis leucine-rich repeat receptor-like kinases BAK1/SERK3 and BKK1/SERK4 are required for innate immunity to hemibiotrophic and biotrophic pathogens." Plant Cell **23**(6): 2440-2455.

Russell, A. R., T. Ashfield and R. W. Innes (2015). "Pseudomonas syringae Effector AvrPphB Suppresses AvrB-Induced Activation of RPM1 but Not AvrRpm1-Induced Activation." Mol Plant Microbe Interact **28**(6): 727-735.

Rusterucci, C., D. H. Aviv, B. F. Holt, J. L. Dangl and J. E. Parker (2001). "The disease resistance signaling components EDS1 and PAD4 are essential regulators of the cell death pathway controlled by LSD1 in arabidopsis." Plant Cell **13**(10): 2211-2224.

Rutter, M. T. and C. B. Fenster (2007). "Testing for adaptation to climate in Arabidopsis thaliana: a calibrated common garden approach." Ann Bot **99**(3): 529-536.

Ryan, C. A. and A. Jagendorf (1995). "Self defense by plants." Proc Natl Acad Sci U S A **92**(10): 4075.

Salk Institute. 2016, from http://signal.salk.edu/atg1001/3.0/gebrowser.php.

Sambrook, J. and D. W. Russell (2001). Molecular cloning : a laboratory manual. Cold Spring Harbor, N.Y., Cold Spring Harbor Laboratory Press.

Saunders, D. G. O., S. Breen, J. Win, S. Schornack, I. Hein, T. O. Bozkurt, N. Champouret, V. G. A. A. Vleeshouwers, P. R. J. Birch, E. M. Gilroy and S. Kamoun (2012). "Host Protein BSL1 Associates with Phytophthora infestans RXLR Effector AVR2 and the Solanum demissum Immune Receptor R2 to Mediate Disease Resistance." Plant Cell **24**(8): 3420-3434.

Schemske, D. W., G. G. Mittelbach, H. V. Cornell, J. M. Sobel and K. Roy (2009). "Is There a Latitudinal Gradient in the Importance of Biotic Interactions?" Annual Review of Ecology Evolution and Systematics **40**: 245-269.

Schiff, C. L., I. W. Wilson and S. C. Somerville (2001). "Polygenic powdery mildew disease resistance in Arabidopsis thaliana: quantitative trait analysis of the accession Warschau-1." Plant Pathology **50**(6): 690-701.

Schulze-Lefert, P. and R. Panstruga (2003). "Establishment of biotrophy by parasitic fungi and reprogramming of host cells for disease resistance." Annu Rev Phytopathol **41**: 641-667.

Schwab, R., S. Ossowski, M. Riester, N. Warthmann and D. Weigel (2006). "Highly specific gene silencing by artificial microRNAs in Arabidopsis." Plant Cell **18**(5): 1121-1133.

Schwessinger, B., M. Roux, Y. Kadota, V. Ntoukakis, J. Sklenar, A. Jones and C. Zipfel (2011). "Phosphorylation-dependent differential regulation of plant growth, cell death, and innate immunity by the regulatory receptor-like kinase BAK1." PLoS Genet **7**(4): e1002046.

Segonzac, C. and C. Zipfel (2011). "Activation of plant pattern-recognition receptors by bacteria." Current Opinion in Microbiology **14**(1): 54-61.

Seo, S., K. Ishizuka and Y. Ohashi (1995). "Induction of Salicylic-Acid Beta-Glucosidase in Tobacco-Leaves by Exogenous Salicylic-Acid." Plant and Cell Physiology **36**(3): 447-453.

Seyfferth, C. and K. Tsuda (2014). "Salicylic acid signal transduction: the initiation of biosynthesis, perception and transcriptional reprogramming." Frontiers in Plant Science **5**.

Shah, J. (2003). "The salicylic acid loop in plant defense." Curr Opin Plant Biol **6**(4): 365-371.

Shah, J., P. Kachroo, A. Nandi and D. F. Klessig (2001). "A recessive mutation in the Arabidopsis SSI2 gene confers SA- and NPR1-independent expression of PR genes and resistance against bacterial and oomycete pathogens." Plant Journal **25**(5): 563-574.

Shapiro, A. D. and C. Zhang (2001). "The role of NDR1 in avirulence gene-directed signaling and control of programmed cell death in arabidopsis." Plant Physiology **127**(3): 1089-1101.

Shimizu, T., T. Nakano, D. Takamizawa, Y. Desaki, N. Ishii-Minami, Y. Nishizawa, E. Minami, K. Okada, H. Yamane, H. Kaku and N. Shibuya (2010). "Two LysM receptor molecules, CEBiP and OsCERK1, cooperatively regulate chitin elicitor signaling in rice." Plant J **64**(2): 204-214.

Shindo, C., G. Bernasconi and C. S. Hardtke (2007). "Natural genetic variation in Arabidopsis: tools, traits and prospects for evolutionary ecology." Ann Bot **99**(6): 1043-1054.

Shirano, Y., P. Kachroo, J. Shah and D. F. Klessig (2002). "A gain-of-function mutation in an Arabidopsis Toll Interleukin1 receptor-nucleotide binding site-leucine-rich repeat type R gene triggers defense responses and results in enhanced disease resistance." Plant Cell **14**(12): 3149-3162.

Shyu, C. and T. P. Brutnell (2015). "Growth-defence balance in grass biomass production: the role of jasmonates." J Exp Bot **66**(14): 4165-4176.

Siemens, D. H., H. Lischke, N. Maggiulli, S. Schurch and B. A. Roy (2003). "Cost of resistance and tolerance under competition: the defense-stress benefit hypothesis." Evolutionary Ecology **17**(3): 247-263.

Slatkin, M. and B. Rannala (2000). "Estimating allele age." Annual Review of Genomics and Human Genetics **1**: 225-249.

Smith, J. M. and A. Heese (2014). "Rapid bioassay to measure early reactive oxygen species production in Arabidopsis leave tissue in response to living Pseudomonas syringae." Plant Methods **10**.

Sohn, K. H., Y. Zhang and J. D. Jones (2009). "The Pseudomonas syringae effector protein, AvrRPS4, requires in planta processing and the KRVY domain to function." Plant J **57**(6): 1079-1091.

Spoel, S. H. and X. Dong (2008). "Making sense of hormone crosstalk during plant immune responses." Cell Host Microbe **3**(6): 348-351.

Spoel, S. H., J. S. Johnson and X. Dong (2007). "Regulation of tradeoffs between plant defenses against pathogens with different lifestyles." Proc Natl Acad Sci U S A **104**(47): 18842-18847.

Stael, S., P. Kmiecik, P. Willems, K. Van Der Kelen, N. S. Coll, M. Teige and F. Van Breusegem (2015). "Plant innate immunity - sunny side up?" Trends Plant Sci **20**(1): 3-11.

Staphnill, A. (2009). Natural genetic variation of basal disease resistance in *Arabidopsis*. Doctor of Philosophy, University of East Anglia.

Stokes, T. L., B. N. Kunkel and E. J. Richards (2002). "Epigenetic variation in Arabidopsis disease resistance." Genes Dev **16**(2): 171-182.

Strauss, S. Y., J. A. Rudgers, J. A. Lau and R. E. Irwin (2002). "Direct and ecological costs of resistance to herbivory." Trends in Ecology & Evolution **17**(6): 278-285.

Symonds, V. V., G. Hatlestad and A. M. Lloyd (2011). "Natural Allelic Variation Defines a Role for ATMYC1: Trichome Cell Fate Determination." Plos Genetics **7**(6).

Szabo, L. J. and W. R. Bushnell (2001). "Hidden robbers: the role of fungal haustoria in parasitism of plants." Proc Natl Acad Sci U S A **98**(14): 7654-7655.

Taiz, L. and E. Zeiger (2010). Plant physiology. Sunderland, MA, Sinauer Associates.

Takai, R., A. Isogai, S. Takayama and F. S. Che (2008). "Analysis of flagellin perception mediated by flg22 receptor OsFLS2 in rice." Mol Plant Microbe Interact **21**(12): 1635-1642.

Tateda, C., Z. Zhang and J. T. Greenberg (2015). "Linking pattern recognition and salicylic acid responses in Arabidopsis through ACCELERATED CELL DEATH6 and receptors." Plant Signal Behav **10**(10): e1010912.

Tateda, C., Z. Zhang, J. Shrestha, J. Jelenska, D. Chinchilla and J. T. Greenberg (2014). "Salicylic acid regulates Arabidopsis microbial pattern receptor kinase levels and signaling." Plant Cell **26**(10): 4171-4187.

Tellier, A. and J. K. M. Brown (2011). "Spatial heterogeneity, frequency-dependent selection and polymorphism in host-parasite interactions." Bmc Evolutionary Biology **11**.

Thaler, J. S. (2002). "Effect of jasmonate-induced plant responses on the natural enemies of herbivores." Journal of Animal Ecology : 141-150.

The European Arabidopsis Stock Center. (2010). "uNASC." from http://www.arabidopsis.info/.

Thomma, B. P., T. Nurnberger and M. H. Joosten (2011). "Of PAMPs and effectors: the blurred PTI-ETI dichotomy." Plant Cell **23**(1): 4-15.

Tian, D. C., H. Araki, E. Stahl, J. Bergelson and M. Kreitman (2002). "Signature of balancing selection in Arabidopsis." Proceedings of the National Academy of Sciences of the United States of America **99**(17): 11525-11530.

Todesco, M., S. Balasubramanian, T. T. Hu, M. B. Traw, M. Horton, P. Epple, C. Kuhns, S. Sureshkumar, C. Schwartz, C. Lanz, R. A. Laitinen, Y. Huang, J. Chory, V. Lipka, J. O. Borevitz, J. L. Dangl, J. Bergelson, M. Nordborg and D. Weigel (2010). "Natural allelic variation underlying a major fitness trade-off in Arabidopsis thaliana." Nature **465**(7298): 632-636.

Todesco, M., S. T. Kim, E. Chae, K. Bomblies, M. Zaidem, L. M. Smith, D. Weigel and R. A. Laitinen (2014). "Activation of the Arabidopsis thaliana immune system by combinations of common ACD6 alleles." PLoS Genet **10**(7): e1004459.

Truman, W., M. T. de Zabala and M. Grant (2006). "Type III effectors orchestrate a complex interplay between transcriptional networks to modify basal defence responses during pathogenesis and resistance." Plant J **46**(1): 14-33.

Tsuchiya, T. and T. Eulgem (2013). "An alternative polyadenylation mechanism coopted to the Arabidopsis RPP7 gene through intronic retrotransposon domestication." Proc Natl Acad Sci U S A **110**(37): E3535-3543.

Turcotte, M. M., M. S. C. Corrin and M. T. J. Johnson (2012). "Adaptive Evolution in Ecological Communities." Plos Biology **10**(5).

Tyler, B. M., S. Tripathy, X. Zhang, P. Dehal, R. H. Jiang, A. Aerts, F. D. Arredondo, L. Baxter, D. Bensasson, J. L. Beynon, J. Chapman, C. M. Damasceno, A. E. Dorrance, D. Dou, A. W. Dickerman, I. L. Dubchak, M. Garbelotto, M. Gijzen, S. G. Gordon, F. Govers, N. J. Grunwald, W. Huang, K. L. Ivors, R. W. Jones, S. Kamoun, K. Krampis, K. H. Lamour, M. K. Lee, W. H. McDonald, M. Medina, H. J. Meijer, E. K. Nordberg, D. J. Maclean, M. D. Ospina-Giraldo, P. F. Morris, V. Phuntumart, N. H. Putnam, S. Rash, J. K. Rose, Y. Sakihama, A. A. Salamov, A. Savidor, C. F. Scheuring, B. M. Smith, B. W. Sobral, A. Terry, T. A. Torto-Alalibo, J. Win, Z. Xu, H. Zhang, I. V. Grigoriev, D. S. Rokhsar and J. L. Boore (2006). "Phytophthora genome sequences uncover evolutionary origins and mechanisms of pathogenesis." Science **313**(5791): 1261-1266.

Untergasser, A., H. Nijveen, X. Rao, T. Bisseling, R. Geurts and J. A. M. Leunissen (2007). "Primer3Plus, an enhanced web interface to Primer3." Nucleic Acids Research **35**: W71-W74.

van der Biezen, E. A., C. T. Freddie, K. Kahn, J. E. Parker and J. D. G. Jones (2002). "Arabidopsis RPP4 is a member of the RPP5 multigene family of TIR-NB-LRR genes and

confers downy mildew resistance through multiple signalling components." Plant Journal **29**(4): 439-451.

Van der Biezen, E. A. and J. D. Jones (1998). "Plant disease-resistance proteins and the gene-for-gene concept." Trends Biochem Sci **23**(12): 454-456.

van der Hoorn, R. A. and S. Kamoun (2008). "From Guard to Decoy: a new model for perception of plant pathogen effectors." Plant Cell **20**(8): 2009-2017.

van Der Schaar, W., C. Alonso-Blanco, K. M. Leon-Kloosterziel, R. C. Jansen, J. W. van Ooijen and M. Koornneef (1997). "QTL analysis of seed dormancy in Arabidopsis using recombinant inbred lines and MQM mapping." Heredity (Edinb) **79 (Pt 2)**: 190-200.

van Leeuwen, H., D. J. Kliebenstein, M. A. L. West, K. Kim, R. van Poecke, F. Katagiri, R. W. Michelmore, R. W. Doerge and D. A. Clair (2007). "Natural variation among Arabidopsis thaliana accessions for transcriptome response to exogenous salicylic acid." Plant Cell **19**(7): 2099-2110.

van Verk, M. C., J. F. Bol and H. J. Linthorst (2011). "WRKY transcription factors involved in activation of SA biosynthesis genes." BMC Plant Biol **11**: 89.

Van Zandt, P. A. (2007). "Plant defense, growth, and habitat: A comparative assessment of constitutive and induced resistance." Ecology **88**(8): 1984-1993.

Vanacker, H., H. Lu, D. N. Rate and J. T. Greenberg (2001). "A role for salicylic acid and NPR1 in regulating cell growth in Arabidopsis." Plant J **28**(2): 209-216.

Vargas, W. A., J. M. Martin, G. E. Rech, L. P. Rivera, E. P. Benito, J. M. Diaz-Minguez, M. R. Thon and S. A. Sukno (2012). "Plant defense mechanisms are activated during biotrophic and necrotrophic development of Colletotricum graminicola in maize." Plant Physiol **158**(3): 1342-1358.

Venugopal, S. C., R. D. Jeong, M. K. Mandal, S. F. Zhu, A. C. Chandra-Shekara, Y. Xia, M. Hersh, A. J. Stromberg, D. Navarre, A. Kachroo and P. Kachroo (2009). "Enhanced Disease Susceptibility 1 and Salicylic Acid Act Redundantly to Regulate Resistance Gene-Mediated Signaling." Plos Genetics **5**(7).

Verhage, A., S. C. van Wees and C. M. Pieterse (2010). "Plant immunity: it's the hormones talking, but what do they say?" Plant Physiol **154**(2): 536-540.

Vetter, M. M., I. Kronholm, F. He, H. Haweker, M. Reymond, J. Bergelson, S. Robatzek and J. de Meaux (2012). "Flagellin Perception Varies Quantitatively in Arabidopsis thaliana and Its Relatives." Molecular Biology and Evolution **29**(6): 1655-1667.

Vleeshouwers, V. G. and R. P. Oliver (2014). "Effectors as tools in disease resistance breeding against biotrophic, hemibiotrophic, and necrotrophic plant pathogens." Mol Plant Microbe Interact **27**(3): 196-206.

Vleeshouwers, V. G., S. Raffaele, J. H. Vossen, N. Champouret, R. Oliva, M. E. Segretin, H. Rietman, L. M. Cano, A. Lokossou, G. Kessel, M. A. Pel and S. Kamoun (2011). "Understanding and exploiting late blight resistance in the age of effectors." Annu Rev Phytopathol **49**: 507-531.

Vlot, A. C., D. A. Dempsey and D. F. Klessig (2009). "Salicylic Acid, a multifaceted hormone to combat disease." Annu Rev Phytopathol **47**: 177-206.

Wagner, S., J. Stuttmann, S. Rietz, R. Guerois, E. Brunstein, J. Bautor, K. Niefind and J. E. Parker (2013). "Structural Basis for Signaling by Exclusive EDS1 Heteromeric Complexes with SAG101 or PAD4 in Plant Innate Immunity." Cell Host & Microbe **14**(6): 619-630.

Wang, D., N. Amornsiripanitch and X. N. Dong (2006). "A genomic approach to identify regulatory nodes in the transcriptional network of systemic acquired resistance in plants." Plos Pathogens **2**(11): 1042-1050.

Wang, G. F., S. Seabolt, S. Hamdoun, G. Ng, J. Park and H. Lu (2011). "Multiple Roles of WIN3 in Regulating Disease Resistance, Cell Death, and Flowering Time in Arabidopsis." Plant Physiology **156**(3): 1508-1519.

Wang, G. Y., J. L. Shi, G. Ng, S. L. Battle, C. Zhang and H. Lu (2011). "Circadian Clock-Regulated Phosphate Transporter PHT4;1 Plays an Important Role in Arabidopsis Defense." Molecular Plant **4**(3): 516-526.

Wang, G. Y., C. Zhang, S. Battle and H. Lu (2014). "The phosphate transporter PHT4;1 is a salicylic acid regulator likely controlled by the circadian clock protein CCA1." Frontiers in Plant Science **5**.

Wang, L., R. M. Mitra, K. D. Hasselmann, M. Sato, L. Lenarz-Wyatt, J. D. Cohen, F. Katagiri and J. Glazebrook (2008). "The Genetic Network Controlling the Arabidopsis Transcriptional Response to Pseudomonas syringae pv. maculicola: Roles of Major Regulators and the Phytotoxin Coronatine." Molecular Plant-Microbe Interactions **21**(11): 1408-1420.

Wang, Q., U. Sajja, S. Rosloski, T. Humphrey, M. C. Kim, K. Bomblies, D. Weigel and V. Grbic (2007). "HUA2 caused natural variation in shoot morphology of A-thaliana." Current Biology **17**(17): 1513-1519.

Wang, X., R. Sager, W. Cui, C. Zhang, H. Lu and J. Y. Lee (2013). "Salicylic acid regulates Plasmodesmata closure during innate immune responses in Arabidopsis." Plant Cell **25**(6): 2315-2329.

War, A. R., M. G. Paulraj, T. Ahmad, A. A. Buhroo, B. Hussain, S. Ignacimuthu and H. C. Sharma (2012). "Mechanisms of plant defense against insect herbivores." Plant Signal Behav **7**(10): 1306-1320.

Wardlaw, A. M. and A. F. Agrawal (2012). "Temporal Variation in Selection Accelerates Mutational Decay by Muller's Ratchet." Genetics **191**(3): 907-916.

Weigel, D. (2012). "Natural variation in Arabidopsis: from molecular genetics to ecological genomics." Plant Physiol **158**(1): 2-22.

Weigel, D. and J. Glazebrook (2006). "In planta transformation of Arabidopsis." CSH Protoc **2006**(7).

Weigel, D. and M. Nordborg (2005). "Natural variation in Arabidopsis. How do we find the causal genes?" Plant Physiol **138**(2): 567-568.

Weigel, D. and M. Nordborg (2015). "Population Genomics for Understanding Adaptation in Wild Plant Species." Annu Rev Genet **49**: 315-338.

Weigelworld. "WMD3 - Web MicroRNA Designer." from http://wmd3.weigelworld.org/cgi-bin/webapp.cgi.

Weymann, K., M. Hunt, S. Uknes, U. Neuenschwander, K. Lawton, H. Y. Steiner and J. Ryals (1995). "Suppression and Restoration of Lesion Formation in Arabidopsis lsd Mutants." Plant Cell **7**(12): 2013-2022.

Wickham, H. (2009). "ggplot2 Elegant Graphics for Data Analysis Introduction." Ggplot2: Elegant Graphics for Data Analysis: 1-+.

Wildermuth, M. C., J. Dewdney, G. Wu and F. M. Ausubel (2001). "Isochorismate synthase is required to synthesize salicylic acid for plant defence." Nature **414**(6863): 562-565.

Willmann, R., H. M. Lajunen, G. Erbs, M. A. Newman, D. Kolb, K. Tsuda, F. Katagiri, J. Fliegmann, J. J. Bono, J. V. Cullimore, A. K. Jehle, F. Gotz, A. Kulik, A. Molinaro, V. Lipka, A. A. Gust and T. Nurnberger (2011). "Arabidopsis lysin-motif proteins LYM1 LYM3 CERK1 mediate bacterial peptidoglycan sensing and immunity to bacterial infection." Proc Natl Acad Sci U S A **108**(49): 19824-19829.

Wilson, I. W., C. L. Schiff, D. E. Hughes and S. C. Somerville (2001). "Quantitative trait loci analysis of powdery mildew disease resistance in the Arabidopsis thaliana accession Kashmir-1." Genetics **158**(3): 1301-1309.

Woolhouse, M. E. J., J. P. Webster, E. Domingo, B. Charlesworth and B. R. Levin (2002). "Biological and biomedical implications of the co-evolution of pathogens and their hosts." Nature Genetics **32**(4): 569-577.

Wu, Y., D. Zhang, J. Y. Chu, P. Boyle, Y. Wang, I. D. Brindle, V. De Luca and C. Despres (2012). "The Arabidopsis NPR1 protein is a receptor for the plant defense hormone salicylic acid." Cell Rep **1**(6): 639-647.

Xia, S. T., Y. T. Cheng, S. Huang, J. Win, A. Soards, T. L. Jinn, J. D. G. Jones, S. Kamoun, S. Chen, Y. L. Zhang and X. Li (2013). "Regulation of Transcription of Nucleotide-Binding Leucine-Rich Repeat-Encoding Genes SNC1 and RPP4 via H3K4 Trimethylation." Plant Physiology **162**(3): 1694-1705.

Xiang, T., N. Zong, Y. Zou, Y. Wu, J. Zhang, W. Xing, Y. Li, X. Tang, L. Zhu, J. Chai and J. M. Zhou (2008). "Pseudomonas syringae effector AvrPto blocks innate immunity by targeting receptor kinases." Curr Biol **18**(1): 74-80.

Xing, W., Y. Zou, Q. Liu, J. N. Liu, X. Luo, Q. Q. Huang, S. Chen, L. H. Zhu, R. C. Bi, Q. Hao, J. W. Wu, J. M. Zhou and J. J. Chai (2007). "The structural basis for activation of plant immunity by bacterial effector protein AvrPto." Nature **449**(7159): 243-U211.

Yamaguchi, Y., G. Pearce and C. A. Ryan (2006). "The cell surface leucine-rich repeat receptor for AtPep1, an endogenous peptide elicitor in Arabidopsis, is functional in transgenic tobacco cells." Proc Natl Acad Sci U S A **103**(26): 10104-10109.

Yang, H. J., Y. Q. Li and J. Hua (2006). "The C2 domain protein BAP1 negatively regulates defense responses in Arabidopsis." Plant Journal **48**(2): 238-248.

Yang, S., J. Li, X. Zhang, Q. Zhang, J. Huang, J. Q. Chen, D. L. Hartl and D. Tian (2013). "Rapidly evolving R genes in diverse grass species confer resistance to rice blast disease." Proc Natl Acad Sci U S A **110**(46): 18572-18577.

Yang, S. H. and J. Hua (2004). "A haplotype-specific Resistance gene regulated by BONZAI1 mediates temperature-dependent growth control in Arabidopsis." Plant Cell **16**(4): 1060-1071.

Yang, Y. X., G. J. Ahammed, C. J. Wu, S. Y. Fan and Y. H. Zhou (2015). "Crosstalk among Jasmonate, Salicylate and Ethylene Signaling Pathways in Plant Disease and Immune Responses." Current Protein & Peptide Science **16**(5): 450-461.

Yasuda, M., A. Ishikawa, Y. Jikumaru, M. Seki, T. Umezawa, T. Asami, A. Maruyama-Nakashita, T. Kudo, K. Shinozaki, S. Yoshida and H. Nakashita (2008). "Antagonistic interaction between systemic acquired resistance and the abscisic acid-mediated abiotic stress response in Arabidopsis." Plant Cell **20**(6): 1678-1692.

Yi, S. Y. and S. Y. Kwon (2014). "How does SA signaling link the Flg22 responses?" Plant Signal Behav **9**(11): e972806.

Yi, S. Y., K. Shirasu, J. S. Moon, S. G. Lee and S. Y. Kwon (2014). "The activated SA and JA signaling pathways have an influence on flg22-triggered oxidative burst and callose deposition." PLoS One **9**(2): e88951.

Yu, I. C., J. Parker and A. F. Bent (1998). "Gene-for-gene disease resistance without the hypersensitive response in Arabidopsis dnd1 mutant." Proceedings of the National Academy of Sciences of the United States of America **95**(13): 7819-7824.

Zhang, J. and M. J. Lechowicz (1995). "Responses to Co2 Enrichment by 2 Genotypes of Arabidopsis-Thaliana Differing in Their Sensitivity to Nutrient Availability." Annals of Botany **75**(5): 491-499.

Zhang, J., F. Shao, Y. Li, H. Cui, L. Chen, H. Li, Y. Zou, C. Long, L. Lan, J. Chai, S. Chen, X. Tang and J. M. Zhou (2007). "A Pseudomonas syringae effector inactivates MAPKs to suppress PAMP-induced immunity in plants." Cell Host Microbe **1**(3): 175-185.

Zhang, N., A. Lariviere, S. J. Tonsor and M. B. Traw (2014). "Constitutive camalexin production and environmental stress response variation in Arabidopsis populations from the Iberian Peninsula." Plant Sci **225**: 77-85.

Zhang, N., S. J. Tonsor and M. B. Traw (2015). "A geographic cline in leaf salicylic acid with increasing elevation in Arabidopsis thaliana." Plant Signal Behav **10**(3): e992741.

Zhang, Y. L., S. Goritschnig, X. N. Dong and X. Li (2003). "A gain-of-function mutation in a plant disease resistance gene leads to constitutive activation of downstream signal transduction pathways in suppressor of npr1-1, constitutive 1." Plant Cell **15**(11): 2636-2646.

Zhang, Y. L. and X. Li (2005). "A putative nucleoporin 96 is required for both basal defense and constitutive resistance responses mediated by suppressor of npr1-1, constitutive 1." Plant Cell **17**(4): 1306-1316.

Zhang, Z., J. Shrestha, C. Tateda and J. T. Greenberg (2014). "Salicylic acid signaling controls the maturation and localization of the arabidopsis defense protein ACCELERATED CELL DEATH6." Mol Plant **7**(8): 1365-1383.

Zheng, X., H. McLellan, M. Fraiture, X. Liu, P. C. Boevink, E. M. Gilroy, Y. Chen, K. Kandel, G. Sessa, P. R. Birch and F. Brunner (2014). "Functionally redundant RXLR effectors from Phytophthora infestans act at different steps to suppress early flg22-triggered immunity." PLoS Pathog **10**(4): e1004057.

Zhou, J., S. Wu, X. Chen, C. Liu, J. Sheen, L. Shan and P. He (2014). "The Pseudomonas syringae effector HopF2 suppresses Arabidopsis immunity by targeting BAK1." Plant J **77**(2): 235-245.

Zhou, N., T. L. Tootle, F. Tsui, D. F. Klessig and J. Glazebrook (1998). "PAD4 functions upstream from salicylic acid to control defense responses in Arabidopsis." Plant Cell **10**(6): 1021-1030.

Zipfel, C., G. Kunze, D. Chinchilla, A. Caniard, J. D. Jones, T. Boller and G. Felix (2006). "Perception of the bacterial PAMP EF-Tu by the receptor EFR restricts Agrobacterium-mediated transformation." Cell **125**(4): 749-760.

Zong, N., T. Xiang, Y. Zou, J. Chai and J. M. Zhou (2008). "Blocking and triggering of plant immunity by Pseudomonas syringae effector AvrPto." Plant Signal Behav **3**(8): 583-585.

8 Appendix

Appendix Table 1. *Arabidopsis thaliana* accessions used in this study

Ecotype ID	Name	Country	Latitude	Longitude
88	CYR	FRA	47.4	0.683333
108	LDV-18	FRA	48.5167	-4.06667
139	LDV-46	FRA	48.5167	-4.06667
159	MAR2-3	FRA	47.35	3.93333
265	PYL-6	FRA	44.65	-1.16667
350	TOU-A1-88	FRA	46.6667	4.11667
351	TOU-A1-89	FRA	46.6667	4.11667
403	Zdarec3	CZE	49.3667	16.2667
410	Doubravnik7	CZE	49.4211	16.3497
424	Draha2	CZE	49.4112	16.2815
428	Borky1	CZE	49.403	16.232
430	Gr-1	AUT	47	15.5
583	LI-YA-030	USA	40.8198	-72.9156
630	LI-OF-065	USA	40.7777	-72.9069
763	Kar-1	KGZ	42.3	74.3667
765	Sus-1	KGZ	42.1833	73.4
766	Dja-1	KGZ	42.5833	73.6333
768	Zal-1	KGZ	42.8	76.35
770	Kyr-1	KGZ	40.046526	72.683613
772	Neo-6	TJK	37.35	72.4667
801	KYC-33	USA	37.9169	-84.4639
870	MIC-31	USA	41.8266	-86.4366
915	LIN S-5	USA	41.8972	-71.4378
932	CHA-41	USA	42.3634	-71.1445
991	Ale-Stenar-41-1	SWE	55.3833	14.05
992	Ale-Stenar-44-4	SWE	55.3833	14.05
997	Ale-Stenar-56-14	SWE	55.3833	14.05
1002	Ale-Stenar-64-24	SWE	55.3833	14.05
1006	Ale-Stenar-77-31	SWE	55.3833	14.05
1061	Brösarp-11-135	SWE	55.7167	14.1333
1062	Brösarp-15-138	SWE	55.7167	14.1333
1063	Brösarp-21-140	SWE	55.7167	14.1333
1066	Brösarp-34-145	SWE	55.7167	14.1333
1070	Brösarp-45-153	SWE	55.7167	14.1333
1074	Brösarp-61-162	SWE	55.7167	14.1333
1137	Gårdby-22-213	SWE	56.6167	16.65
1158	Aledal-6-49	SWE	56.7	16.5167
1166	Aledal-14-73	SWE	56.7	16.5167
1254	Tos-82-387	SWE	59.4333	17.0167
1257	Tos-95-393	SWE	59.4333	17.0167
1303	Ängsö-12-402	SWE	59.5667	16.8667
1313	Ängsö-59-422	SWE	59.5667	16.8667
1317	Ängsö-74-430	SWE	59.5667	16.8667
1318	Ängsö-80-432	SWE	59.5667	16.8667
1363	Ham-7-233	SWE	59.7833	17.5833
1367	Ham-13-241	SWE	59.7833	17.5833
1435	Röd-17-319	SWE	62.8	18.2
1552	Sku-30	SWE	63.0833	18.3667
1585	Hen-16-268	SWE	65.25	15.6
1829	Mdn-1	USA	42.051	-86.509
1853	MNF-Pot-21	USA	43.595	-86.2657
1872	MNF-Pot-75	USA	43.595	-86.2657
1890	MNF-Riv-21	USA	43.5139	-86.1859
1925	MNF-Che-2	USA	43.5251	-86.1843
1954	MNF-Jac-12	USA	43.5187	-86.1739
2016	MNF-Pin-39	USA	43.5356	-86.1788
2171	Paw-26	USA	42.148	-86.431
2202	Pent-23	USA	43.7623	-86.3929
2276	SLSP-31	USA	43.665	-86.496
2278	SLSP-35	USA	43.665	-86.496
2317	Ste-40	USA	42.03	-86.514
4779	UKSW06-179	UK	50.4	-4.9
4807	UKSW06-207	UK	50.4	-4.9
4826	UKSW06-226	UK	50.4	-4.9
4884	UKSW06-285	UK	50.3	-4.9
4900	UKSW06-302	UK	50.3	-4.8
4931	UKSW06-333	UK	50.327643	-4.6
4958	UKSW06-360	UK	50.5	-4.5
5023	UKSE06-118	UK	51.3	0.5
5104	UKSE06-252	UK	51.3	0.5
5151	UKSE06-325	UK	52.2	-1.7
5165	UKSE06-362	UK	51.3	0.4
5210	UKSE06-432	UK	51.2	0.3
5236	UKSE06-470	UK	51.2	0.4
5253	UKSE06-500	UK	51.1	0.6

Continued on next page

Appendix Table 1. Continued from previous page…

Ecotype ID	Name	Country	Latitude	Longitude
5276	UKSE06-533	UK	51.3	1.1
5349	UKSE06-639	UK	51.1	0.4
5353	UKNW06-003	UK	54.5	-3
5470	UKNW06-212	UK	54.7	-3.4
5486	UKNW06-233	UK	54.6	-3.3
5506	UKNW06-281	UK	54.6	-3.1
5535	UKNW06-354	UK	54.6	-3.1
5577	UKNW06-403	UK	54.7	-3.4
5644	UKNW06-481	UK	54.4	-2.9
5720	Cal-2	UK	53.3	-1.6
5726	Cnt-1	UK	51.3	1.1
5741	For-2	UK	56.6	-4.1
5748	Kil-0	UK	56	-4.4
5757	Mc-1	UK	54.6	-2.3
5768	UKID63	UK	54.1	-1.5
5772	Set-1	UK	54.1	-2.3
5778	Sna-1	UK	52.2	1.5
5779	UKID74	UK	51	-3.1
5784	Ty-1	UK	56.4	-5.2
5800	UKID96	UK	57.4	-5.5
5811	UKID107	UK	52.9	-3.1
5818	UKID114	UK	51.8	-0.6
5822	UKID116	UK	56.7333	-5.98333
5829	Ale1-2	SWE	55.3838	14.0612
5830	App1-12	SWE	56.3333	15.9667
5831	App1-14	SWE	56.3333	15.9667
5832	App1-16	SWE	56.3333	15.9667
5835	Bil-3	SWE	63.324	18.484
5836	Boo2-3	SWE	55.86	13.51
5837	Bor-1	CZE	49.4013	16.2326
5856	Dör-10	SWE	63.0167	17.4914
5860	Dra-3	SWE	62.6814	18.0165
5865	Dra1-4	SWE	55.76	14.12
5867	Dra2-1	SWE	55.76	14.12
5874	DraII-6	CZE	49.4112	16.2815
5890	DraIV 1-8	CZE	49.4112	16.2815
5893	DraIV 1-11	CZE	49.4112	16.2815
5907	DraIV 2-9	CZE	49.4112	16.2815
5921	DraIV 3-7	CZE	49.4112	16.2815
5950	DraIV 5-12	CZE	49.4112	16.2815
5964	DraIV 5-28	CZE	49.4112	16.2815
5984	DraIV 6-13	CZE	49.4112	16.2815
5993	DraIV 6-22	CZE	49.4112	16.2815
6008	Duk	CZE	49.1	16.2
6009	Eden-1	SWE	62.877	18.177
6010	Eden-5	SWE	62.877	18.177
6011	Eden-6	SWE	62.877	18.177
6012	Eden-7	SWE	62.877	18.177
6013	Eden-9	SWE	62.877	18.177
6016	Eds-1	SWE	62.9	18.4
6017	Eds-9	SWE	62.9	18.4
6019	Fjä1-2	SWE	56.06	14.29
6020	Fjä1-5	SWE	56.06	14.29
6021	Fjä2-4	SWE	56.06	14.29
6022	Fjä2-6	SWE	56.06	14.29
6023	Fly2-1	SWE	55.7509	13.3712
6024	Fly2-2	SWE	55.7509	13.3712
6025	Gro-3	SWE	62.6437	17.7339
6030	Grön-5	SWE	62.806	18.1896
6034	Hov1-7	SWE	56.1	13.74
6035	Hov1-10	SWE	56.1	13.74
6036	Hov3-2	SWE	56.1	13.74
6038	Hov3-5	SWE	56.1	13.74
6039	Hovdala-2	SWE	56.1	13.74
6040	Kni-1	SWE	55.66	13.4
6041	Lis-3	SWE	56.0328	14.775
6042	Lom1-1	SWE	56.09	13.9
6043	Löv-1	SWE	62.801	18.079
6046	Löv-5	SWE	62.801	18.079
6064	Nyl-2	SWE	62.9513	18.2763
6069	Nyl-7	SWE	62.9513	18.2763
6070	Omn-1	SWE	62.9308	18.3448
6071	Omn-5	SWE	62.9308	18.3448
6073	ÖMö1-7	SWE	56.1481	15.8155
6074	Ör-1	SWE	56.4573	16.1408
6076	Rev-2	SWE	55.6942	13.4504
6077	Rev-3	SWE	55.6942	13.4504
6085	Sparta-1	SWE	55.7097	13.2145
6086	Sr:3	SWE	58.9	11.2
6087	Stu-2	SWE	56.4666	16.1284
6088	Stu1-1	SWE	56.4666	16.1284
6090	T1000	SWE	55.6525	13.2197
6091	T1010	SWE	55.6525	13.215
6092	T1020	SWE	55.6514	13.2233

Continued on next page

Appendix Table 1. Continued from previous page…

Ecotype ID	Name	Country	Latitude	Longitude
6094	T1040	SWE	55.6494	13.2147
6095	T1050	SWE	55.6486	13.2161
6096	T1060	SWE	55.6472	13.2225
6097	T1070	SWE	55.6481	13.2264
6098	T1080	SWE	55.6561	13.2178
6099	T1090	SWE	55.6575	13.2386
6100	T1110	SWE	55.6	13.2
6101	T1120	SWE	55.6	13.2
6102	T1130	SWE	55.6	13.2
6104	T1160	SWE	55.7	13.2
6288	Udu-12	CZE	49.2771	16.6314
6390	Udul 3-36	CZE	49.2771	16.6314
6396	Udul 4-9	CZE	49.2771	16.6314
6413	Ull3-4	SWE	56.06	13.97
6424	Zdrl 1-23	CZE	49.3853	16.2544
6434	Zdrl 2-9	CZE	49.3853	16.2544
6445	Zdrl 2-21	CZE	49.3853	16.2544
6680	ANH-1	GER	51.85	6.4333
6709	Bg-2	USA	47.6479	-122.305
6744	CSHL-5	USA	40.8585	-73.4675
6830	KZ13	KAZ	49.5	73.1
6897	Ag-0	FRA	45	1.3
6898	An-1	BEL	51.2167	4.4
6900	Bil-5	SWE	63.324	18.484
6901	Bil-7	SWE	63.324	18.484
6903	Bor-4	CZE	49.4013	16.2326
6904	Br-0	CZE	49.2	16.6166
6906	C24	POR	40.2077	-8.42639
6907	CIBC-17	UK	51.4083	-0.6383
6908	CIBC-5	UK	51.4083	-0.6383
6909	Col-0	USA	38.3	-92.3
6911	Cvi-0	CPV	15.1111	-23.6167
6913	Eden-2	SWE	62.877	18.177
6915	Ei-2	GER	50.3	6.3
6916	Est-1	RUS	58.3	25.3
6917	Fäb-2	SWE	63.0165	18.3174
6918	Fäb-4	SWE	63.0165	18.3174
6919	Ga-0	GER	50.3	8
6920	Got-22	GER	51.5338	9.9355
6921	Got-7	GER	51.5338	9.9355
6922	Gu-0	GER	50.3	8
6923	HR-10	UK	51.4083	-0.6383
6924	HR-5	UK	51.4083	-0.6383
6926	Kin-0	USA	44.46	-85.37
6927	Knox-10	USA	41.2816	-86.621
6928	Knox-18	USA	41.2816	-86.621
6929	Kondara	TJK	38.48	68.49
6931	Kz-9	KAZ	49.5	73.1
6932	Ler-1	GER	47.984	10.8719
6933	LL-0	ESP	41.59	2.49
6936	Lz-0	FRA	46	3.3
6937	Mrk-0	GER	49	9.3
6938	Ms-0	RUS	55.7522	37.6322
6939	Mt-0	LIB	32.34	22.46
6940	Mz-0	GER	50.3	8.3
6943	NFA-10	UK	51.4083	-0.6383
6944	NFA-8	UK	51.4083	-0.6383
6945	Nok-3	NED	52.24	4.45
6951	Pu2-23	CZE	49.42	16.36
6956	Pu2-7	CZE	49.42	16.36
6957	Pu2-8	CZE	49.42	16.36
6958	Ra-0	FRA	46	3.3
6959	Ren-1	FRA	48.5	-1.41
6960	Ren-11	FRA	48.5	-1.41
6961	Se-0	ESP	38.3333	-3.53333
6963	Sorbo	TJK	38.35	68.48
6964	Spr1-2	SWE	56.3	16
6965	Spr1-6	SWE	58.4173	14.1576
6966	Sq-1	UK	51.4083	-0.6383
6967	Sq-8	UK	51.4083	-0.6383
6968	Tamm-2	FIN	60	23.5
6969	Tamm-27	FIN	60	23.5
6970	Ts-1	ESP	41.7194	2.93056
6971	Ts-5	ESP	41.7194	2.93056
6972	Tsu-1	JPN	34.43	136.31
6973	Ull2-3	SWE	56.0648	13.9707
6974	Ull2-5	SWE	56.0648	13.9707
6975	Uod-1	AUT	48.3	14.45
6976	Uod-7	AUT	48.3	14.45
6979	Wei-0	SUI	47.25	8.26
6981	Ws-2	RUS	52.3	30
6982	Wt-5	GER	52.3	9.3
6984	Zdr-1	CZE	49.3853	16.2544
6985	Zdr-6	CZE	49.3853	16.2544

Continued on next page

Appendix Table 1. Continued from previous page…

Ecotype ID	Name	Country	Latitude	Longitude
6986	Abd-0	UK	57.1539	-2.2207
6987	Ak-1	GER	48.0683	7.62551
6989	Alst-1	UK	54.8	-2.4333
6990	Amel-1	NED	53.448	5.73
6992	Ang-0	BEL	50.3	5.3
6994	Ann-1	FRA	45.9	6.13028
6997	Appt-1	NED	51.8333	5.5833
7000	Aa-0	GER	50.9167	9.57073
7002	Baa-1	NED	51.3333	6.1
7003	Bs-1	SUI	47.5	7.5
7008	Benk-1	NED	52	5.675
7010	Be-0	GER	49.6803	8.6161
7013	Bd-0	GER	52.4584	13.287
7014	Ba-1	UK	56.5459	-4.79821
7025	Bl-1	ITA	44.5041	11.3396
7026	Boot-1	UK	54.4	-3.2667
7028	Bch-1	GER	49.5166	9.3166
7031	Bsch-0	GER	50.0167	8.6667
7033	Buckhorn Pass	USA	41.3599	-122.755
7036	Bu-0	GER	50.5	9.5
7058	Bur-0	IRL	54.1	-6.2
7061	Cal-0	UK	53.2699	-1.64293
7062	Ca-0	GER	50.2981	8.26607
7063	Can-0	ESP	29.2144	-13.4811
7064	Cnt-1	UK	51.3	1.1
7067	Ct-1	ITA	37.3	15
7068	Cerv-1	ITA	42	12.1
7071	Chat-1	FRA	48.0717	1.33867
7072	Chi-0	RUS	53.7502	34.7361
7075	Cit-0	FRA	43.3779	2.54038
7077	Co-1	POR	40.12	-8.25
7081	Co	POR	40.2077	-8.42639
7092	Com-1	FRA	49.416	2.823
7094	Da-0	GER	49.8724	8.65081
7096	Di-G	FRA	47.3239	5.04278
7098	Di-1	FRA	47	5
7102	Do-0	GER	50.7224	8.2372
7103	Dra-0	CZE	49.4167	16.2667
7106	Dr-0	GER	51.051	13.7336
7107	Durh-1	UK	54.7761	-1.5733
7109	Ema-1	UK	51.3	0.5
7111	Edi-0	UK	55.9494	-3.16028
7117	El-0	GER	51.5105	9.68253
7119	En-2	GER	50	8.5
7120	En-D	GER	50	8.5
7123	Ep-0	GER	50.1721	8.38912
7125	Er-0	GER	49.5955	11.0087
7126	Es-0	FIN	60.1997	24.5682
7127	Est	GER	58.6656	24.9871
7130	Et-0	FRA	44.6447	2.56481
7133	Fr-2	GER	50.1102	8.6822
7138	Fi-0	GER	50.5	8.0167
7143	Gel-1	NED	51.0167	5.86667
7147	Gie-0	GER	50.584	8.67825
7148	Gifu-2	JPN	35.45	137.42
7158	Gr-5	AUT	47	15.5
7160	Gre-0	USA	43.178	-85.2532
7161	Gd-1	GER	53.5	10.5
7162	Hs-0	GER	52.24	9.44
7163	Ha-0	GER	52.3721	9.73569
7164	Hau-0	DEN	55.675	12.5686
7165	Hn-0	GER	51.3472	8.28844
7166	Hey-1	NED	51.25	5.9
7167	Hi-0	NED	52	5
7169	Hh-0	GER	54.4175	9.88682
7177	Jm-0	CZE	49	15
7181	Je-0	GER	50.927	11.587
7182	Ka-0	AUT	47	14
7186	Kn-0	LTU	54.8969	23.8924
7192	Kil-0	UK	55.6395	-5.66364
7199	Kl-5	GER	50.95	6.9666
7202	Kb-0	GER	50.1797	8.50861
7203	Krot-0	GER	49.631	11.5722
7206	Kro-0	GER	50.0742	8.96617
7207	Kyoto	JPN	35.0085	135.752
7208	Lan-0	UK	55.6739	-3.78181
7209	La-0	POL	52.7333	15.2333
7213	Ler-0	GER	47.984	10.8719
7217	Lm-2	FRA	48	0.5
7218	Le-0	NED	52.1611	4.49015
7223	Li-2:1	GER	50.3833	8.0666
7231	Li-7	GER	50.3833	8.0666
7236	Litva	LTU		
7244	Mnz-0	GER	50.001	8.26664

Continued on next page

Appendix Table 1. Continued from previous page…

Ecotype ID	Name	Country	Latitude	Longitude
7248	Mv-0	USA	41.3923	-70.6652
7250	Me-0	GER	51.9183	10.1138
7252	Mc-0	UK	54.6167	-2.3
7255	Mh-0	POL	50.95	7.5
7258	Nw-0	GER	50.5	8.5
7263	Nz-1	NZL	-37.7871	175.283
7268	Np-0	GER	52.6969	10.981
7273	No-0	GER	51.0581	13.2995
7276	Ob-0	GER	50.2	8.5833
7280	Old-1	GER	53.1667	8.2
7282	Or-0	GER	50.3827	8.01161
7287	Ove-0	GER	53.3422	8.42255
7288	Oy-0	NOR	60.385543	6.193019
7296	Petergof	RUS	59	29
7298	Pi-0	AUT	47.04	10.51
7305	Pt-0	GER	53.476	10.6065
7306	Pog-0	CAN	49.2655	-123.206
7307	Pn-0	FRA	48.0653	-2.96591
7308	Po-0	GER	50.7167	7.1
7314	Ragl-1	UK	54.3512	-3.41697
7316	Rhen-1	NED	51.9667	5.56667
7319	Rome-1	ITA	42	12.1
7320	Rou-0	FRA	49.4424	1.09849
7322	Rsch-4	RUS	56.3	34
7323	Rubeznhoe-1	UKR	49	38.28
7327	Sf-1	ESP	41.7833	3.03333
7328	Sf-2	ESP	41.7833	3.03333
7329	Santa Clara	USA	37.21	-121.16
7330	Sapporo-0	JPN	43.0553	141.346
7332	Seattle-0	USA	47	-122.2
7333	Sei-0	ITA	46.5438	11.5614
7337	Si-0	GER	50.8738	8.02341
7342	Su-0	UK	53.6473	-3.00733
7343	Sp-0	GER	52.5339	13.181
7344	Sg-1	GER	47.6667	9.5
7346	Ste-0	GER	52.6058	11.8558
7347	Stw-0	RUS	52	36
7349	Ta-0	CZE	49.5	14.5
7350	Tac-0	USA	47.2413	-122.459
7351	Ty-0	UK	56.4278	-5.23439
7353	Tha-1	NED	52.08	4.3
7354	Ting-1	SWE	56.5	14.9
7355	Tiv-1	ITA	41.96	12.8
7356	Tol-0	USA	41.6639	-83.5553
7372	Tscha-1	AUT	47.0748	9.9042
7373	Tsu-0	JPN	34.43	136.31
7375	Tu-0	ITA	45	7.5
7377	Tul-0	USA	43.2708	-85.2563
7378	Uk-1	GER	48.0333	7.7667
7382	Utrecht	NED	52.0918	5.1145
7383	Van-0	CAN	49.2655	-123.206
7384	Ven-1	NED	52.0333	5.55
7387	Vind-1	UK	54.9902	-2.3671
7394	Wa-1	POL	52.3	21
7396	Ws-0	RUS	52.3	30
7404	Wc-1	GER	52.6	10.0667
7411	Wl-0	GER	47.9299	10.8134
7413	Wil-2	LTU	54.6833	25.3167
7415	Wu-0	GER	49.7878	9.9361
7416	Yo-0	USA	37.45	-119.35
7417	Zu-0	SUI	47.3667	8.55
7418	Zu-1	SUI	47.3667	8.55
7419	Db-1	GER	50.3058	8.32213
7424	Jl-3	CZE	49.2	16.6166
7427	Ko-2	DEN		
7430	Nc-1	FRA	48.6167	6.25
7438	N13	RUS	61.36	34.15
7458	Ber	DEN	55.675	12.5687
7460	Da(1)-12	CZE		
7461	H55	CZE	49	15
7471	RLD-1	UNK		
7477	WAR	USA	41.7302	-71.2825
7514	RRS-7	USA	41.5609	-86.4251
7515	RRs-10	USA	41.5609	-86.4251
7516	Vår2-1	SWE	55.58	14.334
7517	Vår2-6	SWE	55.58	14.334
7518	ÖMö2-1	SWE	56.1509	15.7735
7519	ÖMö2-3	SWE	56.1509	15.7735
7520	Lp2-2	CZE	49.38	16.81
7521	Lp2-6	CZE	49.38	16.81
7522	Mr-0	ITA	44.15	9.65
7523	Pna-17	USA	42.0945	-86.3253
7524	Rmx-A02	USA	42.036	-86.511
7525	Rmx-A180	USA	42.036	-86.511

Continued on next page

Appendix Table 1. Continued from previous page…

Ecotype ID	Name	Country	Latitude	Longitude
7526	Pna-10	USA	42.0945	-86.3253
7717	KNO1.37	USA	41.273	-86.625
7917	PNA3.10	USA	42.0945	-86.3253
7947	PNA3.40	USA	42.0945	-86.3253
8077	PT2.21	USA	41.3423	-86.7368
8132	RMX3.22	USA	42.036	-86.511
8213	Pro-0	ESP	43.25	-6
8214	Gy-0	FRA	49	2
8222	Lis-2	SWE	56.0328	14.775
8227	THÖ 03	SWE	62.7989	17.9103
8230	Algutsrum	SWE	56.68	16.5
8231	Brö1-6	SWE	56.3	16
8233	Dem-4	USA	41.1876	-87.1923
8234	Gul1-2	SWE	56.4606	15.8127
8235	Hod	CZE	48.8	17.1
8236	HSm	CZE	49.33	15.76
8237	Kävlinge-1	SWE	55.8	13.1
8238	Kent	UK	51.15	0.4
8239	Köln	GER	51	7
8240	Kulturen-1	SWE	55.705	13.196
8241	Liarum	SWE	55.9473	13.821
8242	Lillö-1	SWE	56.1494	15.7884
8243	PHW-2	ITA	43.7703	11.2547
8244	PHW-34	FRA	48.6103	2.3086
8246	NC-6	USA	35	-79.18
8247	San-2	SWE	56.07	13.74
8249	Vimmerby	SWE	57.7	15.8
8256	Bå1-2	SWE	56.4	12.9
8258	Bå4-1	SWE	56.4	12.9
8259	Bå5-1	SWE	56.4	12.9
8264	Bla-1	ESP	41.6833	2.8
8266	Boo2-1	SWE	55.86	13.51
8275	Cen-0	FRA	49	0.5
8283	Dra3-1	SWE	55.76	14.12
8284	DraII-1	CZE	49.4112	16.2815
8285	DraIII-1	CZE	49.4112	16.2815
8290	En-1	GER	50	8.5
8297	Ge-0	SUI	46.5	6.08
8306	Hov4-1	SWE	56.1	13.74
8307	Hovdala-6	SWE	56.1	13.74
8311	In-0	AUT	47.5	11.5
8312	Is-0	GER	50.5	7.5
8325	Lip-0	POL	50	19.3
8326	Lis-1	SWE	56.0328	14.775
8334	Lu-1	SWE	55.71	13.2
8335	Lund	SWE	55.71	13.2
8337	Mir-0	ITA	44	12.37
8343	Na-1	FRA	47.5	1.5
8351	Ost-0	SWE	60.25	18.37
8353	Pa-1	ITA	38.07	13.22
8354	Per-1	RUS	58	56.3167
8357	Pla-0	ESP	41.5	2.25
8365	Rak-2	CZE	49	16
8366	Rd-0	GER	50.5	8.5
8369	Rev-1	SWE	55.6942	13.4504
8376	Sanna-2	SWE	62.69	18
8378	Sap-0	CZE	49.49	14.24
8386	Sr:5	SWE	58.9	11.2
8387	St-0	SWE	59	18
8419	Wil-1	LTU	54.6833	25.3167
8420	Kelsterbach-4	GER	50.0667	8.5333
8422	Fjä1-1	SWE	56.06	14.29
8423	Hov2-1	SWE	56.1	13.74
8424	Kas-2	IND	35	77
8424	Kas-2	IND	35	77
8426	Ull1-1	SWE	56.06	13.97
8427	Ull2-13	SWE	56.0648	13.9707
8428	Uod-2	AUT	48.3	14.45
8430	Lisse	NED	52.25	4.5667
8472	LP3413.41	USA	41.6862	-86.8513
8584	328ME059	USA	42.093	-86.359
9045	RMXF413.15	USA	42.039	-86.5154
9057	Vinslöv	SWE	56.1	13.9167
9058	Västervik	SWE	57.75	16.6333
9061	Dog-5	TUR	38.3011	42.2239
9063	Dog-7	TUR	38.3011	42.2239
9064	Dog-8	TUR	38.3011	42.2239
9066	Xan-2	AZE	38.6536	48.7992
9067	Xan-3	AZE	38.6536	48.7992
9069	Xan-5	AZE	38.6536	48.7992
9070	Xan-6	AZE	38.6536	48.7992
9073	Lerik1-2	AZE	38.7406	48.6131
9075	Lerik1-4	AZE	38.7406	48.6131
9078	Lerik1-7	AZE	38.7406	48.6131

Continued on next page

Appendix Table 1. Continued from previous page…

Ecotype ID	Name	Country	Latitude	Longitude
9079	Lerik2-1	AZE	38.7833	48.5517
9081	Lerik2-3	AZE	38.7833	48.5517
9082	Lerik2-4	AZE	38.7833	48.5517
9084	Lerik2-6	AZE	38.7833	48.5517
9085	Lerik2-7	AZE	38.7833	48.5517
9089	Nar-3	AZE	38.9522	48.925
9090	Nar-4	AZE	38.9522	48.925
9091	Nar-5	AZE	38.9522	48.925
9094	Istisu-4	AZE	38.9786	48.5594
9095	Istisu-5	AZE	38.9786	48.5594
9096	Istisu-6	AZE	38.9786	48.5594
9098	Istisu-8	AZE	38.9786	48.5594
9099	Istisu-9	AZE	38.9786	48.5594
9100	Lag1-2	GEO	41.8296	46.2831
9102	Lag1-4	GEO	41.8296	46.2831
9103	Lag1-5	GEO	41.8296	46.2831
9104	Lag1-6	GEO	41.8296	46.2831
9105	Lag1-7	GEO	41.8296	46.2831
9106	Lag1-8	GEO	41.8296	46.2831
9111	Lag2-4	GEO	41.8296	46.2831
9113	Lag2-6	GEO	41.8296	46.2831
9114	Lag2-7	GEO	41.8296	46.2831
9115	Lag2-10	GEO	41.8296	46.2831
9119	Bak-3	GEO	41.7942	43.4767
9120	Bak-4	GEO	41.7942	43.4767
9121	Bak-5	GEO	41.7942	43.4767
9124	Bak-9	GEO	41.7942	43.4767
9125	Geg-14	ARM	40.1408	44.8203
9128	Yeg-2	ARM	39.8692	45.3622
9130	Yeg-4	ARM	39.8692	45.3622
9131	Yeg-5	ARM	39.8692	45.3622
9133	Yeg-7	ARM	39.8692	45.3622
9134	Yeg-8	ARM	39.8692	45.3622
9298	Edinburgh-1	UK	55.9681	-3.21833
9312	Ullapool-8	UK	57.9	-5.1525
9314	Gol-2	UK	57.9672	-3.96722
9321	Ådal 1	SWE	62.8622	18.336
9323	Ådal 3	SWE	62.8622	18.336
9332	Bar 1	SWE	62.8698	18.381
9336	Bön 1	SWE	62.8794	18.4473
9339	Böt 1	SWE	57.7133	15.0689
9343	Dja 1	SWE	57.3089	18.1512
9352	Död 2	SWE	57.2608	16.3675
9353	Död 3	SWE	57.2608	16.3675
9356	Eden 17	SWE	62.8762	18.1746
9363	EdJ 2	SWE	62.9147	18.4045
9369	EkS 2	SWE	57.6781	14.9986
9370	EkS 3	SWE	57.6781	14.9986
9371	FäL 1	SWE	63.016	18.3175
9380	FlyA 3	SWE	55.7488	13.3742
9381	Fri 1	SWE	55.8106	14.2091
9382	Fri 2	SWE	55.8106	14.2091
9383	Fri 3	SWE	55.8106	14.2091
9386	Grön 12	SWE	62.806	18.1896
9388	Grön 14	SWE	62.806	18.1896
9390	Had-1	SWE	57.3263	15.8979
9391	Had-2	SWE	57.3263	15.8979
9392	Had-3	SWE	57.3263	15.8979
9394	Hag-2	SWE	56.5804	16.4063
9395	Hal-1	SWE	57.5089	15.0105
9399	Ham-1	SWE	55.4234	13.9905
9402	Hel-3	SWE	57.8765	14.8549
9404	HolA-1 1	SWE	55.7491	13.399
9405	HolA-1 2	SWE	55.7491	13.399
9407	HolA-2 2	SWE	55.7491	13.399
9408	Kal 1	SWE	56.047	13.9519
9409	Kia 1	SWE	56.0573	14.302
9412	Kor 3	SWE	57.2746	16.1494
9413	Kor 4	SWE	57.2746	16.1494
9416	Kru-3	SWE	57.7215	18.3837
9418	Kva 2	SWE	57.2164	18.154
9421	Lan 1	SWE	55.9745	14.3997
9427	Näs 2	SWE	62.8815	18.4055
9433	Nyl 13	SWE	62.9513	18.2763
9434	Öde 2	SWE	62.8959	18.3659
9436	Puk-1	SWE	56.1633	14.6806
9437	Puk-2	SWE	56.1633	14.6806
9442	Sim-1	SWE	55.5678	14.3398
9450	Spro 1	SWE	57.2545	18.2109
9451	Spro 2	SWE	57.2545	18.2109
9452	Spro 3	SWE	57.2545	18.2109
9453	Ste 2	SWE	57.8009	18.5162
9454	Ste 3	SWE	57.8009	18.5162
9455	Ste 4	SWE	57.8009	18.5162

Continued on next page

Appendix Table 1. Continued from previous page…

Ecotype ID	Name	Country	Latitude	Longitude
9470	Tur-4	SWE	57.6511	14.8043
9471	Ull-A-1	SWE	56.0648	13.9707
9476	VårA 1	SWE	55.5796	14.3336
9481	Yst-1	SWE	55.4242	13.8484
9503	11C1	UK	55.8877	-3.21072
9506	IP-Alo-0	POR	40.11	-7.47
9507	IP-Coa-0	POR	38.45	-7.5
9508	IP-Mos-1	POR	40.04	-7.11
9509	IP-Reg-0	POR	39.29	-7.4
9510	IP-Rei-0	POR	38.75	-7.59
9511	IP-Vav-0	POR	38.53	-8.02
9512	IP-Vid-1	POR	38.22	-7.84
9513	IP-Adc-5	ESP	38.77	-4.07
9514	IP-Adm-0	ESP	39.15	-4.54
9515	IP-Ala-0	ESP	39.72	-6.89
9516	IP-Ali-1	ESP	39.9	-5.09
9517	IP-All-0	ESP	42.19	-7.8
9518	IP-Alm-0	ESP	39.88	-0.36
9519	IP-Ang-0	ESP	41.94	2.64
9520	IP-Ara-4	ESP	41.7	-3.68
9521	IP-Bar-1	ESP	41.43	2.13
9522	IP-Bea-0	ESP	36.52	-5.27
9523	IP-Ben-0	ESP	38.37	-2.66
9524	IP-Ber-0	ESP	42.52	-0.56
9525	IP-Bis-0	ESP	42.49	0.54
9526	IP-Cab-3	ESP	41.54	2.39
9527	IP-Cad-0	ESP	40.37	-5.74
9528	IP-Cal-0	ESP	40.94	-1.37
9529	IP-Cap-1	ESP	36.97	-3.36
9530	IP-Car-1	ESP	38.25	-4.32
9531	IP-Cdc-3	ESP	41.21	-4.54
9532	IP-Cdo-0	ESP	42.23	-4.64
9533	IP-Cem-0	ESP	41.15	-4.32
9534	IP-Cmo-3	ESP	40.05	-4.65
9535	IP-Coc-1	ESP	42.31	3.19
9536	IP-Cor-0	ESP	40.83	-2
9537	IP-Cum-1	ESP	38.07	-6.66
9538	IP-Cur-4	ESP	43.12	-8.09
9539	IP-Deh-1	ESP	40.29	-6.67
9540	IP-Elb-0	ESP	41.81	2.34
9541	IP-Fue-2	ESP	38.26	-5.42
9542	IP-Fun-0	ESP	40.79	-4.05
9543	IP-Gra-0	ESP	36.77	-5.39
9544	IP-Gua-1	ESP	39.4	-5.33
9545	IP-Her-12	ESP	39.4	-5.78
9546	IP-Hom-4	ESP	40.82	-1.68
9547	IP-Hor-0	ESP	41.67	2.62
9548	IP-Hoy-0	ESP	40.4	-5
9549	IP-Hum-2	ESP	42.23	-3.69
9550	IP-Iso-4	ESP	43.05	-5.37
9551	IP-Jim-1	ESP	42.28	-5.92
9552	IP-Lab-7	ESP	40.87	-4.5
9553	IP-Ldd-0	ESP	41.58	-4.71
9554	IP-Lso-0	ESP	38.86	-3.16
9555	IP-Mar-1	ESP	39.58	-3.93
9556	IP-Men-2	ESP	39.66	-4.34
9557	IP-Moa-0	ESP	42.46	0.7
9558	IP-Moc-11	ESP	41.57	-5.64
9559	IP-Mon-5	ESP	38.06	-4.38
9560	IP-Mot-0	ESP	38.19	-6.24
9561	IP-Mun-0	ESP	40.71	-5.04
9562	IP-Mur-0	ESP	41.67	2
9563	IP-Nav-0	ESP	40.42	-4.65
9564	IP-Nog-17	ESP	40.45	-1.6
9565	IP-Orb-10	ESP	42.97	-1.23
9566	IP-Oso-0	ESP	42.44	-4.36
9567	IP-Pal-0	ESP	42.34	1.3
9568	IP-Pan-0	ESP	42.76	-0.23
9569	IP-Pds-1	ESP	42.87	-6.45
9570	IP-Pob-0	ESP	41.35	1.03
9571	IP-Pro-0	ESP	43.28	-6.01
9572	IP-Pue-0	ESP	42.75	-3.05
9573	IP-Rds-0	ESP	41.86	2.99
9574	IP-Rel-0	ESP	38.6	-2.7
9575	IP-Ren-6	ESP	42.77	-4.21
9576	IP-Rev-0	ESP	40.86	-4.11
9577	IP-Ria-0	ESP	42.34	2.17
9578	IP-Sac-0	ESP	42.13	-6.7
9579	IP-San-10	ESP	38.33	-3.51
9580	IP-Scm-0	ESP	38.68	-3.57
9581	IP-Sdv-3	ESP	42.84	-5.12
9582	IP-Ses-0	ESP	41.48	-1.63
9583	IP-Sne-0	ESP	37.09	-3.38
9584	IP-Stp-0	ESP	41.19	-3.58

Continued on next page

Appendix Table 1. Continued from previous page…

Ecotype ID	Name	Country	Latitude	Longitude
9585	IP-Svi-0	ESP	43.4	-7.39
9586	IP-Tam-0	ESP	41.03	-3.27
9587	IP-Tdc-0	ESP	41.5	-1.88
9588	IP-Tol-7	ESP	42.11	0.6
9589	IP-Tor-1	ESP	41.6	-2.83
9590	IP-Trs-0	ESP	43.37	-5.49
9591	IP-Vad-0	ESP	42.86	-3.59
9592	IP-Vae-2	ESP	42.1	-5.44
9593	IP-Vaz-0	ESP	42.26	-2.99
9594	IP-Vdm-0	ESP	42.04	1.01
9595	IP-Vdt-0	ESP	40.89	-5.5
9596	IP-Ver-5	ESP	41.95	-7.45
9597	IP-Vig-1	ESP	42.31	-2.53
9598	IP-Vim-0	ESP	41.88	-6.51
9599	IP-Vin-0	ESP	42.8	-5.77
9600	IP-Vis-0	ESP	39.85	-6.04
9601	IP-Voz-0	ESP	41.85	-1.88
9602	IP-Vpa-1	ESP	40.5	-3.96
9603	IP-Vpe-3	ESP	42.83	-4.72
9604	IP-Yan-1	ESP	42.1	-2.35
9605	IP-Zar-0	ESP	40.55	-4.19
9606	Aitba-1	MAR	31.48	-7.45
9607	Panik-1	RUS	53.05	52.15
9608	Karag-2	RUS	51.37	59.44
9609	Adam-1	RUS	51.41	59.98
9610	Lesno-4	RUS	53.04	51.96
9611	Lesno-1	RUS	53.04	51.9
9612	Lesno-2	RUS	53.04	51.94
9613	Balan-1	RUS	55.36	61.41
9614	Kurga-3	RUS	55.53	65.33
9615	Parti-1	RUS	52.99	52.16
9616	Krazo-1	RUS	53.06	51.96
9617	Karag-1	RUS	51.37	59.44
9618	Kurga-2	RUS	55.61	65.08
9619	Basta-1	RUS	51.84	79.48
9620	Basta-2	RUS	51.82	79.48
9621	Basta-3	RUS	51.84	79.46
9622	Bijisk-4	RUS	52.52	85.27
9623	Chaba-1	RUS	53.6	79.39
9624	Chaba-2	RUS	53.6	79.37
9625	Kolyv-2	RUS	51.31	82.59
9626	Kolyv-3	RUS	51.36	82.59
9627	Kolyv-5	RUS	51.32	82.55
9628	Kolyv-6	RUS	51.33	82.54
9629	K-oze-1	RUS	51.35	82.18
9630	K-oze-3	RUS	51.34	82.16
9631	Lebja-1	RUS	51.65	80.79
9632	Lebja-2	RUS	51.67	80.82
9633	Lebja-4	RUS	51.63	80.83
9634	Masl-1	RUS	54.13	81.31
9635	Nosov-1	RUS	51.87	80.6
9636	Noveg-1	RUS	51.75	80.82
9637	Noveg-2	RUS	51.77	80.85
9638	Noveg-3	RUS	51.73	80.86
9639	Panke-1	RUS	53.82	80.31
9640	Rakit-1	RUS	51.87	80.06
9641	Rakit-2	RUS	51.9	80.06
9642	Rakit-3	RUS	51.84	80.06
9643	Sever-1	RUS	52.1	79.31
9644	Zupan-1	CRO	45.07	18.72
9645	Gradi-1	CRO	45.17	18.7
9646	Aiell-1		#N/A	#N/A
9647	Basen-1	ITA	40.37	16.77
9648	Bisig-1	ITA	39.48	16.28
9649	Bivio-1	ITA	39.13	16.17
9650	Corig-1	ITA	39.6	16.51
9651	Filet-1	ITA	40.68	14.87
9652	Fondi-1	ITA	41.36	13.4
9653	Giffo-1	ITA	38.44	16.13
9654	Liri-1	ITA	41.41	13.77
9655	Marce-1	ITA	38.92	16.47
9656	Marti-1	ITA	40.64	17.31
9657	Melic-1	ITA	38.45	16.04
9658	Nicas-1	ITA	38.97	16.34
9659	Pigna-1	ITA	41.18	14.18
9660	Sarno-1	ITA	40.84	14.57
9661	Cimin-1	ITA	39.58	16.21
9662	Stilo-1	ITA	38.47	16.47
9663	Teano-1	ITA	41.33	14.09
9664	Mitterberg-1-179	ITA	46.36	11.28
9665	Mitterberg-1-180	ITA	46.36	11.28
9666	Mitterberg-1-182	ITA	46.36	11.28
9667	Mitterberg-1-183	ITA	46.36	11.28
9668	Mitterberg-2-184	ITA	46.37	11.28

Continued on next page

Appendix Table 1. Continued from previous page…

Ecotype ID	Name	Country	Latitude	Longitude
9669	Mitterberg-2-185	ITA	46.37	11.28
9670	Mitterberg-2-186	ITA	46.37	11.28
9671	Mitterberg-3-187	ITA	46.37	11.28
9672	Mitterberg-3-188	ITA	46.37	11.28
9673	Mitterberg-3-189	ITA	46.37	11.28
9674	Mitterberg-4-190	ITA	46.37	11.29
9675	Mitterberg-4-191	ITA	46.37	11.29
9676	Mitterberg-4-192	ITA	46.37	11.29
9677	Mitterberg-4-193	ITA	46.37	11.29
9678	Mitterberg-4-194	ITA	46.37	11.29
9679	Castelfed-1-195	ITA	46.34	11.29
9680	Castelfed-1-196	ITA	46.34	11.29
9681	Castelfed-1-197	ITA	46.34	11.29
9682	Castelfed-1-198	ITA	46.34	11.29
9683	Castelfed-1-199	ITA	46.34	11.29
9684	Castelfed-2-200	ITA	46.34	11.29
9685	Castelfed-2-201	ITA	46.34	11.29
9686	Castelfed-2-202	ITA	46.34	11.29
9687	Castelfed-2-203	ITA	46.34	11.29
9688	Castelfed-2-204	ITA	46.34	11.29
9689	Castelfed-3-205	ITA	46.34	11.29
9690	Castelfed-3-206	ITA	46.34	11.29
9691	Castelfed-3-207	ITA	46.34	11.29
9692	Castelfed-3-208	ITA	46.34	11.29
9693	Castelfed-3-209	ITA	46.34	11.29
9694	Castelfed-4-210	ITA	46.34	11.29
9695	Castelfed-4-211	ITA	46.34	11.29
9696	Castelfed-4-214	ITA	46.34	11.29
9697	Dolen-1	BUL	41.62	23.94
9698	Goced-1	BUL	41.57	23.85
9699	Kolar-1	BUL	41.37	23.14
9700	Dolna-1	BUL	42.32	23.1
9701	Ivano-1	BUL	43.7	25.91
9702	Kolar-2	BUL	41.38	23.14
9703	Melni-1	BUL	41.53	23.39
9704	Melni-2	BUL	41.53	23.39
9705	Choto-1	BUL	41.5	23.33
9706	Dospa-1	BUL	41.64	24.18
9707	Podvi-1	BUL	41.57	24.84
9708	Kardz-1	BUL	41.62	25.35
9709	Zerev-1	BUL	41.85	23.13
9710	Zerev-1	BUL	41.85	23.13
9711	Dolna-1	BUL	42.32	23.1
9712	Dolna-1	BUL	42.32	23.1
9713	Stara-1	BUL	42.49	25.61
9714	Grivo-1	BUL	41.84	25.75
9715	Krepo-1	BUL	41.99	25.57
9716	Leska-1	BUL	41.54	24.98
9717	Kardz-2	BUL	41.66	25.47
9718	Smolj-1	BUL	41.55	24.75
9719	Koren-1	BUL	41.83	25.69
9720	Malak-1	BUL	41.77	25.68
9721	Schip-1	BUL	42.72	25.33
9722	Groch-1	BUL	41.71	24.41
9723	Slavi-2	BUL	41.42	23.67
9724	Leska-1	BUL	41.54	24.98
9725	Epidauros-1	GRC	37.6	23.08
9726	Faneronemi-3	GRC	37.07	22.04
9727	Olympia-2	GRC	37.63	21.62
9728	Stiav-1	SVK	48.46	18.9
9729	Stiav-2	SVK	48.46	18.9
9730	Bela-1	SVK	48.47	18.94
9731	Stiav-3	SVK	48.46	18.9
9732	Halca-1	SVK	48.47	18.96
9733	Bela-2	SVK	48.47	18.94
9734	Bela-3	SVK	48.47	18.94
9735	Bela-4	SVK	48.47	18.94
9736	Teiu-2	ROU	44.69	25.17
9737	Ulies-1	ROU	45.95	22.62
9738	Bran-1	ROU	45.57	25.42
9739	Toc-1	ROU	46.01	22.33
9740	Mandr-1	ROU	46.16	21.43
9741	Orast-1	ROU	45.84	23.16
9742	Teiu-1	ROU	44.68	25.17
9743	Furni-1	ROU	45.14	25
9744	Iasi-1	ROU	47.16	27.59
9745	Sij 1/96	UZB	41.45	70.05
9746	Malii-1	SRB	43.71	22.3
9747	Zabar-1	SRB	44.38	21.22
9748	Zagub-1	SRB	44.23	21.71
9749	Knjas-1	SRB	43.54	22.29
9750	Sukov-1	SRB	43	22.65
9751	Ruma-1-25	SRB	44.91	19.99
9752	Brest-1	SRB	44	22.07

Continued on next page

Appendix Table 1. Continued from previous page…

Ecotype ID	Name	Country	Latitude	Longitude
9753	Ruma-1-27	SRB	44.91	19.99
9754	Sredn-1	SRB	44.66	21.37
9755	Vajug-1	SRB	44.56	22.56
9756	Staro-2	SRB	44.3	21.08
9757	Staro-1	SRB	44.3	21.08
9758	Altai-5	CHN	47.75	88.4
9759	Anz-0	IRN	37.47	49.47
9760	Baz-0	FRA	48.81	1.66
9761	Bik-1	LBN	33.92	35.7
9762	Etna-2	ITA	37.69	14.98
9764	Qar-8a	LBN	34.1	35.84
9766	Westkar-4	KGZ	42.26	74.16
9767	Had-1b	LBN	34.25	35.92
9768	Rü4-16	GER	48.57	9.16
9769	HE-1	GER	48.55	8.99
9770	KBG2-13	GER	48.53	9.01
9771	Pfn-N2.2-6	GER	48.56	9.11
9772	Höf-1	GER	48.41	8.85
9773	Obn-1	GER	48.52	8.92
9774	Alt-1	GER	48.59	9.22
9775	Berg-1	GER	48.41	8.79
9776	Fell3-7	GER	48.43	8.79
9777	Gn-1	GER	48.57	9.17
9778	Bach-7	GER	48.41	8.84
9779	Bai-10	GER	48.5	8.78
9780	Fell2-4	GER	48.43	8.79
9781	Kus2-2	GER	48.52	9.11
9782	Lu3-30	GER	48.53	9.09
9783	Tü-PK-7	GER	48.52	9.05
9784	Erg2-6	GER	48.5	8.8
9785	Ha-HBT1-2	GER	48.54	9.02
9786	Ha-P-13	GER	48.54	9.01
9787	HI-4	GER	48.5	9
9788	KBG1-14	GER	48.53	9.01
9789	Obh-13	GER	48.39	8.96
9790	Gn2-3	GER	48.58	9.18
9791	Haes-1	GER	48.6	9.2
9792	Lu4-2	GER	48.54	9.09
9793	Rü-N2	GER	48.57	9.16
9794	Tü-B1-2	GER	48.52	9.08
9795	Wank-2	GER	48.5	9.11
9796	Bach2-1	GER	48.41	8.84
9797	Ha-HBT2-10	GER	48.54	9.02
9798	Ha-P2-1	GER	48.54	9.01
9799	Hart-2	GER	48.39	8.85
9800	Ha-S-B	GER	48.54	9.01
9801	Ha-SP-2	GER	48.54	9.01
9802	Kus3-1	GER	48.51	9.11
9803	Müh-2	GER	48.42	8.76
9804	Obe1-15	GER	48.45	8.87
9805	Pfn-10	GER	48.54	9.09
9806	Rü-2	GER	48.56	9.16
9807	Schl-7	GER	48.6	9.22
9808	Tü-B2-3	GER	48.52	9.08
9809	Tü-KB-6	GER	48.52	9.05
9810	Tü-KS-7	GER	48.53	9.07
9811	Tü-NK-12	GER	48.52	9.05
9812	Tü-W1	GER	48.52	9.03
9813	BI-4	GER	48.4	8.77
9814	Fell1-10	GER	48.42	8.79
9815	Ha-HBT3-11	GER	48.54	9.02
9816	Tü-WH	GER	48.55	9.06
9817	Ace-0	ESP	39.84	-6.6
9818	Aln-30	ESP	41.14	-0.25
9819	Amu-0	ESP	42.35	-3.03
9820	Are-0	ESP	41	-4.71
9821	Aru-0	ESP	41.81	2.49
9822	Aul-0	ESP	40.52	-4.02
9823	Bae-0	ESP	43.34	-5.84
9824	Bes-5	ESP	42.91	-4.91
9825	Boa-0	ESP	40.4	-3.88
9826	Bor-0	ESP	42.49	-6.71
9827	Bos-0	ESP	42.78	0.69
9828	Bra-0	ESP	42.5	-6.15
9829	Bur-0	ESP	40.43	-4.75
9830	Bus-0	ESP	36.97	-3.28
9831	Cas-0	ESP	38.54	-3.39
9832	Cat-0	ESP	40.54	-3.69
9833	Cha-0	ESP	40.38	-4.21
9834	Cho-0	ESP	40.51	-3.9
9835	Cir-0	ESP	40.61	-6.57
9836	Cod-0	ESP	41.25	-1.32
9837	Con-0	ESP	37.94	-5.6
9838	Cot-0	ESP	41.83	-5.38

Continued on next page

Appendix Table 1. Continued from previous page…

Ecotype ID	Name	Country	Latitude	Longitude
9839	Coy-0	ESP	40.44	-4.27
9840	Dar-0	ESP	41.13	-1.43
9841	Ees-0	ESP	40.59	-4.15
9842	Ele-0	ESP	39.31	-3.89
9843	Elp-0	ESP	40.53	-3.92
9844	Esn-2	ESP	42.27	0.19
9845	Evs-0	ESP	40.48	-3.96
9846	Ezc-2	ESP	42.31	-3.02
9847	Fel-2	ESP	43.31	-5.7
9848	Glo-1	ESP	40.11	-5.77
9849	Gud-3	ESP	40.65	-4.11
9850	Hec-0	ESP	42.86	-0.7
9851	Hue-3	ESP	42.96	-6.1
9852	Ini-0	ESP	40.46	-3.75
9853	Lac-0	ESP	43.33	-5.91
9854	Laf-1	ESP	43.36	-5.88
9855	Lam-0	ESP	40.57	-3.89
9856	Lch-0	ESP	40.51	-4
9857	Leg-0	ESP	40.33	-3.8
9858	Loz-0	ESP	40.98	-3.8
9859	Lro-0	ESP	40.5	-3.88
9860	Lum-0	ESP	42.24	-2.62
9861	Mac-0	ESP	40.72	-3.21
9862	Mad-0	ESP	40.45	-3.67
9863	Man-0	ESP	43.33	-5.87
9864	Mat-0	ESP	41.76	2.69
9865	Mdc-0	ESP	38.88	-3.53
9866	Mdd-0	ESP	41.89	-2.79
9867	Mie-1	ESP	40.94	-3.22
9868	Moe-0	ESP	41.78	2.37
9869	Moj-0	ESP	36.76	-5.28
9870	Moz-0	ESP	41.91	0.17
9871	Nac-0	ESP	40.75	-3.99
9872	Nag-0	ESP	40.49	-4.11
9873	Ndc-0	ESP	37.94	-5.45
9874	Oja-0	ESP	42.34	-3
9875	Ovi-1	ESP	43.38	-5.87
9876	Pad-0	ESP	41.34	0.99
9877	Pdl-0	ESP	43.02	-5.6
9878	Pee-0	ESP	40.78	-3.62
9879	Per-0	ESP	37.6	-1.12
9880	Pib-1	ESP	42.72	-3.44
9881	Pie-0	ESP	40.46	-5.32
9882	Pil-0	ESP	40.46	-4.26
9883	Piq-0	ESP	42.1	-2.56
9884	Pos-1	ESP	42.25	-3.04
9885	Prd-0	ESP	41.14	-3.68
9886	Pru-0	ESP	42.38	1.73
9887	Pun-0	ESP	40.4	-4.77
9888	Pva-1	ESP	40.93	-3.31
9889	Ras-0	ESP	40.86	-3.87
9890	Rib-1	ESP	43.16	-5.07
9891	Sal-0	ESP	41.93	2.92
9892	Sam-0	ESP	42.68	-6.96
9893	Sca-0	ESP	37.96	-5.37
9894	Sen-0	ESP	42.59	0.76
9895	Sfb-6	ESP	41.78	2.57
9896	Slc-3	ESP	38.47	-3.74
9897	Smt-1	ESP	40.95	-5.63
9898	Som-0	ESP	41.14	-3.58
9899	Tau-0	ESP	42.54	0.84
9900	Tri-0	ESP	37.38	-6.01
9901	Urd-1	ESP	42.27	-2.98
9902	Usa-0	ESP	40.71	-3.24
9903	Val-0	ESP	42.31	-3.1
9904	Vas-0	ESP	40.95	-3.31
9905	Ven-0	ESP	40.76	-4.01
9906	Mah-6	ESP	40	4.25
9907	ENC-2-1	FRA	50.86	3.6
9908	ESP-1-11	FRA	50.72	3.47
9909	GEN-8	FRA	50.59	3.3
9910	BRI-2	FRA	50.68	3.52
9911	ARGE-1-15	FRA	47.16	4.28
9912	CIRY-13	FRA	46.67	4.55
9913	CON-7	FRA	47.24	4.43
9914	IST-29	FRA	47.58	5.33
9915	MAR-4-16	FRA	47.45	3.94
9916	MOL-1	FRA	47.1	4.22
9917	RAD-21	FRA	46.69	4.34
9918	SAUL-24	FRA	47.43	5.21
9919	BRE-14	FRA	48.85	4.45
9920	DIR-9	FRA	48.54	4.32
9921	FOR-23	FRA	48.57	4.41
9922	MIL-2	FRA	48.52	4.7

Continued on next page

Appendix Table 1. Continued from previous page…

Ecotype ID	Name	Country	Latitude	Longitude
9923	PLO-1	FRA	48.58	4.46
9924	PLY-20	FRA	48.59	4.24
9925	RUM-20	FRA	48.91	4.52
9926	TRE-1	FRA	48.86	4.1
9927	ARR-17	FRA	44.05	3.69
9928	BEZ-9	FRA	44.12	3.77
9929	ISS-20	FRA	43.92	3.71
9930	LEC-25	FRA	43.91	4.14
9931	MOU2-25	FRA	43.98	4.31
9932	NOZ-6	FRA	44.12	4.33
9933	VED-10	FRA	43.74	3.89
9934	QUI-8	FRA	44.07	4.08
9935	BAU-15	FRA	50.6	2.93
9936	LCL-16	FRA	50.47	3.46
9937	CATS-6	FRA	50.79	2.69
9938	WAV-8	FRA	50.65	2.99
9939	Aitba-2	MAR	31.48	-7.45
9940	Toufl-1	MAR	31.47	-7.42
9941	Fei-0	POR	40.92	-8.54
9942	Agu-1	ESP	41.32	-1.34
9943	Cdm-0	ESP	39.73	-5.74
9944	Don-0	ESP	36.83	-6.36
9945	Leo-1	ESP	41.8	-3.11
9946	Mer-6	ESP	38.92	-6.34
9947	Ped-0	ESP	40.74	-3.9
9948	Pra-6	ESP	41.05	-3.54
9949	Qui-0	ESP	42.69	-6.93
9950	Vie-0	ESP	42.63	0.76
9951	Kly-1	RUS	51.34	82.57
9952	Kly-4	RUS	51.32	82.55
9953	Koz-2	RUS	51.33	82.19
9954	Leb-3	RUS	51.65	80.82
9955	Stepn-2	RUS	54.09	60.46
9956	Stepn-1	RUS	54.06	60.48
9957	Borsk-2	RUS	53.04	51.75
9958	Shigu-1	RUS	53.33	49.48
9959	Shigu-2	RUS	53.33	49.48
9960	Kidr-1	RUS	51.31	57.56
9961	Krazo-2	RUS	53.09	52
9962	Galdo-1	ITA	40.57	15.32
9963	Lago-1	ITA	39.18	16.26
9964	Mammo-1	ITA	38.36	16.23
9965	Mammo-2	ITA	38.38	16.22
9966	Monte-1	ITA	40.28	15.65
9967	Moran-1	ITA	39.83	16.17
9968	Timpo-1	ITA	39.27	16.27
9969	Valsi-1	ITA	40.18	16.45
9970	Altenb-2	ITA	46.37	11.24
9971	Bozen-1.1	ITA	46.51	11.33
9972	Bozen-1.2	ITA	46.51	11.33
9973	Mitterberg-1-181	ITA	46.36	11.28
9974	Castelfed-4-212	ITA	46.34	11.29
9975	Castelfed-4-213	ITA	46.34	11.29
9976	Rovero-1	ITA	46.25	11.17
9977	Vezzano-2.1	ITA	46.63	10.82
9978	Vezzano-2.2	ITA	46.63	10.82
9979	Voeran-1	ITA	46.36	11.23
9980	Angel-1	ITA	38.62	16.17
9981	Angit-1	ITA	38.76	16.24
9982	Apost-1	ITA	39.01	16.47
9983	Ciste-1	ITA	41.62	12.87
9984	Ciste-2	ITA	41.62	12.87
9985	Slavi-1	BUL	41.43	23.65
9986	Jablo-1	BUL	41.59	25.2
9987	Lecho-1	BUL	41.43	23.5
9988	Bak-2	GEO	41.79	43.48
9989	Bak-7	GEO	41.79	43.48
9990	Lag2.2	GEO	41.83	46.28
9991	Vash-1	GEO	41.24	46.37
9992	Dog-4	TUR	38.3	42.22
9993	Nemrut-1	TUR	38.64	42.24
9994	Ey15-2	GER	48.43	8.77
9995	HKT2.4	GER	48.14	9.4
9996	Nie1-2	GER	48.52	8.8
9997	Rue3.1-31	GER	48.56	9.16
9998	Star-8	GER	48.43	8.82
9999	TueSB30-3	GER	48.53	9.06
10000	Tuescha-9	GER	48.53	9.05
10001	TueV-13	GER	48.52	9.05
10002	TueWal-2	GER	48.53	9.04
10003	WalHaesB4	GER	48.6	9.19
10004	Bolin-1	ROM	44.46	25.74
10005	Copac-1	ROM	46.11	21.95
10006	Kastel-1	UKR	44.64	34.38

Continued on next page

Appendix Table 1. Continued from previous page…

Ecotype ID	Name	Country	Latitude	Longitude
10007	Koch-1	UKR	50.36	29.32
10008	Sij-1	UZB	41.45	70.05
10009	Sij-2	UZB	41.45	70.05
10010	Sij-4	UZB	41.45	70.05
10011	Yeg-1	ARM	39.87	45.36
10012	Istisu-1	AZE	38.98	48.56
10013	Lerik1-3	AZE	38.74	48.61
10014	Xan-1	AZE	38.65	48.8
10015	Sha	AFG	37.29	71.3
10016	Del-10	SRV	44.94	21.18
10017	Petro-1	SRV	44.34	21.46
10018	Dobra-1	SRB	44.84	20.16
10019	KZ10	KAZ	48.67	54.93
10020	Jl-2	CZE	49.17	16.5
10021	Hl-0	GER	52.14	9.38
10022	Uk-3	GER	48.03	7.77
10023	Strand-1			
10024	Tnz-1	TZA		
10025	Bsch-2	GER	50.01	8.67
10026	Bg-5	USA	47.62	-122.35
100000	Wil-1	LTU	54.6833	25.3167
CS28163	Co-2	POR		
CS28072	Bs-5	SUI		
CS78198	Bch-3	GER		
CS78200	Bch-4	GER		
CS2806	Be-1	GER		
CS28068	Bg-1	USA		
CS28075	Bg-9	USA		
CS22344	Bg-4	USA		
CS28073	Bg-6	USA		
CS28074	Bg-7	USA		
CS78195	Bla-11	ESP		
CS28087	Bla-12	ESP		
CS28088	Bla-14	ESP		
CS28080	Bla-2	ESP		
CS28081	Bla-3	ESP		
CS28083	Bla-5	ESP		
CS28090	Bla-9	ESP		
CS78410	Blh-1	CZE		
CS28097	Bs-2	SUI		
CS28110	Bu-11	GER		
CS28111	Bu-13	GER		
CS78209	Chi-1	RUS		
CS28146	CIBC10	UK		
CS28163	Co-2	POR		
CS78212	Co-3	POR		
CS28165	Co-4	POR		
CS28214	Dra-2	CZE		
CS78224	Ei-4	GER		
CS28225	Ei-5	GER		
CS28226	Ei-6	GER		
CS28274	Ga-2	GER		

Appendix Table 2. *Arabidosis thaliana* primers used in this study

Sequence	Target gene/region	Primer name	Orientation	Primer purpose
CTCTCCCTTTCTTCGGCTTT	AT1G14385	G-15043	F	amplifying gene fragments/5.8 Kb chunk (1) for sanger sequencing
AGCCTTTCAAAGCATTTCCA	AT1G14385	G-11927	F	amplifying gene fragments/4.7 Kb chunk (2) for sanger sequencing
TGGTCCGGTTCTCTTTTCTT	BORDER AT1G14385-AT1G14390	G-23251	F	for sequencing the ACD6 gene fragments
ATGTGGCTACCTGCTTTGCT	BORDER AT1G14385-AT1G14390	G-23250	F	for sequencing the ACD6 gene fragments
GTGACCTGACCACCACTCCT	BORDER AT1G14385-AT1G14390	G-12560	F	for sequencing the ACD6 gene fragments
GCACATGTTGCTTTGGTGAC	AT1G14390	G-12674	F	for sequencing the ACD6 gene fragments
ACGGGAATTTCCTCCTCAAG	AT1G14390	G-11929	F	for sequencing the ACD6 gene fragments
GATGTGGACGGGAATACACC	AT1G14390	G-12091	F	for sequencing the ACD6 gene fragments
GAGTTTGTAGCCTATTCAAAGG	BORDER AT1gG14390-AT1G14400	G-14062	F	amplifying gene fragments/6.5 Kb chunk (3) for sanger sequencing
TGTTGCATCCGACATCATTT	BORDER AT1gG14390-AT1G14400	G-14341	F	for sequencing the ACD6 gene fragments
TCCTGGAGGATCAACGTAGC	AT1G14400	G-14412	F	for sequencing the ACD6 gene fragments
CAAAACCGTTTCTTAGGATGGA	AT1G14400	G-14413	R	amplifying gene fragments/5.8 Kb or 4.7 Kb chunks (1) (2) for sanger sequencing
ATCACTGCAATTGCCCATGT	AT1G14400	G-16287	F	amplifying gene fragments/3.6 Kb chunk (4) (5) for sanger sequencing
CGGTTTAGTGGATACCAGTTTACT	AT1G14400	G-12549	R	amplifying gene fragments/6.5 Kb chunk (3) for sanger sequencing
GTGCACTTTGGAAATCAAGC	AT1G14400	G-13166	F	for sequencing the ACD6 gene fragments
CTTAAACCCCGCCTCAACTT	AT1G14400	G-14342	R	for sequencing the ACD6 gene fragments
CTTAAACCCCGCCTCAACTT	AT1G14400	G-12241	F	for sequencing the ACD6 gene fragments
CAAACAGGGTCACGTTGTCA	AT1G14400	G-13168	F	for sequencing the ACD6 gene fragments
CGGGTCATCTTTTAATCTCTGG	AT1G14400	G-12070	F	for sequencing the ACD6 gene fragments
TGTGTGTGGTGGATTGCTTT	AT1G14400	G-12069	R	for sequencing the ACD6 gene fragments
AGACAAGAACGACCTTTGGC	AT1G14400	G-13167	R	for sequencing the ACD6 gene fragments
ATGACTCGAGACATTAACGACTTT	AT1G14400	G-12548	F	for sequencing the ACD6 gene fragments
GGTTTGCGATGGACAGTTCT	AT1G14400	G-12243	F	for sequencing the ACD6 gene fragments
TCATAGGGTGGCCACAAATT	AT1G14400	G-13169	R	for sequencing the ACD6 gene fragments
CACCTATGCAAAACCAACCA	AT1G14400	G-12072	F	for sequencing the ACD6 gene fragments
AGGAAAAACTATTCTACTTGATTCTTG	AT1G14400	G-12071	R	for sequencing the ACD6 gene fragments
AACATGTCTCACAATATAACTTGTCC	AT1G14400	G-12501	F	for sequencing the ACD6 gene fragments

Continued on next page

Appendix Table 2. Continued from previous page…

Sequence	Target gene/region	Primer name	Orientation	Primer purpose
TGGCTCTGAACGATTGTCTAAA	AT1G14400	G-12017	F	for sequencing the ACD6 gene fragments
TTTTTATGGCTCTGAACGATTG	AT1G14400	G-12244	R	for sequencing the ACD6 gene fragments
AAATCTTTTAATTGTAAAGTTGTTTGG	AT1G14400	G-12073	F	for sequencing the ACD6 gene fragments
TTTAACAAAACGCGCAAGTG	AT1G14400	G-12016	R	for sequencing the ACD6 gene fragments
AATTAGATAAAGATATTTATGATTT	AT1G14400	G-19971	R	for sequencing the ACD6 gene fragments
TTTGACCCTGGTAACAAATTGTTTTACCAG	AT1G14400	G-16353	R	for sequencing the ACD6 gene fragments
ATTTCTCTCACAGCGGAGGA	AT1G14400	G-12245	F	for sequencing the ACD6 gene fragments
AGATGTCGAGATGACTCCGG	AT1G14400	G-13171	R	for sequencing the ACD6 gene fragments
CCAATGGAACGTGTCAAGAG	AT1G14400	G-12075	F	for sequencing the ACD6 gene fragments
GCTAAATGGGGTCATCTGGA	AT1G14400	G-12074	R	for sequencing the ACD6 gene fragments
GCTACCTGTCTGGTGAACGC	AT1G14400	G-13300	R	for sequencing the ACD6 gene fragments
AGCCGTAGACGCTGGAAATA	AT1G14400	G-12247	F	for sequencing the ACD6 gene fragments
GTAAAACCAGCTTGGGACGA	AT1G14400	G-12246	R	for sequencing the ACD6 gene fragments
TCATACGGAGCATCCATTGGG	AT1G14400	G-12688	R	for sequencing the ACD6 gene fragments
CCGATCAACAAAGGGTGTTT	AT1G14401	G-12077	F	for sequencing the ACD6 gene fragments
TCTTTTCCAATTCATTCGGC	AT1G14402	G-12076	R	for sequencing the ACD6 gene fragments
AAAACGTTGTCCAGCTTCAAA	AT1G14403	G-12335	F	for sequencing the ACD6 gene fragments
GATGTGGACGGGAATACACC	AT1G14404	G-12019	F	for sequencing the ACD6 gene fragments
CGAAACAAAAGCGGCTTAAG	AT1G14405	G-12248	R	for sequencing the ACD6 gene fragments
ACGTTTGCTGCAGGCTTTAC	AT1G14406	G-12581	F	for sequencing the ACD6 gene fragments
TGGGTATATCAGCGATAGCAAAAA	AT1G14407	G-13176	F	for sequencing the ACD6 gene fragments
TTTGGCCACTAACCCAACTC	AT1G14408	G-12018	R	for sequencing the ACD6 gene fragments
TGGCCACTAACCCAACTCTC	AT1G14409	G-12249	F	for sequencing the ACD6 gene fragments
CTCTTATTTGGGCGCAGTTA	AT1G14410	G-12079	F	for sequencing the ACD6 gene fragments
CAACACCGTAGAGCACACCA	AT1G14411	G-13177	R	for sequencing the ACD6 gene fragments
AGCCGTAGACGCTGGAAATA	AT1G14400	G-12247	F	for sequencing the ACD6 gene fragments
AGAAGAAACATATCCTTTGAA	AT1G14400	G-18613	R	for sequencing the ACD6 gene fragments
GTTTGCTTTTGCCTTTGGAG	AT1G14412	G-12023	F	amplifying gene fragments/ 4.4 Kb chunk for sanger sequencing
AACTCAAGACCTCCCGCTTA	AT1G14413	G-12254	R	amplifying gene fragments/3.6 Kb chunk for sanger sequencing
ATACAGAATTGGGGTGGCAA	AT1G14414	G-12022	R	amplifying gene fragments/4.3 Kb chunk for sanger sequencing
ACTGCACCCGTTTCTCATTC	AT1G14415	G-12026	R	amplifying gene fragments/4.4 Kb chunk for sanger sequencing
GATAAATGTTCGTCGTATCGCCCTCTCTCTTTTGTATTCC	AT1G58602.2	G-33594	F	for constructing amiRNA- I miR-s
GAGGGCGATACGACGAACATTTATCAAAGAGAATCAATGA	AT1G58602.2	G-33610	R	for constructing amiRNA- II miR-a
GAGGACGATACGACGTACATTTTTCACAGGTCGTGATATG	AT1G58602.2	G-33647	F	for constructing amiRNA- III miR*s
GAAAAATGTACGTCGTATCGTCCTCTACATATATATTCCT	AT1G58602.2	G-33676	R	for constructing amiRNA- IV miR*a

Continued on next page

Appendix Table 2. Continued from previous page…

Sequence	Target gene/region	Primer name	Orientation	Primer purpose
GATCATAAATCTGGGTAGTTCATTCTCTCTTTTGTATTCC	AT1G58410.1	G-33653	F	for constructing amiRNA- I miR-s
GAATGAACTACCCAGATTTATGATCAAAGAGAATCAATGA	AT1G58410.1	G-33663	R	for constructing amiRNA- II miR-a
GAATAAACTACCCAGTTTTATGTTCACAGGTCGTGATATG	AT1G58410.1	G-33674	F	for constructing amiRNA- III miR*s
GAACATAAAACTGGGTAGTTTATTCTACATATATATTCCT	AT1G58410.1	G-33606	R	for constructing amiRNA- IV miR*a
GATAATTCTTAGAGCAAAACCGGTCTCTCTTTTGTATTCC	AT1G62630.1, AT1G63350.1, AT1G63360.1	G-38124	F	for constructing amiRNA- I miR-s
GACCGGTTTTGCTCTAAGAATTATCAAAGAGAATCAATGA	AT1G62630.1, AT1G63350.1, AT1G63360.1	G-38125	R	for constructing amiRNA- II miR-a
GACCAGTTTTGCTCTTAGAATTTTCACAGGTCGTGATATG	AT1G62630.1, AT1G63350.1 ,AT1G63360.1	G-38126	F	for constructing amiRNA- III miR*s
GAAAATTCTAAGAGCAAAACTGGTCTACATATATATTCCT	AT1G62630.1, AT1G63350.1, AT1G63360.1	G-38127	R	for constructing amiRNA- IV miR*a
GATACGTTTACAAAGTTCAGCTCTCTCTCTTTTGTATTCC	AT3G46530.1, AT3G46710.1, AT3G46730.1	G-38140	F	for constructing amiRNA- I miR-s
GAGAGCTGAACTTTGTAAACGTATCAAAGAGAATCAATGA	AT3G46530.1, AT3G46710.1, AT3G46730.1	G-38141	R	for constructing amiRNA- II miR-a
GAGAACTGAACTTTGAAAACGTTTCACAGGTCGTGATATG	AT3G46530.1, AT3G46710.1, AT3G46730.1	G-38142	F	for constructing amiRNA- III miR*s
GAAACGTTTTCAAAGTTCAGTTCTCTACATATATATTCCT	AT3G46530.1, AT3G46710.1, AT3G46730.1	G-38143	R	for constructing amiRNA- IV miR*a
GATACGTTTACAAAGTTGGGCTGTCTCTCTTTTGTATTCC	AT3G46530.1, AT3G46710.1, AT3G46730.1	G-38132	F	for constructing amiRNA- I miR-s
GACAGCCCAACTTTGTAAACGTATCAAAGAGAATCAATGA	AT3G46530.1, AT3G46710.1, AT3G46730.1	G-38133	R	for constructing amiRNA- II miR-a
GACAACCCAACTTTGAAAACGTTTCACAGGTCGTGATATG	AT3G46530.1, AT3G46710.1, AT3G46730.1	G-38134	F	for constructing amiRNA- III miR*s

Continued on next page

Appendix Table 2. Continued from previous page…

Sequence	Target gene/region	Primer name	Orientation	Primer purpose
GAAACGTTTTCAAAGTTGGGTTGTCTACATATATATTCCT	AT3G46530.1, AT3G46710.1, AT3G46730.1	G-38135	R	for constructing amiRNA- IV miR*a
GATTTAAGCACTCGAACTAGCTTTCTCTCTTTTGTATTCC	AT3G46530.1, AT3G46710.1, AT3G46730.1	G-38136	F	for constructing amiRNA- I miR-s
GAAAGCTAGTTCGAGTGCTTAAATCAAAGAGAATCAATGA	AT3G46530.1, AT3G46710.1, AT3G46730.1	G-38137	R	for constructing amiRNA- II miR-a
GAAAACTAGTTCGAGAGCTTAATTCACAGGTCGTGATATG	AT3G46530.1, AT3G46710.1, AT3G46730.1	G-38138	F	for constructing amiRNA- III miR*s
GAATTAAGCTCTCGAACTAGTTTTCTACATATATATTCCT	AT3G46530.1, AT3G46710.1, AT3G46730.1	G-38139	R	for constructing amiRNA- IV miR*a
GATTAGTTTGTTCGAAACGTCTCTCTCTCTTTTGTATTCC	AT5G58120.1	G-38154	F	for constructing amiRNA- I miR-s
GAGAGACGTTTCGAACAAACTAATCAAAGAGAATCAATGA	AT5G58120.1	G-38155	R	for constructing amiRNA- II miR-a
GAGAAACGTTTCGAAGAAACTATTCACAGGTCGTGATATG	AT5G58120.1	G-38156	F	for constructing amiRNA- III miR*s
GAATAGTTTCTTCGAAACGTTTCTCTACATATATATTCCT	AT5G58120.1	G-38157	R	for constructing amiRNA- IV miR*a
GATTTAGATAATAGCCGGAGCGATCTCTCTTTTGTATTCC	AT5G58120.1	G-38148	F	for constructing amiRNA- I miR-s
GATCGCTCCGGCTATTATCTAAATCAAAGAGAATCAATGA	AT5G58120.1	G-38149	R	for constructing amiRNA- II miR-a
GATCACTCCGGCTATAATCTAATTCACAGGTCGTGATATG	AT5G58120.1	G-38150	F	for constructing amiRNA- III miR*s
GAATTAGATTATAGCCGGAGTGATCTACATATATATTCCT	AT5G58120.1	G-38151	R	for constructing amiRNA- IV miR*a
GATCTACGCAATATACCTTCCGATCTCTCTTTTGTATTCC	AT5G58120.1	G-38144	F	for constructing amiRNA- I miR-s
GATCGGAAGGTATATTGCGTAGATCAAAGAGAATCAATGA	AT5G58120.1	G-38145	R	for constructing amiRNA- II miR-a
GATCAGAAGGTATATAGCGTAGTTCACAGGTCGTGATATG	AT5G58120.1	G-38146	F	for constructing amiRNA- III miR*s
GAACTACGCTATATACCTTCTGATCTACATATATATTCCT	AT5G58120.1	G-38147	R	for constructing amiRNA- IV miR*a
GATAGATGACAAGTTGACGTCGATCTCTCTTTTGTATTCC	At4g16860, At4g16890, At4g16900, At4g16920, At4g16940, At4g16950, At4g16960	G-34325	F	for constructing amiRNA- I miR-s
GATCGACGTCAACTTGTCATCTATCAAAGAGAATCAATGA	At4g16860, At4g16890, At4g16900, At4g16920, At4g16940, At4g16950, At4g16960	G-34326	R	for constructing amiRNA- II miR-a
GATCAACGTCAACTTCTCATCTTTCACAGGTCGTGATATG	At4g16860, At4g16890, At4g16900, At4g16920, At4g16940, At4g16950, At4g16960	G-34327	F	for constructing amiRNA- III miR*s

Continued on next page

Appendix Table 2. Continued from previous page…

Sequence	Target gene/region	Primer name	Orientation	Primer purpose
GAAAGATGAGAAGTTGACGTTGATCTACATATATATTCCT	AT4G16860, AT4G16890, AT4G16900, AT4G16920, AT4G16940, AT4G16950, AT4G16960	G-34328	R	for constructing amiRNA- IV miR*a
GATTATTTAACCTATCGTCGCAGTCTCTCTTTTGTATTCC	AT4G16860, AT4G16920	G-34333	F	for constructing amiRNA- I miR-s
GACTGCGACGATAGGTTAAATAATCAAAGAGAATCAATGA	AT4G16860, AT4G16920	G-34334	R	for constructing amiRNA- II miR-a
GACTACGACGATAGGATAAATATTCACAGGTCGTGATATG	AT4G16860, AT4G16920	G-34335	F	for constructing amiRNA- III miR*s
GAATATTTATCCTATCGTCGTAGTCTACATATATATTCCT	AT4G16860, AT4G16920	G-34336	R	for constructing amiRNA- IV miR*a
GATATCTATTAATAGCCCCCCCGTCTCTCTTTTGTATTCC	AT4G16860, AT4G16920	G-34337	F	for constructing amiRNA- I miR-s
GACGGGGGGGCTATTAATAGATATCAAAGAGAATCAATGA	AT4G16860, AT4G16920	G-34338	R	for constructing amiRNA- II miR-a
GACGAGGGGGCTATTTATAGATTTCACAGGTCGTGATATG	AT4G16860, AT4G16920	G-34339	F	for constructing amiRNA- III miR*s
GAAATCTATAAATAGCCCCCTCGTCTACATATATATTCCT	AT4G16860, AT4G16920	G-34340	R	for constructing amiRNA- IV miR*a
GATGTCCGCTACAATTCGGCCGTTCTCTCTTTTGTATTCC	AT4G16860, AT4G16920	G-34341	F	for constructing amiRNA- I miR-s
GAACGGCCGAATTGTAGCGGACATCAAAGAGAATCAATGA	AT4G16860, AT4G16920	G-34342	R	for constructing amiRNA- II miR-a
GAACAGCCGAATTGTTGCGGACTTCACAGGTCGTGATATG	AT4G16860, AT4G16920	G-34343	F	for constructing amiRNA- III miR*s
GAAGTCCGCAACAATTCGGCTGTTCTACATATATATTCCT	AT4G16860, AT4G16920	G-34344	R	for constructing amiRNA- IV miR*a
GATGAATGGCAAACGTATTGCACTCTCTCTTTTGTATTCC	AT4G16860, AT4G16920	G-34345	F	for constructing amiRNA- I miR-s
GAGTGCAATACGTTTGCCATTCATCAAAGAGAATCAATGA	AT4G16860, AT4G16920	G-34346	R	for constructing amiRNA- II miR-a
GAGTACAATACGTTTCCCATTCTTCACAGGTCGTGATATG	AT4G16860, AT4G16920	G-34347	F	for constructing amiRNA- III miR*s
GAAGAATGGGAAACGTATTGTACTCTACATATATATTCCT	AT4G16860, AT4G16920	G-34348	R	for constructing amiRNA- IV miR*a

Continued on next page

Appendix Table 2. Continued from previous page…

Sequence	Target gene/region	Primer name	Orientation	Primer purpose
GATACGTTTACAAAGTTGGGCTGTCTCTCTTTTGTATTCC	AT3G46530.1, AT3G46710.1, AT3G46730.1	G-38132	F	for constructing amiRNA- I miR-s
GACAGCCCAACTTTGTAAACGTATCAAAGAGAATCAATGA	AT3G46530.1, AT3G46710.1, AT3G46730.1	G-38133	R	for constructing amiRNA- II miR-a
GACAACCCAACTTTGAAAACGTTTCACAGGTCGTGATATG	AT3G46530.1, AT3G46710.1, AT3G46730.1	G-38134	F	for constructing amiRNA- III miR*s
GAAACGTTTTCAAAGTTGGGTTGTCTACATATATATTCCT	AT3G46530.1, AT3G46710.1, AT3G46730.1	G-38135	R	for constructing amiRNA- IV miR*a
GATTTAAGCACTCGAACTAGCTTTCTCTCTTTTGTATTCC	AT3G46530.1, AT3G46710.1, AT3G46730.1	G-38136	F	for constructing amiRNA- I miR-s
GAAAGCTAGTTCGAGTGCTTAAATCAAAGAGAATCAATGA	AT3G46530.1, AT3G46710.1, AT3G46730.1	G-38137	R	for constructing amiRNA- II miR-a
GAAAACTAGTTCGAGAGCTTAATTCACAGGTCGTGATATG	AT3G46530.1, AT3G46710.1, AT3G46730.1	G-38138	F	for constructing amiRNA- III miR*s
GAATTAAGCTCTCGAACTAGTTTTCTACATATATATTCCT	AT3G46530.1, AT3G46710.1, AT3G46730.1	G-38139	R	for constructing amiRNA- IV miR*a
GATACGTTTACAAAGTTCAGCTCTCTCTCTTTTGTATTCC	AT3G46530.1, AT3G46710.1, AT3G46730.1	G-38140	F	for constructing amiRNA- I miR-s
GAGAGCTGAACTTTGTAAACGTATCAAAGAGAATCAATGA	AT3G46530.1, AT3G46710.1, AT3G46730.1	G-38141	R	for constructing amiRNA- II miR-a
GAGAACTGAACTTTGAAAACGTTTCACAGGTCGTGATATG	AT3G46530.1, AT3G46710.1, AT3G46730.1	G-38142	F	for constructing amiRNA- III miR*s
GAAACGTTTTCAAAGTTCAGTTCTCTACATATATATTCCT	AT3G46530.1, AT3G46710.1, AT3G46730.1	G-38143	R	for constructing amiRNA- IV miR*a
GATCTACGCAATATACCTTCCGATCTCTCTTTTGTATTCC	AT5G58120.1	G-38144	F	for constructing amiRNA- I miR-s
GATCGGAAGGTATATTGCGTAGATCAAAGAGAATCAATGA	AT5G58120.1	G-38145	R	for constructing amiRNA- II miR-a
GATCAGAAGGTATATAGCGTAGTTCACAGGTCGTGATATG	AT5G58120.1	G-38146	F	for constructing amiRNA- III miR*s

Continued on next page

Appendix Table 2. Continued from previous page…

Sequence	Target gene/region	Primer name	Orientation	Primer purpose
GAACTACGCTATATACCTTCTGATCTACATATATATTCCT	AT5G58120.1	G-38147	R	for constructing amiRNA- IV miR*a
GATTTAGATAATAGCCGGAGCGATCTCTCTTTTGTATTCC	AT5G58120.1	G-38148	F	for constructing amiRNA- I miR-s
GATCGCTCCGGCTATTATCTAAATCAAAGAGAATCAATGA	AT5G58120.1	G-38149	R	for constructing amiRNA- II miR-a
GATCACTCCGGCTATAATCTAATTCACAGGTCGTGATATG	AT5G58120.1	G-38150	F	for constructing amiRNA- III miR*s
GAATTAGATTATAGCCGGAGTGATCTACATATATATTCCT	AT5G58120.1	G-38151	R	for constructing amiRNA- IV miR*a
GATTAGTTTGTTCGAAACGTCTCTCTCTCTTTTGTATTCC	AT5G58120.1	G-38154	F	for constructing amiRNA- I miR-s
GAGAGACGTTTCGAACAAACTAATCAAAGAGAATCAATGA	AT5G58120.1	G-38155	R	for constructing amiRNA- II miR-a
GAGAAACGTTTCGAAGAAACTATTCACAGGTCGTGATATG	AT5G58120.1	G-38156	F	for constructing amiRNA- III miR*s
GAATAGTTTCTTCGAAACGTTTCTCTACATATATATTCCT	AT5G58120.1	G-38157	R	for constructing amiRNA- IV miR*a
GATGTTGGCACATAAACTCGGAGTCTCTCTTTTGTATTCC	*RPP1*	G-18131	F	for constructing amiRNA- I miR-s
GACTCCGAGTTTATGTGCCAACATCAAAGAGAATCAATGA	*RPP1*	G-18132	R	for constructing amiRNA- II miR-a
GACTACGAGTTTATGAGCCAACTTCACAGGTCGTGATATG	*RPP1*	G-18133	F	for constructing amiRNA- III miR*s
GAAGTTGGCTCATAAACTCGTAGTCTACATATATATTCCT	*RPP1*	G-18134	R	for constructing amiRNA- IV miR*a
GATTCTTACCGATCCCAGGCGGTTCTCTCTTTTGTATTCC	*RPP1*	G-19483	F	for constructing amiRNA- I miR-s
GAACCGCCTGGGATCGGTAAGAATCAAAGAGAATCAATGA	*RPP1*	G-19484	R	for constructing amiRNA- II miR-a
GAACAGCCTGGGATCCGTAAGATTCACAGGTCGTGATATG	*RPP1*	G-19485	F	for constructing amiRNA- III miR*s
GAATCTTACGGATCCCAGGCTGTTCTACATATATATTCCT	*RPP1*	G-19486	R	for constructing amiRNA- IV miR*a
GATATATCCGTAATGATTGCGGCTCTCTCTTTTGTATTCC	*RPP1*	G-19491	F	for constructing amiRNA- I miR-s
GAGCCGCAATCATTACGGATATATCAAAGAGAATCAATGA	*RPP1*	G-19492	R	for constructing amiRNA- II miR-a
GAGCAGCAATCATTAGGGATATTTCACAGGTCGTGATATG	*RPP1*	G-19493	F	for constructing amiRNA- III miR*s
GAAATATCCCTAATGATTGCTGCTCTACATATATATTCCT	*RPP1*	G-19494	R	for constructing amiRNA- IV miR*a
GATTCAAGGAAACACGTGAGACGTCTCTCTTTTGTATTCC	*RPW8*	G-13382	F	for constructing amiRNA- I miR-s
GACGTCTCACGTGTTTCCTTGAATCAAAGAGAATCAATGA	*RPW8*	G-13383	R	for constructing amiRNA- II miR-a
GACGCCTCACGTGTTACCTTGATTCACAGGTCGTGATATG	*RPW8*	G-13384	F	for constructing amiRNA- III miR*s
GAATCAAGGTAACACGTGAGGCGTCTACATATATATTCCT	*RPW8*	G-13385	R	for constructing amiRNA- IV miR*a
GATGATACTAATGATTGTAGCGCTCTCTCTTTTGTATTCC	*RPW8*	G-37702	F	for constructing amiRNA- I miR-s
GAGCGCTACAATCATTAGTATCATCAAAGAGAATCAATGA	*RPW8*	G-37703	R	for constructing amiRNA- II miR-a
GAGCACTACAATCATAAGTATCTTCACAGGTCGTGATATG	*RPW8*	G-37704	F	for constructing amiRNA- III miR*s
GAAGATACTTATGATTGTAGTGCTCTACATATATATTCCT	*RPW8*	G-37705	R	for constructing amiRNA- IV miR*a
GATTATACGAACCTGTACTTCCTTCTCTCTTTTGTATTCC	*RPW8*	G-37706	F	for constructing amiRNA- I miR-s
GAAGGAAGTACAGGTTCGTATAATCAAAGAGAATCAATGA	*RPW8*	G-37707	R	for constructing amiRNA- II miR-a
GAAGAAAGTACAGGTACGTATATTCACAGGTCGTGATATG	*RPW8*	G-37708	F	for constructing amiRNA- III miR*s
GAATATACGTACCTGTACTTTCTTCTACATATATATTCCT	*RPW8*	G-37709	R	for constructing amiRNA- IV miR*a
GATCAGAACGTAAATCGGATCGCTCTCTCTTTTGTATTCC	*RPW8*	G-37710	F	for constructing amiRNA- I miR-s
GAGCGATCCGATTTACGTTCTGATCAAAGAGAATCAATGA	*RPW8*	G-37711	R	for constructing amiRNA- II miR-a
GAGCAATCCGATTTAGGTTCTGTTCACAGGTCGTGATATG	*RPW8*	G-37712	F	for constructing amiRNA- III miR*s
GAACAGAACCTAAATCGGATTGCTCTACATATATATTCCT	*RPW8*	G-37713	R	for constructing amiRNA- IV miR*a
ATCTTCGCTTGGAGCTTCTC	*FRK1*	G-38244	F	qRT-PCR
TGCAGCGCAAGGACTAGAG	*FRK1*	G-38245	R	qRT-PCR

Continued on next page

Appendix Table 2. Continued from previous page…

Sequence	Target gene/region	Primer name	Orientation	Primer purpose
CTCCATACCCAAGGAGTTATTACAG	*WRKY29*	G-38252	F	qRT-PCR
CGGGTTGGTAGTTCATGATTG	*WRKY29*	G-38253	R	qRT-PCR
CGTGCATCTGTAATATGCTCTAGG	*WRKY46*	G-38254	F	qRT-PCR
GATGATGGTCACTGCTGGAG	*WRKY46*	G-38255	R	qRT-PCR
ACACGTGCAATGGAGTTTGTGG	*PR1*	G-38258	F	qRT-PCR
TTGGCACATCCGAGTCTCACTG	*PR1*	G-38259	R	qRT-PCR
CATGCCATGGCCAAGGAATTAGCAGAG	*SGT1B*	G-38260	F	qRT-PCR
GAAGGCCTATACTCCCACTTCTTGAGCTC	*SGT1B*	G-38261	R	qRT-PCR
CGGGATCCATGAATAATCAAAATGAAGACAC	*NDR1*	G-38262	F	qRT-PCR
GAAGGCCTACGAATAGCAAAGAATACGAG	*NDR1*	G-38263	R	qRT-PCR
GGCGATGAAGCTCAATCCAAACG	*ACTIN*	G-38266	F	qRT-PCR
GGTCACGACCAGCAAGATCAAGACG	*ACTIN*	G-38267	R	qRT-PCR
TCCTGAGGAATGTCCTGTGA	*EDS1*	G-13178	F	qRT-PCR
GAACCGTGTTCAGTTTCCTTG	*EDS1*	G-13179	R	qRT-PCR
GGCGGTATCGATGATTCAGT	*PAD4*	G-13180	F	qRT-PCR
GGTTGAATGGCCGGTTATC	*PAD4*	G-13181	R	qRT-PCR
CGTTTCTCAGCAGTGTCGTC	*NPR1*	G-13184	F	qRT-PCR
CCGTCTCACTGGTACGAAGA	*NPR1*	G-13185	R	qRT-PCR
ATCACTGCAATTGCCCATGT	*ACD6*	G-16287	F	qRT-PCR
ACACGCCACACAACCAAAA	*ACD6*	G-16288	R	qRT-PCR
CGAAGGCGGTTTAATGGATACTGC	*SAG12*	G-12167	F	qRT-PCR
TTAACCGGGACATCCTCATAACCTG	*SAG12*	G-12168	R	qRT-PCR
GAGCCTTACAACGCTACTCTGTCTGTC	*TUB*	N-0078	F	qRT-PCR
ACACCAGACATAGTAGCAGAAATCAAG	*TUB*	N-0079	R	qRT-PCR
AATGATACGGCGACCACCGAGATCTACACTCTTTCCCTACAC GACGCTCTTCCGATCT	Not applicable	G-26787	-	Universal PCR Primer 1 (Used for RAD-seq)
GTGACTGGAGTTCAGACGTGTGCTCTTCCGATCT	Not applicable	G-26788	-	Universal PCR Primer 2(Used for RAD-seq)

Appendix Table 3. Genomic and artificial microRNA constructs used in this study

Plasmid Name	Purpose	Alias	Vector backbone
MZ30	Genomic construct ACD6-Pro-0	pACD6-Pro-0:ACD6-Pro-0:BASTA	pBLuescript SK +
MZ32	Genomic construct ACD6-Pro-0	pACD6-Pro-0:ACD6-Pro-0:BASTA	pGreenIIS_Basta
MZ33	Est-1 :: Pro-0 ACD6 chimera	pACD6-Est-1:ACD6-Pro-0:BASTA	pBLuescript SK +
MZ34	Pro-0 :: Est-1 ACD6 chimera	pACD6-Pro-0:ACD6-Est-1:BASTA	pBLuescript SK +
MZ35	Est-1 :: Pro-0 ACD6 chimera	pACD6-Est-1:ACD6-Pro-0:BASTA	pGreenIIS_Basta
MZ36	Pro-0 :: Est-1 ACD6 chimera	pACD6-Pro-0:ACD6-Est-1:BASTA	pGreenIIS_Basta
MZ51	Genomic construct ACD6-Rmx-A180	pACD6-Rmx-A180:ACD6-Rmx-180:BASTA	pBLuescript SK +
MZ52	Genomic construct ACD6-Rmx-A180	pACD6-Rmx-A180:ACD6-Rmx-180:BASTA	pGreenIIS_Basta
MZ74	artificial miRNA construct for targeted gene approach	amiR-*NB-ARC* (AT1G58602)	pJLblue_rev
MZ76	artificial miRNA construct for targeted gene approach	amiR-*NB-ARC* (AT1G58602)	pGreenIIS_Basta
MZ77	artificial miRNA construct for targeted gene approach	amiR-*NB-LRR* (AT1G58410)	pJLblue_rev
MZ79	artificial miRNA construct for targeted gene approach	amiR-*NB-LRR* (AT1G58410)	pGreenIIS_Basta
MZ108	artificial miRNA construct for targeted gene approach	amiR-*RPW8*	pJLblue_rev
MZ110	artificial miRNA construct for targeted gene approach	amiR-*RPW8*	pGreenIIS_Basta
MZ145	artificial miRNA construct for targeted gene approach	amiR-*CC-NBS-LRR* (AT1G62630, AT1G62650, AT1G62660)	pJLblue_rev
MZ163	artificial miRNA construct for targeted gene approach	amiR-CC-NBS-LRR (AT1G62630, AT1G62650, AT1G62660)	pGreenIIS_Basta
MZ146	artificial miRNA construct for targeted gene approach	amiR-*RPP13* (AT3G46530.1, AT3G46710.1, AT3G46730.1)	pJLblue_rev
MZ164	artificial miRNA construct for targeted gene approach	amiR-*RPP13* (AT3G46530.1, AT3G46710.1, AT3G46730.1)	pGreenIIS_Basta
MZ148	artificial miRNA construct for targeted gene approach	amiR-*RPP13* (AT3G46530.1, AT3G46710.1, AT3G46730.1)	pJLblue_rev
MZ165	artificial miRNA construct for targeted gene approach	amiR-*RPP13* (AT3G46530.1, AT3G46710.1, AT3G46730.1)	pGreenIIS_Basta
MZ149	artificial miRNA construct for targeted gene approach	amiR-*RPP13* (AT3G46530.1, AT3G46710.1, AT3G46730.1)	pJLblue_rev
MZ166	artificial miRNA construct for targeted gene approach	amiR-*RPP13* (AT3G46530.1, AT3G46710.1, AT3G46730.1)	pGreenIIS_Basta
MZ150	artificial miRNA construct for targeted gene approach	amiR-*ADR2* (AT5G58120.1)	pJLblue_rev
MZ167	artificial miRNA construct for targeted gene approach	amiR-*ADR2* (AT5G58120.1)	pGreenIIS_Basta
MZ151	artificial miRNA construct for targeted gene approach	amiR-*ADR2* (AT5G58120.1)	pJLblue_rev
MZ168	artificial miRNA construct for targeted gene approach	amiR-*ADR2* (AT5G58120.1)	pGreenIIS_Basta
EK19 [A]	artificial miRNA construct for targeted gene approach	amiR-*RPP7*	pGreenIIS_Basta
EK20 [A]	artificial miRNA construct for targeted gene approach	amiR-*RPP7*	pGreenIIS_Basta
EK21 [A]	artificial miRNA construct for targeted gene approach	amiR-*RPP7*	pGreenIIS_Basta
EK22 [A]	artificial miRNA construct for targeted gene approach	amiR-*RPP7*	pGreenIIS_Basta
EK26 [A]	artificial miRNA construct for targeted gene approach	amiR-*RPP7*	pGreenIIS_Basta
EK27 [A]	artificial miRNA construct for targeted gene approach	amiR-*RPP7*	pGreenIIS_Basta
EC290 [A]	artificial miRNA construct for targeted gene approach	amiR-*RPP4/5*	pGreenIIS_Basta
EC292 [A]	artificial miRNA construct for targeted gene approach	amiR-*RPP4/5*	pGreenIIS_Basta
EC293 [A]	artificial miRNA construct for targeted gene approach	amiR-*RPP4/5*	pGreenIIS_Basta
EC294 [A]	artificial miRNA construct for targeted gene approach	amiR-*RPP4/5*	pGreenIIS_Basta

Continued on next page

Appendix Table 3. Continued from previous page…

Plasmid Name	Purpose	Alias	Vector backbone
EC295 [A]	artificial miRNA construct for targeted gene approach	amiR-RPP4/5	pGreenIIS_Basta
KB209 [B]	artificial miRNA construct for targeted gene approach	amiR-*RPP1*	pGreenIIS_Basta
KB210 [B]	artificial miRNA construct for targeted gene approach	amiR-*RPP1*	pGreenIIS_Basta
KB211 [B]	artificial miRNA construct for targeted gene approach	amiR-*RPP1*	pGreenIIS_Basta
KB212 [B]	artificial miRNA construct for targeted gene approach	amiR-*RPP1*	pGreenIIS_Basta
KB217 [B]	artificial miRNA construct for targeted gene approach	amiR-*RPP1*	pGreenIIS_Basta
KB226 [B]	artificial miRNA construct for targeted gene approach	amiR-*RPP1*	pGreenIIS_Basta
KB228 [B]	artificial miRNA construct for targeted gene approach	amiR-*RPP1*	pGreenIIS_Basta
MT79 [C]	artificial miRNA construct for targeted gene approach	amiR-*ACD6*	pGreenIIS_Basta

[A] amiRNA constructs made by Dr. Eunyoung Chae; [B] amiRNA constructs made by Dr. Kirsten Bomblies; amiRNA construct made by Dr. Marco Todesco

Appendix Table 4. Adaptors used for multiplexing individuals for RAD-Seq

No.	Index	Restriction Site (PstI)
1	CAGATA	TGCAG
2	GAAGTG	TGCAG
3	TAGCGGAT	TGCAG
4	TATTCGCAT	TGCAG
5	ATAGAT	TGCAG
6	CCGAACA	TGCAG
7	GGAAGACAT	TGCAG
8	AACGCACATT	TGCAG
9	GAGCGACAT	TGCAG
10	CCTTGCCATT	TGCAG
11	GGTATA	TGCAG
12	TCTTGG	TGCAG
13	GGTGT	TGCAG
14	GGATA	TGCAG
15	CTAAGCA	TGCAG
16	ATTAT	TGCAG
17	GCGCTCA	TGCAG
18	ACTGCGAT	TGCAG
19	TTCGTT	TGCAG
20	ATATAA	TGCAG
21	TGGCAACAGA	TGCAG
22	CTCGTCG	TGCAG
23	GCCTACCT	TGCAG
24	CACCA	TGCAG
25	AATTAG	TGCAG
26	GGAACGA	TGCAG
27	ACTGCT	TGCAG
28	TGCTT	TGCAG
29	GCAAGCCAT	TGCAG
30	CGCACCAATT	TGCAG
31	CTCGCGG	TGCAG
32	AACTGG	TGCAG
33	ATGAGCAA	TGCAG
34	CTTGA	TGCAG
35	GCGTCCT	TGCAG
36	ACCAGGA	TGCAG
37	CCACTCA	TGCAG
38	TCACGGAAG	TGCAG
39	TATCA	TGCAG
40	TAGCCAA	TGCAG
41	ATATCGCCA	TGCAG
42	CTCTA	TGCAG
43	GGTGCACATT	TGCAG
44	CTCTCGCAT	TGCAG
45	CAGAGGT	TGCAG
46	GCGTACAAT	TGCAG
47	ACGCGCG	TGCAG
48	GTCGCCT	TGCAG
49	AATAACCAA	TGCAG
50	AATGAACGA	TGCAG
51	ATGGCAA	TGCAG
52	GAAGCA	TGCAG
53	AACGTGCCT	TGCAG
54	CCTCG	TGCAG
55	CTCAT	TGCAG
56	ACGGTACT	TGCAG
57	GCGCCG	TGCAG
58	CAAGT	TGCAG
59	GGAGTCAAG	TGCAG
60	TGAAT	TGCAG
61	CATAT	TGCAG
62	GTGACACAT	TGCAG
63	TATGT	TGCAG
64	TGCAGA	TGCAG
65	CATCTGCCG	TGCAG
66	GGACAG	TGCAG
67	ATCTGT	TGCAG
68	AAGACGCT	TGCAG
69	GAATGCAATA	TGCAG
70	TAGCAG	TGCAG
71	CTTAG	TGCAG
72	TTATTACAT	TGCAG
73	GCCAACAAGA	TGCAG
74	TGCCGCAT	TGCAG
75	CGTGTCA	TGCAG
76	CAACCACACA	TGCAG
77	GCTCCGA	TGCAG
78	CGTTCA	TGCAG
79	CATCACAAG	TGCAG
80	TCCAG	TGCAG

Continued on next page

Appendix Table 4. Continued from previous page…

No.	Index	Restriction Site (PstI)
81	AACTGAAG	TGCAG
82	GATTCA	TGCAG
83	CAAGCCAATT	TGCAG
84	TTGCGCT	TGCAG
85	CGCAGACACT	TGCAG
86	TGTGGA	TGCAG
87	TGGATA	TGCAG
88	ATAGCGT	TGCAG
89	CCATAGA	TGCAG
90	GGCACGCAT	TGCAG
91	ATTAACAATT	TGCAG
92	CAATA	TGCAG
93	TAGTCCAT	TGCAG
94	CGTGACCT	TGCAG
95	CTTCAGA	TGCAG
96	ATCTGCAACA	TGCAG
97	AAGGA	TGCAG
98	TTACT	TGCAG
99	TTATCCAT	TGCAG
100	GGATTG	TGCAG
101	GACGTGA	TGCAG
102	GACGGCA	TGCAG
103	CGTCTG	TGCAG
104	TCTGA	TGCAG
105	AACTT	TGCAG
106	GAGTCACAAT	TGCAG
107	CGGTTGCAT	TGCAG
108	GTCCTGCCA	TGCAG
109	GTTACA	TGCAG
110	GCGGA	TGCAG
111	ATGATACG	TGCAG
112	CTGTTG	TGCAG
113	TCAGTAAT	TGCAG
114	TCACA	TGCAG
115	GTCGT	TGCAG
116	ACGCTAA	TGCAG
117	ATAGG	TGCAG
118	CCTGCCA	TGCAG
119	TAAGACA	TGCAG
120	TGAGA	TGCAG
121	AATGCAG	TGCAG
122	CCGTGA	TGCAG
123	GCCAGACATT	TGCAG
124	GTGCG	TGCAG
125	TTACACA	TGCAG
126	CCGTCACAGT	TGCAG
127	CTGTGT	TGCAG
128	CGCGCCG	TGCAG
129	CTAACA	TGCAG
130	GGCCTG	TGCAG
131	TGACGT	TGCAG
132	ACTGAG	TGCAG
133	GCGCACT	TGCAG
134	GGTAAGCA	TGCAG
135	AATCGGAGG	TGCAG
136	TGGAGCCT	TGCAG
137	GATGGCCAT	TGCAG
138	TGCAA	TGCAG
139	GAGACG	TGCAG
140	CCGTACCACT	TGCAG
141	GTAACG	TGCAG
142	TCCTCACAT	TGCAG
143	TCGTA	TGCAG
144	GTATTGACT	TGCAG
145	GCTCA	TGCAG
146	CAGTAA	TGCAG
147	GGAGAGCAT	TGCAG
148	CCATG	TGCAG
149	CGCTCACACA	TGCAG
150	TGTTACG	TGCAG
151	GATTGGAAGA	TGCAG
152	AATAAGAGT	TGCAG
153	TACAAG	TGCAG
154	TTCAGCCAGT	TGCAG
155	TGAAGCAACT	TGCAG
156	ACAACGCAT	TGCAG
157	GGCGGACGA	TGCAG
158	AATGTA	TGCAG
159	GTACGGACG	TGCAG

NPR1
AT1G64280

>Est-1.MPI_chr1:C/23853329-23858328 Amino_Acid

XRRRHSLKRNSRKGGTSKSTSSTSDTLSSNGLELNDESFAKKLTEQIEMYRQKKQLRKEATDDEGCALQTLDECNMIQDLVASCRPFFRKGLEVsslfvldsllycfwtxldnlktkqsl
sdsstpsfgyrTKSLAKLRSQHEELIRFPAIKVGPSTRKTGTLRDPELSTVIFECTGKMEAIEMAAQAETPFLRQALAVlchvvclitimleslkrislvyixnlcilflvqyigRNELD
LLTMKLEDAAVAFSPPVDRPIQERKDEQELIEVCLRGKLSHKCQEPINNCEVAMTAQKAIMLATRGELTAESASAGKELLSLILQPEKRMAAVHLVTYGRPNRHNVDALDLKLLDTATKV
NCYAVAFHLACADDLNTHDEKLLLKVLEIDDSDLAKHVNSVHKKVKPVELGLEKRRDIIEKVLEEPLSKELSVMDVNSKVIIEKCRDLLKMCAKGCINALKLIVLTDEIVVKDVVDLLHR
qfvfvlvxtlvyehihlwlkicitnxrQYLTILEPIKFIFALYLVELMFDVAPRCAVHCCNEDACESVGKPPPRVRSSYVYALVTVVSDFGVEYDKAIEKLELKVAATNNSDKEKKAAAL
ASKFFSSRASLVCRHFSVERGDSLVLKADSYFDDPSDFVSEFSNSLLQLASVDPGTLVQEAALYVISSDTNDTAVFSTSSIEYSDAFGDITTDMllnrhisixlnfldrsilssvkdvpn
pxldfivmssclwtldvltttlyssadedwpkckvlvplngpfsdkdsikklfiycsalgtrtiftlixvpsmkhqxnkyilleirnplgrfwvlnpssifiyfknkmrntikmyiylyx
kkfklilnvhslxmetxkrqlliifpvyilnxaknvytkyhinykenisftikltxctxviildlringpvirrtrycifvskvvfdnyiysyivnfvhfdyhiykklxskixfcnnyvy
llsrxnnaklkenqimryilkkllxstfafeyctxvfkaxgessqhkgseinssvsfffsdaydgrpeegtsenqqisfsrsxfiflytlsaxsylltlnhqifltsxiptiilyifxqk
grkkskykkfslnfxsliqiikllnvivrxleiadcixniksiikqvikhflkrkilkkfhyiifnlqilriynkxrrgdiitslyqslsxifvwngfixyikhvmrkkqliyirpccvt
cinyllkyfmsvpxiplsyiytflllinrttdlytnsxinnyixyilidkilxyiixslfnpcxkryllqkxsyvpvrsiifysalfdsxinmfchktnnclglfcfeinrkvkyfvilc
xxiykhgvilsgisvqskldkdvvnantpgnkknkkxltpgnsrgnldvreydscfpfcvfscdsgekkayvlnlkeaninylcgrdssrflvvdnsptwtildvgiskidkvkvwskef
ssklvwlehvdeqdkntwqriaglkgeyrvlgsfvdsnpthffswtetklcfrivnnnrsiwhlfgsvqipnsfilrdtkplrlnelrkwtfsdsdfvecmftrhnlhyigrsmcmrrsq
slrqikyrfpnlgivalglsmdwgkvepkpivqyqkttpkfviygrspktykvcllighsadcaeikimgpplfdisvgnnqldsrehvfstrlehgkviyhqifyg

>Pro_0.SALK_chr1:C/23853329-23858328 Amino_Acid

XRRRHSLKRNSRKGGTSKSTSSTSDTLSSNGLELNDESFAKKLTEQIEMYRQKKQLRKEATDDEGCALQTLDECNMIQDLVASCRPFFRKGLEVsslfvldsllycfwtxldnlktkqsl
sdsstpsfgyrTKSLAKLRSQHEELIRFPAIKVGPSTRKTGTLRDPELSTVIFECTGKMEAIEMAAQAETPFLRQALAVlchvvclitimleslkrislvyixnlcilflvqyigRNELD
LLTMKLEDAAVAFSPPVDRPIQERKDEQELIEVCLRGKLSHKCQEPINNCEVAMTAQKAIMLATRGELTAESASAGKELLSLILQPEKRMAAVHLVTYGRPNRHNVDALDLKLLDTATKV
NCYAVAFHLACADDLNTHDEKLLLKVLEIDDSDLAKHVNSVHKKVKPVELGLEKRRDIIEKVLEEPLSKELSVMDVNSKVIIEKCRDLLKMCAKGCINALKLIVLTDEIVVKDVVDLLHR
qfvfvlvxtlvyehihlwlkicitnxrQYLTILEPIKFIFALYLVELMFDVAPRCAVHCCNEDACESVGKPPPRVRSSYVYALVTVVSDFGVEYDKAIEKLELKVAATNNSDKEKKAAAL
ASKFFSSRASLVCRHFSVERGDSLVLKADSYFDDPSDFVSEFSNSLLQLASVDPGTLVQEAALYVISSDTNDTAVFSTSSIEYSDAFGDITTDMllnrhisixlnfldrsilssvkdvpn
pxldfivmssclwtldvltttlyssadedwpkckvlvplngpfsdkdsikklfiycsalgtrtiftlixvpsmkhqxnkyilleirnplgrfwvlnpssifiyfknkmrntikmyiylyx
kkfklilnvhslxmetxkrqlliifpvyilnxaknvytkyhinykenisftikltxctxviildlringpvirrtrycifvskvvfdnyiysyivnfvhfdyhiykklxskixfcnnyvy
llsrxnnaklkenqimryilkkllxstfafeyctxvfkaxgessqhkgseinssvsfffsdaydgrpeegtsenqqisfsrsxfiflytlsaxsylltlnhqifltsxiptiilyifxqk
grkkskykkfslnfxsliqiikllnvivrxleiadcixniksiikqvikhflkrkilkkfhyiifnlqilriynkxrrgdiitslyqslsxifvwngfixyikhvmrkkqliyirpccvt
cinyllkyfmsvpxiplsyiytflllinrttdlytnsxinnyixyilidkilxyiixslfnpcxkryllqkxsyvpvrsiifysalfdsxinmfchktnnclglfcfeinrkvkyfvilc
xxiykhgvilsgisvqskldkdvvnantpgnkknkkxltpgnsrgnldvreydscfpfcvfscdsgekkayvlnlkeaninylcgrdssrflvvdnsptwtildvgiskidkvkvwskef
ssklvwlehvdeqdkntwqriaglkgeyrvlgsfvdsnpthffswtetklcfrivnnnrsiwhlfgsvqipnsfilrdtkplrlnelrkwtfsdsdfvecmftrhnlhyigrsmcmrrsq
slrqikyrfpnlgivalglsmdwgkvepkpivqyqkttpkfviygrspktykvcllighsadcaeikimgpplfdisvgnnqldsrehvfstrlehgkviyhqifyg

FLS2
AT5G46330

>Est-1.MPI_chr5:W/18791802-18796801 Amino_Acid

MKLLSKTFLILTLTFFFFGIALAKQSFEPEIEALKSFKNGISNDPLGVLSDWTIIGSLRHCNWTGITCDSTGHVVSVSLLEKQLEGVLSPAIANLTYLQVLDLTSNSFTGKIPAEIGKLT
ELNQLILYLNYFSGSIPSGIWELKNIFYLDLRNNLLSGDVPEEICKSSSLVLIGFDYNNLTGKIPECLGDLVHLQMFVAAGNHLTGSIPVSIGTLANLTDLDLSGNQLTGKIPRDFGNLL
NLQSLVLTENLLEGEIPAEIGNCSSLVQLELYDNQLTGKIPAELGNLVQLQALRIYKNKLTSSIPSSLFRLTQLTHLGLSENHLVGPISEEIGFLESLEVLTLHSNNFTGEFPQSITNLR
NLTVLTVGFNNISGELPADLGLLTNLRNLSAHDNLLTGPIPSSISNCTGLKLLDLSHNQMTGEIPRGFGRMNLTFISIGRNHFTGEIPDDIFNCSNLETLSVADNNLTGTLKPLIGKLQK
LRILQVSYNSLTGPIPREIGNLKDLNILYLHSNGFTGRIPREMSNLTLLQGLRMYSNDLEGPIPEEMFDMKLLSVLDLSNNKFSGQIPALFSKLESLTYLSLQGNKFNGSIPASLKSLSL
LNTFDISDNLLTGTIPGELLASLKNMQLYLNFSNNLLTGTIPKELGKLEMVQEIDLSNNLFSGSIPRSLQACKNVFTLDFSQNNLSGHIPDEVFQGDMIISLNLSRNSFSGEIPQSFGN
MTHLVSLDLSSNNLTGEIPESLANLSTLKHLKLASNNLKGHVPESGVFKNINASDLMGNTDLCGSKKPLKPCTIKQKSSHFSKRTRVILIILGSAAALLLVLLLVLILTCCKKKEKKIEN
SSESSLPDLDSALKLKRFEPKELEQATDSFNSANIIGSSSLSTVYKGQLEDGTVIAVKVLNLKEFSAESDKWFYTEAKTLSQLKHRNLVKILGFAWESGKTKALVLPFMENGNLEDTIHG
SAAPIGSLLERIDLCVHIASGIDYLHSGYGFPIVHCDLKPANILLDSDRVAHVSDFGTARILGFREDGSTTASTSAFEGTIGYLAPEklttlnfqnpnyaidlleihsyfsxteFAYMR
KVTTKADVFSFGIIMMELMTKQRPTSLNDEDSQDMTLRQLVEKSIGNGRKGMVRVLDMELGDSIVSLKQEEAIEDFLKLCLFCTSSRPEDRPDMNEILTHLMKLRGKANSFREDRNEDRE
VXqqsffddifstlpnsvtkveyfgrktfxfcfslcisvlykveiwfxxtfsytnalgytwilxfliagrsgirfvkflssxwrxrlslpfnhetipllvsdnrqshdgyrehrrxlkdq
chtrqlcrlakxxlxkleslhfhlpgxcfpfsasepqklqdxtdrkpcqxllrmnsslklynfixffnitihfwtnyilfaxslqnkixrixhkklktlnrrqllrfcmaieksxamlv
yavlgsafverplklnvhkkminktnlsfylfsfalmrpqxrntknkhlflnvndrnqqsfrxifyewmanendlgthgfxrxixrrtnekqxsgramaipamkleksrllsfvgtktvl
svlvsskrrxdtwrtrtnrdvseslientgreevtvsykdvysscqheiehrvsrnnrekpfwlpvrhvxsenwclxfnkyasrkrlshrkqtlaiyetgkcksl

>Rmx_A180.SALK_chr5:W/18791802-18796801 Amino_Acid

MKLLSKTFLILTLTFFFFGIALAKQSFEPEIEALKSFKNGISNDPLGVLSDWTIIGSLRHCNWTGITCDSTGHVVSVSLLEKQLEGVLSPAIANLTYLQVLDLTSNSFTGKIPAEIGKLT
ELNQLILYLNYFSGSIPSGIWELKNIFYLDLRNNLLSGDVPEEICKTSSLVLIGFDYNNLTGKIPECLGDLVHLQMFVAAGNHLTGSIPVSIGTLANLTDLDLSGNQLTGKIPRDFGNLL
NLQSLVLTENLLEGEIPAEIGNCSSLVQLELYDNQLTGKIPAELGNLVQLQALRIYKNKLTSSIPSSLFRLTQLTHLGLSENHLVGPISEEIGFLESLEVLTLHSNNFTGEFPQSITNLR
NLTVLTVGFNNISGELPADLGLLTNLRNLSAHDNLLTGPIPSSISNCTGLKLLDLSHNQMTGEIPRGFGRMNLTFISIGRNHFTGEIPDDIFNCSNLETLSVADNNLTGTLKPLIGKLQK
LRILQVSYNSLTGPIPREIGNLKDLNILYLHSNGFTGRIPREMSNLTLLQGLRMYSNDLEGPIPEEMFDMKLLSVLDLSNNKFSGQIPALFSKLESLTYLSLQGNKFNGSIPASLKSLSL
LNTFDISDNLLTGTIPGELLASLKNMQLYLNFSNNLLTGTIPKELGKLEMVQEIDLSNNLFSGSIPRSLQACKNVFTLDFSQNNLSGHIPDEVFQGDMIISLNLSRNSFSGEIPQSFGN
MTHLVSLDLSSNNLTGEIPESLANLSTLKHLKLASNNLKGHVPESGVFKNINASDLMGNTDLCGSKKPLKPCTIKQKSSHFSKRTRVILIILGSAAALLLVLLLVLILTCCKKKEKKIEN
SSESSLPDLDSALKLKRFEPKELEQATDSFNSANIIGSSSLSTVYKGQLEDGTVIAVKVLNLKEFSAESDKWFYTEAKTLSQLKHRNLVKILGFAWESGKTKALVLPFMENGNLEDTIHG
SAAPIGSLLERIDLCVHIASGIDYLHSGYGFPIVHCDLKPANILLDSDRVAHVSDFGTARILGFREDGSTTASTSAFEGTIGYLAPEklttlnfqnpnyaidlleihsyfsxteFAYMR
KVTTKADVFSFGIIMMELMTKQRPTSLNDEDSQDMTLRQLVEKSIGNGRKGMVRVLDMELGDSIVSLKQEEAIEDFLKLCLFCTSSRPEDRPDMNEILTHLMKLRGKANSFREDRNEDRE
VXqqsffddifstlpnsvtkveyfgrktfxfcfslcisvlykveiwfxxtfsytnalgytwilxfliagrsgirfvkflssxwrxrlslpfnhetipllvsdnrqshdgyrehrrxlkdq
chtrqlcrlakxxlxkleslhfhlpgxcfpfsaepqklqdxtdrkpcqxllrmnsslklcnfixffnitihfxtzyilfaxslqnkixrixhkklktlnrrqllrfcmaieksxamlv
yavlgsafverplklnvhkkminktnlsfylfsfalmrpqxrntcnkhlflpvndrnqqsfrxifyewmanendlgthgfxrxixrrtnekqxsgramaipamkleksrllsfvgtktvl
svlvsskrrxdtwrtrtnrdvseslientgreevtvsykdvysscqheiehrvsrnnrekpfwlpvrhvxsenwclxfnkyasrkrlshrkqtlaiyetgkcksl

PAD4
AT3G52430

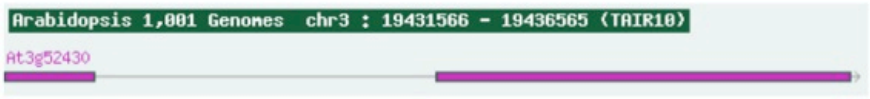

>Est-1.MPI_chr3:W/19431566-19436565 Amino_Acid

MDDCRFETSELQASVMISTPLFTDSWSSCNTANCNGSIKIHDIAGITYVAIPAVSMIQLGNLVGLPVTGDVLFPGLSSDEPLPMVDAAILKLFLQLKvcflflcfffflldaixpiyylq
gmwifefqliiprekntkiikcxygklfhkgflkktkfyhkfysfgfaktnftyxsyyffyvfxyflvelmiitifylnisvlxilmnynpnggffcpfkrllxtitttypnrqxtidnk
xklfsckkfxkdswtqlfqihhleyvivatfgyhkqvnxkfglyaitsvrpsdlknllisexnvigifdtkknkkcxwnwxlyalcfntprrslxmcaqkvfnpxllchhhvfyslfrri
llvfvlslrixksxtktssywfxxvektrsdhxcryklxkwxvxrgvltdfysnlvklsnwqixslnqftlleeivhsegrxsiisfvlvsqpiysnvdcinvqIKEGLELELVGKKLVV
ITGHSTGGALAAFTALWLLSQSSPPSFRVFCITFGSPLLGNQSLSTSISRSRLAHNFCHVVSIHDLVPRSSNEQFWPFGTYLFCSDKGGVCLDNAGSVRLMFNILNTTATQNTEEHQRYG
HYVFTLSHMFLKSRSFLGGSIPDNSYQAGVALAVEALGFSNDDTSGVLVKECIETATRIVRAPILRSAELANELASVLPARLEIQWYKDRCDASEEQLGYYDFFKRYSLKRDFKVNMSRI
RLAKFWDTVIKMVETNELPFDFHLGKKWIYASQFYQLLAEPLDIANFYKNRDIKTGGHYLEGNRPKRYEVIDKWQKGVKVPEECVRSRYASTTQDTCFWAKLEQAKEWLDEARKESSDPQ
RRSLLREKIVPFESYANTLVTKKEVSLDVKAKNSSYSVWEANLKEFKVKMGYENEIEMVVDESDAMETXxdxxqieclicyiticiivvhhvyarlsdecyyifxnkiyrqcstsfarvs
fcvqcaksfscraitlfffflvrskaitlkptcsvmvixfqefxntnixknvrpttxnswrlpiftxskklfipfrfsfpipiflwvnksnkfksnkxtnrdspcssklvssctfsfys
fysqivthtlhtifilytiixlxlsmirylqvlilndsgqifivlsrixcexkmlqyrxlmvxyllixifylixlxvhsinfkrhilvcgspxtkpykxlnvhpithlskeaigflvpfe
tisktiyfgihilxxkkqilvfkylskiqnpxpclpqeatvsaplrgicspklhplsslhasqtlhmhklspthscmrixyilipgdxrrareiwreqrpxhhrlyggqtqtqtrrsrrv
vqdvdpltqssvttttiaslslatsakaadigpkvvpsamflxavavenpaapnhllvtilklaxplilatpvvvhqasilllftpisxiqsltnlyykkiatxplrifwxiilpalpw
tlhgvwtsmmvimiiilirwntlwrnvvimaclhflvksfslxtlmvfglmlcxlvitmxtlaxlrfrlytnrwfisltnpmippisclevgallislpmddpyicixiyefvllyllyk
exytrlyeilxiiscnxesrxilstnlrgnnmctlxiiiyfgysvvfkissriprggpclwirlrfasllelvqfresethvyhgctcesllvslacvdpspkrgc

>Br_0.SALK_chr3:W/19431566-19436565 Amino_Acid

MDDCRFETSELQASVMISTPLFTDSWSSCNTANCNGSIKIQVIAGITYVAIPAVPMIQLGDLVGLPVTGDVIFPGLSSDEPLPMVDAAILKLFLQLKvcflflcfE(f+3)fflldaixpiyylqg
mwifefqliiprekntkiikcxygklfhkgflkktkfyhkfysfgfaktnftyxsyyffyvfxyflvelmiitifylnisvlxilmnynpnggffcpfkrllxtitttypnrqxtidnkx
klfsckkfxkdswtqlfqihhleyvivatfgyhkqvnxkfglyaitsvrpsdlknllisexnvigifdtkkgkkcxwnwxlyalcfntprrsfxmcaqkvfnpxllchhhvfyslfrril
lvfvlslrixksxtktssywfxxvektrsdhxcryklxkwxvxrgvltdfysnlvklsnwqixslnqftlleeivhsegrxsiisfvlvsqpiysnvdcinvqIKEGLELELVGKKLVVI
TGHSTGGALAAFTALWLLSQSSPPSFRVFCITFGSPLLGNQSLSTSISRSRLAHNFCHVVSIHDLVPRSSNEQFWPFGTYLFCSDKGGVCLDNAGSVRLMFNILNTTATQNTEEHQRYGH
YVFTLSHMFLKSRSFLGGSIPDNSYQAGVALAVEALGFSNDDTSGVLVKECIETATRIVRAPILRSAELANELASVLPARLEIQWYKDRCDASEEQLGYYDFFKRYSLKRDFKVNMSRIR
LAKFWDTVIKMVETNELPFDFHLGKKWIYASQFYQLLAEPLDIANFYKNRDIKTGGHYLEGNRPKRYEVIDKWQKGVKVPEECVRSRYASTTQDTCFWAKLEQAKEWLDEARKESSDPQR
RSLLREKIVPFESYANTLVTKKEVSLDVKAKNSSYSVWEANLKEFKVKMGYENEIEMVVDESDAMETXxdxxqieclicyiticiivvhhvyarlsdecyyifxnkiyrqcstsfarvsf
cvqcaksfscraitlfffflvrskaitlkptcsvmvixfqefxntnixknvrpttxnswrlpiftxskklfipfrfsfpipiflwvnksnkfksnkxtnrdspcssklvssctfsfysf
ysqivthtlhtifilytiixlxlsmirylqvlilndsgqifivlsrixcexkmlqyrxlmvxyllixifylixlxvhsinfkrhilvcgspxtkpykxlnvhpithlskeaigflvpfet
isktiyfgihilxxkkqilvfkylskiqnpxpclpqeatvsaplrgicspklhplsslhasqtlhmhklspthscmrixyilipgdxrrareiwreqrpxhhrlyggqtqtqtrrsrrvv
qdvdpltqssvttttiaslslatsakaadigpkvvpsamflxavavenpaapnhllvtilklaxplilatpvvvhqasilllftpisxiqsltnlyykkiatxplrifwxiilpalpwt
lhgvwtsmmvimiiilirwntlwrnvvimaclhflvksfslxtlmvfglmlcxlvitmxtlaxlrfrlytnrwfisltnpmippisclevgallislpmddpyicixiyefvllyllyke
xytrlyeilxiiscnxesrxilstnlrg...ctlqf(h+1)iiyfgysvvlkissriprggpclwirlrfasllelvqfresethvyhgctcesllvslacvdpspkrgc

EDS1
AT3G48090

>Est-1.MPI_chr3:C/17755553-17760552 Amino_Acid

```
XTDTIEDMMYDRLPSHSKHNKPLTIWWKRFTSGELFIEKDDVEGDTIWEGLMGELTKVRVEVEEYPKGKLEEVEAWFCSGCESGSNKLTEQIEELQLGLNLGNVKNWFVDEAIMGNPKLI
YHEYGRQAYIYRTPRGRKMYPGTDENKLHRHYNAIDLPEVLRRYRTALKIWDIDGEFEDPLQCKKMLGLVEDFVGALEARKVNAKFDNEENSVKFSDYYGNKHAQCKPKYEDEIWALKKL
FREQEIVxfgcfwctkhqxvcvssarvqmixscaxxgcvQIIKKQNEVRKKEEELAAQVYQRGRTSqlflfcespnlhncshlxpaacysflslslsvVGLDNLTSEISNEGDLHNFLKK
GMSQVLEEYSHHDRISRFPILSWEQEDSAQSTYFLMQLIADSNNVAVLRKETSFVFTGAPRYPSLELFSSLTELFAEASGTLECVAQNAVTSTDRMVRTYFETIRQESEQVSSKRPDLQA
LVHPLTEEVSAKRALMIRPVIDFRSVFNVFFRSWKERGLAHSFISDGVLPAGFTVCRPELYVNPNRIFYKELYWVTALIATAGGSSHGTFVIQKRSRVAMEVqllllmlswflfffffin
phkxdexlSAQFSTRPDIIAELNKLFAENVTAVDGKGIKRMCPFQVRNLKIEGFSSKNDPDFFDKESFSPQFAFIVVAGAEEKHYRETLYAQKSASWSRTILDGNIGTLAEFAMsryrne
krxhvkkerkeksddqkklgsrsqxniplhlcsxntvwfvgdhswklafipkkkqlqskpxqlsmffsfspikakwtdtkcqhiakymrcsqlkasvkmfmxmqdslkrqtikaqfnqlk
vksdedrxylswrktqstvrpqskatvxhyeskqrfvikxnlshpsknaqlxtktaqspneskteyllfrssxsqkaxldxgsllgslrcsisgtrnreasyxgfxsvvgeqrtrkqtrc
sadcevkvqkiifncsgsxffktqkkpxvlnclwiksesliffgllsfxcffcfftxsvlikktkifglkpfnrrfamyltgvlaxflxsiesseixtslkikilcfilkdehlsryxvv
lgnrfxxkllrlllfeytlkwflvggnxmdrmylfffhieegrxhiwtxlkckxrifvwrqxeqdtktrdafsatidxfnyaslilvhmhtfrqaklscitrpiqyvxikarklqsyidn
aelerkhminkfareeakmlsdrlrkvdalkvpkllfdeageelcrflylsgftlsrigylkysqicfialeyiiimlslrtfltqnrlllclctlhrdrpnpnxlhgxrlnhlgflxfm
yxltksprvhxrsiyfxielssraxsiisxekrfkhgcslnxxexsgnxfdnxsgsfyvgfrlkilyvvvvltlgmitlfydyllrkxxllikhnyllkixdicirxrysxxldxiltiv
kflkrflcygrfrimgmeqlllhvfdvinplnqdxmikvxvlilsxlxsxxlliyrdirplinessmivvpierfasseqxftxfgyvlnsxfkmkkxikkrxilvenxnqsflqimllv
xksrrxynmdlxglcltirxxxilrxirfylklgfikxcwiqisexexfyxvchdskngxiwgfxxerwriwsitfskdcxrccyslcflvltlnkykflncliflc
```

>Br_0.SALK_chr3:C/17755553-17760552 Amino_Acid

```
XTDTIEDMMYDRLPSHSKHNKPLTIWWKRFTSGELFIEKDDVEGDTIWEGLMRELTKVRVEVEEYPKGKLEEVEAWFCSGCESGSNKLTEQIEELQLGLNLGNVKNWFVDEAIMGNPKLI
YHEYGRQAYIYRTPRGRKMYPGTDENKLHRHYNAIDLPEVLRRYRTALKIWDIDGEFEDPLQCKKTLGTVEDFVGALEARKVNAKFDNEENSVKFSDYYGNKHAQCKPKYEMEIWALKKL
FREQCIVxfgcLwctkhqxvcvssarvqmixscaXxgcvQIIKKQNEVRKKEEELAAQVYQRGRTSqlflfcespnlhncshlxpaacysflslslsvVGLDNLTSEISNEGDLHNFLKX
GMSQVLEEYSHHDRISRFPILSWEQEDSAQCTYFLMQLIADSNNVAVLRKETSFVFTGAPRYPSLELFSSLTELIAEASGTLECVACHAVTSTDRMVSRTYFETIRQESEQVSSXRPDLQA
LVHPLTEEVSAKRALSIRPVIDFRNVFNVFFRSWKERGLAHSFISDGVLPAGFTVCRPELYVNPNRIFYKELYWVTALIATAGGSSHGTFVIQKRSRVAMEVqllllmlswflfflffin
phkxdexlSAQFSTRPDIIAELNKLFAENVTAVDGKGIKRMCPFQVRNLKIEGFSSKNDPDFFDKESFSPQFAFIVVAGAEEKHYRETLYAQKSASWSRTILDGNIGTLAEFAMsryrne
krxhvkkerkeksddqkklgsrsqxniplhlcsxntvwfvgdhswklafipkkkqlqskpxqlsmffsfspikakwtdtkcqiiakymrcsqlkasvkmfmxmqdslkrqtikaqfnqlk
vksded.....wrktqstvrpqskatvxhyeskqrfvikxnlshpsknaqlxtktaqspneskteyllfrssxsqkaxldxgsllgslrcsisgtrnreasyxgfxsvvgeqrtrkqtrc
sadcevkvqkiifncsgsxffktqkkpxvlnclwiksesliffgllsfxcffcfftxsvlikktkifglkpfnrrfamyltgvlaxflxsiesseixtslkikilcfilkdehlsryxvvl
gnrfxxkllrlllfeytlkwflvggnxmdrmylfffhieegrxhiwtxlkckxrifvwrqxeqdtktrdafsatidxfnyaslilvhmhtfrqaklscitrpiqyvxikarklqsyidna
elerkhminkfareeakmlsdrlrkvdalkvpkllfdeageelcrflylsgftlsrigylkysqicfialeyiiimlslrtfltqnrlllclctlhrdrpnpnxlhgxrlnhlgflxfmy
xltksprvhxrsiyfxielssraxsiisxekrfkhgcslnxxexsgnxfdnxsgsfyvgfrlkilyvvvvltlgmitlfydyllrkxxllikhnyllkixdicirxrysxxldxiltivk
flkrflcygrfrimgmeqlllhvfdvinplnqdxmikvxvlilsxlxsxxlliyrdirplinessmivvpierfasseqxftxfgyvlnsxfkmkxi+2kx.....enxnqsflqimllvxk
srrxcnmdlxglcltirxxxilrxirffkx+1lgfikxcwiqisexexfyxvchdskngxiwgfxxerwriwsitfskdcxrccyslcfl.....
```

SID2
AT1G74710

>Est-1.MPI_chr1:W/28070391-28075390 Amino_Acid

MASLQFSSQFLGSNTKTHSSIISISRSYSPTPFTRFSRKvfflfcfvffnsvlffggihndxlnfigxfseKYESCSMSMNGCDGDFKTPLGTVETRTMTAVLSPAAATERLISAVSELK
SQPPSFSSGVVRLQvhhzzzziiilcfflrhnpicccmxkneitprgvftlvcgdfvlxlavllhrlcliixdpnrydyxnhtikqssqqrxiypnltvnhklleddxxlskrygyyi
syxfmnkthtrtrsykipxvhrtixlgllgplhvnyneyfllvnftxtksxtfxkexscffsprnlixhcxllvsvamlrxfsxksnnfvfcgpenkxnndxnpicckgkaaikxshshx
naeffkkpksqsnfpaqxtliwiwcrVPIDQQIGAIDWLQAQNEIQPRCFFSRRSDVGRPDLLLDLANENGNGNGNGTVSSDRNLVSVAGIGSAVFFRDLDPFSHDDWRSIRRFLSSTSP
LIRAYGGMRFDPNGKIAVEWEPFGAFYFSVPQvplkidslxeifxvcvvvxladtcagVEFNEPGGSSMLAATIAWDDELSWTLENAIEALQETMLQVSSVVMKLRNRSLGVSVLSKNHV
PTKGAYFPAVEKALEMINQKSSPLNKvvxtleivfvsilktslxvsfxlmflargirVVLARNSRIITDTDIDPIAWLAQLQvcfylwilyssqfsmfrfishxffcvtaREGHDAYQFC
LQPPGAPAFIGNTvgzfizslxxxvllikicahllzliskkyvcdihlcetaPERLFQRTQLGVCSEALAATRPRAASSARDMEIERDLLTSsiftssalnnyriqfsiiillnfcxtvav
PKDDLEFSIVRENIREKLNvssilmlcsfnasflgxxfgifflimlssalqGICDRVVVKPQKTVRKLARVQHLYSQLAGRLTKEDDEvrxxywnsfyisklfissnxlxpfffl svysY
KILAALHPTPAVCGLPAEEARLLIKEIEkistlvqlsssnyrcrdxelcxlkhfassrSFDRGMYAGPIGFFGGEESEFAVGIRSALVEKvslfdlflplkntlxhxllxqnrslrfllq
lvkzcxtvfxftgGLGALIYAGTGIVAGSDPSSEWNELDLKISQvrafvqkmfsdimvlcyqnpnfyslfcccfcsFTKSIEYEATTSLQAINXrksnicixlfclyggxgvltirkqcc
lscklkkkcfnllmgrafsgcnxgrpimnvhrpscydcxxasivfffkdryiqygsktelnltdmtiesnxiyffnfhlarsdpssexsnlcllsrlsknpxnawafqrxcsrvgqvygi
cfyangkyxysfisxrfrsssfvrlrnyfviixlxipsnnltrhifscvvvyrniekyhiikxrintstktqikxdstikkmermxkvknqtkawrxrmesdfplsplxhhiflslftlh
lnxvyxsyltlxltnpfhlfyftnhnalaslrftxiyfvtnytnmnliiytrvrnsfsxylvsfnxnxxnexivystxdlflvyxwklrfhxyxkhvnkiklxrgiysnkksktskkkls
iislprlpxslsqttkpslshylnerrrhsremrrlplrxtrrrftrilrrrgssvsslsklllklvifslkmvkealaltslsismlrrnepplssvtxtlfgtrclisps

>Bs_1.SALK_chr1:W/28070391-28075390 Amino_Acid

MASLQFSSQFLGSNTKTHSSIISISRSYSPTPFTRFSRKvfflfcfvffnsvlffggihndxlnfigxfseKYGSCSMSMNGCDGDFKTPLGTVETRTMTAVLSPAAATERLISAVSELK
SQPPSFSSGVVRLQvhhyiiiiilcfflrhnpicccmxkneitprgvftlvcgdfvlxlavllhrlcliixdpnrydyxnhtikqssqqzxiypnltvnhklleddxxlskrygyyi
syxfmnkthtrtrsykipxvhrtixlgllgplhvnyneyfllvnftxtksxtfxkexscffsprnlixhcxllvsvamlrxfsxksnnfvfcgpenkxnndxnpic..gkaaikyshshx
naeffkkpksqsnfpaqxtliwiwcrVPIDQQIGAIDWLQAQNEIQPRCFFSRRSDVGRPDLLLDLANENGNGNGNGTVSSDRNLVSVAGIGSAVFFRDLDPFSHDDWRSIRRFLSSTSP
LIRAYGGMRFDPNGKIAVEWEPFGAFYFSVPQvplkidslxeifxvcvvvxladtcagVEFNEPGGSSMLAATIAWDDELSWTLENAIEALQETMLQVSSVVMKLRNRSLGVSVLSKNHV
PTKGAYFPAVEKALEMINQKSSPLNKvvxtleivfvsilktslxvsfxlmflargirVVLARNSRIITDTDIDPIAWLAQLQvcfylwilyssqfsmfrfishxffcvtaREGHDAYQFC
LQPPGAPAFIGNTvglficslxxxvllikicahllfiskkyvcdihlcetaPERLFQRTQLGVCSEALAATRPRAASSARDMEIERDLLTSsiftssalnnyriqfsiiillnfcxtvav
PKDDLEFSIVRENIREKLNvssilmlcsfnasflgxxfgifflimlssalqGICDRVVVKPQKTVRKLARVQHLYSQLAGRLTKEDDEvrxxywnsfyisklfissnxlxpfffl svysY
KILAALHPTPAVCGLPAEEARLLIKEIEkistlvqlsssnyrcrdxelcxlkhfassrSFDRGMYAGPIGFFGGEESEFAVGIRSALVEKvslfdlflplkntlxhxllxqnrslrfllq
lvkkcxtvfxftgGLGALIYAGTGIVAGSDPSSEWNELDLKISQvrafvqkmfsdimvlcyqnpnfyslfcccfcsFTKSIEYEATTSLQAINXrksnicixlfclyggxgvltirkqcc
lscklkkkcfnllmgrafsgcnxgrpimnvhrpscydcxxasivfffkdryiqygsktelnltdmtiesnxiyffnfhlarsdpssexsnlcllsrfdsknpfnvwafqrxcsrvgqvygi
cfyangkyxysfisxrfrsssfvrlrnyfviixlxipsnnltrhifscvvvyrnikkyhiikxrintstktqikxdstikkmermxkvknqtkawrxrmesdfplsplxhhiflslftlh
lnxvyxsyltlxltnpfhlfyftnhnalaslrftxiyfvtnytnmnliiytrvrnsfsxylvsfnxnxxnexivystxdlflvyxwklrfhxyxkhvnkiklxrgiysnkksktskkkls
iislprlpxslsqttkpslshylnerrrhsremrrlplrxtrrrftrilrrrgssvsslsklllklvifslkmvkealaltslsismlrrnepplssvtxtlfgtrclisps

>Est-1.MPI_chr1:W/30324219-30329218 Amino_Acid

MTSLSIQPFPEkssllccyxclslcyvfilsyssrapelgllmfyiscxlqnhvhhstlikfefvtlmlrvhxfafcfflmfesllcfyltlpaqvlfxvhliqnrvllrlxllssdfeif
knsmsteISRMARDLDSRKKRRISLDGIAALCEHSKEIIDSLPMLNSPDYFLKPCINELVEREIESPDYCSRVPDFTIGRIGYGYIRFLGNTDVRRLDLDHIVKFHRHEVIVYDDESSKP
VVGEGLNKAAEVTLVVNIPDLTWGKQQVNHIAYKLKQSTERQGATFISFDPDNGLWKFPVPHFSRFGLSDDEAEDIAMDDAPGLGDPVGLDGKKVADIDEEDQMETSELELSHSLPAHLG
LDPEKMKEMRMLMFPNEDEDESEDFREQTSHLMTSLTKRNVRPSQKIAQRNSHQDPPPVVRKTPLALLEYNPGNDKSSPGSILMVQQNKNLAVRKSKTGGFELDISHVTPLTDNYSRNVV
DAALFMGRSFRAGWGPNGVLFHTGKPICSSSSQMVLSSVINKEKIAIDKVVWDRKGKVQKELIDSAFEAPLSLHKELNHVEEEVRFGSFSLKLQNVVTDRVVLSDICRSYIGIIEKQLEV
AGLSTSAKLFLMHQVMVWELIKVLFSERQSTERLMYAASDNEEDVMQDVKEDSAKIDTEALPLIRRAEFSCWLQESVSHRVQEDVSDLNGSSYLEHLFFLLTGRELDSAVELAISKGDVR
LACLLSQAGGSTVNRNDILQQLHLWRRNGLDFNFIEKERIKLYELLAGNIHDALQDFTIDWKRFLGLLMWHHLPPDSSLPIIFRSYQLLLNQAKAPWPVPIYIDEGPADGFVSDNKHSDI
LYYLMLLHSKEEEEFGFLQTMFSAFSSTDDPLDYHMIWHHRGILEAVGAFTSDDLHTLDMGFVAQLLSQGLCHWAIYVVLHIPFREDHPYLHVTVIREILFQYCETWSSMESQRQFIKDL
GIPSEWMHEALvrtpyhssfllllkvlvahcxfthcvagAVYYNYHGDFVKALDQFIECANWQRAHSIFMTSVAHSLFLSAkslhflicrpnystrtxsrcdvgwixlexfvlsllnaaN
HSEIWRIATSMDDRKSEIENWDLGAGIYMSFYLLKSSLQEDADTMVELvclrffivlylltklivqhiisctddtqqdclkhwnlhsydhghkslfildvxtllxmiqttxllgfhrEPL
DSTNESCRNFVGRLNESLAVWGDRLPVEARxvlhtsptcxlialnnrqellmacmnlydpssfyafvciryrxflgydrlhitklkndtxwsnfgwillnlvesiviapklsrwllmttq
pkfavwtdtghtfsvrhflaywlqihsxltnslnaaeVAYSKMAEEICDLLLSDLSKNPSRETQLTCFETAFDAPLPEDVRSTHLQDAVSLFSLYLSETGQISAXxnrhyysvrrsfnll
cvkqsqfvccfcyyttleaxmsxfgrvvlansqilyifceskgenqckwncidfhglfiaelnsqvqlndneatstsnysxllxqreflxwrlymsxxysanilsfgdvfelsscsnarhl
lfiinflfvndixisxirfaeseiykxgixkvcwnifsfffsfffffllnsyllfliatdrefdixlxkxspksekkmqirlqkkekkkvciltrlqstlainrrntew

>Bs_1.SALK_chr1:W/30324219-30329218 Amino_Acid

MTSLSNQPFPEkssllccyxclslcyvfilsyssrVpelgllmfyiscxlqnhvhhstlikfefvtlmlrvhxfafcfflmfesllcfyltlpaqvlfxvhliqnrvllrlxllssdfeif
knsmsteISRMARDLDSRKKRRISLDGIAALCEHSKEIIDSLPMLNSPDYFLKPCINELVEREIESPDYCSRVPDFTIGRIGYGYIRFLGNTDVRRLDLDHIVKFHRHEVIVYDDESSKP
VVGEGLNKAAEVTLVVNIPDLTWGKQQVNHIAYKLKQSTERQGATFISFDPDNGLWKFFVPHFSRFGLSDDEAEDIAMDDAPGLGDPVGLDGKKVADIDEEDQMETSELELSHSLPAHLG
LDPEKMKEMRMLMFPNEDEDESEDFREQTSHLMTSLTKRNVRPSQKIAQRNSHQDPPPVVRKTPLALLEYNPGNDKSSPGSILMVQQNKNLAVRKSKTGGFELDISHVTPLTDNYSRNVV
DAALFMGRSFRAGWGPNGVLFHTGKPICSSSSQMVLSSVINKEKIAIDKVVWDRKGKVQKELIDSAFEAPLSLHKELNHVEEEVRFGSFSLKLQNVVTDRVVLSDICRSYIGIIEKQLEV
AGLSTSAKLFLMHQVMVWELIKVLFSERQSTERLMYAASDNEEDVMQDVKEDSAKIDTEALPLIRRAEFSCWLQESVSHRVQEDVSDLNGSSYLEHLFFLLTGRELDSAVELAISKGDVR
LACLLSQAGGSTVNRNDILQQLHLWRRNGLDFNFIEKERIKLYELLAGNIHDALQDFTIDWKRFLGLLMWHHLPPDSSLPIIFRSYQLLLNQAKAPWPVPIYIDEGPADGFVSDNKHSDI
LYYLMLLHSKEEEEFGFLQTMFSAFSSTDDPLDYHMIWHHRGILEAVGAFTSDDLHTLDMGFVAQLLSQGLCHWAIYVVLHIPFREDHPYLHVTVIREILFQYCETWSSMESQRQFIKDL
GIPSEWMHEALvrtpyhssfllllkvlvahcxfthcvagAVYYNYHGDFVKALDQFIECANWQRAHSIFMTSVAHSLFLSAkslhflicrpnystrtxsrcdvgwixlexfvlsllnaaN
HSEIWRIATSMDDRKSEIENWDLGAGIYMSFYLLKSSLQEDADTMVELvclrffivlylltklivqhiisctddtqqdclkhwnlhsydhghkslfildvxtllxmiqttxllgfhrEPL
DSTNESCRNFVGRLNESLAVWGDRLPVEARxvlhtsptcxlialnnrqellmacmnlydpssfyafvciryrxflgydrlhitklkndtxwsnfgwillnlvesiviapklsrwllmttq
pkfavwtdtghtfsvrhflaywlqihsxltnslnaaeVAYSKMAEEICDLLLSDLSKNPSRETQLTCFETAFDAPLPEDVRSTHLQDAVSLFSLYLSETGQISAXxnrhyysvrrsfnll
cvkqsqfvccfcyyttleaxmsxfgrvvlansqilyifceskgenqckwncidfhglfiaelnsqvqlndneatstsnysxl(1+3)lxqreflxwrnmsxxysaniisfgdvfelsscsnarhll
fiinflfvndixisxirfaeseiykxgixkvcwnifsfffsfffffllnsyl(f+1)lfliatdrefdixlxkxspkse[]kmqirlqkkekkkvciltrlqstlainrrntew